University of Glasgow

Sarker, Swapan Kumar (2017) *Spatial and temporal patterns of mangrove abundance, diversity and functions in the Sundarbans.* PhD thesis.

http://theses.gla.ac.uk/8499/

SPATIAL AND TEMPORAL PATTERNS OF MANGROVE ABUNDANCE, DIVERSITY AND FUNCTIONS IN THE SUNDARBANS

Swapan Kumar Sarker

A thesis submitted in fulfilment of the requirements for
the degree of Doctor of Philosophy

Supervisors: Professor Jason Matthiopoulos & Dr Richard Reeve

Institute of Biodiversity, Animal Health and Comparative Medicine
College of Medical, Veterinary and Life Sciences
University of Glasgow

September 2017

Abstract

Mangroves are a group of woody plants that occur in the dynamic tropical and subtropical intertidal zones. Mangrove forests offer numerous ecosystem services (e.g. nutrient cycling, coastal protection and fisheries production) and support costal livelihoods worldwide. Rapid environmental changes and historical anthropogenic pressures have turned mangrove forests into one of the most threatened and rapidly vanishing habitats on Earth. Yet, we have a restricted understanding of how these pressures have influenced mangrove abundance, composition and functions, mostly due to limited availability of mangrove field data. Such knowledge gaps have obstructed mangrove conservation programs across the tropics.

This thesis focuses on the plants of Earth's largest continuous mangrove forest — the Sundarbans — which is under serious threat from historical and future habitat degradation, human exploitation and sea level rise. Using species, environmental, and functional trait data that I collected from a network of 110 permanent sample plots (PSPs), this thesis aims to understand habitat preferences of threatened mangroves, to explore spatial and temporal dynamics and the key drivers of mangrove diversity and composition, and to develop an integrated approach for predicting functional trait responses of plants under current and potential future environmental scenarios.

I found serious detrimental effects of increasing soil salinity and historical tree harvesting on the abundance of the climax species *Heritiera fomes*. All species showed clear habitat preferences along the downstream-upstream gradient. The magnitude of species abundance responses to nutrients, elevation, and stem density varied between species. Species-specific density maps suggest that the existing protected area network (PAN) does not cover the density hotspots of any of the threatened mangrove species.

Using tree data collected from different salinity zones in the Sundarbans (hypo-, meso-, and hypersaline) at four historical time points: 1986, 1994, 1999 and 2014, I found that the hyposaline mangrove communities were the most diverse and heterogeneous in species composition in all historical time points while the

hypersaline communities were the least diverse and most homogeneous. I detected a clear trend of declining compositional heterogeneity in all ecological zones since 1986, suggesting ecosystem-wide biotic homogenization. Over the 28 years, the hypersaline communities have experienced radical shifts in species composition due to population increase and range expansion of the disturbance specialist *Ceriops decandra* and local extinction or range contraction of many endemics including the globally endangered *H. fomes*.

Applying habitat-based biodiversity modelling approach, I found historical tree harvesting, siltation, disease and soil alkalinity as the key stressors that negatively influenced the diversity and distinctness of the mangrove communities. In contrast, species diversity increased along the downstream – upstream, and riverbank — forest interior gradients, suggesting late successional upstream and forest interior communities were more diverse than the early successional downstream and riverbank communities. Like the species density hotspots, the existing PAN does not cover the remaining biodiversity hotspots.

Using a novel integrated Bayesian modelling approach, I was able to generate trait-based predictions through simultaneously modelling trait-environment correlations (for multiple traits such as tree canopy height, specific leaf area, wood density and leaf succulence for multiple species, and multiple environmental drivers) and trait-trait trade-offs at organismal, community and ecosystem levels, thus proposing a resolution to the 'fourth-corner problem' in community ecology. Applying this approach to the Sundarbans, I found substantial intraspecific trade-offs among the functional traits in many tree species, detrimental effects of increasing salinity, siltation and soil alkalinity on growth related traits and parallel plastic enhancement of traits related to stress tolerance. My model predicts an ecosystem-wide drop in total biomass productivity under all anticipated stress scenarios while the worst stress scenario (a 50% rise in salinity and siltation) is predicted to push the ecosystem to lose 30% of its current total productivity by 2050.

Finally, I present an overview of the key results across the work, the study's limitations and proposals for future work.

Table of Contents

List of Tables

List of Figures

Acknowledgements

First of all, I wish to thank my mentors — Jason Matthiopoulos and Richard Reeve. I am incredibly lucky to have dedicated mentors like you. My enthusiasm for work has just increased day by day during the last four years because of your care, patience, support and trust on me. Jason, I should reveal that you are the most influential person in my life. My perspectives on life and science have been refined in many ways in the last four years. I am privileged to have you as my mentor and friend. Richard, I have learnt from you how to dig deep into research. Thank you for your willingness to meet me at short notice every time. I will miss you both.

Special thanks to my external examiner – Bill Kunin from the Faculty of Biological Sciences, University of Leeds and internal examiner - Grant Hopcraft. I enjoyed the viva, and your comments on the thesis has been extremely useful. I also thank my assessors — David Bailey and Barbara Helm. Your external perspective on my work has been helpful. David, your advice on work-life balance has changed my lifestyle for sure. You and Jason were always keen to see me going back to family in Bangladesh every five months. It always gave my family and me a pleasant feeling. I will always be grateful. I would also like to thank Jill Thompson from the Centre for Ecology and Hydrology. You were very much passionate about my project and made valuable contributions to my soil and trait sampling designs. I would like to say a special thanks to Jana Jeglinski. I could not start producing my spatial maps without your GIS tips. I would also like to thank Sonia Michell for helping me understanding the biodiversity quantification codes.

I am grateful to the Commonwealth Scholarship Commission, UK for funding my PhD studentship. Terry Jacques, Juliette Hargrave and Ellie Fixter – thank you for your kind helps in managing and extending my scholarship. Jason, you spent your Glasgow University start-up fund for my field work. Thank you again.

Everybody at the Bangladesh Forest Department was extremely helpful in all aspects of my fieldwork. Special thanks to Younus Ali, Zaheer Iqbal Ezaz, Jahir Akon, Nirmal K Paul and Mariam Akhter for sharing the past vegetation data. I would like to thank Amir Hossain Chowdhury and Zahir Ahmed for giving all logistic supports during my eight months long fieldwork. I would also like to thank Anwarus Salehin and Mofazzal Hussain: without your field training, it was not possible for

Author's Declaration

I hereby declare that the work presented in this thesis is my own unless otherwise stated or acknowledged. No part of this thesis has been submitted for any other degree. The following lists the contributions made to the material in this thesis by the co-authors and collaborators:

Chapter 2. Published as: "Sarker, S. K., Reeve, R., Thompson, J, Paul, N.K., & Matthiopoulos, J., 2016. *Are we failing to protect threatened mangroves in the Sundarbans world heritage ecosystem?* Scientific Reports, 6, 21234; doi: 10.1038/srep21234." SKS, JM, RR and JT designed research, fieldwork was carried out by SKS with assistance from NKP, SKS analysed data with advice from JM and RR, and SKS prepared the manuscript with comments and edits from JM, RR, JT and NKP.

Chapter 3. Submitted to '*Biological Conservation*' as: "Sarker, S. K., Reeve, R., Mitchell, S. N., & Matthiopoulos, J., *Spatial contraction of distinct and diverse mangrove communities in the Sundarbans world heritage ecosystem*". SKS, JM and RR designed research; SKS collected field data; SKS analysed data with biodiversity quantification code help from SNM and advice from RR and JM; and SKS prepared the manuscript with comments and edits from JM and RR.

Chapter 4. Submitted to '*Diversity and Distributions*' as: "Sarker, S. K., Reeve, R., & Matthiopoulos, J., *Modelling mangrove spatial biodiversity in the Sundarbans World Heritage Ecosystem: A baseline for conservation*". SKS, JM and RR designed research; SKS collected field data; SKS analysed data with advice from RR and JM; and SKS prepared the manuscript with comments and edits from JM and RR.

Chapter 5. Under review in '*Proceedings of the National Academy of Sciences*' as: "Sarker, S. K., Reeve, R., & Matthiopoulos, J., *Solving the fourth-corner problem: Forecasts of whole-ecosystem primary production from spatial, multispecies, trait-based models*". SKS, JM and RR designed research; SKS collected field data; The original concept of the modelling approach and primary code came from JM; RR extended the modelling approach and contributed codes; SKS analysed data

with advice from RR and JM; SKS prepared the first draft and all authors then contributed equally to prepare the final draft.

Swapan Kumar Sarker

September 2017

Abbreviations

ACEP   Atlantic, Caribbean and Eastern Pacific

BFD   Bangladesh Forest Department

CS   Community size

DAS   Density of all stems for each plot

DP   Disease prevalence

DR   Distance of each plot from the nearest riverbank

FP   Forest productivity

HH   Historical harvesting

HSM   Habitat Suitability Model

IWP   Indo-west Pacific

LS   Leaf succulence

MC   Metacommunity

PAN   Protected area network

PSP   Permanent sample plots

REDD   Reduced Emissions from Deforestation and Degradation

SC   Subcommunity

SLA   Specific leaf area

SLR   Sea level rise

TER   Trait-environment relationships

TTR   Trait-trait relationships

URP   Upriver position

WD   Wood density

Chapter 1 . General Introduction

1.1 What are mangroves?

Mangroves are woody plants that grow at the interface between land and sea. They first appeared along the shores of the Tethys Sea and then diverged from their terrestrial relatives during the Late Cretaceous to Early Tertiary (Ricklefs et al. 2006). Mangrove forests (30°N and 30°S latitude, $1.37\text{-}1.5 \times 10^5$ km^2) occur in the dynamic tropical and subtropical intertidal zones (Giri et al. 2011) and consist of approximately seventy taxonomically diverse plant species from two plant divisions, twenty-seven genera, twenty families and nine orders (Duke et al. 1998). Mangroves have many highly specialized adaptations to cope with extreme environmental conditions such as saline anaerobic sediments, high temperature and regular flooding (Mitra 2013). The adaptation mechanisms in mangroves are mainly of three forms: morphological, physiological and anatomical (Naskar & Palit 2015). Morphological adaptations in many mangroves include pneumatophores (breathing roots) to grow in anaerobic sediments and viviparous propagules to promote seed dispersal and formation of new forest stands. Physiological adaptations include salt exclusion, extrusion or accumulation to reduce salt stress on plant body. Anatomical adaptations may include thick cuticle and sunken stomata to ensure efficient water use by mangroves under limited freshwater availability. Collectively, these mechanisms ensure the long-term persistence and propagation success of mangroves living under extreme environments (Duke et al., 1998).

Based on the development of adaptive mechanisms over time and habitat preferences, mangrove plants are categorized into two groups: exclusive and non-exclusive mangroves (Wang et al., 2010). Exclusive mangroves are highly adapted and their geographic ranges are strictly confined to the intertidal environmental settings (they do not expand into terrestrial communities). On the other hand, non-exclusive mangroves lack such derived traits and tend to grow in a relatively benign environment of the intertidal zone. They can even expand their ranges towards terrestrial plant communities (Tomlinson 1986). For example, the flagship

species of the Sundarbans mangrove ecosystem – *Heritiera fomes* – is a non-exclusive species while the other major species such as *Excoecaria agallocha*, *Ceriops decandra* and *Xylocarpus mekongensis* are exclusive mangrove species. These species show a number of differences in their life-history and morphological traits and reproductive processes. *H. fomes* is an evergreen mangrove tree species that grows up to 25 m in height and produces pneumatophore. It regenerates through seed and the germination type is hypogeal (Mahmood 2015). The regeneration is more successful under moderate crown cover than the open areas. This species has moderate light demands although prefers shade at the early stage of growth (Siddiqi 2001). Flowering time for this species is April – June and the fruiting time is May – July. *E. agallocha* is a deciduous tree that grows up to 5 – 15 m with irregular crown structure. The species mostly shows epigeal germination and do not have pneumatophores. It also has the ability to copice (Mahmood 2015). Flowering time for this species is April – July and the fruiting time is May – September. *Ceriops decandra* is an evergreen, slow growing tree that grows up to 4 m in height and can survive for long periods under extreme environmental conditions. The species shows viviparous germination and also has good coppicing ability (Mahmood 2015). Flowering time for this species is March – May and the fruiting time is April – July. *X. mekongensis* is a deciduous tree that grows up to 20 m in height with peg or cone-shaped pneumatophores. Germination type is hypogeal in this species. Flowering time for this species is March – May and the fruiting time is April – August (Siddiqi 2001).

1.2 Mangroves are threatened world-wide

Mangrove forests support coastal livelihoods worldwide and provide numerous ecosystem services, including nutrient cycling (Feller et al. 2010), storm/tsunami protection (Ostling et al. 2009), carbon sequestration (Alongi 2014), and fisheries production (Carrasquilla-Henao & Juanes 2017). Mangroves are the most carbon-dense forests in the world (1,023 Mg C ha^{-1}) (Donato et al. 2011). The estimated monetary value of the ecosystem services provided by mangrove forests is US $4185 ha^{-1} y^{-1} (Friess 2016). Despite such ecological and economic contributions, mangroves are declining rapidly because of land clearing, coastal development, over-harvesting, aquaculture expansion, altered hydrology, nutrient over-

enrichment and changes in rainfall and sea surface temperature (Polidoro et al. 2010; Daru et al. 2013; Ghosh et al. 2017). Since the 1950s, the world-wide mangrove forest coverage has declined by 50% (Feller et al. 2010) and the geographic range and population sizes of most of the mangrove plant species have contracted (Polidoro et al. 2010). The current rate of mangrove deforestation is 1-2% per year (Alongi 2015). Different aspects of climate change such as sea level rise (SLR), altered precipitation patterns and increased temperature and storminess may further accelerate the loss (Ward et al. 2016). This loss and degradation may seriously limit the capacity of mangroves to provide valuable ecosystem services for current and future generations.

1.3 Modelling mangrove abundance

The influence of climate change on mangrove forests' worldwide distribution is now well accepted. Studies have shown differential responses of mangroves to fine-scale variations in salinity (Alongi 2015; Banerjee et al. 2017; Hoppe-Speer et al. 2011), nutrients (Naidoo 2009; Reef et al. 2010), and hydroperiod (Crase et al. 2013). Hence, future global climate scenarios and changes in fine-scale environmental conditions may cause species compositional shifts and range contraction (in an adverse situation, e.g. drought and high salinity) or expansion (in suitable condition, e.g. adequate rainfall, low salinity and improved nutrient supply) of individual mangrove species. Quantifying the relationship between environmental variables and observed species abundance or occurrence using habitat suitability models (HSMs), has been a widely used approach to address these challenges for diverse taxa including upland plants (Smolik et al. 2010; Pottier et al. 2013), birds (Moudrý & Šímová 2013), butterflies (Eskildsen et al. 2013), fish (Gasper et al., 2013), seals (Anderwald et al. 2012), and dolphins (Hastie et al., 2005). Theoretical background and practical guidelines for constructing HSMs have been explicitly described by Guisan & Zimmermann (2000), Austin (2002), Guisan & Thuiller (2005), Franklin (2010) and Miller (2010).

HSMs are static in nature and assume equilibrium or pseudo-equilibrium between the environment and observed species patterns. These static models fail to capture the response of species under changing environmental conditions and have limited ability to cope with non-equilibrium situations (e.g. invasion, climate change) because they assume that habitats are closed, stable and without

competition (Guisan & Zimmermann 2000; Dormann 2007). Despite such fundamental limitations, HSMs have been widely used for forecasting or hindcasting species distributions in space and time (Elith & Leathwick 2009). The outputs of HSMs — species distribution/density maps — can be used for identifying critical habitats of threatened mangrove species. HSMs can also be used to locate appropriate mangrove restoration sites by matching maps of critical environmental variables and species historical ranges or habitat preferences (Hirzel & Le Lay, 2008). HSMs have been increasingly used to project the potential effects of global warming on species distributions and ecosystem properties (Franklin 2010). Global biodiversity databases (e.g. GBIF, BISS etc.) have little information on mangroves (Ellison 2001). In this context, HSM research on mangroves can contribute baseline data in these databases. So far, mangrove-related global and regional conservation work has not focused on species-specific distributions in space although such information about either abundant or endangered species is important for identifying critical habitats and no-take zones and also for establishing coastal protected areas (Polidoro et al. 2010).

Mangrove modelling research has been dominated by topics such as mangrove demography (Khoon & Eong 1995), stand structure and dynamics (Luo et al., 2010; Rakotomavo & Fromard, 2010), ecosystem services (Barbier et al. 2011), food webs (Siple & Donahue 2013), evolution and molecular ecology (Daru et al. 2013; Triest 2008) and biological invasion (Geller et al., 2010). Moreover, application of remote-sensing technology to provide spatio-temporal information on mangroves has been an active area of research during the last two decades (Giri et al., 2011; Heumann, 2011; Kuenzer et al., 2011). However, the use of HSMs for mangroves has been limited. Only recently, Record et al. (2013) provided the first example of applying species and community distribution models to coastal mangroves worldwide. However, fine-scale environmental data-driven regional or local HSMs that offer realistic predictions for both species and habitat conservation (Franklin 2010) are limited for mangroves.

1.4 Modelling mangrove biodiversity

1.4.1 Biodiversity quantification: state-of-the-art

Understanding the processes that shape biodiversity and explaining biodiversity patterns across space and time are crucial for identifying vulnerable ecosystems, habitats or species and for developing realistic conservation plans (Meynard et al. 2011). These processes are, however, scale-dependent. For example, biodiversity at a local scale may be related to competition or random dispersal whereas regional diversity may be related to environmental filtering (Swenson et al. 2012). Two prominent theories — 'niche theory' (Hutchinson 1957) and 'neutral theory' (Hubbell 2001) — have quite different explanations about the processes that shape biodiversity. Niche theory asserts that the amount of resource use varies across species, so only species having differentiated niches can coexist in a particular ecological community. The neutral theory assumes that community individuals have the same chance to reproduce and death, and relative abundances of species vary for demographic stochasticity or 'ecological drift'. It further assumes that demographic processes take place at the local scale and demographic drift may be responsible for species extinction. Demographic drift may also be responsible for species extinction from the regional species pool. The regional species pool may gain novel species via speciation and contributes to local diversity via propagule dispersion. The neutral theory of Hubbell thus proposes 'limited dispersal' instead of 'niche specialization', as the main mechanism responsible for spatial variation across ecological communities.

Biodiversity is simplified by partitioning regional species diversity (γ) into local (α) and turnover (β). α (alpha) diversity represents species diversity of a specific site, β (beta) diversity represents species compositional variation among sites, and γ (gamma) diversity is the sum of diversity for the various sites within an ecosystem. Species richness and numerous indices that incorporate relative abundances of species are two principle measurement schemes of alpha diversity. α diversity can be estimated in many ways (Maurer & Mcgill 2011). However, Shannon's index of diversity (Shannon & Weaver 1949) and measures based on Simpson's concentration (Simpson 1948) are the most commonly used indices. Jost (2006, 2007) has strongly criticized the use of index values of these indices in making

ecological statements and suggested using the 'effective number of species' which he termed 'true diversity'.

β diversity can be defined in two ways: directional turnover and non-directional variation. In the case of directional turnover, species compositional change is measured along a specified gradient (e.g. spatial, temporal or environmental), and in case of non-directional variation, variation in species composition is measured without reference to any specific gradient (Legendre & De Cáceres 2013). Both β diversity versions are frequently used to explain the connections between local and regional diversity, and for visualizing spatial patterns of species assemblages (De Cáceres et al. 2012). Various β diversity indices have been proposed to quantify species compositional variation (directional or non-directional). Whittaker (1960) first proposed a non-directional β diversity index for species richness ($β = γ/α$), and Nekola & White (1999) developed a directional β index by introducing the slope of the similarity decay in species composition with geographic distance. After these initial approaches, the number of indices has been increasing. Currently, the most popular indices belong to two families: additive ($α + β = γ$)(Lande 1996) and multiplicative ($α \times β = γ$)(Whittaker 1972).

While debates on several aspects of diversity measurements (e.g. partitioning diversity, scale, theoretical clarity, biological meaning) are ongoing (Barwell et al. 2015), a variety of approaches have been taken by ecologists (Jost, 2006, 2007, 2010; Mendes et al., 2008; Tuomisto, 2010a, 2010b; Veech & Crist, 2010) to develop a unified index of diversity measurement. Most of these approaches, abundance-based in nature, have tried to integrate several components of diversity (e.g. evenness, scale etc.) into a single unified equation. However, Leinster & Cobbold (2012) criticized these approaches for not accounting for the species relative abundances. Reeve et al. (2016) have recently proposed a unified framework that resolves these problems and offers direct diversity comparison between constituent communities of an ecosystem, thus allowing identification of distinct, diverse or homogeneous communities. The main motivation behind their approach is to overcome the limitations of traditional diversity indices and to make diversity comparisons easier and informative.

1.4.2 Mangrove biodiversity research: state-of-the-art

Spatial modelling of distributions of individual species has been, so far, the most popular strategy in ecology and biogeography (Franklin 2010). Community-level biodiversity modelling is gaining popularity for its ability to account for the rare species and to combine complex species and environmental data into a structured form which allows us to produce various spatial outputs such as maps of diversity indices, community types (sites with similar species composition), species groups (species with similar distributions), and gradients of compositional variation (Bonthoux et al., 2013). A variety of approaches: (1) 'assemble first, predict later', (2) 'predict first, assemble later' and (3) 'assemble and predict together' (Ferrier & Guisan 2006) are followed to produce these outputs. In the 'assemble first, predict later' approach, biological survey data are first used to estimate plot-level biodiversity indices which are then modelled as a function of environmental covariates. In the 'predict first, assemble later' approach, individual species in a study area are first modelled separately as a function of the environmental covariates to generate species distribution layers and then these layers are combined to calculate biodiversity indices for all grid cells. In the 'assemble and predict together' approach, a single integrated modelling framework is first used to predict the spatial distributions of all species simultaneously and then these predictions are used to calculate biodiversity indices for all grid cells. While these approaches have been widely applied to identify hotspots and to prioritize conservation sites for a variety of taxa (e.g. upland tree species, birds, and fish), they have rarely been used for the mangrove taxa.

Testing 'zonation' (distinct ordering of mangrove plants from shore to inland) and explaining the 'biodiversity anomaly' (mangrove species richness declines when we move along the latitudinal gradient) are the two research agendas that have dominated the mangrove biodiversity literature. Numerous studies have tested the existence of mangrove species zonation patterns. Although zonation is considered a common pattern in mangrove distributions world-wide (Siddiqi 2001), Bunt (1996) and Bunt & Stieglitz (1999) could not identify any clear-cut mangrove distribution patterns in Australia. Ellison et al. (2000) criticized the previous studies for being descriptive and tested species zonation patterns in the Bangladesh Sundarbans using quantitative methods. They did not notice any

distinct species zonation patterns. The number of mangrove plant species declines when we move along the latitudinal gradient – highest species richness (58 plant species) in the Indo-west Pacific (IWP) zone and lowest (12 plant species) in the Atlantic, Caribbean and Eastern Pacific (ACEP) regions. Mangrove ecologists put tremendous efforts to explain the cause of this 'anomalous' drop in species richness from IWP to ACEP (Ellison et al. 1999; Ellison 2001; Ricklefs et al. 2006).

Limited understanding of how fine-scale environmental variations and human pressures effect mangrove communities, has obstructed the success of mangrove conservation initiatives in many countries (Lewis 2005). Mangrove biodiversity research programs have mostly relied on the species richness index which does not account for between-species population variability. Robust abundance-based unified equations for biodiversity quantification could be a promising tool to capture local spatial variability in species diversity and composition in the tropical mangrove ecosystems.

1.5 Quantifying trait-environment relationships

A central challenge in plant ecology is to understand and predict the spatial and temporal changes in species composition and the associated changes in ecosystem function under varying biotic and abiotic conditions. While using species-centric approaches has been a common practice to handle this challenge, plant ecologists now consider trait-based approaches as the most appropriate choice (Diaz et al. 2007; Laughlin 2014; Chain-Guadarrama et al. 2017). Trait-based approaches are based on the idea that the fitness of plant species depends on how their traits respond to environmental drivers, thus facilitating more mechanistic prediction of species-, community- and ecosystem-level attributes (e.g. abundance, community composition, and biomass productivity etc.) under changing environmental conditions (Cadotte et al. 2011; Reich 2014). Plant functional traits are any measurable feature (morphological, physiological or anatomical) that influence a plant's performance (Violle et al. 2007). Thus, functional traits play important roles in determining: which plant species can grow and survive under what environmental conditions, to what extent they acquire resources and maintain primary growth, and how they interact with co-existing species (Westoby & Wright 2006). How these roles are mediated by dynamic environmental conditions in

natural forest ecosystems, collectively, influence the ecosystem processes, functioning and services (Hooper et al. 2005; Cadotte et al. 2011).

Disentangling the association between traits and environmental drivers i.e. "performance filter" (Webb et al. 2010) is the building block of trait-based ecology because predicting filtered trait distributions based on a projection of the performance filter across space and time can determine species abundance and community composition which in turn defines ecosystem functions and services under changing environment. However, linking traits to environmental variables and abundances has been a long-standing problem known as the fourth-corner problem in community ecology. Ecologists have proposed both multivariate (Dolédec et al. 1996; Legendre et al. 1997; Dray & Legendre 2008; ter Braak et al. 2012; Dray et al. 2014) and univariate (Pollock et al. 2012; Jamil et al. 2012; Jamil et al. 2013; Jamil et al. 2014; Brown et al. 2014) approaches to resolve the problem. Existing multivariate approaches (e.g. RLQ ordination, permutation tests etc.) offer a broad qualitative impression of trait-environment associations and help in selecting important traits and environmental variables in a trait-based study. However, these approaches have limited ability to quantify the strength of the associations between traits and environmental drivers. On the other hand, recent advancements in trait-based univariate (regression) approaches offer the flexibility of model selection, validation, and predictions. Although these approaches may potentially scale up individual traits to the community and ecosystem level processes (Funk et al. 2017), currently their usage is limited for single species and single traits.

Persistent environmental pressures may eliminate species over ecological time scales (species sorting) and modify trait values over evolutionary time scales (natural selection), resulting in altered species composition, relative abundance, and finally productivity in local communities (Verberk et al. 2013). Species sorting and natural selection do not act independently on a single trait, but rather, on species whose survival in a specific environment is controlled by multiple interacting traits. However, existing trait-based univariate approaches mostly deal with single species (Jamil et al. 2012) and have limited statistical ability to model multiple species, traits, and environmental variables simultaneously and to incorporate complex interactions between multiple traits of multiple competing

species under a dynamic environment. These shortcomings thus may yield excessively uncertain predictions when forecasting species, community and ecosystem responses under future environmental scenarios (Webb et al. 2010; Verberk et al. 2013; Violle et al. 2014).

Therefore, substantial methodological improvements are still required for linking the underlying concepts of trait-environmental relationships to quantitative approaches that will allow a predictive basis to community ecology and provide theoretical linkages between community ecology, ecosystem ecology, and functional biogeography. Webb et al. (2010) stated that traits-based ecology is now at a critical juncture where further advancements require an integrated quantitative approach that can analyse hierarchically structured trait data consistently to explain the dynamic nature of the trait–environment relationship and allow for robust spatial and temporal predictions of trait distributions with precise estimates of uncertainties. Verberk et al. (2013) consider that failure in detecting the response traits, in addressing the linkages and interactions among traits, and in differentiating which trait combinations maintain plants' growth and survival under stress, are the predominant constraints responsible for low discriminatory power and poor mechanistic understanding of current trait-based approaches. Funk et al. (2017) have identified three outstanding issues (i.e. selecting appropriate traits; unfolding intraspecific trait variation and integrating this variation into models; and scaling functional trait data to community- and ecosystem-level processes) that need to be resolved to advance traits-based ecology. To do so they and many others (Webb et al. 2010; Verberk et al. 2013) have suggested a need for new model development.

1.6 Study site: the Sundarbans

The Sundarbans is Earth's largest continuous mangrove forest covering 10,017 km^2 in Bangladesh and India. This forest is part of the Ganges-Brahmaputra delta which originated following the fragmentation of Gondwanaland in the early Cretaceous (Islam & Wahab 2005). The Bangladesh part of the Sundarbans (21°30′ — 22°30′N, 89° 00′ – 89°55′E) covers 6017 km^2. Of this 69% is forest land, and the rest encompasses rivers, small streams and canals. The forest is washed out by the tide twice a day and its hydrology depends on the fresh water discharge from the Ganges and the saltwater influx from the Bay of Bengal.

The Bangladesh Sundarbans supports the livelihood of 3.5 million coastal people (Islam et al. 2014), harbours breeding and nursing grounds for many marine organisms (Sandilyan & Kathiresan 2012), protects them from natural disasters (Danielsen et al. 2005), and houses the remaining habitats of many globally endangered plant and animal species (Siddiqi 2001). Because of these contributions, UNESCO declared the Bangladesh Sundarbans a World Heritage Site in 1997 (Gopal & Chauhan 2006). It was also declared a globally important RAMSAR wetland ecosystem under the Ramsar Convention in 1992 (Siddiqi 2001).

The Sundarbans has lost half of its original size within the last 150 years due to the conversion of mangrove habitats to agricultural land and human settlements (Siddiqi 2001). Historical forest exploitation, gradual reduction in freshwater flows (3700 m^3/s to 364 m^3/s) since the construction of the Farakka dam in India in 1974, salinity intrusion, oil spills, cyclones, water and soil pollution have severely degraded the Sundarbans ecosystem by depleting the populations of many threatened mangroves, including the globally endangered *Heritiera fomes* (Ellison et al. 2000). Some studies (Ellison et al. 2000; Iftekhar & Islam 2004; Iftekhar & Saenger 2008; Mukhopadhyay et al. 2015; Aziz & Paul 2015) have described the negative effects of these forces on Sundarbans' forest structure and functions.

Along with the historical and ongoing degradations, different aspects of climate change, particularly, sea level rise (SLR) (Karim & Mimura 2008) are likely to have a significant influence on the Sundarbans. However, spatially explicit baseline information on the remaining populations and spatial distributions, diversity, species composition, and functions of the mangroves are still lacking. This scarcity of information has been a major impediment to national and international conservation efforts in the Sundarbans (Islam et al. 2014; Aziz & Paul 2015).

1.7 Aims of the thesis

The overall aim of this thesis is to quantify the habitat preferences of threatened mangroves in the Sundarbans world heritage ecosystem, to explore spatial and temporal dynamics and the key drivers of mangrove biodiversity, and to develop an integrated approach for predicting functional trait responses of plants under current and future environmental scenarios. The thesis comprises four data chapters (Chapters 2 – 5).

Chapter 2 determines habitat preferences and develops spatial density maps of the four most dominant mangrove tree species (i.e. *Heritiera fomes, Excoecaria agallocha, Ceriops decandra* and *Xylocarpus mekongensis*).

Chapter 3 determines the spatial heterogeneity in alpha, beta, and gamma diversity at four historical time points (1986, 1994, 1999 and 2014) to uncover the temporal dynamics in species composition in the established ecological zones (hypo-, meso-, and hypersaline) in the Sundarbans. Specific questions that I ask here include: Which ecological (i.e. salinity) zone supports the most/least diverse mangrove communities? Is the most diverse ecological zone also the most heterogeneous (i.e. variable between plots) in species composition? How has compositional heterogeneity in the broader ecological zones developed over the 28 years? How has the geographic range and density of mangroves changed since 1986? I also develop spatial biodiversity maps to answer the following questions: Where are the historical and contemporary biodiversity hotspots located? Which habitats have changed most in species composition over time?

Chapter 4 uncovers the influences of fine-scale habitat conditions and historical events in shaping the spatial distributions of mangrove alpha, beta and gamma diversity. My more specific questions include: What are the key drivers of mangrove biodiversity? How do the predictive abilities of environmental data-driven biodiversity models compare with those of covariate-free direct interpolation approaches? Where are the biodiversity hotspots in the Sundarbans currently located? Are these hotspots well protected?

Chapter 5 proposes a Bayesian hierarchical modelling approach to quantify trait-environment relationships for multiple traits, species, and environmental drivers simultaneously, while accounting for trade-offs between different traits. I then apply this integrated approach on field data comprising nine prominent tree species, eight important environmental drivers, and four key plant morphological traits (canopy height, specific leaf area, wood density, and leaf succulence) and ask: (1) Which set of theoretical hypotheses, is best supported by the data? (2) How do the different traits of each species respond to the array of environmental drivers? (3) Is there covariation between the responses of functional traits? Using the model-based predictions, I then develop trait and productivity maps under present and future environmental scenarios.

Finally, Chapter 6 provides a broader discussion of previous chapters' results and proposals for future improvements.

Chapter 2 . The spatial distribution and habitat preferences of threatened mangroves in the Sundarbans: Implications for conservation

Note: This chapter has been published in 'Scientific Reports' (Appendix 1)

2.1 Abstract

The Sundarbans world heritage ecosystem is under threat from historical and future human exploitation and sea level rise. Limited scientific knowledge on the spatial distributions of the threatened tree species and their habitat requirements has obstructed conservation efforts in this global priority ecosystem. Using tree counts and environmental data collected from 110 permanent sample plots (PSPs), in this chapter, I developed habitat suitability models (HSMs) and species density maps for the four most dominant mangrove species: *Heritiera fomes*, *Excoecaria agallocha*, *Ceriops decandra* and *Xylocarpus mekongensis*. Generalized additive models of mangrove abundance data revealed steep responses to salinity gradients. Globally endangered *H. fomes* abundance declined as soil salinity increased. Responses to nutrients, elevation and stem density varied between species. *X. mekongensis* preferred upstream habitats while the rest preferred downstream and intermediate-stream areas. Historical harvesting had negative influences on all species, except *E. agallocha*. The most suitable habitats of the threatened species currently occur outside the existing protected area network (PAN). This study, therefore, recommends a reconfiguration of the existing PAN to include these suitable habitats and ensure their immediate protection. Finally, I discuss how the habitat insights and spatial predictions generated by my models can guide future forest studies and spatial conservation planning.

2.2 Introduction

The mangrove biome (137,760 km^2 in 118 countries) is under severe threat. We have lost nearly 50% of the biome since the 1950s due to deforestation, habitat degradation and coastal development (Feller et al. 2010). If the current trend of human exploitation and habitat degradation continues, the whole mangrove biome may vanish in the next 100 years (Duke et al. 2007). About 16% of the total mangrove plant species (~ 70) are at elevated risk of extinction and 10% are near-

threatened (Polidoro et al. 2010). However, we have limited knowledge about the habitat preferences and current spatial distributions of these threatened plants in many stressed coastal regions in the tropics, particularly, the Sundarbans, which is a UNESCO World Heritage Site and a RAMSAR wetland ecosystem of global importance (Siddiqi 2001).

The Sundarbans contains one third of the global mangrove plant species (Ghosh et al. 2016) and acts as a repository of numerous globally endangered flora and fauna (Iftekhar & Islam 2004). However, natural (e.g. tropical cyclones, tsunamis) and anthropogenic (e.g. tree harvesting, aquaculture, oil spills) pressures (Ellison et al. 2000; Aziz & Paul 2015) have heavily degraded the Sundarbans ecosystem, resulting in local extinction of at least three mangrove plant species of the *Bruguiera* genus and six mammal species including Javanese rhinoceros (*Rhinoceros sondiacus*) and wild buffalo (*Bulbulus bulbalis*) in the last two centuries (Iftekhar & Islam 2004). The population of *Heritiera fomes*, a globally endangered tree species, has declined by 76% since the 1950s. Nearly 70% of the *H. fomes* trees are currently affected by the 'top dying' disease (Chowdhury et al. 2008). Declines in other major mangrove tree species (e.g. *Excoecaria agallocha* and *Xylocarpus mekongensis*) have also been reported (Iftekhar & Saenger 2008). We also know little about the current spatial distributions of *Ceriops decandra*, a globally near-threatened species (Siddiqi 2001).

In the Sundarbans, the freshwater river flows help to modulate salt-water toxicity and keep the ecosystem suitable for mangrove trees. However, since the construction of the Farakka dam (in 1974) in the Ganges upstream, the freshwater supply into the Sundarbans has reduced by 65% (Iftekhar & Islam 2004), resulting in increased salinity levels, reduced nutrient status, and overall degradation of the entire ecosystem (Mukhopadhyay et al. 2015). The rate of sea level rise (SLR) along the Bangladesh coast was substantially higher than the global average in the last century (Karim & Mimura 2008). Future SLR is likely to alter the habitat conditions, regional hydrology, vegetation structure and functions in the Sundarbans (Ghosh et al. 2016). Therefore, ongoing habitat degradation and future SLR together may alter the current spatial distributions of these mangrove species and forest community composition.

Determining the drivers and spatial distributions of threatened species is vital for their management and conservation. However, lack of such knowledge has obstructed the success of conservation initiatives in many countries (Lewis 2005), including Bangladesh (Islam et al. 2014). Only recently have coastal mangrove distributions been modelled at global (Record et al. 2013) and regional (Crase et al. 2015) scales and we are now in urgent need of Habitat Suitability Models (HSMs), based on fine-scale species abundance and environmental data to assist us in protecting threatened ecosystems such as the Sundarbans. HSMs and their outputs (i.e. habitat maps) are widely used during different phases of resource management and spatial conservation planning (Guisan & Thuiller 2005). These maps are also used to identify areas appropriate for establishing protected areas, evaluate threats to those areas, and design reserves (Guisan et al. 2013). For example, a baseline distribution map of the mangrove species could be an important tool for the forest managers to make decisions on future mangrove planting and forest protection via tracking population changes over time.

In this chapter, I used tree counts and environmental data collected from a network of 110 permanent sample plots (PSPs) in the Sundarbans to generate spatially explicit baseline information on the distribution and habitat preferences of the four most abundant mangrove species: *H. fomes*, *E. agallocha*, *C. decandra* and *X. mekongensis*. I identified the key environmental variables related to their spatial distribution and generated species-specific spatial density maps using both geostatistical and regression approaches. I then demonstrated the potential applications of these habitat insights and spatial maps for future forest studies, spatial conservation planning, biodiversity protection and monitoring programs.

2.3 Methods

2.3.1 Study system

The Bangladesh Sundarbans (21°30′ − 22°30′N, 89° 00′ – 89°55′E) is part of the Earth's largest river delta at the Ganges-Brahmaputra estuary (Fig. 2.1). Geologically, the Sundarbans is of recent origin (about 7000 years old) and was formed through the silt deposition by the Ganges-Brahmaputra river system (Iftekhar & Islam 2004). The soil is finely textured, poorly drained and rich in alkali metal contents (Siddiqi 2001). Of its total area (6017km^2), about 69% is land and

the rest comprises rivers, small streams and canals (Wahid et al. 2007). Most parts of the forest are inundated twice a day. The water level is associated with the joint effects of the seawater tides and freshwater input from the Ganges. Freshwater flow increases during the monsoon (June–September) and sharply drops during the dry season (October to May) due to reduced water influx from the Ganges. The climate is humid and tropical. Average annual precipitation is 1700 mm. Average maximum annual temperature is between 29.4° and 31.3°C (Gopal & Chauhan 2006).

2.3.2 Tree surveys

To monitor biodiversity and forest stock the Bangladesh Forest Department (BFD) established a network of 120 PSPs in the Sundarbans in 1986 (Fig. 2.1). Each PSP is 0.2 ha in size (100 x 20 m) and divided into 5 20 x 20 m subplots. Of these, 110 PSPs were positioned to represent the ecological zones (i.e. hyposaline, mesosaline and hypersaline) and the forest types (Iftekhar & Saenger 2008). The remaining 10 relatively smaller sized PSPs (20 x 10 m) were established to monitor forest regeneration, and were not considered in this thesis. As part of the 2008 – 2014 forest inventories, my fieldwork team, together with the BFD tagged every tree with stem diameter ≥ 4.6 cm (because mangroves grow very slowly and this threshold value has been used in all previous forest inventories in the Sundarbans since the early 1900's (Iftekhar & Saenger 2008)), recorded at 1.3 m from the ground with a unique tree number and recorded tree counts for each of the 110 PSPs.
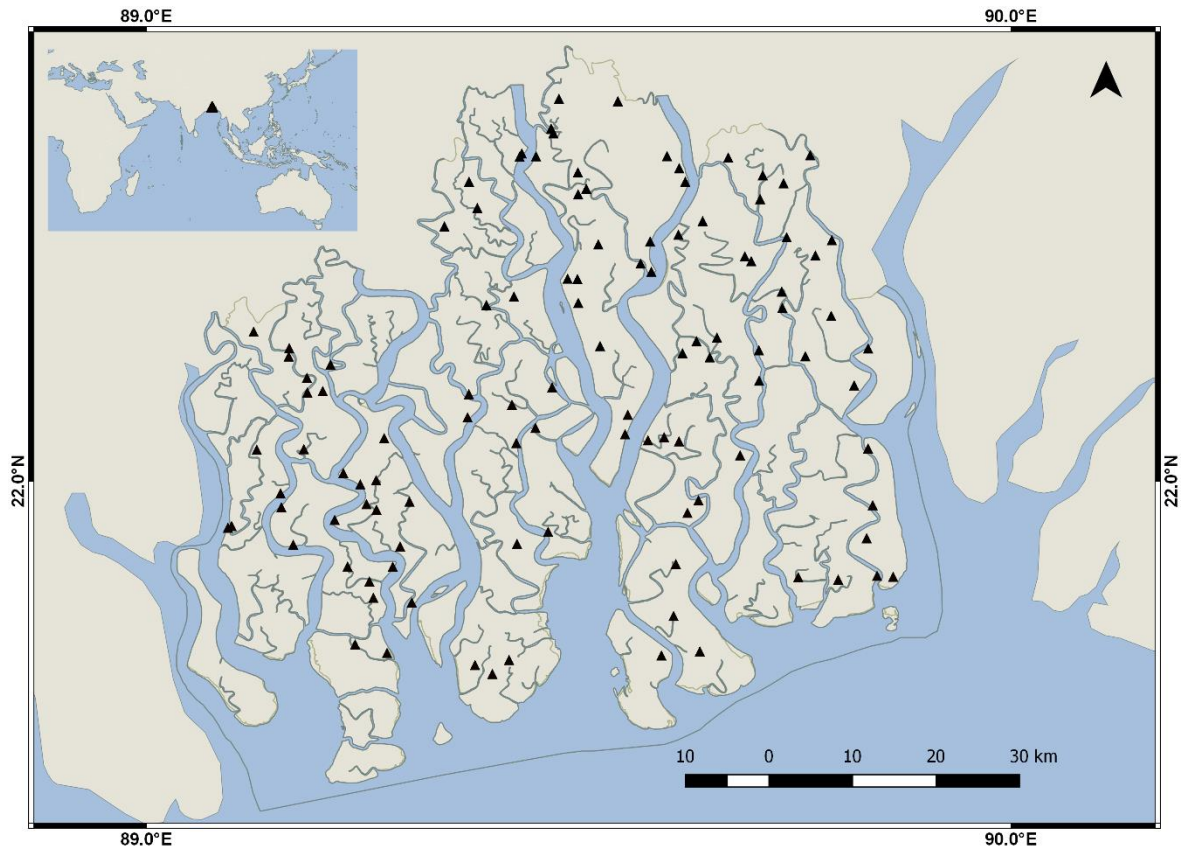
Fig. 2.1 Sampling sites (triangles) in the Sundarbans, Bangladesh. The thin grey lines represent the canals.

2.3.3 Environmental data

Environmental data were collected from all 110 PSPs during January − June 2014. I adopted a soil sampling design (Fig. 2.2), collected 9 soil samples from each PSP (to a depth of 15 cm) to account for the within-plot variation in soil parameters. For soil texture analysis (percentage of sand, slit and clay), I used the hydrometer method (Gee & Bauder 1986). I determined soil salinity (as electrical conductivity − EC) in a 1:5 distilled water:soil dilution (Hardie & Doyle 2012) using a soil conductivity meter − Extech 341350A-P Oyster. I took field measurements for soil pH and oxidation reduction potential (ORP) using digital soil pH and ORP (Extech RE300 ExStik) meters. Soil NH_4 concentration was measured following the Kjeldahl method (Bremner & Breitenbeck 1983).
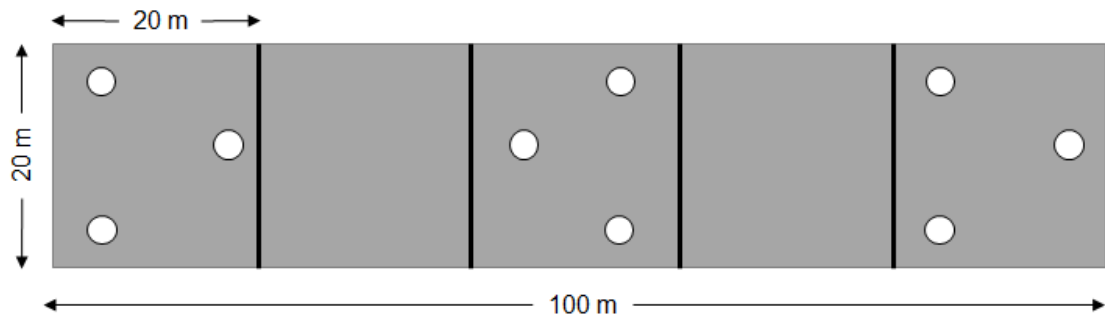
Fig. 2.2 Soil sampling design. Total 9 soil samples (circles, 0 – 30 cm depth) were (3 samples/subplot) collected in the ends and middle of the 20 x 20 subplots in each PSP.

I measured total phosphorus (P) using the molybdovanadate method and a 721-spectrophotometer. Soil potassium (K), magnesium (Mg), iron (Fe), zinc (Zn), copper (Cu), and sulphide concentrations were measured using an atomic absorption spectrophotometer (AA-7000) at the soil chemistry laboratory of the Civil and Environmental Engineering Department in the Shahjalal University of Science and Technology, Bangladesh. I analysed each of the nine soil samples first and then averaged the results. Five elevation (above-average sea level) readings for each PSP were randomly extracted from the digital elevation model with accuracy (i.e. accuracy at pixel level) ±1 m for the Sundarbans region (IWM 2003). Then I averaged these readings to reduce the error associated with the digital elevation model. A proportional distance from the river-sea interface, measured using the map of the Sundarbans, was used to calculate and classify "upriver position" (henceforth, URP) of each PSP (Norman C. Duke et al. 1998). Here 'downstream' represents the lower third (0 – 33% upriver from the sea) of the estuarine system, 'intermediate' represents the middle third (34 – 66% upriver from the sea), and 'upstream' represents the upper third (67 – 100% upriver from the sea). This scheme is useful for understanding how individual mangrove's habitat preference vary along the downstream– upstream gradient.

2.3.4 Covariate selection

To develop a biologically informative covariate set for my HSMs, I followed Twilley & Rivera-Monroy's (2005) conceptual framework. This framework comprises three broad categories of variables (i.e. resources, regulators and hydroperiod) that are

believed to control mangrove forest structure and function (Krauss et al. 2008; Reef et al. 2010; Crase et al. 2013). Resources (i.e. nutrients) are used by plants and their availability is related to tree productivity. Here, I selected soil NH_4, P, K, Mg, Fe and Zn based upon the detailed explanation of nutrient requirements of mangrove plants available in the mangrove literature (Reef et al. 2010). Regulators are non-resource variables that influence the growth and establishment of mangroves. I employed soil salinity as the main regulator. Hydroperiod (the duration, frequency and depth of inundation) is recognized as an important determinant of mangrove distribution (Crase et al. 2013). PSP level hydroperiod data are not available for the Sundarbans, so I selected elevation as a proxy that reflects the possible variation in hydroperiod across the Sundarbans. I also selected URP of each PSP as a covariate to account for the effects of the river systems on mangrove distributions along the downstream-upstream gradient.

The relative abundance of a mangrove species may influence the abundance of another through biotic interactions i.e. competition or facilitation (Wisz et al. 2013). In fact, each tree interacts with the trees that are in its neighbourhood through multiple concurrent interactions (Le Roux et al. 2013). Given the super-dominance of *E. agallocha* and *H. fomes* (see section 2.3.2) and tree structural complexities (i.e. multiple stems in *C. decandra*) which might have increased tree measurement (i.e. diameter) errors, I initially considered two alternative measures of abundance: (1) density of all stems for each plot, and (2) total basal area for each plot as biotic variables. HSMs of species with basal area as a covariate had lower explanatory and predictive powers, compared to models with density of all stems. Therefore, I selected density of all stems for each plot (hereafter, DAS) as a simple proxy for biotic interaction.

The Sundarbans has a long exploitation history (Siddiqi 2001). Illegal tree harvesting is also common (Iftekhar & Islam 2004). Hence, I incorporated historical harvesting (henceforth, HH) as a covariate in my HSMs due to its potential influence on present tree densities in the PSPs. HH denotes the number of cut trees (detected by counting stumps) in each PSP from the first census (1986) to the last census (2014).

I checked for multi-collinearity in my set of candidate covariates using the *vifstep* function of 'usdm' package (Naimi 2015) in R 3.2.2 (R Core Team 2016), which

first calculates Variance Inflation Factors (VIF) for all predictor variables, then removes the one with highest VIF that exceeds the threshold of 2.5 and repeats the procedure until no variable with VIF > 2.5 remains. This led to the exclusion of Zn from my covariate set (Appendix 2A).

2.3.5 Habitat suitability analyses

I used generalized additive models (GAMs) (Wood 2006) with a Poisson likelihood and a log-link for their ability to handle complex, non-monotonic relationships between the response and the predictor variables (Guisan et al. 2002). Moreover, by using non-parametric smoothing functions, GAMs can often construct biologically insightful relationships between response and covariates without a-priori hypotheses (Guisan & Thuiller 2005). Smoothed responses used cubic basis splines executed within the 'mgcv' package (Wood 2011) in R.

Using the 'dredge' function in the 'MuMIn' package (Barton 2015), I fitted candidate models with all possible combinations of covariates and ranked them using the Akaike Information Criterion (AIC) (Burnham & Anderson 2002). I then obtained the relative support for each model by calculating the ΔAIC (the difference between the best model's AIC value and the AIC value for each of the other models). Kullback–Leibler information loss is minimal between models with ΔAIC ≤ 2 (Burnham & Anderson 2002). So, I used the 'ΔAIC ≤ 2' criterion to select my confidence set of models for each mangrove species. I then calculated Akaike weights (AICw) to inspect relative support for each model in the confidence set. AICw values range from 0 to 1 and the sum of all AICw across the confidence set is 1. When there was only one model with ΔAIC ≤ 2, it was unambiguous that it outperformed all possible candidate models. When there were multiple competing models, I used AIC-weighted model averaging to reduce model selection uncertainty and bias. I determined Relative Importance (RI) of each covariate by summing the AICw of the models in which the covariate was retained. RI values range between 0 and 1, where 0 indicates that the target covariate is never included in the competing models, 1 indicates inclusion of the covariate in all the competing models. I ranked the covariates based on their RI values. Residual diagnostic plots for the best GAMs did not show violations of the Poisson dispersion assumption.

Goodness-of-fit of the models was measured using the R^2 (coefficient of determination) statistic between the observed and estimated abundance values. For validation purposes, I partitioned my dataset into a calibration (88 PSPs, 80% of the full data) and validation (22 PSPs, 20% of the full data) subsets. The validation dataset was randomly chosen to cover the whole Sundarbans and was employed to assess the predictive power of the fitted models via the R^2 statistic applied to the model's predictions for the validation data. I also mapped the actual and predicted abundances of both calibration and validation set to check for any spatial patterns of prediction errors.

2.3.6 Spatial mapping

I mapped mangrove species densities over the entire Sundarbans using two different approaches: (1) direct interpolation of plot-level raw abundance using geostatistical methods, and (2) habitat-based predictions from my HSMs. Environmental data collection is demanding, whereas tree abundance measurements are taken regularly at the PSPs. Therefore, it is useful to know how close the predictions of the habitat models were compared to simple interpolation methods. To directly interpolate individual mangrove species abundances, I used ordinary kriging (OK), a widely-used interpolation technique. Selecting an appropriate variogram model is a prerequisite for kriging success. I fitted three different variogram models to each mangrove: Spherical, Exponential and Gaussian, and selected the model with least sum of squared errors. The spherical model offered best fit for *H. fomes*, the exponential model provided best fit for *E. agallocha* and *C. decandra*, and the Gaussian model for *X. mekongensis* (see Appendix 2B for the semivariograms of the species).

For producing covariate surfaces, I fitted Spherical, Exponential and Gaussian variogram models to each covariate, and selected the model with least sum of squared errors (see Appendix 2C for the semivariograms of the covariates). I then used these covariate surfaces (Appendix 2D) to generate model-averaged predictions of species density over the entire Sundarbans.

Each grid-cell of the interpolated surface was 625 m^2 (25m x 25m). The covariate surfaces were constructed by OK using the 'gstat' package (Pebesma 2004) in R. A protected area network (PAN) comprising three Wildlife Sanctuaries (WS) – East WS, West WS, and South WS has been operational since the 1970s. I superimposed

the PAN on my species density maps for evaluating its spatial extent to cover the current density hotspots of the threatened tree species. I also compared the predictive abilities of the direct and habitat-based approaches. Here, I used the normalized root mean square error (NRMSE) statistic derived from the leave-one-out cross-validation procedure. For normalization, the root mean square error statistic was divided by the range of the actual species abundances. Both habitat-based and direct predictions of the mangrove tree abundances were mapped using the 'raster' package (Hijmans 2015) in R. I further mapped the prediction discrepancy between these two approaches, to look for any spatial patterning in the prediction errors.

2.4 Results

2.4.1 Tree surveys

A single survey of each of the 110 PSP's carried out between 2008 − 2014 gave a total of 49409 trees of 20 species from 13 families and 18 genera (Table 2.1). The most abundant mangrove tree species was *E. agallocha* (59.69% of total trees), followed by *H. fomes* (30.89%), *C. decandra* (6.12%) and *X. mekongensis* (0.82%). The remaining 16 species were extremely rare comprising only 2.49% of the total count.

Table 2.1 Taxonomy and global conservation status of the mangrove species surveyed in the 110 permanent sample plots (PSPs) in the Bangladesh Sundarbans. *IUCN global population trend, [†] Not assessed for the IUCN Red List, LC = Least concern, DD = Data deficient, NT = Near threatened, VU= Vulnerable, EN = Endangered, D = Decreasing.

Latin name	Family	IUCN conservation status	Global population trend[*]
Aegiceras corniculatum	Myrsinaceae	LC	D
Amoora cucullata	Meliaceae	NA[†]	NA
Avicennia officinalis	Avicenniaceae	LC	D
Bruguiera sexangula	Rhizophoraceae	LC	D
Cerbera manghas	Apocynaceae	NA	NA
Ceriops decandra	Rhizophoraceae	NT	D
Cynometra ramiflora	Fabaceae	NA	NA
Excoecaria agallocha	Euphorbiaceae	LC	D
Excoecaria indica	Euphorbiaceae	DD	D
Heritiera fomes	Malvaceae	EN	D
Intsia bijuga	Leguminosae	VU	D
Lumnitzera racemosa	Combretaceae	LC	D
Hypobathrum racemosum	Rubiaceae	NA	NA
Pongamia pinnata	Leguminosae	LC	Stable
Rhizophora mucronata	Rhizophoraceae	LC	D
Sonneratia apetala	Lythraceae	LC	D
Talipariti tiliaceum	Malvaceae	NA	NA
Tamarix dioica	Tamaricaceae	NA	NA
Xylocarpus granatum	Meliaceae	LC	D
Xylocarpus mekongensis	Meliaceae	LC	D

2.4.2 Habitat models

The best GAMs for estimating species abundances explained the variability of *H. fomes* (68%), *E. agallocha* (84%), *C. decandra* (73%) and *X. mekongensis* (75%) (Table 2.2). Salinity, K, DAS (total density of individuals), URP (upriver position) and HH (historical harvesting) were included in the best GAMs of all mangrove species. Mg and Fe were included (RI = 1.00) in the best GAMs for *H. fomes*, *E. agallocha* and *X. mekongensis*, with P (RI = 1.00) for *H. fomes*, *E. agallocha*, and *C. decandra*, and also elevation (RI = 1.00) for *H. fomes* and *X. mekongensis*. The partial response plots of the best GAM (Fig. 2.3) indicated that *H. fomes* abundance decreased with increasing soil salinity (> 7 dS m^{-1}). In contrast, increasing salinity was associated with increasing abundances of *E. agallocha* (> 7 dS m^{-1}), *C. decandra* (> 6.2 dS m^{-1}), and *X. mekongensis* (> 7 dS m^{-1}).

Responses to nutrients varied between species. The high abundance of *H. fomes* was associated with low chemical concentrations of P (< 30 mg Kg^{-1}), K (< 6 gm Kg^{-1}), Mg (< 2.75 gm Kg^{-1}) and Fe (< 30 gm Kg^{-1}) in the soil. In contrast, the high abundance of *E. agallocha* was associated with relatively high concentrations of P (> 30 mg Kg^{-1}), K (> 6 gm Kg^{-1}), Mg (> 2.75 gm Kg^{-1}) and Fe (> 30 gm Kg^{-1}), and low concentrations of NH$_4$ (< 0.70 gm Kg^{-1}). High *C. decandra* abundance was related to high K (> 5 gm Kg^{-1}) and low NH$_4$ (< 0.70 gm Kg^{-1}) and P (< 30 mg Kg^{-1}) concentrations. High *X. mekongensis* abundance was related to low K (< 5 gm Kg^{-1}) and Mg (< 1.60 gm Kg^{-1}). *H. fomes* and *X. mekongensis* preferred elevated sites. *H. fomes* abundance showed a declining trend after a certain value of DAS (> 500 trees/0.2 ha). In turn, *E. agallocha*, *C. decandra* and *X. mekongensis* displayed positive responses to increasing DAS. The abundances of *E. agallocha* (URP > 65%) and *C. decandra* (URP > 50%) sharply decreased with increasing URP, indicating their high preference for down- and mid-stream habitats. In contrast, *H. fomes* and *X. mekongensis* abundances increased with increasing URP (> 50%, indicating their preference for upstream habitats). High HH was related to low abundances of *H. fomes*, *C. decandra* and *X. mekongensis*. In contrast, *E. agallocha* had high abundance in the sites that experienced high HH.

Table 2.2 Results of generalized additive models (GAMs) built for the four major mangrove species of the Bangladesh Sundarbans. DE = deviance explained, RI = relative variable importance in the model selection process. Covariates: soil salinity, elevation above average-sea level (ELE), soil NH_4, total phosphorus (P), potassium (K), magnesium (Mg), iron (Fe), upriver position (URP), density of all stems for each plot (DAS) and historical harvesting (HH).

Species	Model rank	Salinity	ELE	NH₄	P	K	Mg	Fe	URP	DAS	HH	ΔAIC	ΔAICw	Adj-R²	DE (%)
H. fomes	1	+	+	−	+	+	+	+	+	+	+	0.00	0.99	0.67	68
	RI	1.0	1.0	0.0	1.0	1.0	1.0	1.0	1.0	1.0	1.0				
E. agallocha	1	+	−	+	+	+	+	+	+	+	+	0.00	0.66	0.83	84
	2	+	+	−	+	+	+	+	+	+	+	1.39	0.33		
	RI	1.0	0.67	0.67	1.0	1.0	1.0	1.0	1.0	1.0	1.0				
C. decandra	1	+	−	+	+	+	−	−	+	+	+	0.00	0.46	0.65	73
	2	−	+	+	+	+	−	−	+	+	+	0.53	0.35		
	3	+	+	+	+	+	−	−	+	+	+	1.84	0.18		
	RI	0.65	0.65	1.0	1.0	1.0	0.0	0.0	1.0	1.0	1.0				
X. mekongensis	1	+	+	−	−	+	+	−	+	+	+	0.00	0.75	0.84	75
	RI	1.0	1.0	0.0	0.0	1.0	1.0	0.0	1.0	1.0	1.0				

Fig. 2.3 Effects of covariates inferred from the best GAMs fitted to the abundances of the four prominent mangrove species in the Sundarbans. The solid line in each plot is the estimated spline function (on the scale of the linear predictor) and shaded areas represent the 95% confidence intervals. Estimated degrees of freedom are provided for each smoother following the covariate names. Zero on the y-axis indicates no effect of the covariate on mangrove abundances (given

that the other covariates are included in the model). Covariate units: soil salinity = dS m^{-1}, elevation = m (above average-sea), NH_4 = gm Kg^{-1}, P = mg Kg^{-1}, K = gm Kg^{-1}), Mg = gm Kg^{-1}, Fe = gm Kg^{-1}, URP = % upriver, DAS = density of all stems for each plot, and historical harvesting (HH) = total number of harvested trees in each plot since 1986.

The predictive abilities of the GAMs were R^2 = 0.75 for *H. fomes*, R^2 = 0.78 for *E. agallocha*, and R^2 = 0.51 for *C. decandra*. The predictive ability of the GAMs for *X. mekongensis* was somewhat lower (R^2 = 0.24) than the other species (possibly due to its high densities in the northern upstream areas and sporadic occurences in the remaining Sundarbans). When GAMs were used to estimate mangrove abundances for all 110 PSPs, a strong association (*H. fomes*, R^2 = 0.67; *E. agallocha*, R^2 = 0.83; *C. decandra*, R^2 = 0.65; *X. mekongensis*, R^2 = 0.84) was found between the actual and estimated abundances. Spatial maps of the actual and estimated abundances of the mangroves (both calibration and validation datasets) looked similar and the residuals did not show spatial clustering (Appendices 2E & 2F).

2.4.3 Mangrove distribution maps

Spatial density maps of the species produced through GAMs and direct interpolation (kriging raw abundances) are presented in Figs. 2.4 and 2.5. The *E. agallocha* GAM had better predictive ability than ordinary kriging (OK) (Table 2.3). For *H. fomes* and *X. mekongensis*, both approaches had almost identical predictive performances. Figure 2.6 represents the habitat mapping uncertainties related to these methods.
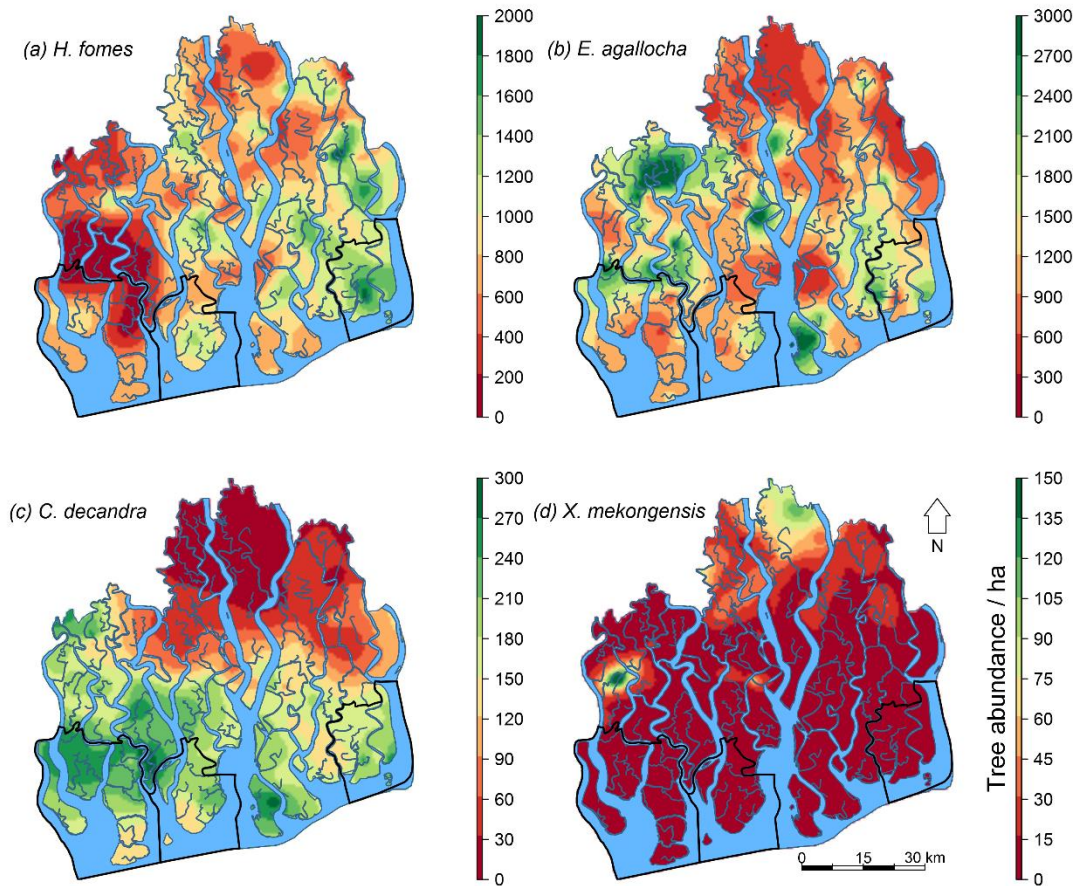
Fig. 2.4 Spatial density ha⁻¹ of the mangrove species in the Sundarbans based on habitat-based models (GAMs). Areas inside the bold black lines represent the three protected areas.

Overall, my species density maps reveal that the *H. fomes* density hotspots were restricted to the eastern Sundarbans. *E. agallocha* density was highest in the north-western region. *C. decandra* density was highest in the western and southern regions and *X. mekongensis* density was highest in a few specific areas in the northern (Kalabogi and Koyra) and north-western (Koikhali) regions. All the three protected areas (i.e. East WS, West WS and South WS) that are distributed in the downstream areas (Figs. 2.4 & 2.5) do not include the density hotspots for any of the species.
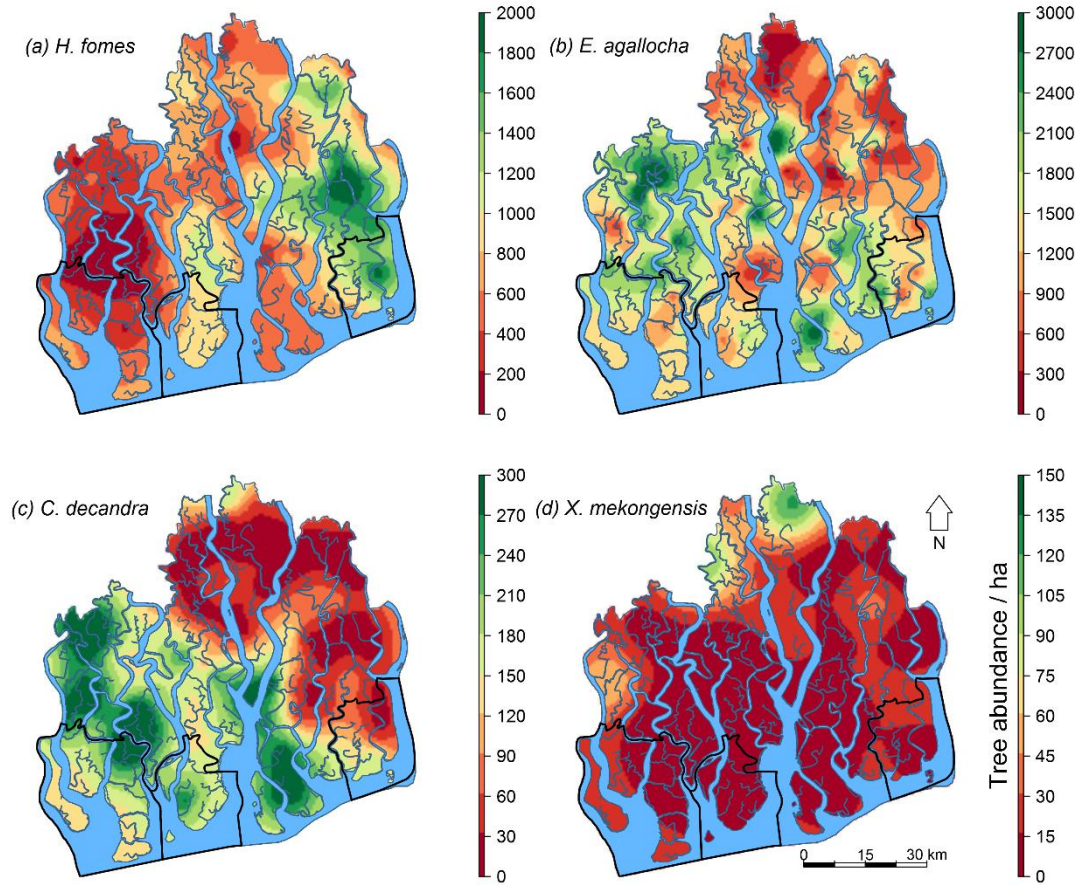
Fig. 2.5 Spatial density ha^{-1} of the mangrove species in the Sundarbans based on geostatistical technique (OK). Areas inside the bold black lines represent the three protected areas.

Table 2.3 Comparison of predictive accuracy (through leave-one-out cross validation) between the habit-based models (GAMs) and ordinary kriging (OK) based on the normalized root mean square error (NRMSE) of the predicted species abundances versus the actual abundances. NRMSE is expressed here as a percentage, where lower values indicate less residual variance.

	GAMs	OK
	NRMSE (%)	
H. fomes	20	20
E. agallocha	14	23
C. decandra	26	21
X. mekongensis	15	16
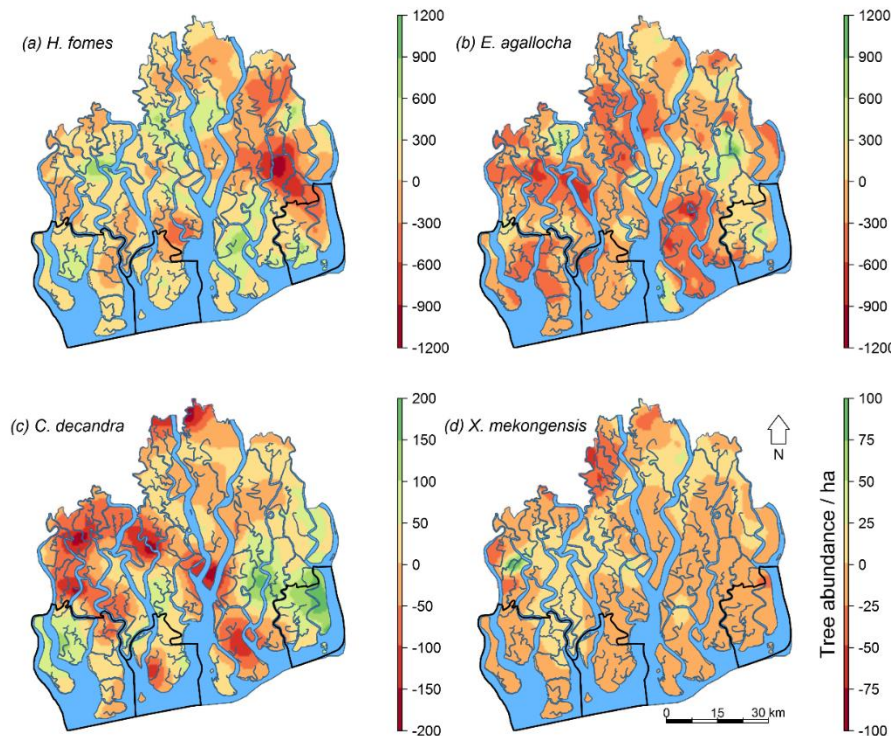
Fig. 2.6 Spatial distributions of the predicted abundance differences between the GAMs and ordinary kriging for the four species.

2.5 Discussion

This study is the first to quantify mangrove habitat preferences and to identify the key drivers regulating mangroves spatial distributions in the Sundarbans. The high explanatory and predictive power of the HSMs confirm their usefulness for making regional habitat maps.

2.5.1 Habitat models

High salinity stress can impede mangrove growth and development (Nandy et al. 2007) and affect structural development of mangrove forests (Washington et al. 2001). My results showed that the response of the mangrove species varied steeply along the salinity gradient in the Sundarbans (Fig. 2.3). *H. fomes* showed a strong negative response while the remaining mangrove species showed a strong positive response to increasing soil salinity. Although mangrove plants are not salt lovers, they manage to tolerate salt stress via elaborate adaptations (i.e. anatomical, physiological, and morphological) (Vovides et al. 2014). However, extreme salt stress impedes growth and development via toxicity, altered osmolarity and reduced photosynthesis of many mangroves (Nandy et al. 2007). When mangroves experience salt stress, depletion of leaf protein is necessary to modulate the salt stress (Parida & Das 2005). This protein depletion mechanism facilitates the synthesis of new stress-related proteins for keeping appropriate water potential to modulate the salt stress. The protein depletion rate is much lower in *H. fomes* than *E. agallocha* and *C. decandra* (Dasgupta et al. 2012) which goes some way towards explaining their dissimilar responses to salt concentration. Low photosynthesis rate, the presence of high stomatal density (indicates uncontrolled transpiration), a thin cuticle and near-absence of water storage tissues (indicates inefficient water storage and use) in the leaves (see Das 1999) further suggest that highly saline habitats are unsuitable for *H. fomes*. The positive response of *E. agallocha* to increased salinity may be due to its high protein depletion rate (Dasgupta et al. 2012), optimal photosynthesis under salt stress and salt accumulation ability in leaves (Nandy et al. 2009). Additionally, this positive response may also be the result of *E. agallocha*'s release from competition with the less salt-tolerant *H. fomes*. Chen & Ye's (2014) finding that the salt tolerance ability of *E. agallocha* increases with its age provides further supports for such results. The positive response of *C. decandra* to increased salinity may be due to

its high protein depletion rate and salt exclusion ability of roots. *C. decandra* is a 'disturbance specialist' for its superior ability to invade highly saline and degraded (polluted, silted, and eroded) habitats (Harun-or-Rashid et al. 2009). *X. mekongensis* responded positively to increased salinity. This finding is in agreement with Hossain et al. (2014) reporting high germination and seedling growth in *X. mekongensis* under extremely saline conditions.

My results reveal that the magnitude of response to nutrients varied between species. NH_4 and P were found to be the key limiting factors for forest productivity in many tropical ecosystems (Baribault et al. 2012). In the Sundarbans, *E. agallocha* and *C. decandra* could grow abundantly in the NH_4-poor habitats. *E. agallocha* prefers relatively P-rich habitats (> 30 mg Kg^{-1}) while *H. fomes* grows abundantly in the P limited sites (< 30 mg Kg^{-1}). Soil K helps to modulate salinity-induced drought stress in plants by enhancing the water uptake and retention capacity of plants (Sardans & Peñuelas 2015). Relatively greater densities of *E. agallocha* and *C. decandra* in the hypersaline and relatively K-rich habitats (i.e. north-western and southern Sundarbans) imply that these species might have developed strategies for efficient utilization of K in salinity stressed habitats. Fe and Mg play important roles in metabolic and physiological processes in plants (Alongi 2010). *E. agallocha* prefers Fe-rich habitats, whilst *H. fomes* prefers Fe-poor habitats. The Mg preference range of *E. agallocha* (> 2.75 gm Kg^{-1}) is somewhat higher than that of *H. fomes* (< 2.75 gm Kg^{-1}) and *X. mekongensis* (< 1.60 gm Kg^{-1}). This difference may be associated with the mechanisms (e.g. chemical composition of the source rock material, the weathering process etc.) that regulate the availability of Mg to plants (Gransee & Führs 2013). I acknowledge that fitted response curves for each mangrove species only reveals how its abundances are related to multiple covariates within their observed habitat conditions. Since these covariates include proxies for biotic interactions, these curves do not necessarily reveal the physiological limits (i.e. the fundamental niche) of the mangroves.

Although the Sundarbans is a deltaic swamp with a narrow elevation gradient (0.50 m – 4.0 m above mean sea level), it is characterized by diverse elevation values. The western zone is more elevated than the eastern zone because of tectonic activity and higher sediment deposition (Iftekhar & Islam 2004). This disparity may

be responsible for variable inundation levels in different parts of the ecosystem with subsequent changes in soil salinity and nutrients, and may ultimately have forced the mangrove trees to be distributed in distinct zones (Bunt 1996). Ellison et al. (2000) tested this hypothesis using randomization tests and data from 11 sampling stations in the Sundarbans, and concluded that the mangrove trees in the Sundarbans do not show any distinct patterns (i.e. absence of zonation) along the elevation gradient. In contrast, my results show that *H. fomes* (> 2.00 m) and *X. mekongensis* (> 2.75 m) display a clear preference for elevated sites (Fig. 2.3). I could reveal these patterns because of my larger sample size of 110 PSPs distributed over the entire region, and my multivariate and nonlinear modelling methodology.

The inclusion of DAS in the best GAMs with maximum RI (1) scores indicates the importance of adding biotic variables in HSMs. *H. fomes* abundance tends to drop when the DAS value is > 500 trees/0.2 ha, indicating the super dominance of generalists such as *E. agallocha* (shows a positive linear response to DAS). Ellison et al. (2000) observed a negative association between *H. fomes* and *E. agallocha*. On the contrary, *X. mekongensis* abundance is greater in the highly-populated northern habitats (Figs. 2.4 & 2.5) where the species coexists with *H. fomes* and *Bruguiera sexangula*. My correlative inferences might not necessarily reflect the causal mechanisms of biotic interactions (competition or facilitation) on species distributions. Nevertheless, they help to improve the explanatory and predictive power of HSMs and may form the basis for more mechanistic studies.

Like DAS, URP (representing the downstream − upstream gradient) was also retained in the best GAMs with maximum RI scores, demonstrating the influence of river systems on mangroves' spatial distributions. The river system covers about 1700 km^2 and frequently change channels. Erosion and compensatory accretion are common along the river banks. The freshwater supply from these rivers mainly controls the amount of alluvium deposit in the forest floor, which in turn regulate the availability of plant nutrients (Siddiqi 2001). The negative response of *E. agallocha* and *C. decandra* abundances to increasing URP indicate their preference for habitats distributed between the downstream to intermediate positions (0 – 66% upriver from the sea). On the other hand, *H. fomes* and *X. mekongensis's* clear positive response to URP (> 50%) would support a characterization of these

species as upland specialists. These differences in mangrove habitat preferences along the downstream — upstream gradient may be related to the change in regional hydrology since the construction of the Farakka dam (1974) on the Ganges in India which has silted up most of its southbound distributaries heading towards the Sundarbans' river system. As a result, the carrying capacities of the major river (e.g. Sibsa and Posur) systems have radically changed with about 65% reduction in the freshwater flow (Wahid et al. 2007).

2.5.2 Mangrove distribution maps

H. fomes is now facing extinction in the Indian Sundarbans and Myanmar (Blasco et al. 2001). The Bangladesh Sundarbans now supports the sole remaining viable population of this globally endangered mangrove (Iftekhar & Islam 2004). Figures 2.4 & 2.5 represent that the eastern region of the Bangladesh Sundarbans supports the highest *H. fomes* populations, the central and northern regions support intermediate densities, and the species is almost absent in the western region. This may indicate historical range contraction of the species even in the Bangladesh Sundarbans as palynological evidence suggests its past dominance in the western region (Gopal & Chauhan 2006). The sharp negative response of *H. fomes* to increasing HH (Fig. 2.3) implies that this has been one of the main target species for illegal harvesting. In fact, *H. fomes* stem density has declined by 50% (1960 — 1990) all over the Sundarbans because of habitat degradation and mass exploitation (Iftekhar & Saenger 2008). *H. fomes* favours freshwater dominated habitats and shows a negative response to increased soil salinity. Therefore, the highest abundances in the eastern region may be related to its proximity to the freshwater dominated Baleshwar River. However, the freshwater supply to the eastern zone has been dropping because of heavy siltation in the internal channels (Wahid et al. 2007). Therefore, further harvesting and reductions in freshwater supply could push this species over the brink of extinction.

E. agallocha habitat maps indicate this species' wide distribution across the entire Sundarbans, except the upstream-dominated northern region. Contrary to *H. fomes*, *E. agallocha* is a salt tolerant fast growing and reproducing species with high ability to colonize open and degraded habitats (Harun-or-Rashid et al. 2009). *E. agallocha* abundance increased in the sites with high historical harvesting intensity (Fig. 2.3). Natural calamities (i.e. tropical cyclones and tsunamies) and

tree mortality have created large forest gaps in the Sundarbans and the amount of open areas has been increasing by 0.05% each year (Iftekhar & Islam 2004). Hence, I assume that these conditions may favour *E. agallocha* to increase its density and expand its range even to the upstream-dominated northern region.

C. decandra hotspots are now distributed in the south and south-western zones (Figs. 2.4 & 2.5*)*. Intermediate *C. decandra* densities in the central and south-eastern regions provide a clear indication of its landward range expansion. Interestingly, although *C. decandra* belongs to the 'Near Threatened' status globally, its populations seem to be increasing and the species may be expanding its landward range.

High-density populations of *X. mekongensis* are currently restricted to Kalabogi, Koyra and Koikhali regions in the Sundarbans. The distribution of the species is patchy in the rest of the ecosystem. *X. mekongensis* abundances show a strong negative response to increasing historical harvesting intensity (Fig. 2.3). Because of its high timber price in the black market, this has been the target species for illegal harvesting since the colonial regime (Raju 2003). At present, most of the *X. mekongensis* trees (64%) are infected by the heart rot disease (Siddiqui & Khair 2012). Hence, *X. mekongensis* is under severe pressure in the Sundarbans, and could be at higher risk of local extinction.

2.5.3 Implications for conservation

My species density maps advocate the immediate protection of the remaining suitable habitats (hotspots) of *H. fomes* and *X. mekongensis*, the two species most at risk of local and global extinction. However, the existing protected area network, comprising East, West, and South Wildlife Sanctuaries, does not include the hotspots of any of these threatened species (Figs. 2.4 & 2.5). According to the Bangladesh Wildlife Preservation Order 1973 (amended in 1974) these sanctuaries were established to ensure completely undisturbed habitat for the protection of wildlife, vegetation, soil and water (Islam et al. 2014). The capacity of these sanctuaries to conserve biodiversity with limited physical and technological resources, has been highly disputed (Islam et al. 2014). Given the circumstances, a preventative approach involving the design of a new or extended network of protected areas with improved logistics support is a plausible option offering

expediency and cost effectiveness over long term forest restoration projects (Possingham et al. 2015).

The usefulness of HSMs in guiding species habitat restoration, protection, and replanting projects is well documented (Franklin 2010). Although recognising the potential existence of environmental stressors should be the first step in reforestation and restoration planning, a limited understanding of mangroves habitat requirements has limited the success of such initiatives in many countries (Lewis 2005). In the Sundarbans, previous replanting campaigns (based on educated guesses) were also unsuccessful (Islam et al. 2014). In this context, the regional HSMs of this study with detailed information on the mangroves' habitat requirements, may guide the future mangrove replanting initiatives. The absence of a persistent soil seed bank of *H. fomes* and *X. mekongensis* in the Sundarbans has recently been identified (Harun-or-Rashid et al. 2009). Thus, this study recommends planting of endemics such as *H. fomes* in the forest gaps, to safeguard these habitats from invasive species (Biswas et al. 2007).

The Sundarbans has a history of extensive exploitation particularly during the 1980s (Siddiqi 2001). The Bangladesh government enforced a full logging ban in 1989 (Sarker et al. 2011). Despite such law enforcement, illegal felling of trees is common (Iftekhar & Islam 2004). My results also indicate the negative effects of historical harvesting on the populations of the threatened mangrove species. This exploitation is also directly linked with the habitat loss of many mangrove-dependent animals including the globally endangered Royal Bengal tiger (Aziz et al. 2013). My mangrove distribution maps may guide ongoing and future protection and monitoring initiatives of the government to combat illegal logging through recording mangrove population changes or predicting changes and identifying areas (or species) that may be most affected by future harvesting and other human interventions (e.g. settlement and shrimp farming).

The predictive performances of the GAM-based and the direct interpolation approach are nearly identical, and the habitat suitability maps show high spatial congruence, except in few areas where the direct interpolation method underestimated *H. fomes* and *C. decandra* densities (Fig. 2.5 and Appendix 2B). This localized density underestimation may be related to the limited ability of the direct interpolation method in capturing fine scale environmental variations

(Appendix 2C) that might shape mangrove density distributions (Franklin 2010). These uncertainties also suggest allocating more sampling efforts in these areas. Miller et al. (2007) asserted that the direct interpolation approach is inappropriate for species habitat mapping because of its limited ability to accommodate environmental and biotic predictors.

2.6 Conclusions

This study demonstrates the usefulness of habitat modelling as a tool for predicting mangrove abundances and provides novel insights into the underlying ecology of these species. The HSMs and complementary habitat maps provide spatially explicit information on the remaining habitats of the threatened mangrove species, and form the baseline for designing cost-effective field inventories, biodiversity assessment and monitoring programs. Most importantly, the Bangladesh Forest Department can readily use the distribution maps in their existing protection and monitoring initiatives designed to combat illegal logging in the Sundarbans. The relative performance of the direct interpolation-based species distribution maps against the habitat-based spatial density maps indicates their usefulness when environmental data are not available. I could not make HSMs for the remaining 16 mangrove species in my data due to their low prevalence. Future studies may usefully extend their sampling efforts beyond the existing PSP network to record these rare mangroves.

Chapter 3 . Spatio-temporal patterns in mangrove biodiversity in the Sundarbans

3.1 Abstract

Rapid global change and human pressure have turned mangrove forests into one of the world's most threatened ecosystems. Yet, we have a restricted understanding of how mangrove species composition and diversity have changed, mostly due to limited availability of mangrove field data. Such knowledge gaps have obstructed mangrove conservation programs across the tropics, but particularly in the Sundarbans. In this chapter, I established spatially explicit baseline biodiversity information for the Sundarbans using long-term mangrove tree data collected from a network of 110 permanent sample plots at four historical time points: 1986, 1994, 1999 and 2014. I determined the spatial and temporal heterogeneity in alpha, beta, and gamma diversity in three ecological zones (hypo-, meso-, and hypersaline) and also uncovered how the geographic range and populations of the mangroves changed in these zones. Spatially, the hyposaline mangrove communities were the most diverse and distinct (most heterogeneous in species composition) while the hypersaline communities were the least diverse and most homogeneous in all historical time points. Since 1986, I have detected a declining trend of compositional heterogeneity (between-site variability in species composition) and a significant spatial contraction of distinct and diverse communities over the entire ecosystem. Temporally, the western and southern hypersaline communities have undergone radical shifts in species composition for population increase and range expansion of the invasive species *Ceriops decandra* and local extinction or range contraction of endemics including the globally endangered *Heritiera fomes*. The legislated network of protected areas does not cover the surviving biodiversity hotspots located in the hyposaline habitats. In addition to suggesting the immediate coverage of these hotspots under protected area management, my novel biodiversity insights and spatial maps can form the basis for future spatial conservation planning, biodiversity assessment, monitoring and protection initiatives for the Sundarbans.

3.2 Introduction

Historical anthropogenic pressures and rapid environmental changes have turned highly productive tropical and sub-tropical mangrove forests into Earth's one of the most threatened and rapidly vanishing habitats, causing worldwide loss of coastal livelihoods and ecosystem services (Lee et al. 2014; Malik et al. 2015; Friess 2016). Floristic composition and diversity play key roles in sustaining these services. However, since 1950, we have lost nearly 50% of global mangrove coverage (Feller et al. 2010). The current rate of mangrove deforestation is 1 — 2% per year (Alongi 2015). The loss may further accelerate due to future sea level rise (SLR) (Ward et al. 2016). Despite the drastic nature of these losses, we have a limited understanding of spatial and temporal changes in biodiversity in tropical mangrove plant communities.

Different aspects of biodiversity such as species alpha, beta and gamma diversity, represent different fundamental aspects of natural communities which can be of particular conservation interest (Socolar et al. 2015). For example, spatial maps of species richness (a measure of alpha diversity) can guide us locating the biodiversity hotspots while analyses of long-term changes in species composition (beta diversity) can provide insights on species invasion, extinction and biotic homogenisation (Smart et al. 2006; Gaston & Fuller 2008; Jarnevich & Reynolds 2010). Therefore, to serve long-term conservation and protection of threatened flora, fauna and habitats, we need to look at all aspects of biodiversity.

Mangrove ecologists have, thus far, mostly relied on alpha diversity, in particular, the species richness index (Ellison 2001; Record et al. 2013; Osland et al. 2017) that does not account for the abundance-related heterogeneity in vegetation structure. In fact, explaining why mangrove tree species richness decreases along the latitudinal gradient (termed a 'biodiversity anomaly', Ricklefs et al. 2006) has dominated the mangrove biodiversity literature in the last two decades. While such global studies offer a broader insight on biodiversity patterns, management and conservation initiatives are essentially implemented based on regional or local needs. Nevertheless, limited availability of long-term mangrove field data has been a major constraint for conducting spatio-temporal biodiversity studies in threatened tropical coastal regions (Ellison 2001), but particularly in the Sundarbans.

The Sundarbans has already lost half of its original size over the last 150 years, mostly due to deforestation, habitat degradation and conversion of mangrove habitats to agricultural land (Siddiqi 2001). The remaining Sundarbans has now transformed into a highly stressed ecosystem due to a historical and ongoing reduction in freshwater flows in the river system, siltation, salinity intrusion, water and soil pollution (Ellison et al. 2000; Wahid et al. 2007). Increasing salinity and historical forest exploitation have strongly affected the populations of many threatened tree species (Chapter 2). Further deterioration of the ecosystem through salinity intrusion and SLR is likely to significantly affect the remaining populations and spatial distributions of the endangered, rare as well as the common species.

Based on soil salinity, the Bangladesh Sundarbans was divided into three ecological zones i.e. hyposaline zone (< 2 dS m^{-1}), mesosaline zone (2 – 4 dS m^{-1}) and hypersaline zone (> 4 dS m^{-1}) in the 1980s (Siddiqi 2001). Management and conservation decisions are made based on the status of tree growth and forest stock in these ecological zones (Iftekhar & Saenger 2008). The salinity level over the entire Sundarbans has already increased by 60% since 1980 due to a reduction in the freshwater supply from the transboundary rivers for dam constructions in 1974 (Aziz & Paul 2015). Yet, we know little about how the mangrove tree communities of different salinity zones have changed for such alteration in habitat conditions. Collectively, such knowledge gaps and the lack of baseline biodiversity maps, has been a major impediment to national and international conservation efforts in the Sundarbans.

In this chapter, using mangrove tree data spanning 28 years, collected in 1986, 1994, 1999, and 2014, from 110 permanent sample plots (PSPs) in the Sundarbans, I looked at different aspects of the mangrove communities. My main goal was to understand the spatial structure of the biodiversity components — within-plot (alpha), between-plot (beta), and total (gamma) diversity — at these four historical time points and to disentangle the temporal dynamics in species composition both within the ecological zones and across the whole Sundarbans ecosystem. More precisely, I asked the following questions: Which ecological (i.e. salinity) zone supports the most/least diverse mangrove communities? Is the most diverse ecological zone also the most heterogeneous (i.e. variable between plots)

in species composition? How has compositional heterogeneity in the broader ecological zones developed over the 28 years? How has the geographic range and density of mangroves changed since 1986? I also developed spatial maps of all aspects of biodiversity to answer the following questions: Where are the historical and contemporary biodiversity hotspots located? Which habitats have changed most in species composition over time? Finally, I demonstrated the potential applications of these new maps and insights in the ongoing and future biodiversity research, forest protection, reforestation and restoration programs.

3.3 Methods

3.3.1 Tree data

Tree data were collected from the PSP network comprising 110 equal-sized PSPs (0.2 ha, 100 x 20 m, divided into five 20 x 20 m subplots, Fig. 3.1) in the Bangladesh Sundarbans during four complete forest censuses: 1986, 1994, 1999 and 2014. Every tree with d.b.h (diameter at breast height – 1.3 m from the ground) ≥ 4.6 cm was tagged with a unique tree number and identified. The PSP network represents the ecological (i.e. salinity) zones and the forest types (for details see Iftekhar & Saenger 2008). The hyposaline zone comprises 50 PSPs representing the *H. fomes, H. fomes − Execration agallocha*, and *E. agallocha − H. fomes* forest types. The mesosaline zone comprises 30 PSPs representing the *H. fomes – E. agallocha*, and *E. agallocha − H. fomes* forest types. The hypersaline zone comprises 30 PSPs representing the *E. agallocha − Ceriops decandra* and the *C. decandra − E. agallocha* forest types.
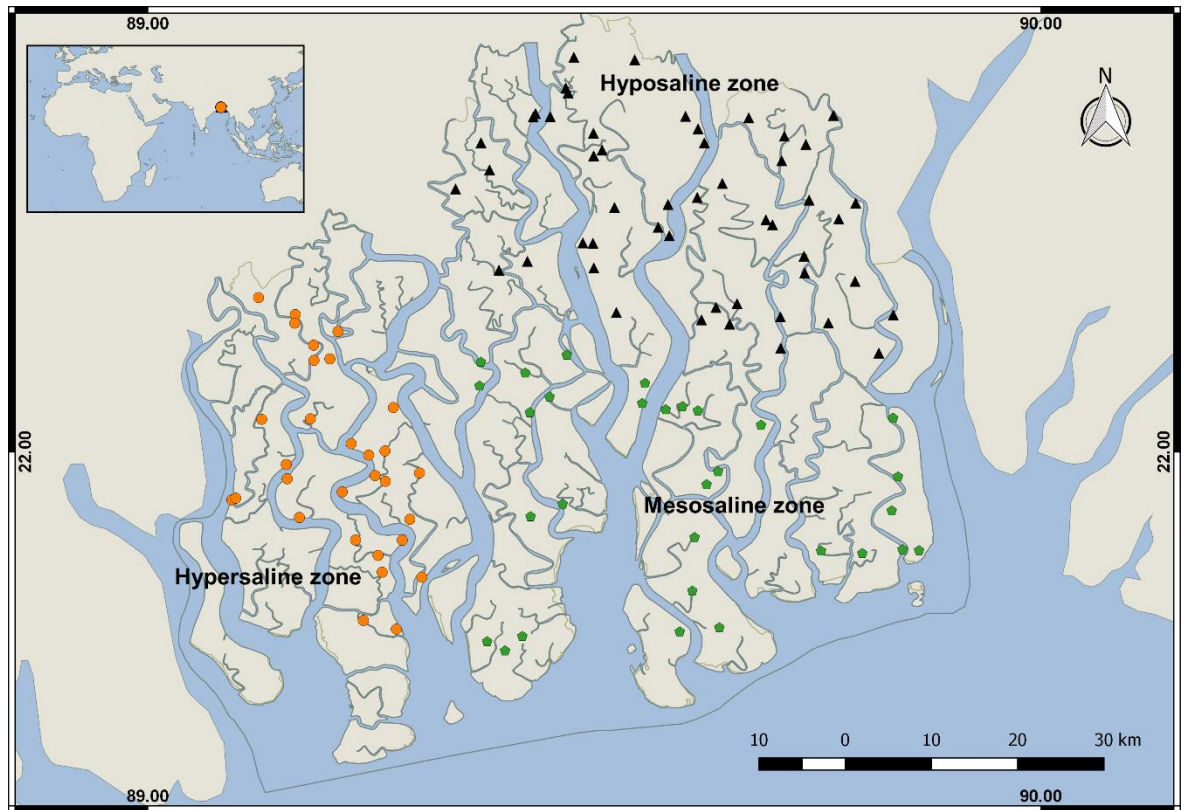
Fig. 3.1 Permanent Sample Plots (PSPs) in the Sundarbans, Bangladesh. Black triangles, green pentagons, and orange circles represent the PSPs located within the hypo-, meso- and hypersaline ecological zones, respectively.

3.3.2 Biodiversity partitioning

I used the framework developed by Reeve et al. (2016) for partitioning biodiversity because it allowed me to investigate the hierarchical structure of mangrove biodiversity in a highly complex ecosystem like the Sundarbans by assessing biodiversity at three different spatial scales, at the scale of the ecosystem as a whole, of the three salinity zones, and of the 110 individual PSPs, and also, at four different time points (1986, 1994, 1999, and 2014). This framework, based on Rényi's notion of generalised relative entropy (Rényi 1961), and extending Hill (1973), Jost (2006; 2007) and Leinster and Cobbold's (2012) notions of ecosystem diversity, partitions ecosystem diversity in a way that allows us to understand the true subcommunity alpha, beta and gamma diversity structure and dynamics. As the alpha, beta and gamma diversity measures proposed by Reeve et al. (2016) are independent from each other, they do not necessarily reflect variations of a mathematical formulation rather they help to provide biological insights over

individual communities across an ecosystem. Figure 3.2 presents how I adopted this framework to investigate spatial and temporal biodiversity patterns in the Sundarbans based on my long-term (28-year) dataset.
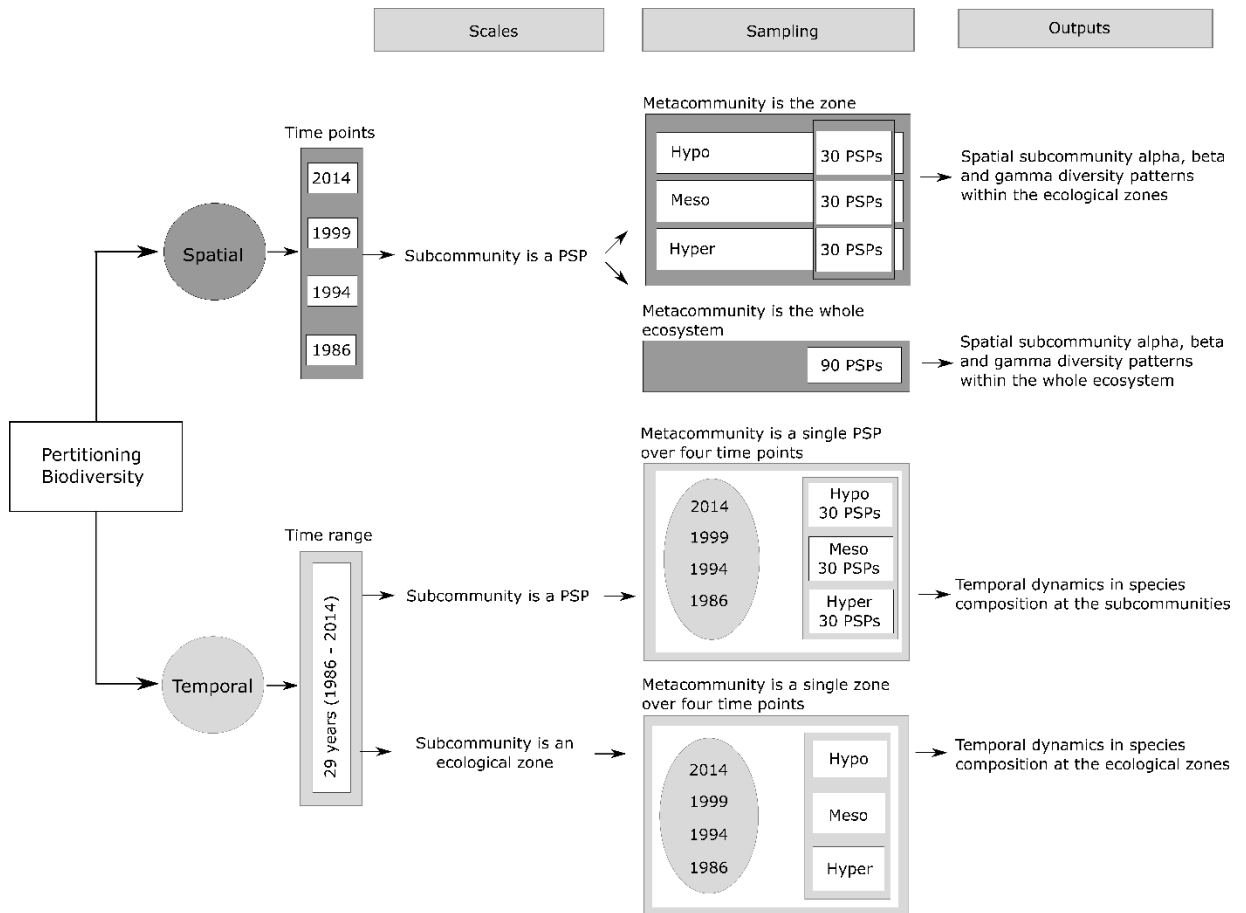
Fig. 3.2 Biodiversity partitioning scheme used in this chapter to explain spatial subcommunity (SC) alpha, beta, and gamma diversity structures across the ecological zones (i.e. hypo-, meso-, and hypersaline zones) and the whole ecosystem (Sundarbans) in four historical time points (in 1986, 1994, 1999 and 2014), and to investigate temporal dynamics in species composition across the individual subcommunities as well as the individual ecological zones over the 28 years.

All of the analyses are based on the comparison between the biodiversity of a larger part of the data (called a *metacommunity*) with the biodiversity of its subsets (called *subcommunities*). The definition of the *metacommunity* (hereafter, MC) and its partitioning into *subcommunities* (hereafter, SCs) is done in a way suitable to the question being asked. For example, in a spatial analysis,

a MC will be the ecosystem or a single ecological zone at a time point, and in a temporal analysis, either a single PSP or one ecological zone at all four time points combined. Each PSP represents a SC in a spatial analysis and a single time point at whatever spatial scale is being examined in temporal analyses. For the spatial analyses, I used two MC levels — ecological zone and the whole Sundarbans ecosystem — to investigate how the biodiversity components (i.e. alpha, beta and gamma) in each SC looks like in relation to its ecological zone or in relation to the whole ecosystem. To avoid bias from the uneven distribution of PSPs among the ecological zones (50 in hyposaline, 30 in mesosaline, and 30 in the hypersaline zone), I repeatedly subsampled 30 PSPs from the hyposaline zone at random in the analyses (100 iterations). Thus, in analyses, each ecological zone as a MC comprised 30 PSPs i.e. SCs, and the whole Sundarbans ecosystem as a MC comprised 90 SCs, 30 from each of the three ecological zones. This diversity framework, which extends and enhances existing approaches, allowed me to use identical diversity and partitioning analyses to address all of my spatial and temporal questions to ensure consistency across the whole study. In particular, I was able to make spatial and temporal comparisons of the PSPs and zones to identify which were the most diverse individually (alpha diversity), which were the most representative of the MC in terms of having similar species composition — or conversely which were the most distinct individually and heterogeneous as a whole (beta diversity), and which contribute the most to overall MC diversity (gamma diversity).

I used the normalised alpha diversity (denoted $\overline{\alpha}$) which represents the diversity of a single SC (PSP) in isolation, or the average diversity of SCs across an ecological zone or the whole ecosystem to identify the zones with the richest local biodiversity. Because the SC value of $\overline{\alpha}$ is a local measure, it is independent of the MC composition, and so the value of $\overline{\alpha}$ of a SC is the same when estimated for a MC comprising 30 SCs (any ecological zone) as well as for a MC comprising 90 SCs (the whole ecosystem).

The normalised beta diversity measure, $\overline{\rho}$, measures representativeness and assesses how well a SC represents the species composition of its MC. For a SC, it takes its lowest value when every tree is completely dissimilar to every other tree in the rest of the MC, at which point its value is the proportion of the total number

of trees in that SC, reflecting the fact that the SC represents only itself. It is maximised (with value 1) only when the species distribution of the SC is identical to that of the MC, since it represents the whole MC perfectly. Low representativeness therefore suggests high spatial heterogeneity in species composition within the MC, and high representativeness suggests spatial homogeneity. At a community and MC level, high values of $\bar{\rho}$ therefore suggest that the system is homogeneous at the spatial scale of the SC, with the same species found everywhere with the same relative abundances, and low values at the MC level suggest that the MC is very heterogeneous at the same (SC) scale. Low values at the community level again suggest that its constituent SCs poorly represent the MC, but this could be either for the same reason (high heterogeneity among SCs) or because the community itself poorly represents the MC. The two cases can be distinguished by making the community, here the ecological zone, into a MC. If the heterogeneity remains, then the former is true, if not then the latter. I used this, to investigate to what extent each SC represents the species composition of its ecological zone and also the whole ecosystem.

The gamma diversity, γ, is the conventional gamma diversity (Hill 1973; Jost 2006; Leinster & Cobbold 2012) at the MC level that reflects the total species diversity in an unpartitioned ecosystem or an ecological zone. Here, I partitioned the MC gamma diversity into SC (PSP) gamma diversity that measures each PSP's average contribution to (or influence on) the MC diversity per tree. This diversity measure combines the alpha diversity of a SC with its beta diversity to assess the overall contribution of the PSP to the MC (Reeve et al. 2016).

The values of all these diversity measures (alpha, beta, and gamma; subcommunity/PSP, community/zone, and metacommunity/whole ecosystem) are moderated by a viewpoint parameter, q, which takes a value between 0 and ∞, where $q = 0$ relates to species richness, $q = 1$ relates to Shannon entropy (Shannon & Weaver 1949), and $q = 2$ relates to Simpson's concentration index (Simpson 1948), but the latter two measures put more weight on the more dominant species than species richness. For all of my analyses, I report the results using the above three values (0, 1, and 2) of q, writing them as $^{0}\bar{\alpha}$, $^{1}\bar{\rho}$, $^{2}\gamma$, etc.

3.3.3 Spatial and temporal biodiversity analyses

Four spatial snapshots (species counts over the plot matrix obtained in 1986, 1994, 1999 and 2014) were analysed individually to determine spatial SC level alpha, beta and gamma diversity relative to two MC levels: the ecological zone level and the whole-ecosystem level. I then averaged the alpha, beta, and gamma diversity values of the SCs and also calculated the 95% confidence intervals. This helped me to identify spatially which ecological zone was the most/least diverse (alpha), how representative/heterogeneous the SCs were at the four historical time points (beta), and which SCs contributed most/least to the overall diversity of the ecological zones as well as the whole Sundarbans ecosystem (gamma).

To understand long-term dynamics in species composition across the SCs of the Sundarbans' ecosystem, I estimated their temporal representativeness ($\overline{\rho}$). Following Reeve et al. (2016), here each PSP's summed composition over the four census times (1986 – 2014) formed the MC and each PSP composition in each census time was the SC. I calculated the temporal MC $\overline{\rho}$ following the same method as before for the spatial analysis. Temporal $\overline{\rho}$ values of the PSPs of each of the ecological zones were then averaged (and confidence intervals calculated) to understand which zones contained PSPs that changed the most in terms of their composition (seen as low representativeness). I also pooled the species data of the SCs (30 PSPs) of each zone and estimated temporal $\overline{\rho}$ for each of the hypo-, meso-, and hypersaline zones as a whole to understand how each ecological zone changed in species composition over the 28 years. All the diversity analyses were performed using the R statistical software, version 3.2.3 (R Core Team 2016).

3.3.4 Biodiversity mapping

Here I considered the MC comprising of all 110 PSPs surveyed at the four time points to ensure maximum area coverage and estimated the SC alpha, beta and gamma diversity. Using these SC level values, I developed spatial maps of each of the diversity facets for the four census points through ordinary kriging (OK) which is the most widely used geostatistical interpolation technique. OK uses a linear combination of weights at observed locations to provide unbiased prediction at unsampled locations (Bivand et al 2013). Because selecting an appropriate semivariogram model is a prerequisite for kriging success, I fitted three different

semivariogram models to each mangrove: Spherical, Exponential and Gaussian, and selected the model with least sum of squared errors. The spherical model offered best fit for all the biodiversity measures and the semivariograms for them are presented in Appendices 3A, 3B and 3C. OK was performed using the 'gstat' package version $1.1 - 5$ (Pebesma 2004) and the spatial maps were constructed using the 'raster' package version $2.5 - 8$ (Hijmans 2015) in R. I followed a similar mapping procedure to build surfaces for temporal beta diversity ($\overline{\rho}$). This approach of mapping temporal $\overline{\rho}$ in a spatial context helped me to identify areas with high temporal dynamics in species composition. I also superimposed the existing protected area network (PAN) onto my biodiversity maps to examine its ability to support the historical and current biodiversity hotspots in the Sundarbans.

3.3.5 Mangrove population dynamics and range analyses

In Sundarbans, many rare endemic tree species are facing extinction risk (Chapter 2). Information on historical and current population sizes of these critical species is essential for their protection and conservation. Hence, I calculated the percentage contribution of each species to the total composition (sum of populations of all species) of each ecological zone for the first (1986) and the last census (2014). Then I calculated the percentage composition change for each species of each ecological zone from 1986 to 2014.

Following Gillette et al. (2012), I determined how the mangrove species' range expanded or contracted in the hypo-, meso- and hypersaline zones over the 28 years. Historical and concurrent environmental changes in the Sundarbans may promote the geographic expansion of some species (especially invasive or disturbance specialists) and geographic contraction of others (especially endemics). This disproportionate expansion of generalist or invasive species relative to endemics is the key mechanism behind biotic homogenization (McKinney & Lockwood 1999). To test this, I subtracted the number of PSPs in each ecological zone at which a mangrove species occurred in 1986 from the number of PSPs in which it occurred in 2014. The resulted value was then standardized by the number of total PSPs in which the species was present in both times. This value lies between -1 to 1 (positive values indicating range expansion). New species (i.e. introduction) in the ecological zone get the highest value (= 1), and the species that disappeared from the zone (i.e. local extinction) get the lowest

value (= -1). A species has value 0 value if it occurs exactly in the same number of PSPs both in 1986 and 2014, meaning that the species range remains unchanged over time.

3.4 Results

3.4.1 Spatial and temporal dynamics

Spatially, the subcommunities (SCs) of the hyposaline zone were the most individually diverse ($^1\overline{\alpha}$, Fig. 3.3a) and simultaneously the most heterogeneous in species composition (lowest representativeness, $^1\overline{\rho}$, Fig. 3.3b, c) in all historical time points, leading to the SCs being the largest contributors to the overall diversity (per tree, $^1\gamma$, Fig. 3.3d, e) of the ecosystem over the 28 years. The SCs of the hypersaline zone were the least diverse in all historical time points although alpha diversity increased in this zone (also in the mesosaline zone) in the last 15 years (as a result of the invasion of the disturbance specialist *C. decandra*).

The SCs of the mesosaline zone were spatially the most homogeneous in species composition (i.e. high representativeness) and stable over time. In contrast, since 1986, the SCs of both the hypo- and hypersaline zones showed trends of increasing representativeness, $\overline{\rho}$, (i.e. decreasing compositional heterogeneity) and decreasing contribution, γ, to the overall diversity of the ecosystem, indicating biotic homogenization and increasing dominance of generalists. Similar patterns were observed when rare species were given the same importance as the dominant species (*q* = 0) and the relative abundances of the dominant species were considered (*q* = 2) (Appendices 3D & 3E).

The SCs of the hypersaline zone and the zone itself (sample plots pooled) had the least temporal beta ($\overline{\rho}$) diversity i.e. representativeness (Appendix 3F), suggesting that the hypersaline habitats saw the highest turnover in species composition in the Sundarbans over the 28 years.
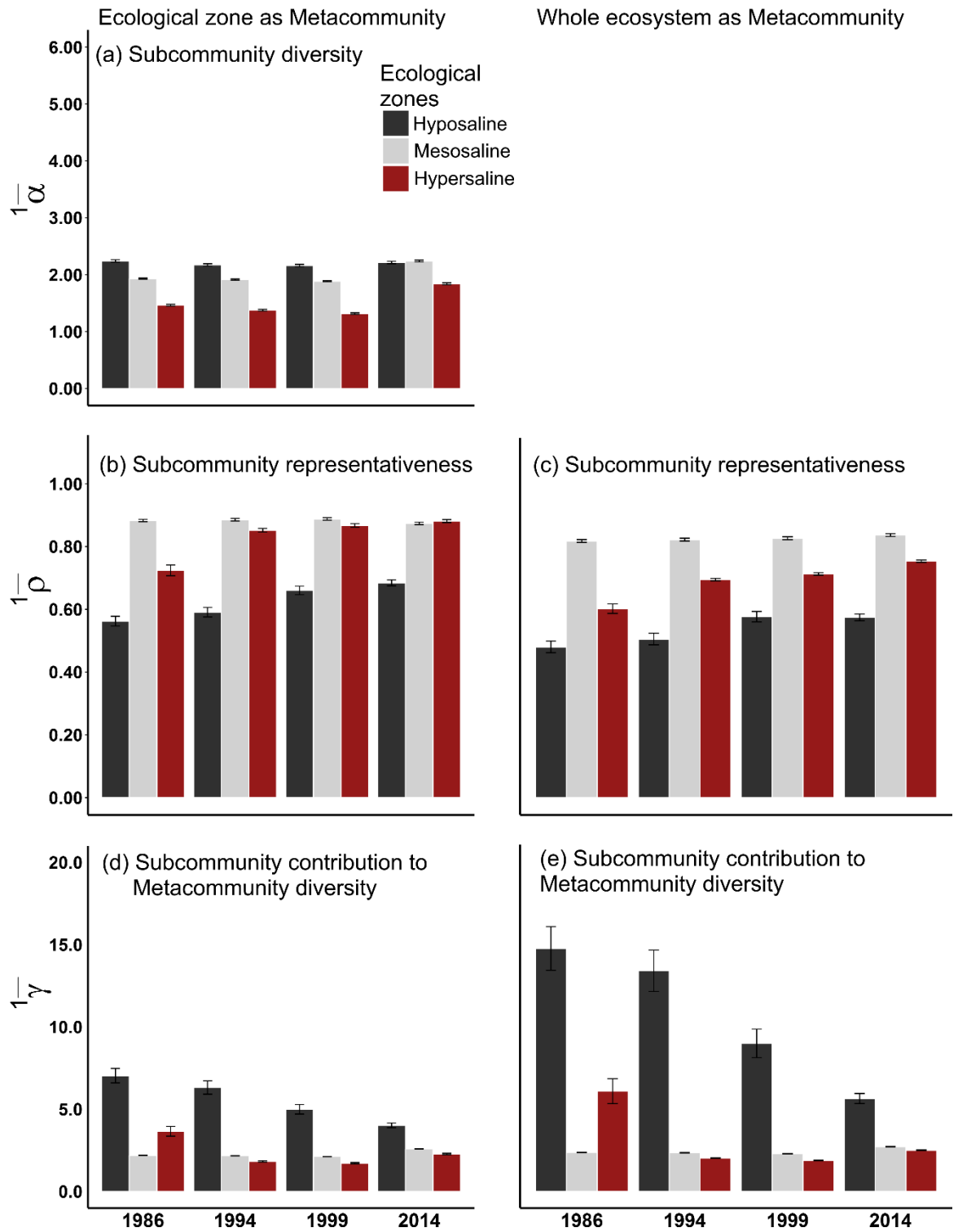
Fig. 3.3 Spatial subcommunity alpha, beta, and gamma diversities (viewpoint parameter, q = 1) in the ecological zones of the Sundarbans in four time points since 1986.

3.4.2 Biodiversity maps

Both historically and currently, the hyposaline habitats of the northern Sundarbans support the most biodiverse ($^1\overline{\alpha}$, Fig. 3.4a) SCs. Spatial coverage of the unrepresentative i.e. heterogeneous PSPs ($^1\overline{\rho}$, Fig. 3.4b) and also the SCs contributing most to the overall diversity ($^1\gamma$, Fig. 3.4c) of the ecosystem have declined over the 28 years and are now only restricted to the northern hyposaline habitats. The established protected area network does not cover these biodiversity hotspots. The spatial biodiversity maps for $q = 0$ and $q = 2$ showed similar patterns (Appendices 3G & 3H). The semivariograms of the biodiversity indices (Appendices 3A, 3B, and 3C) indicates that the variation in alpha diversity between sampling locations is relatively better explained by their proximity to each other, compared to the beta and gamma diversity indices, suggesting a fair amount of uncertainty remains in predicting beta and gamma diversity using direct interpolation technique.
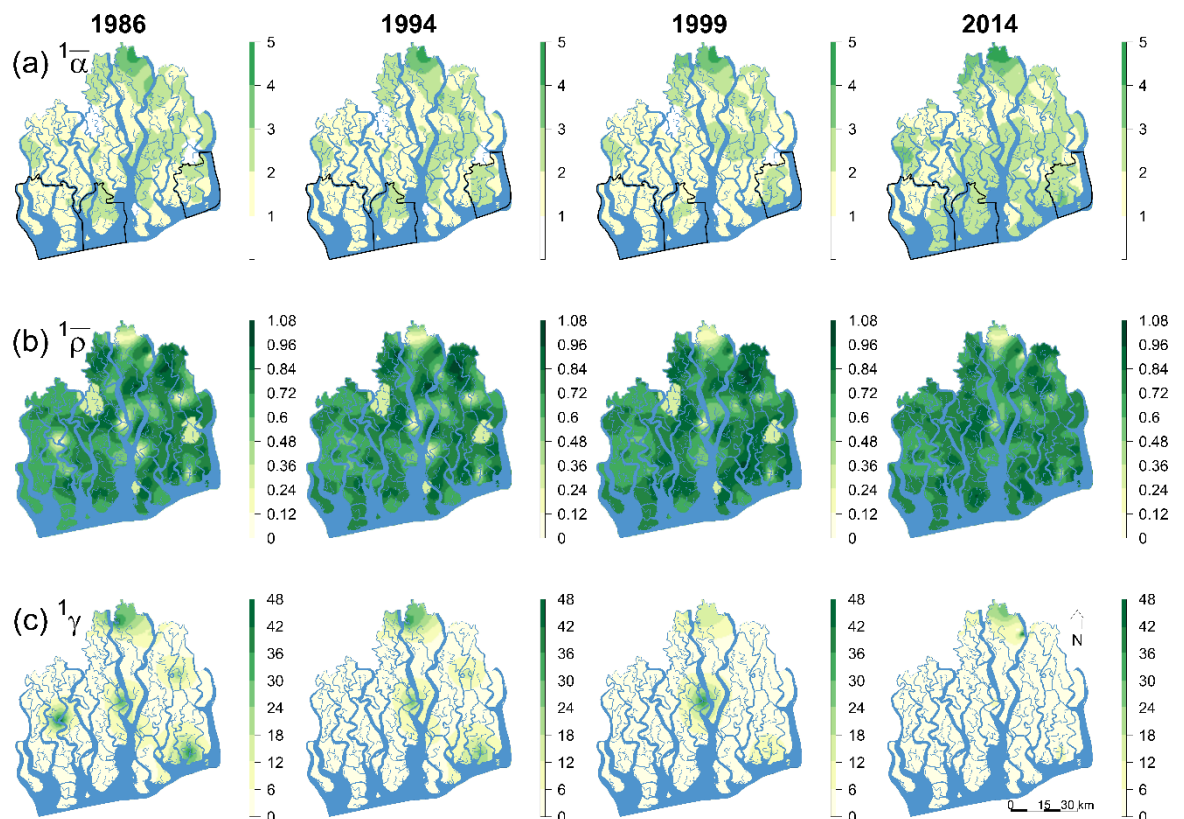
Fig. 3.4 Spatial distributions of subcommunity alpha, beta and gamma diversities (for viewpoint parameter, $q = 1$) over the entire Sundarbans generated through ordinary kriging. The black contours represent the three protected areas.

The western and southern habitats in the hypersaline and mesosaline zones and a part of the northern hyposaline zone (specifically the Kalabogi region) experienced radical temporal shifts in species composition since 1986 (Fig. 3.5).

3.4.3 Mangrove population and range dynamics

With 21 historical species presence, the hyposaline zone was the most species-rich ecological zone in the Sundarbans (Table 3.1). Since 1986, the percentage composition declined for 13 species in the hyposaline zone, for 8 species in the mesosaline zone, and for all species in the hypersaline zone, except *C. decandra*. Between 1986 and 2014, the contribution of the invading species *C. decandra* to the total composition increased by about 97% in the hyposaline, 96% in the mesosaline, and 67% in the hypersaline zone. Conversely, the contribution of the climax species *H. fomes* substantially declined in the meso (-16.48%) and hypersaline (-21.66%) zones.

Fig. 3.5 Spatial maps showing the distributions of temporal change in subcommunity beta diversity (viewpoint parameter, q = 0, 1, and 2) during 1986 – 2014 generated through ordinary kriging. The black contours represent the three protected areas.
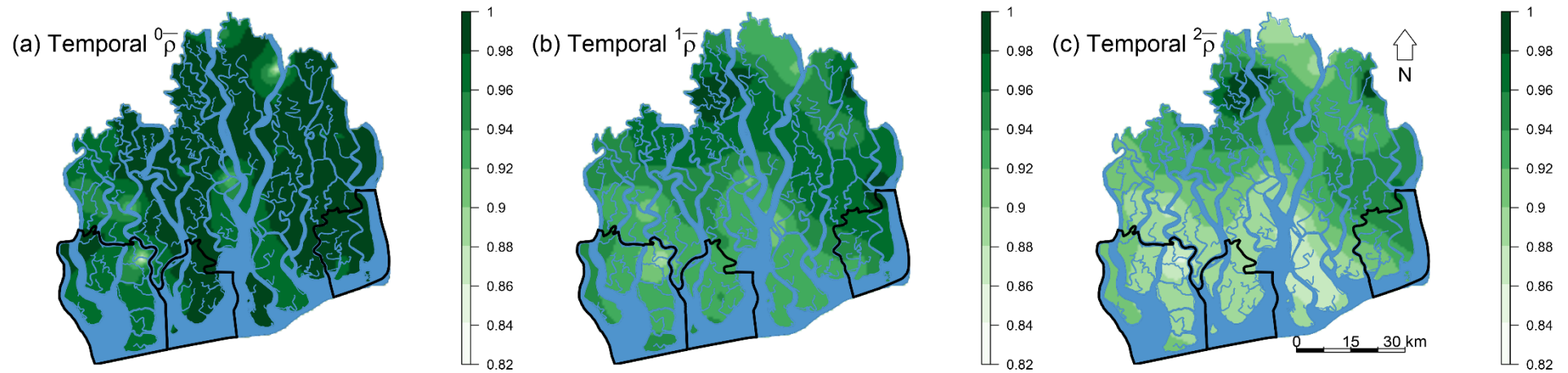
Table 3.1 Mangrove populations change during 1986 – 2014.

	Hyposaline zone			Mesosaline zone			Hypersaline zone		
	Abundance		% CC*	Abundance		% CC	Abundance		% CC
Species	1986	2014		1986	2014		1986	2014	
Excoecaria agallocha	9572 (46.97)	8635 (46.59)	-0.41	7338 (47.95)	9301 (56.34)	8.04	9505 (85.32)	11558 (80.45)	-2.94
Heritiera fomes	8525 (41.43)	8253 (44.53)	3.12	7754 (50.67)	5998 (36.33)	-16.48	1215 (10.91)	1009 (7.02)	-21.66
Avicennia officinalis	568 (2.79)	193 (1.04)	-45.60	1 (0.01)	--	-100.00	6 (0.05)	4 (0.03)	-31.84
Sonneratia apetala	436 (2.14)	116 (0.63)	-54.73	--	--	0.00	5 (0.04)	3 (0.02)	-36.49
Amoora cucullata	350 (1.72)	337 (1.82)	2.85	51 (0.33)	33 (0.20)	-25.02	57 (0.51)	41 (0.29)	-28.39
Bruguiera sexangula	290 (1.42)	339 (1.83)	12.49	1 (0.01)	1 (0.01)	-3.79	4 (0.04)	5 (0.03)	-1.56
Xylocarpus mekongensis	198 (0.97)	297 (1.60)	24.51	38 (0.25)	41 (0.25)	0.01	76 (0.68)	69 (0.48)	-17.37
Cynometra ramiflora	180 (0.88)	14 (0.08)	-84.24	71 (0.46)	19 (0.12)	-60.25	--	--	--
Cerbera manghas	130 (0.64)	21 (0.11)	-69.83	--	--	--	--	--	--
Talipariti tiliaceum	59 (0.29)	31 (0.17)	-26.76	--	--	--	--	--	--
Aegiceras corniculatum	33 (0.16)	15 (0.08)	-33.35	--	--	--	--	--	--
Excoecaria indica	8 (0.04)	4 (0.02)	-29.05	--	--	--	--	--	--
Tamarix dioica	8 (0.04)	3 (0.02)	-41.61	--	--	--	--	--	--
Barringtonia racemosa	7 (0.03)	0 (0.00)	-100.00	--	--	--	--	--	--
Ceriops decandra	4 (0.02)	258 (1.39)	97.22	20 (0.13)	1098 (6.65)	96.15	257 (2.31)	1669 (11.62)	66.87
Sonneratia caseolaris	3 (0.01)	0 (0.00)	-100.00	--	--	--	--	--	--
Intsia bijuga	2 (0.01)	3 (0.02)	24.51	--	--	--	--	--	--
Lannea coromandelica	2 (0.01)	0 (0.00)	-100.00	--	--	--	--	--	--
Xylocarpus granatum	1 (0.005)	9 (0.05)	81.64	14 (0.09)	12 (0.07)	-11.45	16 (0.14)	9 (0.06)	-39.26
Pongamia pinnata	1 (0.005)	2 (0.01)	37.48	--	--	--	--	--	--
Sapium indicum	1 (0.005)	0 (0.00)	-100.00	--	--	--	--	--	--
Petunga roxburghii	--	3 (0.02)	100.00	--	4 (0.02)	100.00	--	--	--
Salacia chinensis	--	--	--	12 (0.08)	--	-100.00	--	--	--
Rhizophora mucronata	--	--	--	--	1 (0.01)	100.00	--	--	--
Lumnitzera racemosa	--	--	--	3 (0.02)	1 (0.01)	-52.79	--	--	--
Totals	20378	18533		15303	16509		11141	14367	

*Compositional change

Over the 28 years, *C. decandra* and *I. bijuga* considerably expanded their range, *C. ramiflora* contracted its range, *B. racemose*, *S. caseolaris*, *L. coromandelica* and *S. indicum* faced local extinction, and *P. roxburghii* newly arrived in the hyposaline zone (Fig. 3.6). In the mesosaline zone, *P. roxburghii* and *R. mucronata* recently arrived, *C. decandra* widely expanded its range, *A. cucullata* and *C. ramiflora* substantially contracted their range, and *A. officinalis* and *S. chinensis* faced local extinction. The range of the highly salt tolerant *C. decandra* and the pioneer species *S. apetala* considerably expanded in the hypersaline zone while the range of the salt intolerant *H. fomes* and *A. cucullata* contracted over time.

Fig. 3.6 Mangrove species range change during 1986 – 2014 in the Sundarbans.
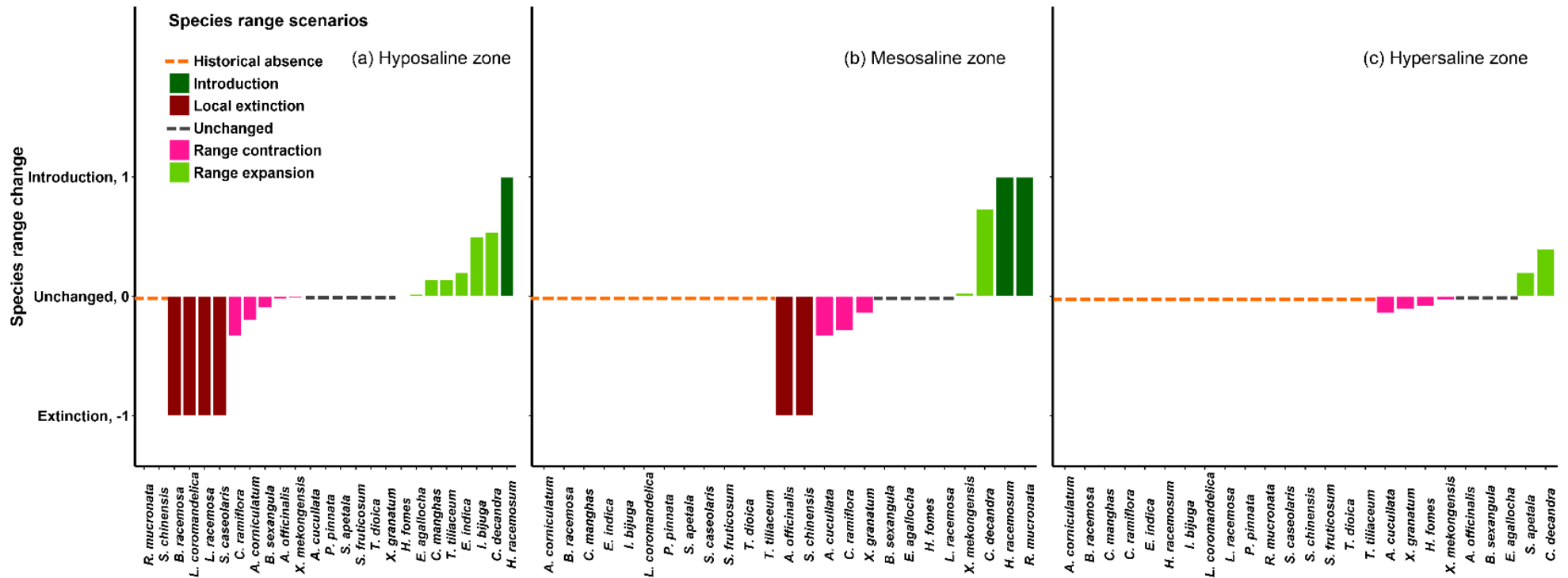
3.5 Discussion

3.5.1 Spatial structure and temporal dynamics

Salinity limits mangrove establishment, growth and development and mangrove species occupy distinct positions of coastal areas due to differential salt tolerance ability (Parida & Das 2005). In the Sundarbans, the most diverse (alpha) and distinct (least representative) SCs were distributed in the hyposaline zone (Fig. 3.3) where the soil salinity level usually stays below 2 dS m^{-1} because of adequate fresh water supply from the nearby Baleswar — Passur river system (Siddiqi 2001). This salinity level can allow widespread coexistence of both non-halophytes (species that survive optimally in fresh water dominated mangrove habitats, but likely to die at hypersaline soils, e.g. *A. cucullata, I. bijuga, C. ramiflora* and *T. tiliaceum*) and facultative halophytes (species that grow well in fresh water dominated habitats but unable to survive at high salinity levels, e.g. *H. fomes, B. sexangula and X. mekongensis*) (Krauss & Ball 2013). This might have contributed to the high diversity and distinctiveness of the hyposaline SCs. In contrast, the hypersaline zone (the salinity level often exceeds 4 dS m^{-1}) supported the least diverse (alpha) SCs because of the super dominance of obligate halophytes (species that show optimum growth and reproduction in hypersaline conditions, e.g. *C. decandra* and *E. agallocha*).

My results showed a clear trend of increasing representativeness (decreasing heterogeneity) in the hyposaline and hypersaline SCs since 1986 (Fig. 3.3). In line with that, the contribution of these SCs to the overall diversity of the ecological zones was also declining substantially. These results indicate that the previously distinct SCs of two extreme environmental settings (low and high saline conditions) are becoming homogeneous in species composition over time. This pattern might be closely related to increasing salinity (Aziz & Paul 2015) and historical tree harvesting which has resulted in local extinction, range contraction and population decline of many salt-intolerant species (including the climax species *H. fomes*) and widespread colonization of many opportunistic obligate halophytes, particularly, *C. decandra* (Table 3.1, Fig. 3.6).

Surprisingly, alpha diversity increased in the SCs of all the ecological zones, particularly in the last census time – 2014. This sudden shift is related to the

radical range expansion of *C. decandra* during the last 15 years including the introduction and localized population growth of some non-halophytes in the meso- and hyposaline habitats (Table 3.1, Fig. 3.6). This scenario is in agreement with the basic homogenization theory that assumes that changes in alpha diversity can be independent of between-habitat homogenization because replacement of locally distinct SCs (containing rare species) with generalists would reduce heterogeneity, but the SCs may remain the same/increase in species number (Olden & Poff 2003; Smart et al. 2006). Over the four historical time points, the SCs of the mesosaline zone showed stable and higher representativeness (i.e. homogeneity in species composition) compared to the SCs of the other ecological zones. This compositional stability might be due to prevailing intermediate environmental conditions in this zone which support both facultative and obligate halophytes. Previous studies (Flowers et al. 2010; Krauss & Ball 2013) on other mangrove systems also reported stable forest structure and optimum tree growth and physiological functions at moderate salinity concentrations.

3.5.2 Spatial biodiversity maps

My spatial biodiversity maps (Fig. 3.4, Appendices 3G & 3H) indicated that both historical and current biodiversity hotspots (alpha) were confined to the northern (specifically the Kalabogi region) hyposaline habitats in the Sundarbans. These upstream habitats are only inundated by spring high tides so receive the lowest amount of saltwater from the Bay of Bengal (Chowdhury, De Ridder, et al. 2016). These habitats now also support the most unrepresentative i.e. distinct SCs comprising the remaining assemblages of the unique *H. fomes – B. gymnorhiza – X. mekongensis* forest type (Iftekhar & Saenger 2008). The mangrove assemblages of the rest of the ecosystem are currently more or less homogeneous followed by a gradual decline in spatial coverage of the distinct communities in all historical time points since 1986. Except the upstream northern habitats, all areas were also poor in alpha diversity in all historical time points (except an increase in 2014 in the south and southeastern downstream areas, mostly due to the invasion of *C. decandra*). This ecosystem-wide compositional homogeneity and poor alpha diversity might be somewhat related to the historical decline in areas that supported unique tree assemblages and to concurrent hyper-dominance of generalists — *E. agallocha* and *C. decandra* (Iftekhar & Saenger 2008).

It is worth mentioning here that the semivariograms of the different biodiversity measures (Appendices 3A, 3B, and 3C) suggests that the variation in alpha diversity between sampling points can be better described by their proximity to each other, compared to the beta and gamma diversity indices. This indicates that a considerable amount of uncertainty remains when we interpolate between community variability in species composition and the contribution of each community to the overall biodiversity of the ecosystem through kriging. Therefore, future studies should consider incorporating fine-scale variability in habitat conditions in their habitat-based biodiversity models to produce more reliable beta and gamma diversity maps of the region.

3.5.3 Conservation implications

Similar to the species density maps in Chapter 2, the established protected area network does not cover the remaining biodiversity hotspots (Fig. 3.4, Appendices 3G & 3H) that support most of the remaining populations of *X. mekongensis* and *H. fomes*, the two species most at risk of local and global extinction. Hence, in addition to bringing threatened mangrove species under immediate protection, this study advocates bringing the remaining biodiversity hotspots under protected area management to ensure their immediate protection and long-term conservation of the many threatened species living there.

I found that already many mangrove tree species have faced local extinction and the abundance and geographic range of many of the remaining species have substantially declined over the last three decades (Table 3.1, Fig. 3.6). These results suggest that conservation initiatives should immediately focus on the endangered (e.g. *H. fomes*) as well as the rare endemics (e.g. *C. ramiflora, C. manghas and A. cucullata* etc.) whose populations and geographic ranges have declined drastically in recent times because further exploitation of these threatened species may push them to the brink of extinction. My results further suggest prioritisation of rare endemic species in the future mangrove replanting projects.

Illegal felling of mangrove trees is becoming increasingly common (Iftekhar & Saenger 2008) in the Sundarbans. The Bangladesh Forest Department has started implementing a SMART (Spatial Monitoring and Reporting Tool) patrol management

system in the Sundarbans for adequate forest protection. My biodiversity maps can guide this ongoing initiative as well as the long-term forest protection and conservation programs. More precisely, my results suggest these conservation and protection efforts to primarily focus on the remaining biodiversity hotspots located in the northern upstream hyposaline zone.

3.6 Conclusions

Using 28 years mangrove census data, I report, for the first time, on how species composition and diversity of the mangrove assemblages have changed across space and time in the Sundarbans. I quantified species-specific ranges as well as population dynamics under different environmental settings. My biodiversity maps offer spatially explicit information on the remaining biodiversity hotspots and the areas that have experienced the highest turnover in species composition since 1986. These novel results can guide future biodiversity research, biodiversity assessment and monitoring programs in the Sundarbans. The Bangladesh Forest Department can also readily use my biodiversity maps with complementary information on population size and range dynamics of the species (particularly for endangered and rare endemics) in their ongoing and future mangrove conservation and protection initiatives. The presence of many rare species (with very few historical occurrences) in my long-term datasets advocates for the extension of the current PSP network. Due to the unavailability of long-term environmental data for the Sundarbans, I used the established ecological (i.e. salinity) zones to describe the spatio-temporal patterns of different aspects of biodiversity. The projected SLR range along the Bangladesh coast may alter the regional hydrology with associated changes in salinity and nutrient availability in the ecological zones, so we need to account for the fine-scale habitat conditions in future biodiversity studies to make robust and practically useful biodiversity predictions.

Chapter 4 . Uncovering the drivers of mangrove biodiversity in the Sundarbans

4.1 Abstract

Tropical mangrove forests are amongst the most threatened and rapidly vanishing habitats on Earth. Yet, we have a restricted understanding of the drivers and spatial patterns of biodiversity in threatened mangrove plant communities. Using species, environmental and historical disturbance data from the 110 permanent sample plots (PSPs) in the Sundarbans, in this chapter, I provide the first comprehensive and consistent quantification and habitat-based modelling of all fundamental aspects of biodiversity (i.e. alpha, beta and gamma diversity) in threatened mangrove communities. I applied Generalized Additive Models (GAMs) to determine the key drivers shaping the spatial distributions of mangrove diversity and composition in the Sundarbans. Baseline biodiversity maps were constructed using covariate-driven habitat models and their predictive performances were compared with covariate-free (i.e. direct interpolation) approaches to see whether the inclusion of habitat variables bolster spatial predictions of biodiversity indices or we can rely on purely spatial approaches when environmental data are not available. I found that historical tree harvesting, disease, siltation and soil alkalinity were the key stressors causing loss of alpha and gamma diversity in threatened mangrove communities. Both alpha and gamma diversity increased along the downstream-to-upstream and riverbank-to-forest interior gradients. Mangrove communities subjected to intensive past tree harvesting, disease prevalence and siltation were more representative (beta diversity) i.e. homogeneous in species composition. In contrast, the heterogeneity of the communities increased along the salinity and downstream-to-upstream gradients. Overall, the habitat-based models showed better predictive ability than the covariate-free approach. Nevertheless, a small margin of differences in predictive ability between the approaches demonstrates the utility of direct interpolation approaches when environmental data are unavailable. Given that the surviving biodiversity hotspots (comprising many globally endangered tree species) are located outside the established protected area network (PAN) and

hence open to constant human exploitation, this study suggests bringing them immediately under protected area management.

4.2 Introduction

Tropical and subtropical mangrove forests (30° N and 30° S) support coastal livelihoods worldwide and provide ecosystem services including nutrient cycling, coastal protection, carbon sequestration, and fisheries production (Lee et al. 2014). However, they are amongst the most threatened and rapidly vanishing habitats on Earth (Polidoro et al. 2010; Richards & Friess 2016). The mangrove biome has already lost about 50% of its coverage since the 1950s for land conversion, deforestation, and habitat degradation (Feller et al. 2010). The International Union for Conservation of Nature (IUCN) has listed 40% of mangrove tree species as Threatened (Polidoro et al. 2010). Increasing anthropogenic pressures and anticipated sea level rise (SLR) are likely to alter the structure and functions of the remaining mangrove forests (Duke et al. 2007).

Making spatial predictions of biodiversity is important for pinpointing the locations or communities requiring immediate or long-term protection and conservation actions, in evaluating threats to those communities, and in monitoring spatial distributions and temporal dynamics in biodiversity (Socolar et al. 2015). A variety of biodiversity modelling approaches (e.g. stacked species distribution models, macroecological models, ordination, and stochastic models) (Ferrier & Guisan 2006; Mateo et al. 2017) have been applied to understand the spatial patterns of species richness and composition in different forest ecosystems (e.g. neo-tropical, boreal and temperate forests). However, their application to mangrove forests is limited (but see Record et al. 2013) due to the scarcity of field data (Ellison 2001), thus resulting in poor understanding of mangrove biodiversity patterns.

Each of the three established aspects of biodiversity (alpha, beta and gamma, Whittaker 1960) characterizes different fundamental attributes of natural communities which can be of specific conservation interest. For example, spatial maps of alpha diversity can help in specifying the most species rich (i.e. biodiversity hotspots) habitats while beta diversity maps can determine the most heterogeneous (i.e. distinct) communities. Thus far, mangrove biodiversity studies have mostly relied on alpha diversity, in particular, the species richness index

(Ellison 2001; Record et al. 2013; Osland et al. 2017) that does not account for the variability in species relative abundances (Shannon & Weaver 1949). At a regional scale, mangrove plant communities may look spatially homogeneous because mangrove forests are relatively species-poor compared to the upland tropical forests. In turn, at finer scales, considerable heterogeneity in species relative abundances becomes apparent (Farnsworth 1998). Therefore, in addition to the richness index, we need to consider heterogeneity in species relative abundances while measuring biodiversity indices (Barwell et al. 2015). Most importantly, looking at how different aspects of biodiversity respond to variations in environmental drivers is important for constructing more informative and practically useful biodiversity maps.

Constructing maps of biodiversity indices can help to investigate spatio-temporal variations in natural communities, to locate habitats or communities or species require immediate protection and to support spatially explicit conservation planning (Devictor et al. 2010). Both habitat-based and covariate-free (direct interpolation methods such as kriging) approaches are used for mapping biodiversity indices. Although covariate-free approaches have been criticized for low predictive ability (Granger et al. 2015), the relative performance of the approaches has rarely been tested using field data.

Testing the 'zonation' hypothesis (i.e. the distinct ordering of tree species along the shore-to-inland gradient, Ellison et al. 2000) and explaining the 'biodiversity anomaly' (i.e. why mangrove plant species richness drops along the latitudinal gradient, Ricklefs et al. 2006), have been the key agendas dominating the mangrove biodiversity literature in the last two decades. While such studies have substantially improved our insight on species sorting and richness, limited attention has been paid to understanding how abiotic, biotic and historical anthropogenic pressures have contributed to spatial variations in mangrove diversity and composition. Such knowledge gaps have obstructed the success of conservation initiatives in many tropical coastal regions (Lewis 2005), particularly in the Sundarbans (Islam et al. 2014).

Using a newly introduced abundance-based framework for biodiversity partitioning (Reeve et al. 2016) and a habitat-based biodiversity modelling approach, my main goal was to uncover the influences of fine-scale habitat conditions and historical

events in shaping the spatial distributions of mangrove alpha, beta and gamma diversity. My more specific questions included: What are the key drivers of mangrove biodiversity? How do the predictive abilities of environmental data-driven biodiversity models compare with those of covariate-free direct interpolation approaches? Where are the biodiversity hotspots in the Sundarbans currently located? Are these hotspots well protected? Finally, I discussed the potential applications of these novel insights and biodiversity maps for future mangrove research, biodiversity protection, monitoring, and spatial conservation planning.

4.3 Methods

4.3.1 Data collection

Tree and environmental data were collected from 110 PSPs (100 x 20 m, divided into 5 20 x 20 m subplots, Fig. 4.1) established by the Bangladesh Forest Department (BFD) in 1986. As part of the 2008 – 2014 surveys, my field team, together with the BFD tagged every tree (d.b.h ≥ 4.6 cm at 1.3 m from the ground) with a unique tree number and recorded tree counts for the PSPs. In total, we recorded 49409 trees from 20 mangrove species (Table 2.1, Chapter 2). The top four dominant species contributed to about 98% of the total count, indicating sporadic occurrences of many rare species in the ecosystem.

Environmental data were collected in 2014 (January – June). I collected 9 soil samples from each PSP (soil depth = 15 cm) implementing a soil sampling design (Fig. 2.2, Chapter 2) to account for the within-plot variations in soil variables. I then determined soil sand, silt and clay percentages, salinity, pH, oxidation reduction potential (ORP), NH_4, P, K, Mg, Fe, Zn, Cu and sulphide concentrations (see section 2.3.3 in Chapter 2). For each soil variable, I recorded the average reading from 9 soil samples. I retrieved elevation readings (above-average sea level) and calculated the "upriver position" (URP) for each PSP (Duke et al. 1998).
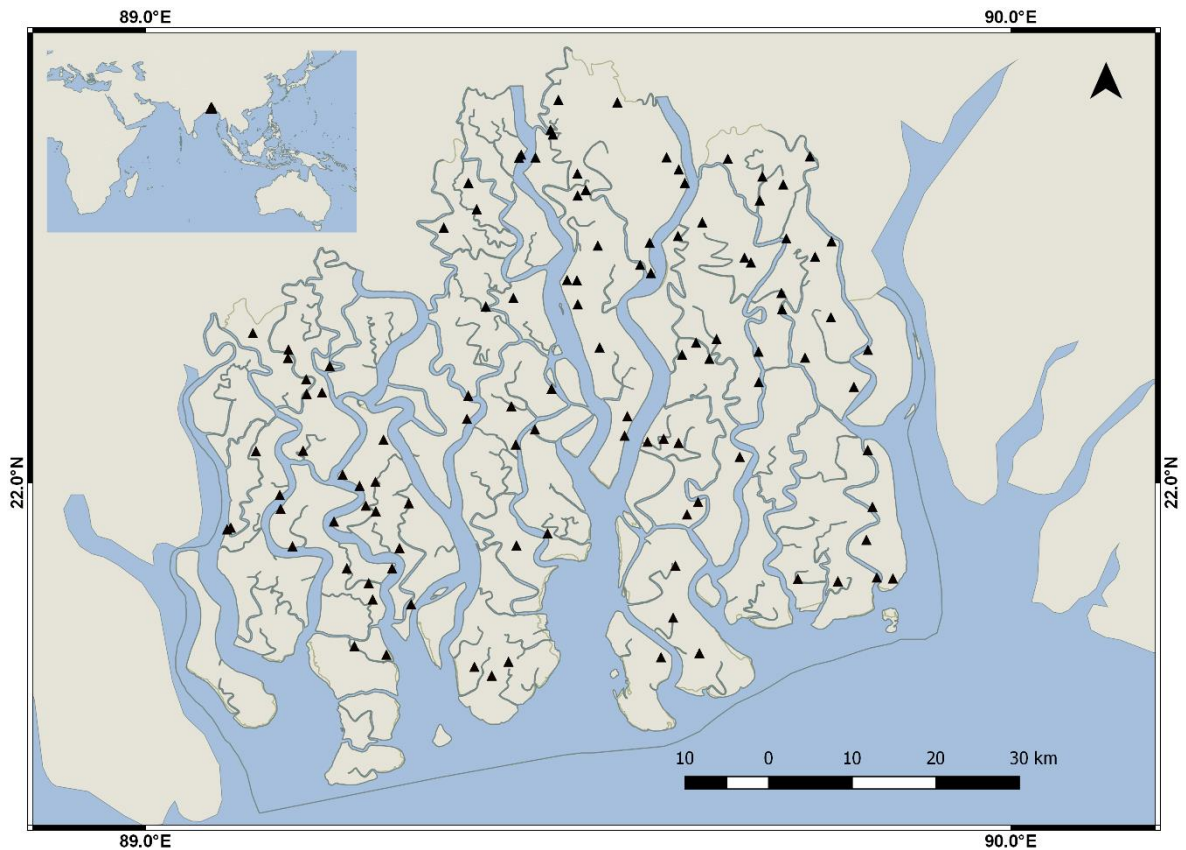
Fig. 4.1 Sampling sites (triangles) in the Sundarbans, Bangladesh. Blue areas represent water bodies.

4.3.2 Covariate selection

Similar to Chapter 1, here I followed the conceptual framework of Twilley & Rivera-Monroy (2005) to construct a biologically informative variable set for my mangrove biodiversity models. As described earlier in Chapter 2, this framework comprises three broad categories of variables (i.e. resources, regulators and hydroperiod) that are believed to explain vegetation structure and productivity in coastal mangrove forests. I selected three essential plant macro-nutrients (i.e. soil NH_4, P and K) as resource variables; soil salinity, pH and silt as regulators; and elevation as a simple proxy of hydroperiod.

Biotic interactions (e.g. competition or facilitation) between plants can influence species composition at a local scale (Howard et al. 2015). Competitive exclusion of weak competitors by superior competitors in stressed mangrove habitats may lead to species-poor mangrove communities dominated by a single or few

opportunistic species (Saenger 2002). To account for such influences, initially, I considered two candidate biotic variables: (1) 'community size' – total number of individuals in each PSP, and (2) total basal area in each PSP. Diversity models using the basal area as a covariate had lower explanatory powers, compared to models with 'community size (CS)'. Therefore, I selected CS as a proxy of biotic interactions.

I incorporated URP of each PSP in my covariate set to account for the influence of the river systems on species composition along the downstream — upstream gradient. In riverine estuaries, tidal inundation levels, soil physical and chemical properties can significantly vary along the riverbank — inner forest gradient (Berger et al. 2008) which influence colonization success and survival of mangrove plants. To account for such variations in estuarine settings, I included the straight-line distance of each PSP from the nearest riverbank (henceforth, DR).

Tropical coastal ecosystems are prone to both natural and anthropogenic disturbances (Sherman et al. 2000). Natural disturbances (such as tree disease and mortality) and anthropogenic disturbances (such as tree harvesting) offer rooms for tree recruitment through gap creation, thus influence vegetation composition (Duke 2001). Therefore, a clear understanding of community dynamics in mangrove forests is not possible without a comprehensive understanding of the historical and concurrent disturbance events. To account for the influences of natural and human disturbances on current diversity and species composition in the Sundarbans, I incorporated historical harvesting (HH) and disease prevalence (DP) as covariates in my models. Here HH and DP represent the total number of illegally harvested and diseased (for example, 'top dying' disease (dieback of the foliage and twigs in part of the crown) of *H. fomes*, 'heart rot' disease of *X. mekongensis* etc.) trees in each PSP from historical records (1986 to 2014). Finally, using Variance Inflation Factors (Robinson & Schumacker 2009), I checked for multi-collinearity in the covariates (Appendix 4A) and removed covariates leading to VIF greater than 2.5. This led to the removal of ORP from my covariate set (Appendix 4B).

4.3.3 Biodiversity partitioning

For partitioning biodiversity, I again applied the framework of Reeve et al. (2016). As in Chapter 3, each PSP represents a *subcommunity* (SC), and here the PSPs together (1 - 110) form the *metacommunity* (MC). This partitioning scheme allows us to understand and easily compare the diversity and species composition in every single SC in relation to the MC (the whole Sundarbans ecosystem) and again I measured SC alpha ($\overline{\alpha}$), beta ($\overline{\rho}$), and gamma (γ) diversity. I considered three values i.e. 0, 1 and 2 for the viewpoint parameter, *q,* and presented all my results using these three *q* values, writing them as $^{0}\overline{\alpha}$, $^{1}\overline{\rho}$, $^{2}\gamma$, etc.

4.3.4 Biodiversity modelling

I constructed generalized additive models (GAMs, Wood 2006) to quantify how different biodiversity components responded to different variables. Guided by data and using non-parametric smoothing functions, GAMs can capture response-predictors relationships without a priori knowledge of the functional form of these relationships (Guisan & Thuiller 2005). These advantageous features of GAMs are well suited for uncovering unknown biodiversity — environment linkages in dynamic ecosystems such as the Sundarbans where multiple environmental gradients have interactive effects on species distributions (Chapter 2). All analyses were done in R version 3.2.3 (R Core Team 2016). Biodiversity GAMs were built using cubic basis splines with the Gamma error distribution using the 'mgcv' package version $1.8 - 7$ (Wood 2011). Model selection and model averaging were carried out using the 'MuMIn' version 1.15.1 (Barton 2015) package.

I exhaustively fitted GAMs for each diversity index with all possible combinations of covariates. Then I ranked the fitted GAMs using the second-order AIC (AICc) because the ratio between sample size and the number of covariates was < 40 (Burnham & Anderson 2002). Models whose AIC_c had values less than 2 from the best model (ΔAIC_c <2) were retained as competing models (Burnham & Anderson 2002). The relative support for each of the competing models was then determined using their Akaike weights (AIC_{cw}, vary between 0 to 1, and the sum of all AIC_{cw} across the competing models is 1). To reduce model selection uncertainty and bias, I then conducted model averaging to predict the diversity indices. To determine the strength of the covariates, I ranked them based on their Relative

Importance (RI) values. RI of each covariate was calculated by totalling the AIC_{cw} of the models in which the covariate was included. RI values vary between 0 and 1, where 0 specifies that the target covariate is not included in any of the competing models while 1 means that the covariate is included in all competing models. I measured goodness-of-fit of the biodiversity models using the R^2 (coefficient of determination) statistic between the observed and estimated values of the diversity indices.

4.3.5 Biodiversity mapping

I applied two different approaches to make spatial biodiversity predictions. First, I used the habitat-based models (GAMs) and interpolated covariate surfaces to produce model-averaged predictions. Second, I used a direct interpolation method, ordinary kriging (OK), that simply relied on the empirical spatial autocorrelation between neighbouring PSPs (did not consider environmental covariates) to make purely spatial predictions. I compared these two approaches because environmental data collection is challenging, whereas tree surveys are conducted annually at the PSPs. Hence, it is useful to know how close the predictions of the habitat-based biodiversity models were compared to direct interpolation methods. The size of each grid-cell of the interpolated surfaces was 625 m^2 (25m x 25m). I compared the predictive abilities of GAMs with OK, using the normalized root mean square error (NRMSE) statistic resulting from a leave-one-out cross-validation (LOOCV) procedure. OK was performed using the 'gstat' package version 1.0 −26 (Pebesma 2004) in R.

As mentioned earlier, the largest mangrove protected area network (PAN) comprising three Wildlife Sanctuaries (WS) − East WS, West WS, and South WS, has been operational in the Sundarbans since the 1970s. To evaluate its capacity to support the remaining biodiversity hotspots in the Sundarbans, I superimposed this onto my spatial biodiversity maps. All the biodiversity maps were constructed using the 'raster' package version 2.4 − 18 (Hijmans 2015) in R.

4.4 Results

4.4.1 Habitat-based biodiversity models

The explanatory power and the goodness-of-fit of the alpha, beta and gamma diversity GAMs varied when I increased weight on species relative abundances (q = 0, 1 and 2) in the subcommunities (SCs). $^1\overline{\alpha}$ (Shannon entropy) GAM explained more deviance (DE = 71%) and showed better fit (Adj. R^2 = 0.71) compared to those for $^0\overline{\alpha}$ (species richness) and $^2\overline{\alpha}$ (Simpson's concentration) (Table 4.1), suggesting, for alpha diversity, the model with a moderate focus (q = 1) on species relative abundances in the SCs could capture more signal compared to the models that only considered species presence-absence (q = 0) or put more importance to the more dominant species (q = 2) in the SCs. Like $^1\overline{\alpha}$, the $^1\gamma$ GAM could capture more signal than $^0\gamma$ and $^2\gamma$ GAMs. In contrast, for beta diversity, with DE = 65% and Adj. R^2 = 0.70, the $^2\overline{\rho}$ GAM captured more signal than the $^0\overline{\rho}$ and $^1\overline{\rho}$ GAMs, implying that my covariates could more successfully explained the variability in species composition across the SCs when the variability was mostly contributed by more dominant species.

4.4.2 Drivers and responses of biodiversity components

The relative importance (RI) of the covariates in influencing biodiversity indexes also varied when I changed the weight on species relative abundances in the SCs. For example, while historical harvesting (HH) had no influence on $^0\overline{\rho}$ (possibly due to high number of shared species between SCs or HH did not lead to species extirpation), it had stronger effects on $^1\overline{\rho}$ and $^2\overline{\rho}$, indicating that the influence of past tree harvesting in shaping current community composition becomes clearer when I accounted for the variability in species relative abundances across the SCs.

In general, several abiotic and biotic drivers had combined effects on the spatial distributions of the biodiversity indexes. SC alpha diversity was mainly influenced by community structure (CS), upriver position (URP), distance to riverbank (DR) and silt (Table 4.1 and Appendix 4C). CS, URP, salinity, HH, silt and disease prevalence (DP) were the predominant drivers for spatial variations in SC beta

diversity. SC gamma diversity was mostly influenced by CS, URP, salinity, DR, HH, pH and silt.

Table 4.1 Results of GAMs for nine diversity measures. Summaries of model fit in rightmost three columns are only shown for the best model (DE = deviance explained). Numbers in the main part of the table (enclosed in box) represent the Relative Importance (RI) of each covariate. Dark-shaded cells highlight covariates that were retained in the best model for each biodiversity index. Light-shaded cells represent covariates retained in other models within the candidate set. Dashed boxes indicate no participation of that covariate in any of the candidate models. The covariate short-hands are: community size (CS), upriver position (URP), salinity, distance to riverbank (DR), historical harvesting (HH), acidity (pH), silt concentration, disease prevalence (DP), soil total phosphorus (P), soil potassium (K), elevation above average-sea level (ELE), and soil NH_4.

Diversity types		CS	URP	Salinity	DR	HH	pH	Silt	DP	P	K	ELE	NH$_4$	AICcw	DE (%)	Adj-R^2
Alpha	${}^0\bar{\alpha}$	1	1	--	0.57	0.40	--	0.08	0.06	--	0.34	--	--	0.16	41	0.45
	${}^1\bar{\alpha}$	1	1	0.20	1	0.82	0.80	1	--	0.80	0.80	--	--	0.42	71	0.71
	${}^2\bar{\alpha}$	1	1	0.28	0.15	0.11	0.40	--	--	1	0.72	0.42	--	0.28	68	0.65
Beta	${}^0\bar{\rho}$	0.71	0.21	1	0.58	--	--	--	0.94	0.66	0.61	--	--	0.12	51	0.51
	${}^1\bar{\rho}$	1	1	0.86	0.25	0.93	0.47	0.35	1	0.29	--	--	--	0.22	58	0.42
	${}^2\bar{\rho}$	1	1	0.84	0.46	1	0.84	1	0.84	0.83	0.67	--	0.46	0.37	65	0.70
Gamma	${}^0\gamma$	1	1	0.36	1	0.30	0.91	0.30	1	0.10	--	0.18	0.27	0.12	75	0.86
	${}^1\gamma$	1	1	1	1	1	1	1	0.35	0.65	--	0.65	0.65	0.65	86	0.90
	${}^2\gamma$	1	1	0.73	1	1	--	1	--	0.72	0.72	--	--	0.28	72	0.74

The partial response plots of the best alpha, beta, and gamma diversity GAMs (for $q = 0$, 1 and 2) showed similar relationships across the models (Fig. 4.2, Appendices 4D & 4E). While alpha diversity (for $^1\bar{\alpha}$) increased with increasing DR (> 1500 m) and URP (> 80%), it decreased with increasing HH (> 175 tree cuts/0.2 ha), silt (> 20%), CS (> 450 trees/0.2 ha) and pH (> 7.25). The response of alpha diversity varied for different nutrients. The K concentration that maximised $^1\bar{\alpha}$ was 5.5 gm Kg^{-1} while increasing soil P (> 35 mg Kg^{-1}) was related to decreasing $^1\bar{\alpha}$. Mangrove communities showed increasing representativeness (for $^2\bar{\rho}$) i.e. homogeneity in species composition with increasing HH (> 150 tree cuts/0.2 ha), silt (> 20 %), DP (> 25 diseased trees/0.2 ha), and CS (> 450 trees/0.2 ha). In contrast, communities showed decreasing representativeness i.e. increasing heterogeneity in species composition with increasing salinity (> 6.5 dS m^{-1}) and URP (> 70%). Gamma diversity (for $^1\gamma$) showed strong positive responses to increasing DR (> 1000 m), salinity (> 8 dS m^{-1}), and URP (> 70%), and negative responses to increasing HH (> 175 tree cuts/0.2 ha), silt (> 20%), CS (> 500 trees/0.2 ha) and pH (> 7.25).
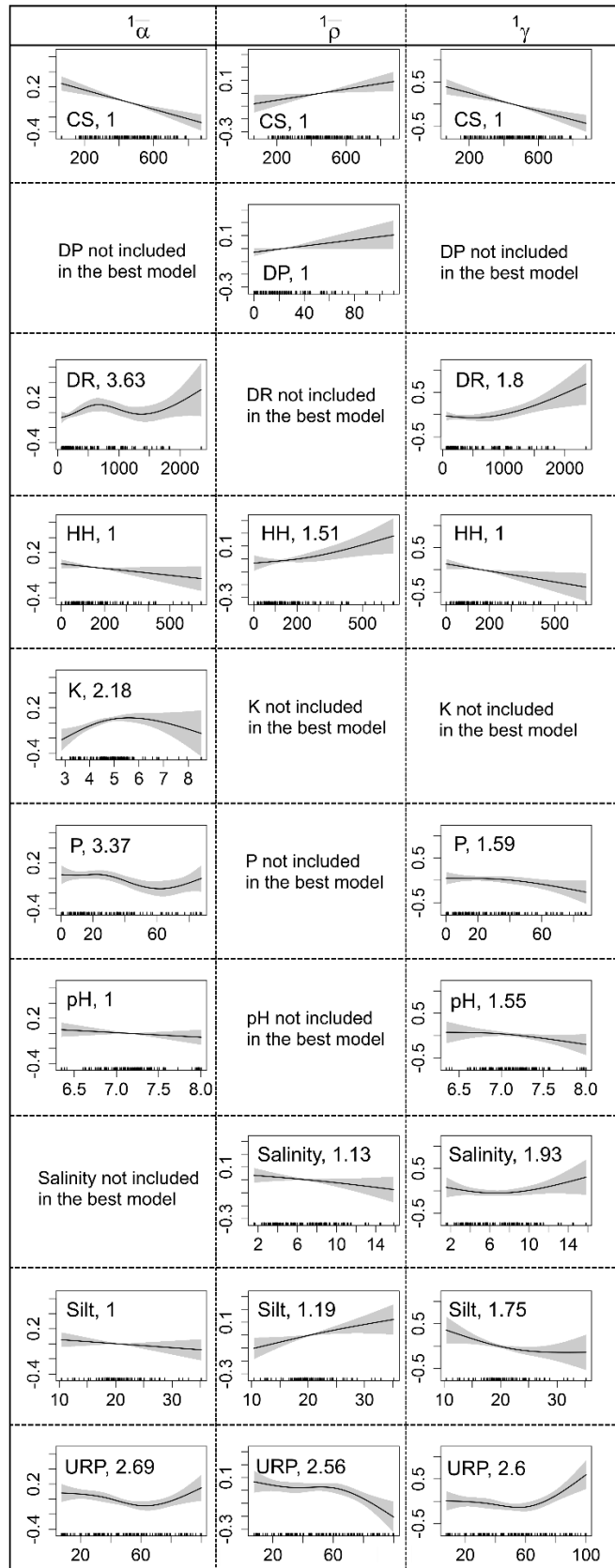
Fig. 4.2 Effects of covariates inferred from my best GAMs fitted to the biodiversity indices for q = 1. The solid line in each plot is the estimated spline function (on the scale of the linear predictor) and shaded areas represent the 95% confidence intervals. Estimated degrees of freedom are presented for each smooth following

the covariate names. Zero on the y-axis indicates no effect of the covariate on biodiversity index values. Covariate units: CS = total number of individuals in each plot, URP = % upriver, soil salinity = dS m^{-1}, DR = distance (m) of each plot from the riverbank, Historical harvesting (HH) = total number of harvested trees in each plot since 1986, silt (%), disease prevalence (DP) = total number of diseased trees in each plot since 1986, P = mg Kg^{-1} and K = gm Kg^{-1}.

4.4.3 Biodiversity maps

Spatial alpha, beta and gamma diversity maps produced via GAMs are presented in Fig. 4.3. Alpha diversity maps (first row) uncovered that hotspots in species richness ($q = 0$), Shannon entropy ($q = 1$) and Simpson's concentration ($q = 2$) were restricted to the northern (specifically the Kalabogi region) and eastern (specifically the Sharankhola region) Sundarbans. Beta (second row) and gamma (third row) diversity maps revealed that the entire Sundarbans looks homogeneous when I considered only species presence or absence ($q = 0$) i.e. not accounted for the between-species variability in relative abundances. Allowing increasing weight on species abundance ($q = 1$ and 2) revealed that the most heterogeneous (or distinct) mangrove communities and the communities that contributed most to the overall biodiversity of the ecosystem were restricted to the northern upstream habitat. Additionally, like my interpolated biodiversity maps in Chapter 3, habitat-based maps in this chapter show that the established protected area network (PAN) does not currently include the most diverse and distinct (i.e. biodiversity hotspots) mangrove communities. Prediction error was always reduced by the use of environmental covariates, but particularly for alpha and gamma diversity. Regarding beta diversity, while the predictive ability of the GAMs was better than that of kriging for $^{0}\overline{\rho}$ and $^{1}\overline{\rho}$, both approaches had similar prediction error (24%) for $^{2}\overline{\rho}$ (Table 4.2).
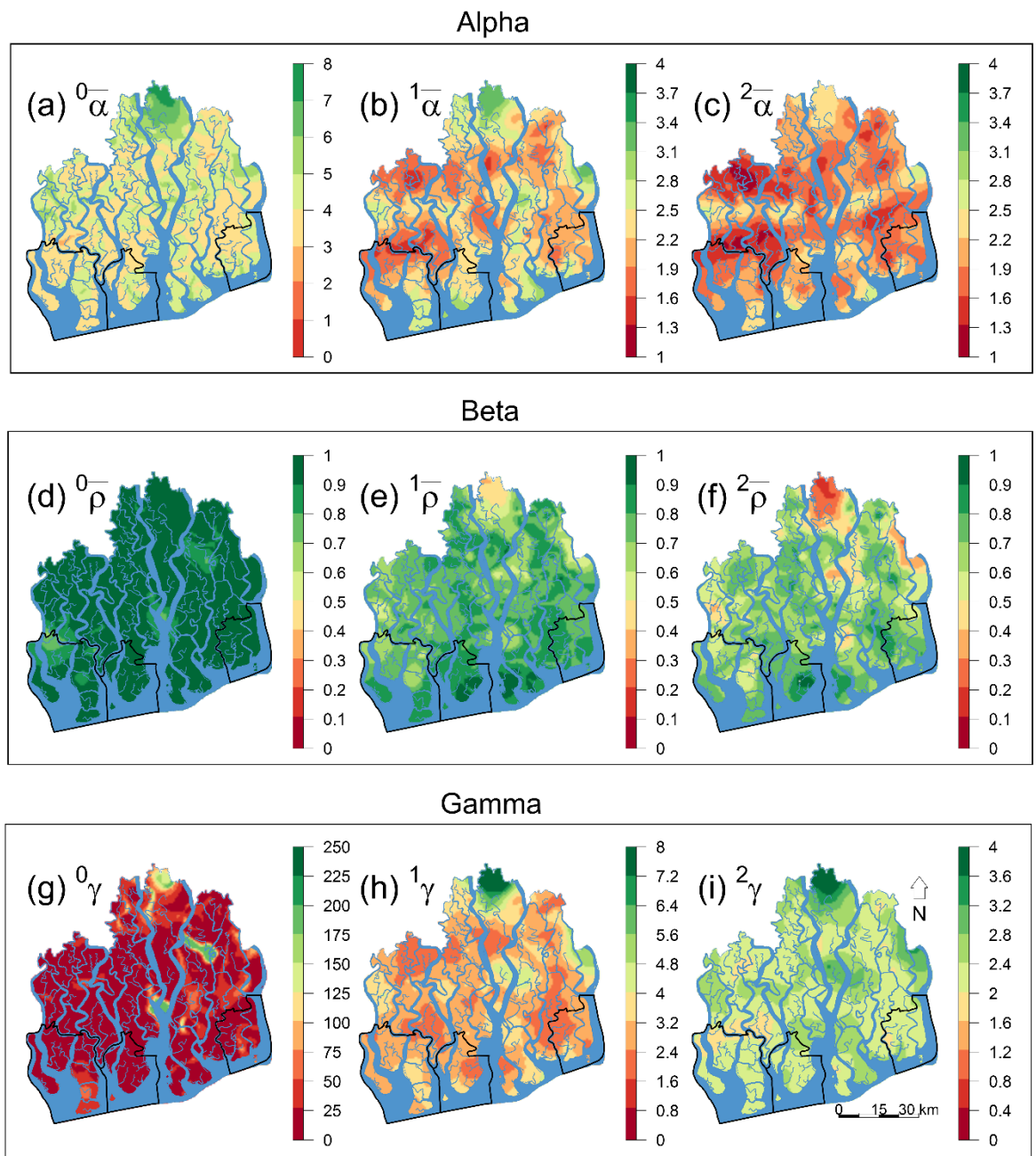
Fig. 4.3 Spatial distributions of SC alpha, beta and gamma diversities (for *q* = 0 - 2) over the entire Sundarbans generated through GAMs. Higher values of α and γ indicate greater species diversity and community contribution to the overall diversity of the ecosystem. Lower values of ρ indicate greater heterogeneity in species composition (i.e. community distinctness) and higher values of ρ represent greater representativeness (i.e. homogeneity) in species composition. The black contours represent the three protected areas.

Table 4.2 Comparison of predictive accuracy (through leave-one-out cross validation) of the habit-based (GAMs) and Kriged diversity models using

normalized root mean square error (NRMSE) of the predicted versus the actual diversity values. NRMSE is expressed here as a percentage, where lower values indicate less residual variance.

Diversity types		GAMs	Kriging
		NRMSE (%)	
Alpha	$^0\bar{\alpha}$	17	18
	$^1\bar{\alpha}$	14	16
	$^2\bar{\alpha}$	14	16
Beta	$^0\bar{\rho}$	21	24
	$^1\bar{\rho}$	19	22
	$^2\bar{\rho}$	24	24
Gamma	$^0\gamma$	13	17
	$^1\gamma$	10	11
	$^2\gamma$	11	13

4.5 Discussion

This chapter provides a baseline quantification and habitat-based modelling of all three aspects of biodiversity (alpha, beta and gamma) in threatened mangrove communities. Contrary to the common assumption that one or two straightforward environmental gradients (salinity and inundation) control mangrove biodiversity (Ellison 2001), my results highlight that several environmental drivers, biotic interactions and historical events have combined effects on spatial patterns of mangrove diversity and species composition. High explanatory and predictive power of the biodiversity models confirm their usefulness in constructing spatially explicit predictions of different aspects of biodiversity. The ability of the models to reveal previously unknown linkages between the biodiversity aspects and

abiotic, biotic and disturbance variables have yielded novel biological insights and thus now prompt many ecological questions for future studies.

4.5.1 Drivers and responses of biodiversity components

Inclusion of URP in the best biodiversity GAMs (with maximum RI scores, except URP for $^{0}\bar{\rho}$, Table 4.1), suggest strong influence of the downstream/upstream gradient in shaping spatial distributions of all aspects of biodiversity in the Sundarbans. Species diversity (alpha), SC contribution to the overall diversity of the ecosystem (gamma) and heterogeneity of the communities (beta) increased along the downstream/upstream gradient (URP > 65%), suggesting downstream and intermediate-stream areas are no more suitable for many salt-intolerant species (e.g. *H. fomes*) that were abundant in the past (Gopal & Chauhan 2006) while the most suitable habitats supporting widespread coexistence of salt-intolerant, salt-tolerant and rare species are currently restricted to the late successional upstream area, corroborating my individual species level findings in Chapter 2.

CS was also retained in all the best GAMs (with maximum RI scores), demonstrating the importance of including biotic variables in habitat-based biodiversity models. Increasing CS contributed to decreasing species diversity (alpha and gamma) and increasing homogeneity (representativeness), providing a strong signal for biotic filtering in harsh estuarine settings. From the response plots (Fig. 4.2, Appendices 4D & 4E), it appears that this pattern arises when SCs have > 450 trees. These SCs are, indeed, distributed in the western and south-western Sundarbans. Chapter 2 revealed the super dominance of *E. agallocha* and *C. decandra* in these mangrove communities. Ellison et al. (2000) showed negative associations between these generalists and facultative endemics, particularly, *H. fomes*. In fact, the super-dominant saturated communities can support higher numbers of small-diameter individuals (larger CS) that may not compete but offer limited space for new species to colonise and grow. On the other extreme, northern mangrove communities which are dominated by large-diameter, late-successional species (e.g. *H. fomes* and *X. mekongensis*) are usually less populated and support many rare endemics. These late-successional communities are more diverse and distinct than the densely-populated communities (Fig. 4.3).

My analyses uncovered a strong impact of HH and DP in shaping current distributions of the biodiversity components in the Sundarbans, implying the importance of integrating past disturbance events in habitat-based models for more accurate predictions. I found a significant negative effect of HH on alpha and gamma diversities, although DP had no visible effect. This discrepancy may be related to local extinction of many rare endemics during past formal and informal logging activities while DP that did not lead to species extirpation but reduced their relative abundances (Banerjee et al. 2017). However, for beta diversity, both HH and DP contributed to increasing homogeneity in species composition across the SCs (Fig. 4.2). This again indicates that the diseases have not infected all trees equally rather they have only infected and removed a few endemics such as *H. fomes* (top-dying disease) and *X. mekongensis* (heart rot disease) which have resulted in increasing homogeneity in the mangrove communities. Therefore, by using the approach of Reeve et al. (2016) to look at how DP simultaneously effects alpha, beta and gamma diversity, we are able to get indications of the pathogenicity of the disease (i.e. whether it is a generalist and infects and removes all species equally or if it is a specializes on specific host species). Mangrove habitats with past logging history are usually nutrient-poor, absorb higher amounts of heavy metals, and are prone to species invasion (Ngole-Jeme et al. 2016). Harvesting- and disease-induced tree mortalities have created large as well as small forest gaps in the Sundarbans. Intriguingly, the large diameter tree species (i.e. *H. fomes* and *X. mekongensis*) that still dominate the less saline habitats, recruit poorly in the forest gaps (Iftekhar & Islam 2004). Instead, these forest gaps are increasingly colonized by the disturbance specialists (e.g. *C. decandra*) (Mukhopadhyay et al. 2015). Therefore, increasing colonization and dominance of disturbance specialists in the historically disturbed SCs are the possible mechanisms responsible for increasing similarity among mangrove communities. This result somewhat contrasts with the Intermediate Disturbance Hypothesis which states that diversity of coexisting species is maximum at intermediate intensities of disturbance (Connell 1978).

Highly silted mangrove communities in the Sundarbans are not only poor in alpha and gamma diversities but also almost similar in species composition (Fig. 4.2). These results are in agreement with Mitra & Zaman (2016), reporting limited growth and regeneration of many mangroves due to sediment burial of aerial roots

in the Sundarbans. Sediment burial of aerial roots (inhibiting root aeration) is a major reason for worldwide mangrove mortality (De Deurwaerder et al. 2016). However, at the species level, the sensitivity of individual species to sediment burial can vary substantially. For example, Thampanya et al., (2002), in their experimental work on Thailand mangroves, observed 100% mortality in *Avicennia officinalis*, 70% in *Rhizophora mucronata*, and 40% in *Sonneratia caseolaris* under extreme sediment accretion level (32 cm). The Sundarbans is an active delta where the river network annually transports about 2.4 billion tons of sediments (Mitra & Zaman 2016). Therefore, future research is required to understand species-specific sensitivities and adaptations (e.g. modified rooting architecture) to siltation because this will help to forecast which species may colonize the newly formed islands, and which sites are compatible for replanting in future siltation scenarios.

Although in their pioneering work, Ellison et al. (2000) found no evidence for 'zonation' in the Sundarbans, I detected a clear pattern of increasing alpha and gamma diversities along the riverbank/forest interior gradient. Communities that are at least 1500 m away from the riverbank had higher alpha diversity and 800 m away had higher contribution to the overall ecosystem diversity compared to the near-bank communities, implying late successional forest interior communities were more diverse than the early successional riverbank communities.

Salinity has been considered a key limiting factor for species richness in coastal ecosystems (Feller et al. 2010). It appears from my analyses that salinity had no effect on species richness although the importance of salinity slightly increased for Shannon entropy and Simpson concentration, implying the role of salinity becomes clearer when I accounted for between-species variability in relative abundance. Regarding beta diversity, increasing salinity contributed to increasing compositional heterogeneity among the SCs (Fig. 4.2). This pattern suggests high plot-to-plot variation in composition in the degraded saline soils for population declines and range contraction of many salt-intolerant species (e.g. *H. fomes*) and increasing colonization success of the salt-tolerant generalists such as *E. agallocha* and *C. decandra* (Iftekhar & Saenger 2008; Aziz & Paul 2015; Mukhopadhyay et al. 2015).

Nitrogen (N), phosphorus (P), and potassium (K) were found to be the important soil nutrients limiting mangrove forest structure in many tropical coastal regions (Lovelock et al. 2006; Naidoo 2009; Da Cruz et al. 2013). Interestingly, these resource variables received less support in my biodiversity models, reconfirming the high importance of regulators and historical disturbances in structuring mangrove communities (Twilley & Rivera-Monroy 2005).

4.5.2 Mangrove biodiversity maps

GAM-based baseline biodiversity maps for the Sundarbans (Fig. 4.3) reveal that currently the most species-rich ($^0\overline{\alpha}$) tree communities are confined to the northern (specifically, Kalabogi) and eastern (specifically, Sarankhola) regions. Due to the proximity of Baleshwar and Posur rivers (Aziz & Paul 2015), these areas receive a greater amount of freshwater than the rest of the ecosystem which may help to keep them suitable for many salt-intolerant and rare plant species. The remaining ecosystem is relatively species-poor. $^1\overline{\alpha}$ (Shannon entropy) and $^2\overline{\alpha}$ (Simpson's concentration index) maps not only show similar patterns but also pinpoint the areas i.e. the north-western and south-western Sundarbans where the super-dominance of generalists has resulted in lower alpha diversity. These areas are prone to high salinity fluctuation and saltwater flooding throughout the year which together was found to inhibiting regeneration and growth of many plant species (Ghosh et al. 2016). Spatial variability in species composition becomes clearer when more weight was put on the dominant species ($^1\overline{\rho}, ^2\overline{\rho}$), compared to the rare species ($^0\overline{\rho}$). In general, the most distinct communities and the communities that contribute most to the overall biodiversity of the whole ecosystem ($^0\gamma,\ ^1\gamma,\ ^2\gamma$), are currently restricted to the northern upstream habitats housing many endangered tree species (Chapter 2). Like alpha diversity, the rest of the ecosystem also looks homogeneous in terms of species composition.

Restricted distributions of diverse and distinct mangrove communities in a few specific areas indicate for historical pressures on Sundarbans's floral composition, as reported by many (Gopal & Chauhan 2006; Aziz & Paul 2015; Ghosh et al. 2016). The freshwater supply from the transboundary rivers into the Sundarbans has substantially declined (3700 m^3/s to 364 m^3/s) since the construction of the Farakka dam (1974) in India (Mirza 1998). The average soil salinity has already

increased by 60% since 1980 (Aziz & Paul 2015). Illegal harvesting of trees and heavy siltation in the internal channels are ongoing (Rahaman et al. 2015). Chapter 2 results revealed that the coverage of distinct and diverse areas has substantially reduced in the Sundarbans over the 28 years. Findings in this Chapter lead me to conclude that additional harvesting, siltation, cuts in freshwater supply and range expansions of the generalists under projected SLR (Mukhopadhyay et al. 2015) may convert the whole Sundarbans into a species-poor homogeneous mangrove ecosystem.

The existing approaches for biodiversity mapping without including environmental data (i.e. (1) predicting diversity from stacked species distribution layers, and (2) estimating a diversity index in few sites and then predicting these estimated values for an entire study area using geostatistical interpolation methods) are shown to produce inaccurate spatial predictions of diversity indices (Granger et al. 2015). In this study, in general, the environmental data-driven GAMs showed better predictive ability than the covariate-free direct interpolation method (Table 4.2), thus, supporting the inclusion of fine-scale environmental, biotic and historical disturbance data for more accurate mapping of biodiversity indices. However, similar performances of these approaches in predicting $^2\bar{\rho}$, and small differences in prediction error for $^0\bar{\alpha}$ (species richness) and $^0\gamma$, indicates the utility of direct interpolation methods when environmental data are not available.

4.5.3 Conservation applications

SLR is likely to have drastic impacts on riverine and sea-dominated mangrove forests worldwide, particularly, the Sundarbans. Under the projected SLR range by 2100 (30 – 100 cm) which is significantly higher than the global range (26 – 59 cm) (Karim & Mimura 2008), the Sundarbans is likely to lose 10 – 23% of its present area (Payo et al. 2016) with alteration to soil biogeochemistry (Banerjee et al. 2017) and estuarine hydrology (Wahid et al. 2007). Given the severity of these future environmental impacts on Sundarbans' threatened plant communities, identifying the existing and future environmental stressors of mangrove biodiversity is important. This chapter identified siltation, soil salinity and pH as the dominant environmental stressors responsible for decreasing species diversity and community distinctness (Table 4.1, Fig. 4.2, Appendices 4D & 4E). These novel

habitat insights and baseline biodiversity maps have valuable applications in designing and implementing climate-smart mangrove enhancement (reducing abiotic stresses that caused mangroves' biodiversity loss), restoration (restoring specific areas where certain mangrove species/distinct assemblages previously existed) and reforestation initiatives in the Sundarbans. Previous studies (McKee & Faulkner 2000; Lewis 2005; Kodikara et al. 2017) show that considerable uncertainty remains in rebuilding the degraded mangrove habitats to their previous state. However, my results about the key stressors and their spatial distributions can help the forest managers about deciding which mangrove communities or which stressors to target for future reforestation and restoration initiatives.

My biodiversity maps (Fig. 4.3) again reveal that the established protected area network (PAN), covering 23% area of the entire Sundarbans, does not include the most diverse and distinct communities (i.e. biodiversity hotspots). With restricted distributions in the northern and eastern regions, these unique communities support the remaining populations of many globally endangered tree species (Chapter 2). These biodiversity hotspots are very close to the local communities and vulnerable to opportunistic tree harvesting (Iftekhar & Islam 2004), so this study suggests bringing them under protected area management for long-term conservation of the threatened species living there.

My results have important implications for devising nutrient enrichment programs in coastal ecosystems. The negative response of alpha diversity to increasing soil P and K concentrations suggest that the mangroves of the Sundarbans may suffer from nutrient toxicity in highly silted hypersaline habitats. Although nutrient enrichment programs were previously implemented in estuarine mangrove forests to support plant growth and development, such programs resulted in widespread mortality of many plant species worldwide (Lovelock et al. 2009). Therefore, this study suggests for taking extreme caution while implementing nutrient enrichment programs in the Sundarbans and elsewhere and also advocates for experimental and field-based studies that explicitly investigate the responses of individual mangrove species to nutrients under different environmental settings.

The biodiversity maps can guide the biodiversity protection and monitoring initiatives in the Sundarbans. Also, these maps can contribute to successful

implementation of the REDD+ (Reduced Emissions from Deforestation and Degradation) (Gardner et al. 2012) initiatives for enhancing carbon stock (through biodiversity conservation) as well as financial returns.

4.6 Conclusions

In this Chapter, I have provided a baseline quantification and habitat-based modelling of all three aspects of biodiversity (alpha, beta and gamma), to determine their drivers and to make predictions about their spatial patterning in the Sundarbans. I found that several environmental drivers, biotic interactions and historical events had combined effects on the biodiversity components. Specifically, historical harvesting, increasing community size, siltation, salinity intrusion, disease, soil alkalinity and nutrient toxicity were the dominant stressors responsible for reducing species diversity and community distinctness. Although habitat-based models showed better predictive ability than the covariate-free approach, the small margin of differences in predictive ability between the approaches demonstrates the utility of direct interpolation approaches when environmental data are unavailable. My baseline biodiversity maps uncovered that the most diverse and distinct mangrove communities (biodiversity hotspots), comprising many globally endangered tree species, had restricted distributions in the freshwater-dominated northern and eastern regions. Although these biodiversity hotspots are susceptible to human exploitation, they were not included in the existing PAN, thus suggesting for an immediate expansion of the protected area. I believe details on the drivers and their capacity to influence mangroves' diversity and composition, and the biodiversity maps, collectively, will contribute to designing and implementing climate-smart mangrove enhancement, restoration, reforestation and nutrient enrichment initiatives. Also, my maps can guide the existing and future mangrove biodiversity protection, monitoring and REDD+ initiatives. The existing PSP network covers 83% (20 out of 24) of the true mangrove species in the Sundarbans, suggesting that future studies may need to extend their sampling efforts beyond the current PSP network. Elevation, as a proxy of hydroperiod, received the least support in my models. Given that projected SLR is likely to alter the regional hydrology in the Sundarbans with changes in soil-biogeochemistry and tidal inundation, this study suggests adding hydroperiod as a predictor in future biodiversity models.

Chapter 5 . Solving the fourth-corner problem: Forecasts of functional traits and ecosystem productivity from spatial, multispecies, trait-based models

5.1 Abstract

Forecasting productivity and stress across an ecosystem is complicated by the multiple interactions between competing species even within a trophic level, the unknown levels of intraspecific trait plasticity and complex dependencies between those traits in individual trees. Integrating these factors requires a previously missing conceptual and quantitative synthesis of how multiple species and their functional traits interact with each other and with the various changing environmental attributes (an unresolved challenge known in community ecology as the "fourth-corner problem"). I proposed such a synthesis and applied it to the world's largest mangrove forest, the Sundarbans. This sentinel ecosystem is being impacted simultaneously by both climate change and multiple types of human exploitation. Across the ecosystem, I found extensive variability in environmental parameters, especially both relatively benign and extreme conditions of salinity and siltation, the former in upriver areas, the latter a result of damming of freshwater entering the ecosystem. I identified the retreat in growth-related traits and a plastic enhancement of survival-related traits, both clear indications of stress, and quantify both the trait-environment relationships involved and strong intraspecific trade-offs between traits, which vary between mangrove tree species. This Bayesian model allowed me to predict that if historical increases in salinity and siltation are maintained, whole-ecosystem productivity will decline by 30% by 2050. My spatially explicit modelling approach provides the foundations for trait-based predictions in plant ecology, bridges community and ecosystem ecology through simultaneously modelling trait-environment correlations and trait-trait trade-offs at organismal, community and ecosystem levels, and is readily applicable across the Earth's ecosystems.

5.2 Introduction

Understanding and predicting the effects of global environmental changes on the Earth's forest ecosystems is a core challenge confronting community ecology, ecosystem ecology, and the nascent field of functional biogeography. To address this challenge, the use of plant functional traits, rather than taxonomic identities, has gained momentum (Diaz et al. 2007; Kraft et al. 2008; Lavorel et al. 2011; Soudzilovskaia et al. 2013; Kunstler et al. 2015; Kraft et al. 2015; Faucon et al. 2017). Functional traits are any measurable morphological or physiological feature that may influence overall fitness or performance (e.g. growth, survival) of primary producers (Violle et al. 2007). In nature, productivity and stress levels of primary producers are affected by a complex causal network encompassing multiple functional traits, multiple species and multiple environmental drivers (Fig. 5.1).

Fig. 5.1 Productivity and stress levels in plant species are governed by community composition, functional traits and spatio-temporal environmental heterogeneity, but these three determinants also interact with each other in non-trivial ways.

Changes in traits via natural selection and species sorting (species elimination under persistent stress), may alter plant performance, community structure and primary production (Webb et al. 2010) but, again, natural selection and species sorting do not act independently on single traits, single species or as a result of single environmental stressors (Verberk et al. 2013). Therefore, attempting to model productivity and stress without integrating these complex dependencies between traits, species and the environment constricts our mechanistic insights and limits reliable predictions.

Linking trait(s) to environmental drivers has been a longstanding problem – known as "the fourth-corner problem" in community ecology (Legendre et al. 1997). For its resolution, ecologists have proposed trait-based approaches such as the fourth-corner correlation (Legendre et al. 1997; Dray & Legendre 2008), the multivariate RLQ (Dolédec et al. 1996; Dray et al. 2014), the Community Weighted trait Means (CWM) (Lavorel et al. 2007), and regression methods (Pollock et al. 2012; Jamil et al. 2012; Jamil et al. 2013; Brown et al. 2014; Warton et al. 2015). Among these, the fourth-corner correlation and RLQ approaches have received much historical attention (Kleyer et al. 2012). Using a combination of environmental (R), species (L) and trait (Q) data tables and permutation tests, these approaches look at pairwise associations between a single trait and single environmental variable using significance testing of association hypotheses. Ecologists routinely apply them for identifying the response traits i.e. 'traits that mediate the response of plant species to the environment' (Pakeman 2011). While such trait-based approaches hold promise (Funk et al. 2017), substantial methodological difficulties remain (Webb et al. 2010; Verberk et al. 2013; Dray et al. 2014) that limit their utility for community ecology, ecosystem ecology and functional biogeography. For example, detection of pairwise trait-environment relationships (TER) cannot detect the effect of multiple environmental drivers acting on the same functional trait, and significance testing says little about the strength of TER. Most importantly, they lack an integrated modelling framework to translate the TER into forecasts of community and ecosystem dynamics.

Recently proposed regression approaches relax these limitations by supporting model selection, validation, and quantitative predictions. They model species abundance (or presence-absence) as a function of traits and environmental

variables and their interaction terms (a product of a single trait with a single environmental variable) to describe TER (ter Braak et al. 2017). However, such approaches have focused on one species at a time (Jamil et al. 2012) and ignored intraspecific covariation between traits (Funk et al. 2017), hence not managing to account for the complex interactions between species, traits and the environment. This may be the cause of their limited predictive power (Funk et al. 2017; ter Braak et al. 2017). The CWM approach has been widely applied to directly correlate community level trait values with environmental variables (Peres-Neto et al. 2017). However, quantifying TER only using community level data, likely understates individual heterogeneity [aggregation bias, (Webb et al. 2010)], thus resulting in inaccurate TER quantification and inconsistent parameter estimations (Verberk et al. 2013; Peres-Neto et al. 2017). The shortcomings of existing trait-based approaches have raised concerns (Webb et al. 2010; Verberk et al. 2013; Violle et al. 2014; Funk et al. 2017) about how accurately they will forecast species, community and ecosystem responses under future environmental scenarios.

Trait distributions within individual species are nested within communities. These communities operate within their ecosystem context and respond dynamically to multiple environmental drivers (Webb et al. 2010). Thus, trait-based modelling frameworks that integrate the underlying concepts of TER, formalise ecological hypotheses [for example, habitat filtering (Weiher & Keddy 1995) and limiting similarity (MacArthur & Levins 1967; Chesson 2000) hypotheses] as models and test them in a single analysis using all data, can provide the foundations for trait-based predictions in plant ecology. This may also bring stronger theoretical linkages between community and ecosystem ecology. However, by looking at species, traits and the environment in a fragmented way, existing trait-based approaches offer limited scope for rigorous hypotheses testing, model selection and spatial predictions. We therefore need a synthetic approach for coexisting species, their traits, environmental variables and associated uncertainties.

In this Chapter, I have developed a spatially-explicit, Bayesian regression model that uses multiple explanatory variables (the environmental drivers) and multiple interacting responses (the different traits describing each of several species). My model accounts for intraspecific variations in traits, integrates fundamental

ecological hypotheses into the model-building process, offers model selection and generates spatial predictions for traits with associated estimates of uncertainty.

I applied the approach to the Sundarbans. This sea-dominated, dynamic ecosystem is ideal for testing mechanistic trait-based approaches because it comprises many globally endangered tree species that need to maintain their fitness under constant environmental stress (Chapter 2). I focused on nine prominent tree species [constituting 99% of the total tree populations in the Sundarbans, (Iftekhar & Saenger 2008)], eight prominent environmental drivers, and four key traits [canopy height (Height), specific leaf area (SLA), wood density (WD), and leaf succulence (LS)] covering the "leaf economic spectrum" (Wright et al. 2004) and the "wood economic spectrum" (Chave et al. 2009) and reflecting the "acquisitive − conservative continuum" (Reich et al. 1997; Grime et al. 1997; Díaz et al. 2015). Using my integrated approach, I asked: 1) Which set of theoretical hypotheses about trait responses to the environment, is best supported by the data? 2) How do the different traits of each species respond to the array of environmental drivers? 3) Is there covariation between the responses of functional traits? Finally, I explored the fate of the Sundarbans by developing trait and productivity maps under present and future environmental scenarios, with corresponding measures of prediction uncertainty.

5.3 Methods

5.3.1 Species, trait and environmental data

I collected data from 110 0.2 ha permanent sample plots (PSPs) covering the entire Sundarbans (Fig. 5.2) and recorded a total of 49409 trees from 20 species (Table 2.1, Chapter 2). The top four dominant species (i.e. *E. agallocha*, *H. fomes*, *C. decandra* and X. mekongensis) together contributed 98% of the total count. In this Chapter, I focused on species that occurred in > 5% of the PSPs.

I collected nine soil samples from each PSP (soil depth = 15 cm) implementing a novel soil sampling design (Fig. 2.2, Chapter 2) to account for within-plot variation in soil parameters and used the average value of the samples. My biologically informative variable set for the trait-based models comprised three broad categories of variables: (1) resources, (2) regulators and (3) disturbance (Guisan

& Thuiller 2005). Resource variables included NH4, P, and K, regulators include salinity, silt, pH, and upriver position (URP). URP (the proportional distance of a PSPs from the river-sea interface) accounts for the influence of the downstream — upstream gradient on species functions and composition (Duke et al. 1998). I used historical harvesting (HH, the total number of tree cuts in each PSP since 1986) as the disturbance variable to account for its possible influences on current species compositions and functions.
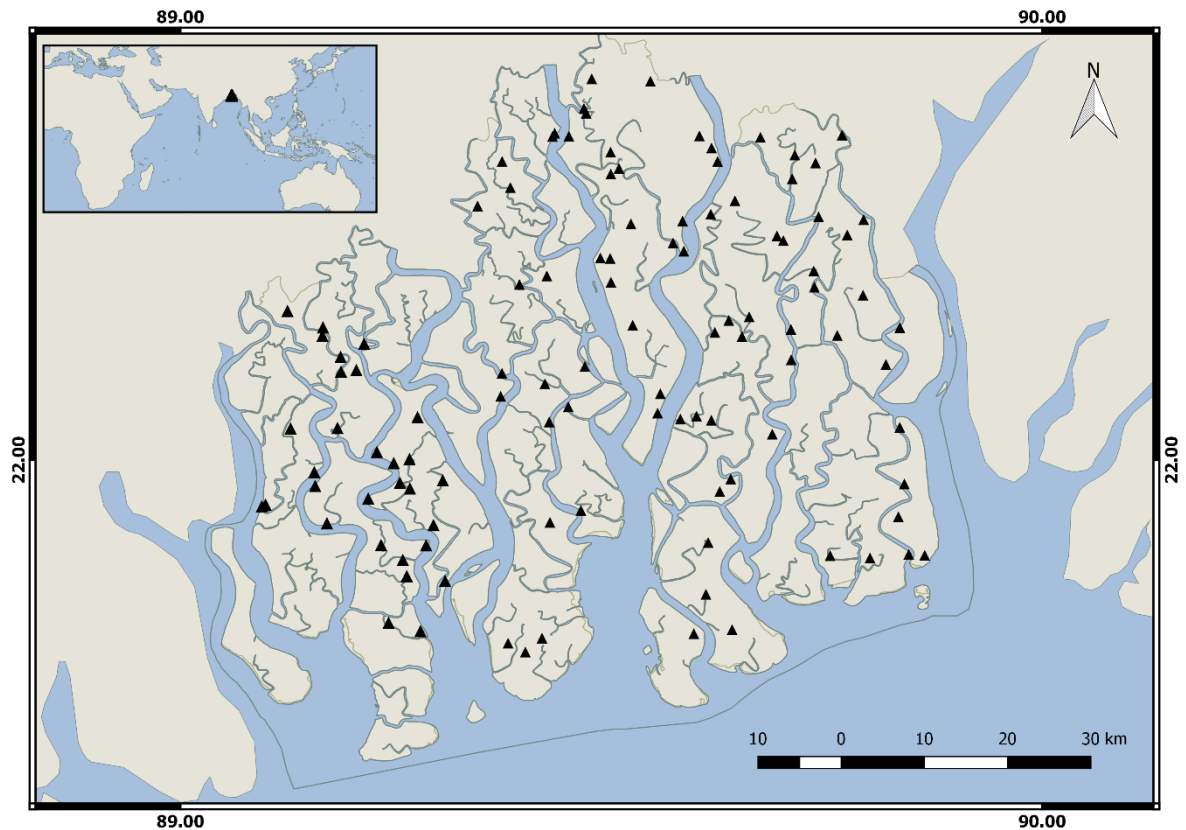
Fig. 5.2 Sampling sites (triangles) for species, environmental and trait data collection in the Sundarbans, Bangladesh. Blue areas represent water bodies.

I selected and measured four core functional traits — canopy height, wood density (WD), specific leaf area (SLA), and leaf succulence (LS). Height and SLA are growth stimulating traits that represent plant's acquisitive resource-use strategy. Height is central to a plant's resource (carbon) acquisition strategy for its role in regulating plant's ability to compete for light (Díaz et al. 2015). SLA reflects the efficiency of leaf for light capture per unit biomass invested, hence regulates the relative growth rate of trees (Pérez-Harguindeguy et al. 2013). In contrast, WD

and LS are survival-related traits that represent a plant's conservative resource-use strategy under stress. WD controls tree hydraulics, architecture, defence and growth potential. LS offers accumulation of water and dissolved ions in leaves under salinity stress. Therefore, LS is a prominent indicator of species' resistance to salinity and drought (Wang et al. 2011).

I measured all functional traits following standard trait measurement protocols (Pérez-Harguindeguy et al. 2013). From each PSP, I recorded trait measurements for 3 individual trees per species. For each tree, I collected a wood sample and at least three matured leaves from the sun-exposed branches for laboratory measurements. All trait samples, as well as the environmental data, were collected in 2014 (January – June). I determined canopy height (m) using a Suunto clinometer. For specific leaf area, I (1) measured green weights of the leaves immediately after collection in the field, (2) derived fresh area of the leaves using their images (captured by a digital camera — Nikon D5500) in Adobe Photoshop CS6, (3) quantified dry mass of the leaves using a digital balance (precision ~ 0.001 g) after keeping the green leaves in an oven at 65°C for 72 hours, and (4) calculated SLA as fresh leaf area (cm^2)/dry mass (g). Leaf succulence was calculated as leaf green mass (g) – leaf dry mass (g)/fresh leaf area (dm^{-2}) (Wang et al. 2011). For WD, I (1) collected wood cores using an increment borer, (2) estimated fresh volume of the cores using the formula of a cylinder ($V=\pi r^2 l$, where r = radius of the core, and l = length of the core), (3) quantified dry mass of the cores using a digital balance (precision ~ 0.001 g) after keeping the fresh cores in an oven at 105°C for 72 hours, and (4) calculated WD as dry mass (g)/fresh wood volume (cm^3).

5.3.2 Model development and inference

Using functional traits as response variables and environmental drivers as predictor variables, I developed a Bayesian hierarchical model to account for interactions between traits, between traits and environmental variables, and their variability across the species. The response and predictor variables were standardized to increase fitting robustness and facilitate comparisons between the strength of different effects. I started with a simple model assuming all constituent species of the ecosystem show a similar functional response to the environmental filters. Then, I iteratively increased the complexity of the model

and compared the performance of the models using the DIC (deviance information criterion), the Bayesian analog of the Akaike Information Criterion (Spiegelhalter et al. 2002). I obtained posterior distributions and 95% CI (credible intervals) for the parameters using Markov Chain Monte Carlo (MCMC) in the symbolic language JAGS version 4.2.0 (Plummer 2015) with the 'runjags' interface version 2.0.2 - 8 (Denwood 2016) in software R version 3.2.3 (R Core Team 2016) (JAGS codes for the models are in Appendix 5F). To evaluate the convergence of the two MCMC chains, I inspected the trace plots and ensured that the potential scale reduction factor (Gelman-Rubin statistic) for all monitored parameters was < 1.05 (Gelman et al. 2004). For reducing the chance of any relic effects of initial values, I discarded the first 5000 samples as burn-in and then simulated two independent MCMC chains for 60000 iterations. Spatially explicit trait and fine-scale environmental data on tropical and sub-tropical coastal ecosystems are exceedingly rare (Ellison 2001). Indeed, credible previous trait and environmental data on the Sundarbans are unavailable. Therefore, I used non-informative priors in all models to allow data to dominate posterior parameter estimation. For assessing the goodness-of-fit of the best model, I used R^2 values from regressions of observed vs. predicted traits.

5.3.3 Mapping traits and productivity

Using kriged surfaces (Appendix 2B, Chapter 2) of the environmental variables, the best Bayesian model predicted functional trait distributions for the four most prominent species (together contributed 98% of the total count). Then, using previously derived species density maps (Fig. 2.4, Chapter 2), I averaged the summed posterior trait values of each species weighted by their relative abundance in each grid cell to produce community trait maps for the entire ecosystem.

To develop whole-ecosystem biomass productivity maps, I first built species-specific trait-based productivity models. I then linked these models with the species traits and density maps to generate productivity predictions. I modelled biomass productivity of individual trees (taking basal area as a proxy) as a linear function of the functional traits using a GLM framework. I fitted all possible candidate models with all possible combinations of predictor variables. I then used the 'ΔAIC ≤ 2' criterion (Burnham & Anderson 2002) to determine a set of

competing models and performed model averaging to predict plot level species-specific productivity. Finally, I linked the GLM approach with the Bayesian mean posterior trait surfaces and species density predictions to produce spatial productivity maps for the whole ecosystem.

5.3.4 Forecasting traits and productivity

Salinity intrusion and siltation have strong influences on species abundances and community composition in the Sundarbans (Chapters 2, 3 & 4). The SLR rate along the Bangladesh coast in the 20th century was significantly higher than the global average. The soil salinity level has already increased by 60% since 1980 due to drop in freshwater supplies from the transboundary rivers (Aziz & Paul 2015). Assuming continuation of such historical pressures which may further affect plant functions via physiological stress and shifting relationships among species, I updated the environmental and species distribution maps for five future stress scenarios (E1 = 10, E2 = 20, E3 = 30, E4 = 40 and E5 = 50% increase in salinity and siltation), and then used them to forecast traits and forest productivity under these novel environments. Here, I considered E5 as the worst stress scenario for the ecosystem by 2050.

To evaluate the robustness of these forecasts, I used samples from the joint posterior distribution of all model parameters to simulate traits and productivity distributions for both current and future environmental scenarios. Using these simulations, I then mapped the posterior probability of deterioration of traits [a decrease in growth (Height and SLA) trait values and an increase in survival (WD and LS) trait values] and productivity at each grid cell, averaged across all grid cells in the ecosystem, in response to each of the future stress scenarios, to uncover the uncertainty related to my forecasts. All maps were generated using the 'raster' package version 2.4 – 18 (Hijmans 2015) in R.

5.4 Results

5.4.1 Integrated modelling approach

My approach is an extension of the multivariable regression models typically used to quantify species-habitat associations (Elith & Leathwick 2009) on the basis of one response and multiple explanatory variables. I have augmented this approach by allowing it to model several interdependent response variables (multiple functional traits from multiple species), using a Bayesian hierarchical modelling framework. This allowed a single model, fitted simultaneously to all my data, to capture TER for 4 traits, 9 tree species, and 8 environmental drivers, while accounting for trade-offs between different traits. Based on this inferential template, several trait-based models (Fig. 5.3) were developed, prompted from the viewpoints of distinct ecological hypotheses. Conducting formal model selection among these competing versions of the model, allowed me to understand how TER can differ across species, to generate species-specific and community-wide trait predictions, and finally to translate these spatial predictions into spatial forecasts of whole-ecosystem productivity.

Initially, the traits of all constituent tree species were assumed to respond identically to environmental drivers (Model I, my base model), formulating the hypothesis that extreme habitat filtering drives different species to show similar functional responses in stressful environments (Weiher & Keddy 1995). This was challenged with two alternative hypotheses. In Model II, I incorporated variability in trait-trait relationships (TTR) for different species to capture the effects of taxonomic variability on trait plasticity. On the other hand, to formalise the consequences of the 'limiting similarity' hypothesis (MacArthur & Levins 1967; Chesson 2000), in Model III I allowed trait responses to environmental drivers (the trait-environment relationships, TER) to vary across species, implying that resource partitioning and specialization (morphological or physiological) cause different coexisting species to show dissimilar functional responses to environmental drivers . Fig. 2 shows the relative quality of fit of the trait-based models in terms of the deviance information criterion (DIC) (Spiegelhalter et al. 2002). Both models very strongly improved DIC over Model I (ΔDIC > 1000), with Model III being preferred and therefore selected for future model comparisons (but see Model VIII below).
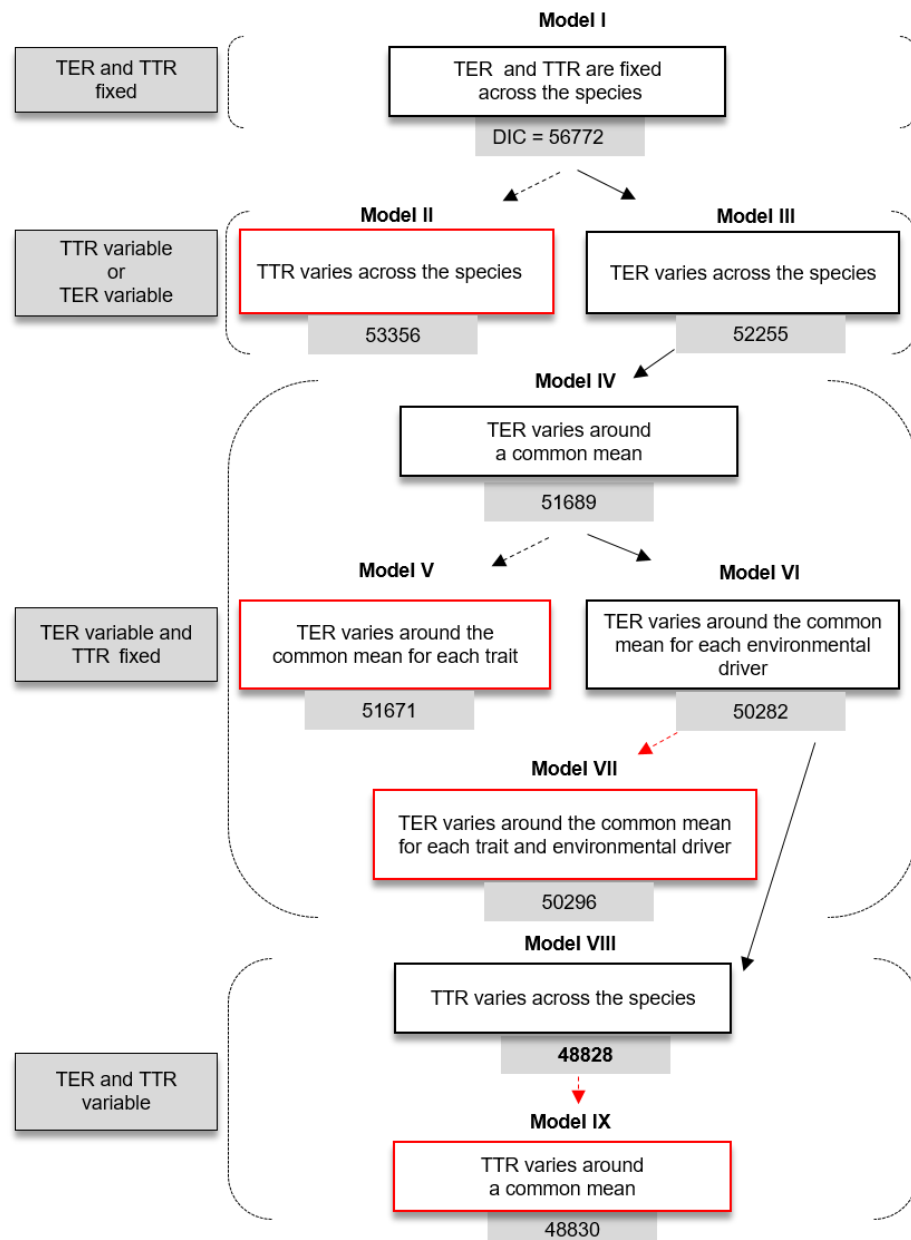
Fig. 5.3 Flow chart of the different ecological hypotheses compared via model selection. The different versions (I to IX) of my model were constructed by partitioning the variability in the data in different ways to estimate trait-environment relationships (TER) across multiple species by taking account of the intraspecific trait-trait relationships (TTR) at various hierarchical levels. The performances of the trait-based models were evaluated using DIC (the deviance information criterion, whose numerical value is displayed under each model), with arrows denoting tests made. Black arrows indicate that a new model improved DIC over the older model, red did not, solid arrows point to new models that were selected (the models outlined in black). Dashed arrows point to new models that were not selected (the models outlined in red).

In extreme environments such as mangrove forests, species can usually tolerate a certain level of stress via specialization (Feller et al. 2010). Hence, it is likely that all species show an average functional response to environmental filters. Nevertheless, the strength of the response around that average may vary for different species and for different traits depending on how severe the stress conditions are and how one trait facilitates or constrains another.

I incorporated these ecological hypotheses into models IV to VII. Model IV tested the hypothesis that although the mangrove species differed in their response to the environmental drivers regarding their traits, that variability is around a common interspecific average response. This model was also strongly preferred (ΔDIC > 500), so the next models investigated the variability around that mean. Model V tested whether the amount of variability around the mean is different for each trait and Model VI tested whether it is different for each environmental driver. Model V was weakly preferred over Model IV (ΔDIC > 10), but Model VI was very strongly preferred (ΔDIC > 1000), so Model VI was selected. Model VII then tested whether the amount of variability around the average response is also different for each trait (as Model V), but it was not preferred over Model VI.

This completed my analysis of the trait-environment relationships, so Model VIII tested whether the TTR is different for each species (recapitulating Model II, which was set aside in favour of Model III). This was still very strongly preferred (ΔDIC > 1000), so Model IX (analogously to Model IV) tested whether, although the TTR is different for each species, that variability is around a common interspecific mean. Model IX was not preferred over Model VIII, indicating that there was no common mean for the trait-trait relationships.

5.4.2 Model comparison summary

Model VIII (DIC = 48828) which is nested within Models I, III, IV and VI, was identified as the preferred model (ΔDIC > 1000 for all models it was nested within), showing evidence that tree species growing in a stressed ecosystem like a mangrove forest have a typical functional response to the environmental filters with inter-specific variability around this average, and the amount of variability is further contingent upon the nature and magnitude of the filters. I further

observed inter-specific variability in trait-trait relationships across the species, but the data provided no evidence for further patterns within the TTRs.

The explanatory power of the best model was high (regressions of observed vs. predicted trait values yielded — canopy height: R^2 = 0. 68, specific leaf area: R^2 = 0.64, wood density: R^2 = 0.94 and leaf succulence: R^2 = 0.67) and plots of predictions vs. observations indicate that the model made unbiased predictions (Appendix 5A). The potential scale reduction factor (Gelman-Rubin statistic) for all monitored regression parameters was < 1.05, indicating model convergence.

5.4.3 Drivers of functional traits

Soil salinity and siltation are the dominant environmental drivers that limit species canopy height (Fig. 5.4, Table 5.1). However, the intensity of such detrimental effects varies across the species. Salt-induced drop in canopy height is highest in the most prominent tree species (*H. fomes*) of the ecosystem [posterior mean ϕ = -0.59, 95% CI = (-0.69, -0.50)]. In contrast, increasing URP (i.e. more available freshwater) favours height increase in many species, including the pioneer species *S. apetala* [ϕ = 0.18, 95% CI = (0.05, 0.32)] and the climax *H. fomes* [ϕ = 0.16, 95% CI = (0.08, 0.24)]. Soil pH, salinity, siltation, and K have limiting effects on specific leaf area (SLA) of many species. In contrast, I identified a strong positive response of SLA to URP and NH4 – suggesting that nitrogen-rich upstream habitats favour plants' resource-acquisition in tropical coastal environments.

While the growth traits (Height and SLA) show a strong negative response to increasing salinity, siltation and pH, I discovered a clear positive response of the survival traits (WD and LS) to these dominant environmental filters (Fig. 5.4, Table 5.1), suggesting a substantial growth-survival trade-off across the species. Nevertheless, the strength of this positive response or positive filtering (adaptive shifts in trait values to increase resistance to stress) varies across the species, trait types, and environmental drivers. For example, salinity is the dominant positive filter for *H. fomes* [ϕ = 0.19, 95% CI = (0.15, 0.22)], siltation for *B. sexangula* [ϕ = 0.12, 95% CI = (0.04, 0.20)] and pH for *X. mekongensis* [ϕ = 0.11, 95% CI = (0.07, 0.15)] in terms of WD, while salinity is the predominant positive filter for LS and the filtering is highest in *X. mekongensis* [ϕ = 0.34, 95% CI = (0.25, 0.43)].
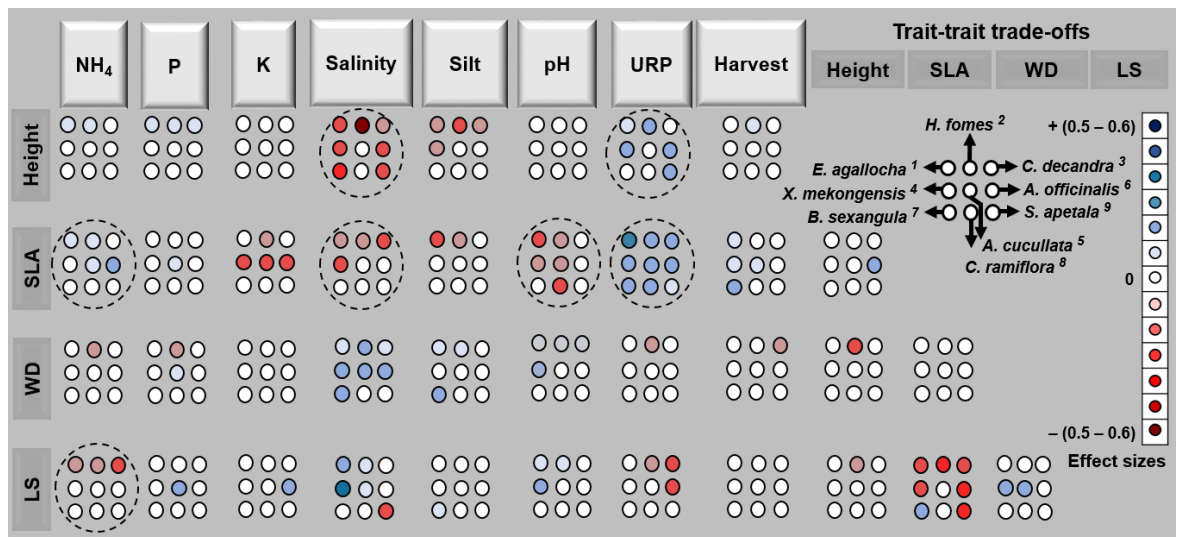
Fig. 5.4 Effects of environmental drivers (URP = upriver position) on the functional traits (Canopy height = Height, SLA = specific leaf area, WD = wood density, LS = leaf succulence) and intraspecific covariation among the functional traits. Each circle represents a species. Species are ordered (left to right, then top to bottom) based on their overall abundance (e.g. *E. agallocha*[1] is the most abundant and *S. apetala*[9] is the least abundant species). The fill-colours of the circles indicate the type and strength of the trait response (red for a negative response and blue for a positive one, see scale on right). A dashed circle around all 9 species indicates that the average species trait response to this environmental driver is strong (negative or positive, i.e. 95% credible intervals do not include 0). Regarding intraspecific covariation among the traits, the colour gradient represents the posterior correlations between traits. Posterior means and 95% credible interval values for the parameters are presented in Tables 5.1 and 5.2.

5.4.4 Covariation among the functional traits

SLA and LS show negative associations in most species (Fig. 5.4, Table 5.2), and for *H. fomes* I found broader trade-offs between growth and survival traits. I also noticed an apparent facilitation between the growth traits in *A. officinalis*, and between the survival traits in *X. mekongensis* and *A. cucullata*.

Table 5.1 Posterior mean and 95% credible intervals of the standardized regression coefficients from the best model (Model VIII), representing the effects of the environmental drivers on canopy height (CH), specific leaf area (SLA), wood density (WD) and leaf succulence (LS) of nine tree species in the Sundarbans. Average CH, SLA, WD and LS responses across species are included at the bottom of the table. The highlighted numbers indicate a significant response to each driver: red for a negative and blue for a positive response. Here, I defined significance as the event of the 95% credible intervals not including 0.

Species	Traits	NH$_4$	P	K	Salinity	Silt	pH	URP	Harvesting
E. agallocha	CH	0.05 (0.00; 0.10)	0.08 (0.03; 0.13)	-0.04 (-0.09; 0.01)	-0.20 (-0.26; -0.15)	-0.08 (-0.13; -0.04)	0.02 (-0.03; 0.06)	0.09 (0.04; 0.15)	0.00 (-0.05; 0.05)
	SLA	0.10 (0.02; 0.17)	0.04 (-0.03; 0.12)	-0.06 (-0.13; 0.02)	-0.09 (-0.17; 0.00)	-0.11 (-0.18; -0.03)	-0.15 (-0.23; -0.08)	0.26 (0.18; 0.35)	0.10 (0.02; 0.18)
	WD	-0.01 (-0.03; 0.01)	-0.02 (-0.05; -0.01)	0.00 (-0.03; 0.02)	0.06 (0.04; 0.09)	0.04 (0.02; 0.06)	0.03 (0.01; 0.05)	-0.02 (-0.05; 0.01)	-0.02 (-0.05; 0.01)
	LS	-0.07 (-0.13; 0.02)	0.03 (-0.03; 0.09)	0.00 (-0.06; 0.06)	0.12 (0.06; 0.19)	-0.04 (-0.09; 0.02)	0.10 (0.05; 0.16)	-0.02 (-0.09; 0.04)	-0.04 (-0.10; 0.02)
H. fomes	CH	0.08 (0.01; 0.15)	0.08 (0.01; 0.16)	-0.05 (-0.12; 0.02)	-0.59 (-0.69; -0.50)	-0.14 (-0.21; -0.07)	-0.05 (-0.13; 0.01)	0.16 (0.08; 0.24)	0.10 (0.02; 0.18)
	SLA	0.06 (0.02; 0.09)	0.01 (-0.02; 0.05)	-0.05 (-0.09; -0.02)	-0.06 (-0.10; -0.02)	-0.06 (-0.09; -0.03)	-0.06 (-0.09; -0.02)	0.18 (0.14; 0.22)	-0.04 (-0.08; 0.01)
	WD	-0.05 (-0.08; 0.02)	-0.01 (-0.04; 0.02)	0.01 (-0.02; 0.05)	0.19 (0.15; 0.22)	0.08 (0.05; 0.11)	0.07 (0.04; 0.10)	-0.04 (-0.07; 0.01)	0.00 (-0.03; 0.04)
	LS	-0.03 (-0.07; 0.01)	0.00 (-0.04; 0.04)	0.00 (-0.04; 0.04)	0.04 (0.01; 0.08)	0.02 (-0.01; 0.05)	0.05 (0.02; 0.08)	-0.08 (-0.11; 0.04)	0.00 (-0.04; 0.03)
C. decandra	CH	0.01 (-0.01; 0.03)	0.03 (0.01; 0.05)	0.00 (-0.02; 0.02)	-0.04 (-0.07; -0.02)	-0.03 (-0.06; -0.01)	0.01 (-0.01; 0.03)	0.01 (-0.03; 0.04)	-0.01 (-0.04; 0.03)
	SLA	0.00 (-0.04; 0.04)	0.01 (-0.02; 0.05)	0.01 (-0.02; 0.04)	0.01 (-0.03; 0.04)	-0.02 (-0.06; 0.02)	-0.03 (-0.06; 0.01)	0.14 (0.09; 0.20)	-0.04 (-0.10; 0.02)
	WD	-0.01 (-0.04; 0.03)	0.00 (-0.04; 0.03)	0.00 (-0.03; 0.04)	0.09 (0.06; 0.13)	0.01 (-0.03; 0.05)	0.03 (0.00; 0.06)	0.02 (-0.03; 0.07)	-0.05 (-0.11; 0.01)
	LS	-0.15 (-0.24; 0.07)	0.07 (-0.01; 0.14)	0.02 (-0.05; 0.09)	0.03 (-0.06; 0.13)	0.03 (-0.06; 0.12)	0.04 (-0.03; 0.12)	-0.18 (-0.30; 0.07)	-0.01 (-0.12; 0.10)

X. mekongensis	CH	0.01 (-0.05; 0.08)	0.05 (-0.02; 0.12)	0.00 (-0.07; 0.07)	-0.15 **(-0.21; -0.08)**	-0.10 **(-0.16; -0.03)**	0.04 (-0.02; 0.10)	0.14 **(0.07; 0.21)**	-0.05 (-0.13; 0.02)
	SLA	0.05 (-0.02; 0.12)	0.04 (-0.04; 0.11)	-0.13 **(-0.21; -0.05)**	-0.12 **(-0.20; -0.05)**	-0.01 (-0.08; 0.06)	-0.09 **(-0.16; -0.03)**	0.15 **(0.08; 0.23)**	0.08 **(0.01; 0.16)**
	WD	0.01 (-0.04; 0.06)	0.03 (-0.01; 0.08)	0.01 (-0.04; 0.06)	0.13 **(0.08; 0.17)**	-0.01 (-0.06; 0.04)	0.11 **(0.07; 0.15)**	0.04 (-0.01; 0.09)	0.00 (-0.05; 0.06)
	LS	-0.04 (-0.13; 0.04)	0.02 (-0.06; 0.11)	0.01 (-0.07; 0.09)	0.34 **(0.25; 0.43)**	-0.07 (-0.15; 0.02)	0.11 **(0.03; 0.19)**	-0.03 (-0.12; 0.06)	-0.07 (-0.16; 0.02)
A. cucullata	CH	0.00 (-0.06; 0.06)	0.00 (-0.06; 0.08)	-0.01 (-0.07; 0.05)	0.01 (-0.07; 0.08)	-0.06 (-0.13; 0.01)	0.00 (-0.06; 0.07)	-0.02 (-0.09; 0.04)	-0.05 (-0.12; 0.03)
	SLA	0.10 **(0.03; 0.16)**	0.08 **(0.01; 0.16)**	-0.11 **(-0.18; -0.04)**	-0.15 **(-0.24; -0.07)**	0.07 (-0.01; 0.16)	-0.07 **(-0.15; 0.00)**	0.16 **(0.08; 0.23)**	0.09 **(0.01; 0.18)**
	WD	-0.03 (-0.09; 0.02)	0.09 **(0.02; 0.15)**	0.04 (-0.02; 0.11)	0.12 **(0.04; 0.20)**	0.04 (-0.03; 0.11)	-0.01 (-0.08; 0.06)	-0.04 (-0.10; 0.03)	-0.07 (-0.14; 0.01)
	LS	-0.05 (-0.13; 0.03)	0.16 **(0.06; 0.26)**	-0.01 (-0.10; 0.07)	0.11 **(0.01; 0.22)**	0.03 (-0.07; 0.12)	-0.03 (-0.12; 0.06)	-0.07 (-0.16; 0.02)	0.05 (-0.05; 0.15)
A. officinalis	CH	0.05 (-0.06; 0.18)	0.04 (-0.09; 0.16)	-0.03 (-0.13; 0.08)	-0.15 **(-0.30; -0.07)**	0.00 (-0.11; 0.12)	0.05 (-0.08; 0.18)	0.13 **(0.00; 0.26)**	-0.05 (-0.17; 0.07)
	SLA	0.15 **(0.04; 0.25)**	0.05 (-0.06; 0.16)	-0.11 **(-0.19; -0.02)**	0.08 (-0.02; 0.18)	-0.01 (-0.11; 0.08)	-0.04 (-0.16; 0.07)	0.14 **(0.04; 0.24)**	0.00 (-0.10; 0.10)
	WD	-0.01 (-0.07; 0.06)	-0.01 (-0.08; 0.06)	0.03 (-0.03; 0.09)	0.02 (-0.03; 0.07)	0.00 (-0.06; 0.05)	0.02 (-0.06; 0.10)	0.04 (-0.02; 0.10)	0.01 (-0.06; 0.08)
	LS	-0.05 (-0.16; 0.06)	-0.03 (-0.14; 0.09)	0.14 **(0.04; 0.26)**	-0.06 (-0.18; 0.05)	-0.03 (-0.13; 0.07)	0.01 (-0.11; 0.13)	-0.14 **(-0.25; 0.02)**	-0.02 (-0.12; 0.09)
B. sexangula	CH	-0.04 (-0.16; 0.09)	0.03 (-0.10; 0.15)	-0.05 (-0.16; 0.07)	-0.23 **(-0.36; -0.09)**	-0.02 (-0.12; 0.08)	0.01 (-0.10; 0.12)	0.12 (-0.01; 0.25)	-0.06 (-0.17; 0.04)
	SLA	0.05 (-0.08; 0.17)	0.00 (-0.14; 0.13)	-0.06 (-0.18; 0.06)	0.07 (-0.11; 0.26)	0.02 (-0.11; 0.15)	-0.02 (-0.14; 0.12)	0.19 **(0.04; 0.35)**	0.17 **(0.03; 0.32)**
	WD	0.02 (-0.09; 0.12)	0.07 (-0.04; 0.18)	0.06 (-0.04; 0.15)	0.11 **(0.01; 0.20)**	0.12 **(0.04; 0.20)**	0.03 (-0.06; 0.13)	0.05 (-0.07; 0.16)	-0.02 (-0.10; 0.06)
	LS	-0.03 (-0.13; 0.08)	0.02 (-0.08; 0.13)	0.03 (-0.06; 0.12)	0.01 (-0.08; 0.11)	0.10 **(0.03; 0.18)**	0.00 (-0.10; 0.09)	0.01 (-0.10; 0.14)	-0.05 (-0.11; 0.03)
C. ramiflora	CH	0.06 (-0.02; 0.15)	0.00 (-0.09; 0.11)	-0.02 (-0.13; 0.08)	0.00 (-0.15; 0.15)	0.00 (-0.06; 0.06)	0.00 (-0.10; 0.11)	-0.02 (-0.11; 0.07)	-0.03 (-0.09; 0.03)
	SLA	0.03 (-0.07; 0.13)	0.05 (-0.07; 0.16)	-0.09 (-0.21; 0.02)	-0.03 (-0.22; 0.15)	0.06 (-0.03; 0.15)	-0.12 **(-0.24; 0.00)**	0.16 **(0.05; 0.27)**	-0.03 (-0.10; 0.05)

	WD	0.03 (-0.07; 0.12)	0.07 (-0.04; 0.19)	0.05 (-0.06; 0.16)	0.04 (-0.12; 0.22)	0.03 (-0.05; 0.10)	0.04 (-0.07; 0.15)	0.00 (-0.10; 0.10)	0.03 (-0.04; 0.10)
	LS	-0.06 (-0.15; 0.02)	-0.07 (-0.18; 0.03)	0.00 (-0.10; 0.10)	-0.02 (-0.16; 0.12)	-0.03 (-0.09; 0.03)	-0.01 (-0.11; 0.09)	-0.01 (-0.10; 0.08)	0.00 (-0.06; 0.05)
S. apetala	CH	0.08 (-0.04; 0.22)	0.11 (-0.02; 0.25)	-0.05 (-0.17; 0.05)	-0.18 **(-0.33; -0.03)**	0.02 (-0.13; 0.16)	-0.03 (-0.16; 0.10)	0.18 **(0.05; 0.32)**	-0.01 (-0.16; 0.13)
	SLA	0.02 (-0.08; 0.12)	0.07 (-0.03; 0.17)	0.01 (-0.06; 0.08)	-0.04 (-0.11; 0.04)	-0.02 (-0.14; 0.10)	-0.02 (-0.11; 0.07)	0.07 **(0.01; 0.16)**	0.02 (-0.11; 0.16)
	WD	0.00 (-0.11; 0.11)	-0.01 (-0.12; 0.09)	-0.01 (-0.08; 0.07)	0.04 (-0.04; 0.11)	0.03 (-0.08; 0.15)	0.03 (-0.06; 0.13)	0.00 (-0.08; 0.08)	-0.02 (-0.15; 0.12)
	LS	-0.08 (-0.20; 0.04)	0.07 (-0.04; 0.19)	0.04 (-0.05; 0.13)	-0.14 **(-0.25; -0.03)**	0.10 (-0.03; 0.23)	-0.03 (-0.15; 0.08)	-0.02 (-0.12; 0.09)	-0.02 (-0.15; 0.13)
Average effect	CH	0.03 (-0.02; 0.08)	0.04 (-0.01; 0.09)	-0.03 (-0.07; 0.02)	-0.11 **(-0.19; -0.03)**	-0.04 (-0.09; 0.01)	0.01 (-0.05; 0.06)	0.07 **(0.02; 0.13)**	-0.02 (-0.07; 0.04)
	SLA	0.05 **(0.01; 0.10)**	0.03 (-0.02; 0.09)	-0.06 **(-0.11; -0.01)**	-0.02 (-0.10; 0.05)	-0.01 (-0.06; 0.04)	-0.06 **(-0.11; -0.01)**	0.13 **(0.07; 0.20)**	0.03 (-0.02; 0.09)
	WD	0.00 (-0.05; 0.04)	0.02 (-0.03; 0.07)	0.02 (-0.02; 0.06)	0.05 (-0.02; 0.13)	0.03 (-0.02; 0.08)	0.03 (-0.01; 0.08)	0.00 (-0.05; 0.06)	-0.01 (-0.06; 0.04)
	LS	-0.06 **(-0.11; 0.01)**	0.03 (-0.03; 0.08)	0.02 (-0.03; 0.07)	0.03 (-0.05; 0.11)	0.01 (-0.04; 0.06)	0.02 (-0.03; 0.08)	-0.05 (-0.11; 0.01)	-0.02 (-0.07; 0.04)

Table 5.2 Intraspecific covariation among the traits. Blue numbers indicate significant positive and red numbers indicate significant negative posterior correlations between traits. Here, I defined significance as the event of the 95% credible intervals not including 0.

Species	Height – SLA	Height - WD	Height - LS	SLA - WD	SLA - LS	WD - LS
E. agallocha	-0.03 (- 0.11; 0.04)	-0.06 (-0.18; 0.04)	0.03 (-0.06; 0.10)	-0.01 (-0.11; 0.07)	**-0.15 (-0.25; -0.06)**	0.06 (-0.04; 0.13)
H. fomes	0.05 (-0.03; 0.13)	**-0.19 (-0.33; -0.09)**	**-0.1 (-0.22; -0.01)**	-0.02 (-0.14; 0.08)	**-0.27 (-0.45; -0.14)**	0.09 (-0.02; 0.17)
C. decandra	-0.06 (-0.24; 0.07)	-0.10 (-0.29; 0.04)	-0.03 (-0.17; 0.08)	-0.08 (-0.26; 0.05)	**-0.19 (-0.35; -0.07)**	0.06 (-0.06; 0.14)
X. mekongensis	-0.03 (-0.17; 0.06)	-0.08 (-0.26; 0.04)	-0.06 (-0.19; 0.02)	0.05 (-0.08; 0.15)	**-0.20 (-0.36; -0.08)**	**0.13 (0.03; 0.21)**
A. cucullata	-0.03 (-0.28; 0.12)	-0.04 (-0.3; 0.11)	-0.07 (-0.30; 0.08)	-0.17 (-0.47; 0.01)	-0.05 (-0.27; 0.08)	**0.18 (0.02; 0.27)**
A. officinalis	**0.14 (0.02; 0.21)**	0.02 (-0.20; 0.13)	-0.07 (-0.23; 0.03)	-0.11 (-0.44; 0.09)	**-0.29 (-0.60; -0.11)**	0.17 (-0.04; 0.28)
B. sexangula	0.01 (-0.15; 0.11)	-0.10 (-0.46; 0.09)	0.01 (-0.32; 0.17)	-0.07 (-0.29; 0.06)	**0.19 (0.05; 0.26)**	0.22 (-0.06; 0.35)
C. ramiflora	0.00 (-0.54; 0.21)	-0.02 (-0.62; 0.21)	-0.12 (-1.0; 0.16)	-0.10 (-0.62; 0.12)	-0.05 (-0.67; 0.18)	-0.18 (-0.95; 0.09)
S. apetala	0.08 (-0.24; 0.21)	0.05 (-0.29; 0.19)	-0.1 (-0.40; 0.06)	-0.08 (-0.93; 0.18)	**-0.30 (-0.90; -0.01)**	0.24 (-0.10; 0.36)

5.4.5 Trait and productivity maps

My integrated Bayesian approach offers species-specific as well as community-wide spatial trait predictions under current and future stress scenarios regarding salinity intrusion and siltation, and link them with the trait-based productivity models to forecast ecosystem productivity. It further evaluates the robustness of such forecasts by propagating parameter uncertainty through sampling from the joint posterior distribution of all model parameters and simulating traits and productivity distributions for both current and future stress scenarios.

Spatial maps (Fig. 5.5) revealed that the most productive tree communities are currently distributed in the freshwater dominated eastern and northern Sundarbans. If historical increases in salinity and siltation are maintained, my model predicts a significant productivity loss over the entire ecosystem under all future stress scenarios (10, 20, 30, 40 and 50% increase in salinity and siltation) (Fig. 5.6A) although there is the possibility of local productivity gains in a few of the communities, particularly under the least stress future scenarios (Appendix 5B). The worst stress scenario (a 50% rise in salinity and siltation) is predicted to push the ecosystem to lose 30% of its current total productivity by 2050 (Fig. 5.6A).
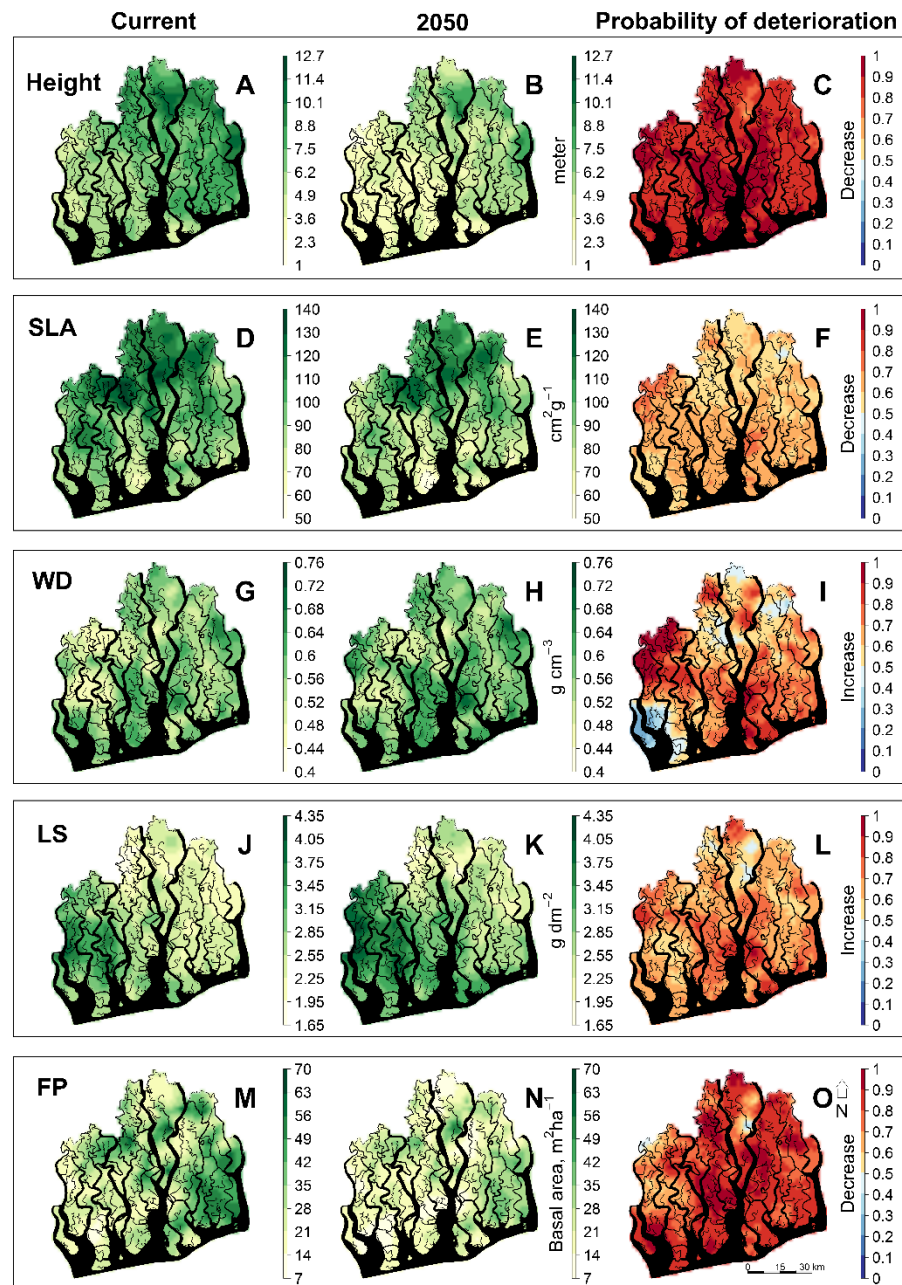
Fig. 5.5 Current status (first column) and worst-case scenario for the year 2050 (second column), of community-weighted posterior mean of tree canopy height (Height), specific leaf area (SLA), wood density (WD), leaf succulence (LS) and forest productivity (FP) in the Sundarbans world heritage ecosystem. Uncertainties related to these forecasts are mapped as the posterior probability of deterioration (see section 5.3.4 and Appendices 5B & 5C) in the third column. Deterioration is considered to be a decrease in productivity and growth trait (Height and SLA) values, or an increase in survival trait (WD and LS) values.
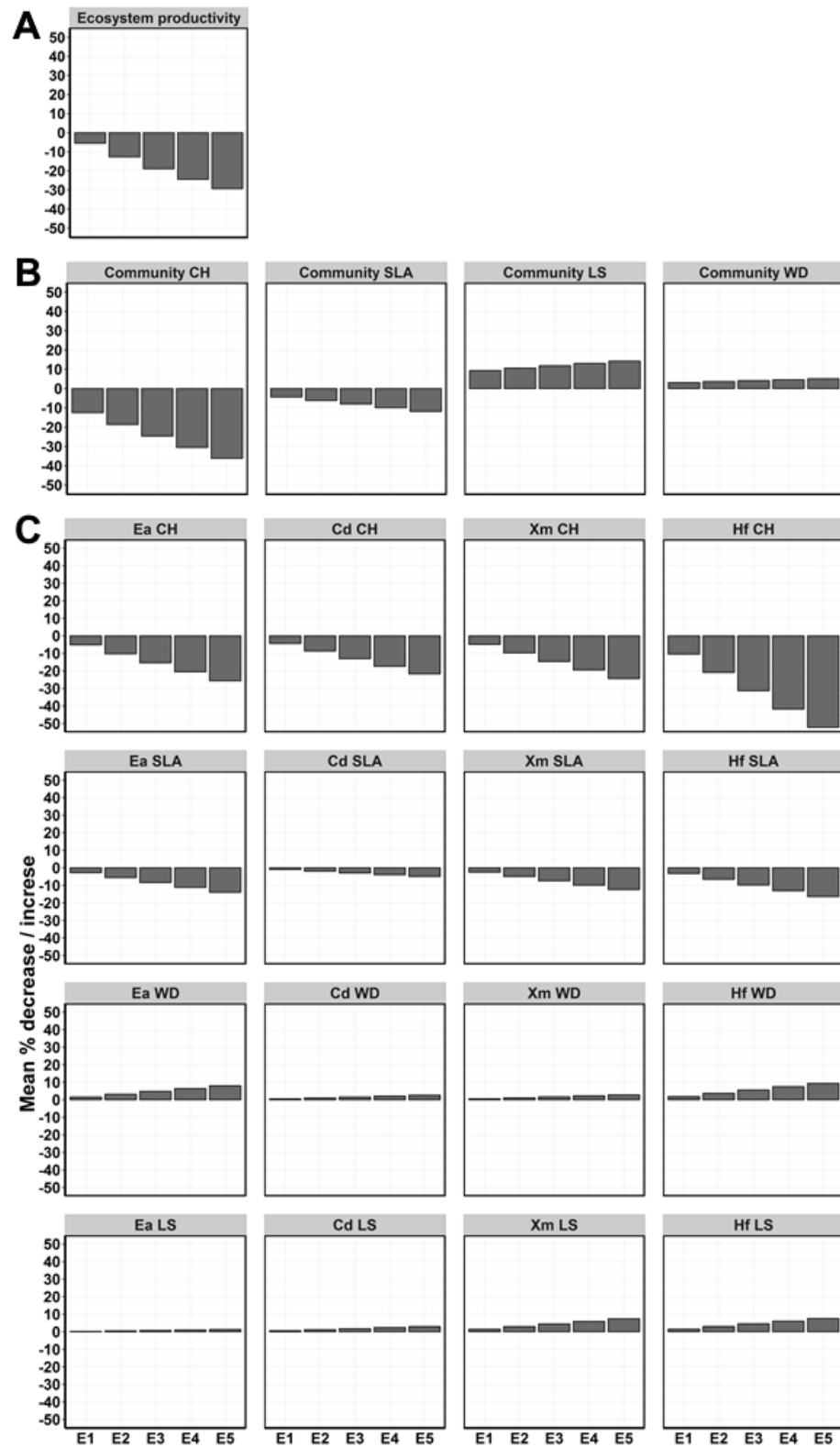
Fig. 5.6 Bar charts show the response of the ecosystem to each of five future stress scenarios, E1 to E5, representing a 10% to 50% increase in both salinity and siltation for the whole Sundarbans ecosystem by 2050. (A) shows mean percentage decline in whole ecosystem productivity; (B) shows mean percentage decline in community canopy height (CH) and community specific leaf area (SLA), and increase in community wood density (WD) and community leaf succulence (LS);

(C) shows mean percentage decline in CH and SLA, and increase in WD and LS for four prominent mangrove tree species under five future stress scenarios. The species short-hands are *Excoecaria agallocha* (Ea), *Ceriops decandra* (Cd), *Xylocarpus mekongensis* (Xm) and *Heritiera fomes* (Hf). Decreases in CH and SLA and increases in LS and WD are considered to be deteriorations in the traits.

The eastern and northern regions currently support the tallest mangrove communities. However, if the habitat degradation trend is continued, it is highly likely that these tallest communities will turn into dwarf communities, following an average of 36% height loss by 2050 (Fig. 5.6B, Appendix 5C). In turn, I predict a community-wide increase in the values of LS (14%) and WD (5%) – indicating highly plastic responses of the mangrove species to ensure efficient water use and mechanical support under the extreme stress scenarios, by 2050. Community SLA showed more stable patterns between time-points.

My species-specific trait predictions (Figs. 5.7, 5.8, 5.9 & 5.10) further determined that although every constituent species of the ecosystem will lose height under the future stress scenarios, the loss will be substantially higher for the climax species *H. fomes* (52%) by 2050 (Fig. 5.7, Appendix 5D). The increase in WD (9%) is also highest for this species. In turn, the disturbance specialist species ─ *C. decandra* - which is expected to undergo ecosystem-wide range expansion by 2050 (Appendix 5E), loses the least amount of height and SLA, compared to others.
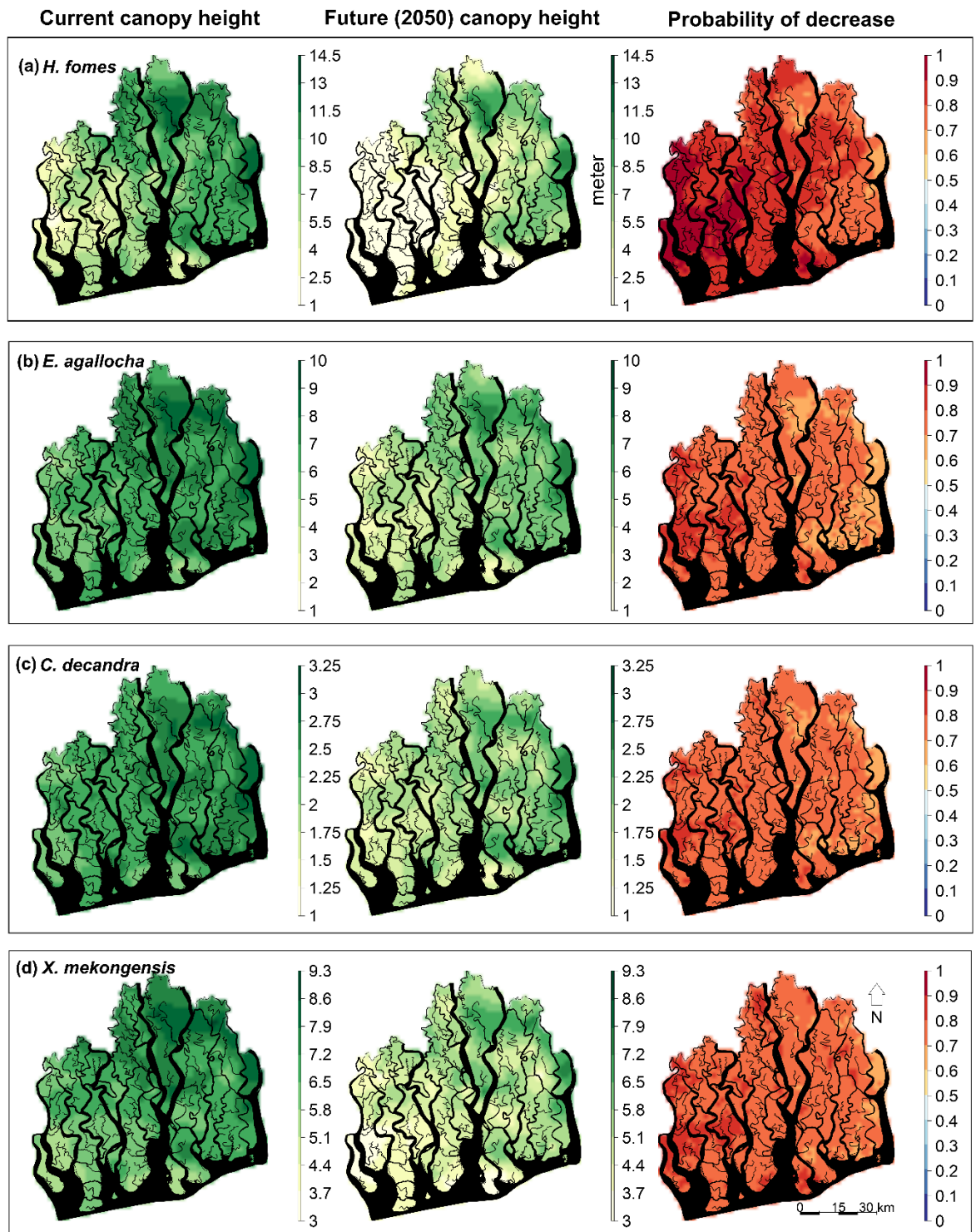
Fig. 5.7 Current status (first column) and worst-case scenario for the year 2050 (second column), of posterior mean of tree canopy height for four prominent mangrove tree species in the Sundarbans world heritage ecosystem. Uncertainties related to these forecasts are mapped as the posterior probability of a decrease in canopy height in the third column.
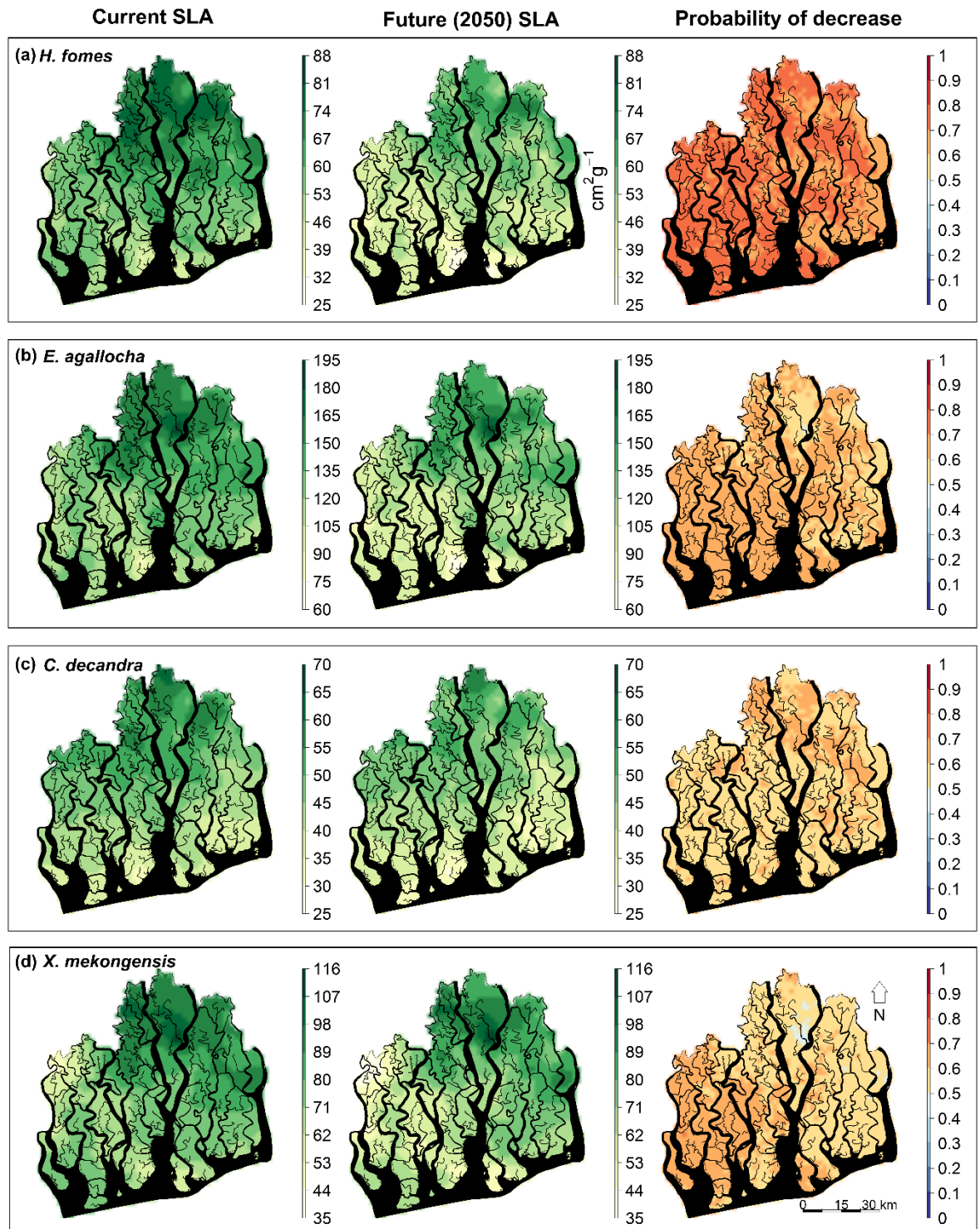
Fig. 5.8 Current status (first column) and worst-case scenario for the year 2050 (second column), of posterior mean of tree SLA for four prominent mangrove tree species in the Sundarbans world heritage ecosystem. Uncertainties related to these forecasts are mapped as the posterior probability of a decrease in SLA in the third column.
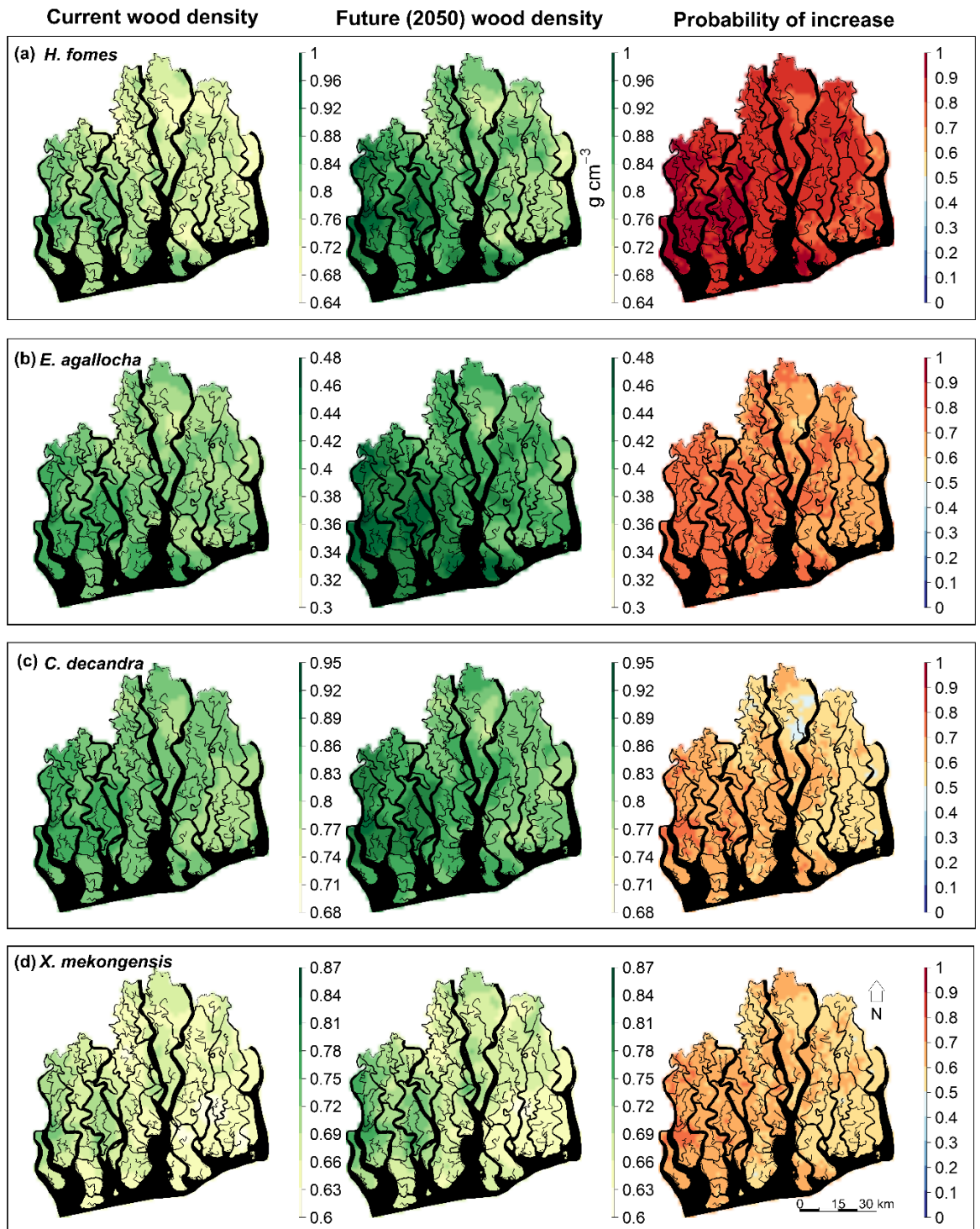
Fig. 5.9 Current status (first column) and worst-case scenario for the year 2050 (second column), of posterior mean of tree wood density for four prominent mangrove tree species in the Sundarbans world heritage ecosystem. Uncertainties related to these forecasts are mapped as the posterior probability of an increase in wood density in the third column.
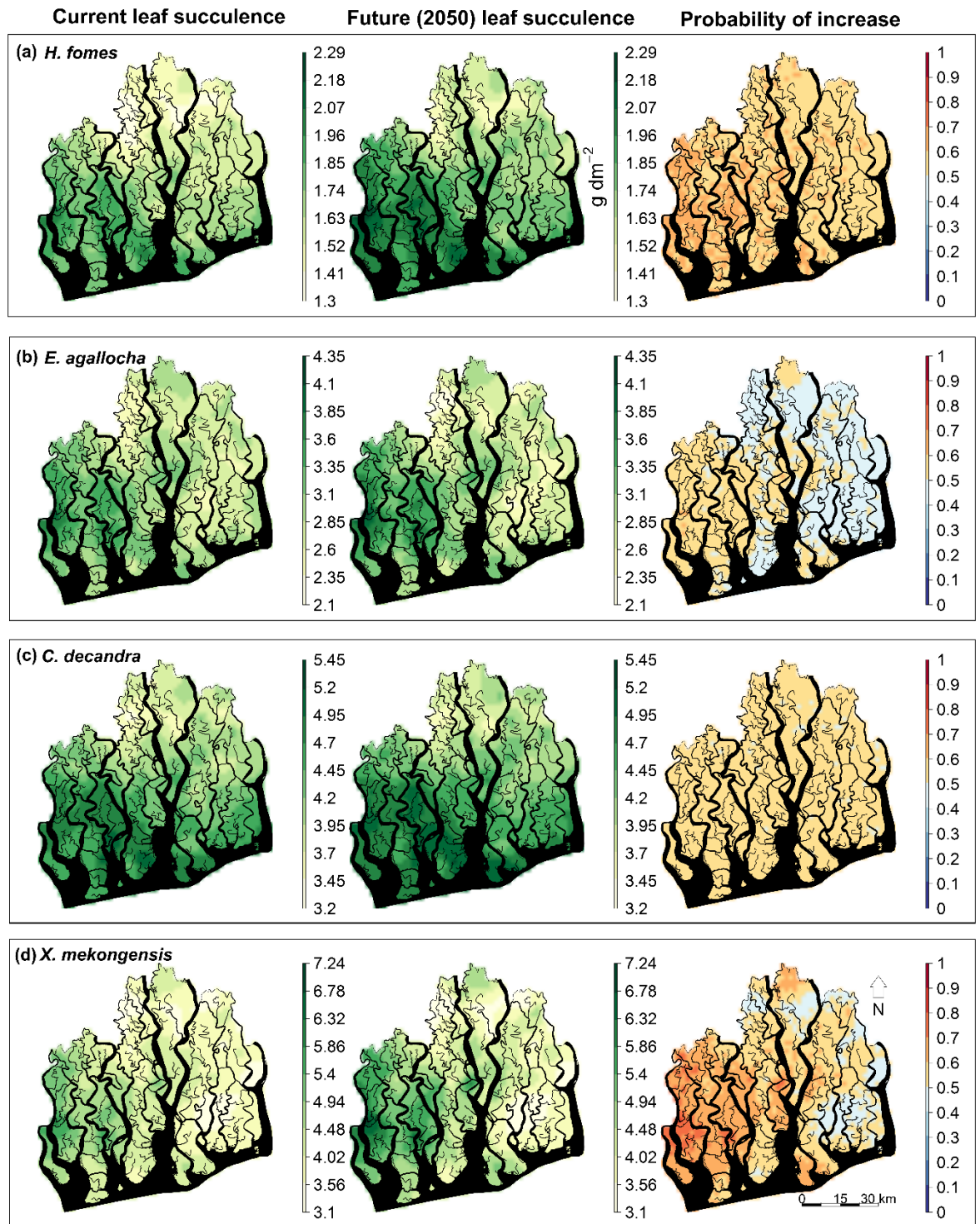
Fig. 5.10 Current status (first column) and worst-case scenario for the year 2050 (second column), of posterior mean of tree leaf succulence for four prominent mangrove tree species in the Sundarbans world heritage ecosystem. Uncertainties related to these forecasts are mapped as the posterior probability of an increase in leaf succulence in the third column.

5.5 Discussion

Primary production in tropical forest ecosystems is affected by the complex interactions between species' functional traits and the scene set by different environmental drivers. These are interconnected processes that collectively (through forest species composition and individual species function) determine fundamental functional aspects of the entire forest, such as its productivity. Looking at subsets of this causal network (e.g. statistical relationships between single traits and the environment) can only reveal part of the biological signal in the data. By underrepresenting the complexity of the connections between traits, species and environment (a challenge known as the "fourth-corner problem"), any predictive model of future forest dynamics stands to suffer from increased imprecision and by failing to propagate parameter uncertainty through to the prediction stages we risk ascribing unjustifiable confidence in any such predictions. In this paper, I have developed an analytical approach that follows a more holistic view of forest ecosystems, both by developing a model as complex as the data would support and by fully propagating parameter uncertainty into the predictions. This approach resolves the "fourth-corner problem", contributes to the clarification of different theoretical hypotheses about how complex forest ecosystems function, uncovers the environmental drivers of functional traits, and generates predictions about how traits and forest productivity will be affected by the environmental change in the future.

My integrated Bayesian approach allowed different ecological hypotheses to be tested in a single analysis simultaneously using all available data. In extreme environments, such as the tropical inter-tidal zones, tree communities may comprise functionally redundant species (Ricotta et al. 2016). Therefore, the studied species might have shown homogeneous functional responses to the stressors. Model I (Fig. 5.3) which represents this expectation (i.e. the 'habitat filtering' hypothesis (Weiher & Keddy 1995)) received the least support in my analyses. Rather, I found better support for Model III (representing the 'limiting similarity' hypothesis (MacArthur & Levins 1967; Chesson 2000)), suggesting that resource partitioning and specialization cause different coexisting mangrove species to show disparate functional trait responses to the environmental drivers. However, Model VIII, which considers both the 'habitat filtering' (by assuming that all species show an average functional trait response to the environmental drivers)

and the 'limiting similarity' (by assuming that the amount of variability around the average functional trait response depends on the nature and magnitude of the drivers) hypotheses, received the most support from my data. This suggests that habitat filtering and limiting similarity jointly explain mangroves' trait responses to the environment.

Applying my approach to the dynamic Sundarbans ecosystem, I determined salinity, siltation, pH and upriver position as the key drivers governing plants' trait responses (Fig. 5.4, Table 5.1). Further, I discovered diverging trait responses among the species and the strength of such responses to the environmental drivers was found to vary across the trait categories. For example, among the traits, height was more affected by salinity than the other drivers and the magnitude of the effect was significantly higher on the climax species *H. fomes* than the generalists — *E. agallocha* and *C. decandra*. These species-specific differences in canopy height (and for other traits) responses could be related to the variability in water stress, nutritional imbalance, and salt stress that the species experience under variable saline environments (Rasool et al. 2013).

Simultaneous plastic decreases in growth traits (Height and SLA) and plastic increases in survival traits (WD and LS) along the soil salinity, siltation and pH gradients, suggest conservative resource-use (low resource acquisition and turnover rates, and slow growth rates) as the dominant ecological strategy in many species to ensure their long-term survival under unfavourable environments (Rosado et al. 2016). The growth and survival traits showed opposing responses to increasing upriver-position (i.e. more available freshwater), suggesting that the same species can increase resource acquisition and growth under benign environmental conditions.

My model predicts an ecosystem-wide productivity loss under all future stress scenarios and forecasts a 30% loss of its current total productivity under the highest stress scenario by 2050 (Fig. 5.6A, Appendix 5B). This productivity loss is mainly associated with the community-wide decreases (36%) in height, by 2050 (Fig. 5.6B, Appendix 5C). Trait maps (Fig. 5.5) reveal that community SLA and WD show more stable patterns between the stress scenarios. This could be the result of turnover in species composition rather than stasis in stress conditions (Appendix 5E). For example, while the climax species — *H. fomes* (medium SLA and high WD)

— is projected to lose most of its suitable habitat by 2050, both generalist — *E. agallocha* (high SLA and low WD) — and disturbance specialist species — *C. decandra* (low SLA and high WD) — are likely to replace most of the degraded habitats and are projected to undergo ecosystem-wide range expansions. My species-specific predictions further uncovered spatial variability in plastic responses of the traits under projected stress conditions. I found that, under increasing stress, every species will lose canopy height and SLA, but the loss will be substantially higher for the climax species *H. fomes* (52% height and 16% SLA loss by 2050) (Fig. 5.6C, Appendix 5D) which is in agreement with the previous results that the species has narrower salt-tolerance than the generalists because of its limited ability to balance water and salt uptake (Das 1999). Plastic increases in conservative trait values (WD and LS) were also predicted to be highest for this species, implying maximum stress on the species contributing the most biomass.

While my approach incorporated multiple species, intra-specific variations in traits, in common to other existing approaches (Dolédec et al. 1996; Legendre et al. 1997; Lavorel et al. 2007; Pollock et al. 2012; Jamil et al. 2012; Jamil et al. 2013; Dray et al. 2014; Brown et al. 2014; Warton et al. 2015), it did not consider competitive interactions between species. Species-species interactions can lead to trait divergence (i.e. limited trait similarity) or sometimes trait convergence when traits have a strong influence on the competitive ability of the coexisting species which in turn may affect the species composition and biomass productivity in forest communities. However, my empirical inferences can inform more mechanistic models of tree dynamics (Purves et al. 2008; Grueters et al. 2014; Chauvet et al. 2017) that will better capture tree interaction dynamics.

In addition, several fundamental unknowns might also interfere with my forecasts. The first is the climate- or local stress-induced trait acclimation and adaptation that could potentially affect the accuracy of the projected trait values and productivity. However, variability in acclimation potential among different tree species and different trait types have yet to be discovered in mangrove ecosystems and elsewhere (Van Bodegom et al. 2014). The second unknown is the degree to which environment–trait relationships and trait–trait interactions will remain the same under future climatic and stress conditions (i.e. whether they undergo abiotic/biotic filtering).

Another area of improvement is to consider traits that directly measure the fitness or reproductive success of individual species. The fitness of individual species depends mainly on its ability to use and conserve resources or to tolerate abiotic and biotic stresses (Grime 2001). Therefore, the ideal trait for predicting species, community and ecosystem level productivity under variable stress scenarios is one whose function directly reflects the physiological or mechanical mechanisms controlling resource acquisition or conservation or stress tolerance in primary producers. Physiological (or hard) traits such as the relative growth rate of plants (RGR) which directly measures biomass allocation in plants, offer such an opportunity. However, their quantification is costly and time demanding and cannot be measured for large numbers of species in many regions of the world (Weiher et al. 1999). All the traits in this study are 'soft' or 'morphological' traits. The functional interpretations of them are rather indirect which might have resulted in increased uncertainty in parameter estimations and spatial predictions of traits and productivity. The positive side of including them is that they are available for all tree species whatever the scale is and closely represent many 'hard' traits. For example, I considered SLA as a surrogate of RGR as species with high SLA-leaves have higher RGR (Pérez-Harguindeguy et al. 2013). Future models incorporating available 'hard' traits or a mixture of 'soft' and 'hard' traits may offer a better mechanistic understanding of trait-environment relationships, and more accurate predictions of shifts in trait range under future environmental conditions and resulting consequences for ecosystem functioning.

My integrated approach not only advances our understanding of previously unknown functional trait responses of threatened taxa such as mangroves under variable stress conditions, but also provides forest managers a much-needed functional basis to tailor science-driven management and conservation actions particularly for conservation priority areas like the Sundarbans. Inadequate knowledge of how different mangrove species respond in dynamic coastal environments has previously led to unsuccessful conservation efforts in many tropical regions (Lewis 2005), including the Sundarbans (Islam et al. 2014). Therefore, determining the environmental drivers that limit mangroves' growth and survival is crucial before designing and implementing habitat restoration and reforestation programs. For example, my finding that soil salinity, alkalinity and siltation are the most limiting environmental drivers of mangroves' primary

growth and resource acquisition, especially for the climax species, can target the selection of species and sites for future reforestation and restoration initiatives.

My finding that currently the productivity hotspots are confined to the hyposaline eastern and northern regions in the Sundarbans and the projected 30% decline in productivity, lends strong support for immediate habitat enhancement programs (e.g. river dredging for increasing freshwater flows and for reducing silt deposition) in the eastern and northern regions. Most importantly, the productivity maps can be important tools for implementing the United Nations REDD+ (Reduced Emissions from Deforestation and Degradation) initiatives and guiding national strategy while negotiating for payments for ecosystem services (Rahman et al. 2015).

The application of my proposed approach is not limited to mangrove forests rather this is a generalizable foundation for powerful modelling of trait-environment linkages under changing climate and for predicting their consequences on ecosystem functions and services in other forest ecosystems of the world (e.g. boreal, temperate, and other tropical forests). The increasing availability of spatially explicit global datasets for plant functional traits (Kattge et al. 2011), species distributions (Hudson et al. 2014), and high-resolution environmental layers (Shangguan et al. 2014) provide opportunities for such applications, especially within dynamic global vegetation models (Scheiter et al. 2013).

5.6 Conclusions

This integrated Bayesian approach provides the foundations for trait-based predictions in plant ecology through simultaneously modelling trait-trait and trait-environment correlations (for multiple traits, species, and environmental drivers) at organismal, community and ecosystem levels, thus resolving many fundamental methodological problems of the existing ordination/permutation and univariate approaches, and bridges community, ecosystem ecology, and functional biogeography. These novel developments allow us to (1) integrate fundamental ecological hypotheses into the model building process, (2) quantify the strength of the trait-environment relationships, (3) identify the degree of intraspecific covariation among multiple traits, (4) predict species-specific and community-level trait distributions with accurate estimates of uncertainty, and (5) forecast whole-ecosystem productivity under future environmental conditions. Applying this approach to the Sundarbans, I discovered (1) joint effects of habitat filtering and limiting similarity in shaping trait responses to environment with parallel contribution of intraspecific variability in trait-trait interactions, (2) substantial intraspecific trade-offs among the functional traits in many tree species, (3) serious detrimental effects of increasing salinity, siltation and soil alkalinity on functional traits associated with plants' resource acquisition and growth, (4) plastic enhancement of traits related to stress tolerance, indicative of plants prioritizing survival over growth, and (5) ecosystem-wide drop in biomass productivity under all anticipated stress scenarios with an average of 30% productivity loss by 2050 in the worst scenario. These findings advance our understandings on how species living in stressed ecosystems respond to environmental change and provide policymakers and managers with a much-needed functional basis for developing strategic approaches and setting targets for forest conservation, restoration, and ecosystem management. Because of its high computational efficiency, my integrated approach is applicable to any forest ecosystem across broad global scales, to predict shifts in ecosystem functioning and services under a rapidly changing climate.

Chapter 6 . General Discussion

6.1 An overview of my thesis findings

My overall aim of this thesis was to understand mangroves' habitat requirements and spatial distributions, to explore spatio-temporal patterns and drivers of Sundarbans' biodiversity, and to develop an integrated approach for predicting species trait responses and forest productivity under changing environments. In Chapter 2, using GAMs on mangrove abundances, I determined habitat preferences and spatial distributions of the four major mangrove tree species. The climax species *H. fomes* showed a strong negative response to salinity and human harvesting. *H. fomes* and *X. mekongensis* preferred upstream habitats while the remaining species preferred downstream to intermediate-stream areas. The magnitude of responses to nutrients, elevation, and the biotic interaction term varied between species. Spatial maps show that the established protected area network (PAN) does not cover the density hotspots of any of the tree species.

In Chapter 3, using long-term mangrove tree data collected at four historical time points (1986, 1994, 1999 and 2014), I uncovered the spatial heterogeneity in alpha, beta, and gamma diversity and temporal dynamics in species abundances, geographic range, and composition in the existing ecological zones (hypo-, meso-, and hypersaline) of the Sundarbans. Here, I also developed regional biodiversity maps to pinpoint the historical and current biodiversity hotspots and to specify the areas that experienced shifts in species composition over time. I found that the hyposaline zone supported the most diverse and heterogeneous communities (in terms of species composition) at all historical time points. In contrast, the hypersaline zone comprised the least diverse and most homogeneous communities. Most importantly, I detected a clear trend of decreasing heterogeneity in the mangrove communities of all ecological zones since 1986, providing a strong signal for ecosystem-wide biotic homogenization. Biodiversity maps revealed that the established PAN neither supported the historical biodiversity hotspots nor the existing hotspots. They further identified the western and southern hypersaline zones as the areas that have experienced the greatest species compositional shifts (biotic differentiation) since 1986.

In Chapter 4, using GAMs on tree count, environmental and historical disturbance data, my objectives were to determine the key drivers for different aspects (alpha, beta and gamma) of mangrove biodiversity and to develop habitat data-driven baseline biodiversity maps for the Sundarbans. I found historical tree harvesting, siltation, disease and soil alkalinity as the key stressors that negatively influenced the diversity (alpha) and distinctness (beta) of the mangrove communities. In contrast, species diversity increased along the downstream – upstream, and riverbank – forest interior gradients, suggesting the late successional upstream and forest interior communities are more diverse than the early successional downstream and riverbank communities. Like the species density hotspots, the existing PAN does not cover the remaining biodiversity hotspots.

In Chapter 5, I developed an integrated Bayesian modelling approach to quantify trait-environment correlations for multiple traits, species, and environmental drivers simultaneously while accounting for the intraspecific variation in traits. The approach thus resolves the 'fourth-corner problem' (Legendre et al. 1997) and provides a foundation for mechanistic trait-based predictions in plant ecology. Applying this approach on the Sundarbans, I found (1) combined effects of habitat filtering and limiting similarity in shaping trait responses to environment with parallel contribution of intraspecific variability in trait-trait interactions, (2) substantial intraspecific trade-offs among the functional traits in many tree species, (3) serious detrimental effects of increasing salinity, siltation and soil alkalinity on plant primary growth, and parallel plastic enhancement of traits related to stress tolerance and (4) ecosystem-wide drop in biomass productivity under all anticipated stress scenarios.

Although each data chapter had separate aims and answered specific questions, they mainly covered three central themes: habitat preferences of mangroves, spatio-temporal patterns and drivers of mangrove biodiversity, and species trait responses to environmental drivers. I collect the insights for each of the themes below and then briefly discuss the practical implications of my findings, limitations and potential areas for future improvements.

6.1.1 Habitat preferences of mangroves

Habitat suitability analyses in Chapter 2 uncovered that multiple environmental drivers (i.e. salinity, upriver position, harvesting, nutrients) simultaneously influence spatial distributions of mangroves. This contrasts with the common mangrove-centric assumption that only a few abiotic stressors (e.g. temperature, tidal waves etc.) shape mangrove distributions in the harsh tropical inter-tidal zones (Ellison 2001).

All the mangroves showed steep responses to increasing salinity although the magnitude of the responses clearly varied between species. *H. fomes* showed a strong negative response while the remaining species showed clear positive responses. These results are in agreement with previous studies (Ball 2002; Dangremond et al. 2015) reporting that differential salt tolerance and salinity optima among mangrove species contribute to spatial variability in mangrove populations in tropical coastal areas.

Changes in river hydro-geomorphological features along the downstream-upstream gradient alter habitat qualities which in turn may cause spatial variability in species distributions (Angiolini et al. 2011). Likewise, I found differential habitat preferences of the Sundarbans' mangroves along the downstream-upstream gradient. Most suitable habitats of *H. fomes* and *X. mekongensis* are now located in the upstream areas although records show their widespread distributions over the entire forest in the 19th century (Gopal & Chauhan 2006). This shift in habitat preferences may be related to riparian degradation through hydrological modification (e.g. a 60% drop in the freshwater flow in the Sibsha and Posur river system), increasing river-bank erosion and siltation which have modified the fluvial geomorphology of the waterbodies in the Sundarbans (Wahid et al. 2007).

Before the Bangladeshi government enforced a full logging ban in 1989 (Sarker et al. 2011), the Sundarbans was managed for sustainable timber production in the Pakistani (1948 − 1970) and the British (1600 − 1947) regimes (Ghosh et al. 2015). Despite the enforcement of a full logging ban, tree harvesting by local communities is common (Iftekhar & Saenger 2008). My results showed that past harvesting has had substantial negative effects on the populations of *H. fomes*, *X.*

mekongensis and *C. decandra*. Siddiqi (2001) reported intensive past harvesting of *C. decandra* by local communities for fuelwood, and selective logging of *H. fomes* and *X. mekongensis* by the BFD for timber supply. Interestingly, *E. agallocha* showed the opposite pattern: a clear trend of population increase in the highly-exploited areas in the past. Frequent tropical cyclones, past industrial and illegal logging, and tree mortality have resulted in large as well as small forest gaps in the Sundarbans and the size of open areas has been increasing by 0.05% each year (Iftekhar & Islam 2004). *E. agallocha* is a salt tolerant fast producing species that can easily colonise open and degraded habitats (Harun-or-Rashid et al. 2009). I assume that these conditions may favour *E. agallocha* to increase its density even in the *H. fomes and X. mekongensis* dominated stands. Increasing dominance of *E. agallocha* in the previously *H. fomes* dominated stands, and increasing coverage of mono-specific *E. agallocha* stands - 0.69% per year during 1981-1997 (Iftekhar & Saenger 2008) - provide support for my assumption.

In common with other terrestrial plant communities, nutrient availability is recognized as a major driver for spatial variability in abundance, composition and productivity in mangrove communities (Feller et al. 2010). Often, mangrove soils are poor in nutrients and nutrient availability is irregularly driven by a complex interaction between abiotic and biotic variables (Reef et al. 2010). Mangroves have developed several nutrient conservation strategies (e.g. resorption of nutrients before leaf shedding, evergreenness) to maintain growth and development under such conditions. Moreover, mangroves can show high plasticity in their ability to opportunistically exploit nutrients when they become available depending on their physiological requirements, thus for a specific nutrient the responses of different species may vary (Reef et al. 2010). Likewise, I found that the magnitude of response to nutrients varied between mangroves in the Sundarbans.

H. fomes prefers NH_4 rich habitats while the others can grow abundantly in NH_4-poor habitats. Terrestrial plants put considerable respiration effort to uptake and assimilate N and those are well adapted to the efficient uptake and assimilation of NH_4 require much less respiration efforts (i.e. less metabolic cost) compared to uptake and assimilation of other N forms (Reef et al. 2010). This indicates that *H. fomes* might have increased its capacity to efficiently utilize NH_4 as the main N

source for saving metabolic cost under increasing salinity stress in the Sundarbans. Conversely, the apparent preference of salt-tolerant mangroves for NH_4-poor habitats may be related to their preference for other forms of N, or they may suffer from NH_4 toxicity (Kronzucker et al. 1997). Soil P is a key constraint for forest productivity in the tropics (Baribault et al. 2012). Interestingly, in the Sundarbans, all the mangroves show a preference for habitats with relatively lower P availability. K is a key soil macro-nutrient that can modulate salinity-induced drought stress by improving the water uptake and retention capacity of plants (Sardans & Peñuelas 2015). The salt-tolerant species such as *E. agallocha, C. decandra and X. mekongensis* maintain high abundances in the K-rich habitats (north-western Sundarbans). Fe and Mg are required in minute quantities for successful mangrove growth because of their roles in metabolic and physiological processes (Alongi 2010). Responses to Fe substantially varied between species. Interestingly, mangroves mostly accumulate Fe in roots (Alongi 2010). *H. fomes* and *X. mekongensis* have extensive aerial root system (i.e. pneumatophores). *E. agallocha* has spreading surface roots, and *C. decandra* has extensive knee roots (Siddiqi 2001). These differential rooting structures may be related to diverse Fe use efficiency in the mangroves. *H. fomes*'s higher preference range for Mg than *X. mekongensis* may be related to the distribution and chemical properties of the source rock material, the weathering process, and salinity levels which control the availability of Mg to mangrove plants (Gransee & Führs 2013).

The above responses to nutrients indicate that the mangroves of Sundarbans may be highly plastic in their ability to utilize nutrients (i.e. withstand low-nutrient conditions, but able to exploit high levels of nutrients when other stresses are withdrawn). Future research is required to understand the plasticity levels in different mangroves, and their nutrient acquisition, and conservation strategies under different stress scenarios (e.g. salt stress and flooding).

Species distribution maps reveal that currently, the eastern region of the Sundarbans supports the remaining *H. fomes* hotspots, the north-western region supports the *E. agallocha* hotspots, the western and southern regions support the *C. decandra* hotspots, and few specific areas in the northern (Kalabogi and Koyra) and north-western (Koikhali) regions support the *X. mekongensis* hotspots. *H. fomes* was the most abundant species both in the Bangladesh and Indian parts of

the Sundarbans just 200 years ago (Siddiqi 2001). Currently, the species is at the elevated risk of extinction in the Indian Sundarbans. Historical obstruction of freshwater influx from the Ganga-Bhagirathi-Hooghly river system, salinity intrusion, deposition of industrial effluents, and aquaculture expansion which have gradually transformed it into world's one of the most degraded mangrove ecosystems (Kathiresan 2010). The more stress tolerant species *C. decandra* is now the climax species in the heavily degraded Indian Sundarbans.

Most of the world's *H. fomes* trees are now restricted only to the less saline eastern region of the Bangladesh Sundarbans. Evidence of widespread distribution of *H. fomes* in the western region (currently, the hypersaline zone) in the past (Gopal & Chauhan 2006), suggests historical range contraction of the species in the Bangladesh Sundarbans. *C. decandra* has already replaced a substantial amount of *H. fomes* range: 0.08% year^{-1} during the period 1981−1997 (Iftekhar & Saenger 2008). Gopal & Chauhan (2006) have documented an annual replacement of about 0.4% of the total forest area by *C. decandra*. Therefore, the Indian Sundarbans case should be taken as a warning regarding the future availability of suitable habitats for *H. fomes* and other salt-intolerant (freshwater loving) species in the Bangladesh Sundarbans.

6.1.2 Spatio-temporal patterns and drivers of mangrove biodiversity

Species diversity, composition, abundance, and geographic range of the mangroves have substantially changed in the Sundarbans over the last three decades (Chapter 3). This finding is consistent with recent remote-sensing technique-based studies (Giri et al. 2007; Mukhopadhyay et al. 2015; Ghosh et al. 2015) reporting species and vegetation cover changes in the Sundarbans since the 1980s. Chapter 4 further determined the drivers for spatial variability in diversity and species composition.

At all historical time points (1986, 1994, 1999 and 2014), the hyposaline mangrove communities remained the most diverse (alpha) while the hypersaline communities remained the least diverse. Chapter 2 has already revealed widespread distributions of the facultative halophyte *H. fomes* in the less saline nitrogen rich upstream areas that also allow co-existence of other salt-intolerant non-halophytes (Siddiqi 2001). In turn, two obligate halophytes: *E. agallocha and*

C. decandra showed super-dominance in the highly saline down – intermediate stream habitats. Therefore, the relatively higher diversity in the hyposaline communities may be closely related to suitable habitat conditions that supported historical coexistence of both facultative (e.g. *H. fomes*) as well as other opportunistic non-halophytes.

Surprisingly, in the last 15 years, alpha diversity sharply increased in the communities of the southern meso- and western hypersaline areas. My temporal beta diversity analyses detected that these areas have also experienced radical shifts in species composition over the 28 years. Salinity fluctuation is highest in these areas and often the salinity level remains high for longer, inhibiting the regeneration process and inducing disease outbreaks in many salt-intolerant species, including *H. fomes* (Ghosh et al. 2016). Habitat-based biodiversity models in Chapter 4 uncovered that historical harvesting, increasing siltation, salinity, pH and community size (dominance of generalists) have strong negative effects on alpha diversity while increasing upstream and forest interior environment have strong positive effects on alpha diversity as well as the gamma diversity. Chapter 4 further showed that increasing salinity could promote increasing heterogeneity in the communities. This is due to the increasing colonization success of the opportunistic stress-tolerant species (e.g. *E. agallocha* and *C. decandra*) in the degraded saline soils in the Sundarbans (Iftekhar & Saenger 2008; Aziz & Paul 2015; Mukhopadhyay et al. 2015) with associated population declines and range contraction of many stress-intolerant species (Chapter 3). Therefore, range and population expansion of the stress-tolerant species and range contraction and population loss of the stress-intolerant species under increasing salt stress, harvesting, siltation, and soil alkalinity could be the possible mechanisms that resulted in sudden alpha diversity increase and alteration to the species composition (particularly in the southern meso- and western hypersaline communities) over the 28 years.

A disproportionate expansion of generalist (or invasive) species relative to specialist endemics which results in reduced distinctness in natural communities is the key mechanism responsible for biotic homogenization (Olden 2006). Chapter 3 revealed (1) increasing similarity (decreasing distinctness) among mangrove communities since 1986, (2) range expansion of the widespread stress-tolerant

species (e.g. *E. agallocha* and *C. decandra*) and range contraction of the local endemics, (3) increasing abundance of the stress-tolerant species and decreasing abundance of the stress-intolerant endemics including the climax *H. fomes*, and (4) local extinction of many rare mangrove species. These findings strongly comply with the basic assumptions of the biotic homogenization theory (McKinney & Lockwood 1999; Olden & Poff 2003; Olden & Rooney 2006).

Chapter 4 determined historical tree harvesting, increasing disease prevalence, siltation, soil alkalinity, nutrient toxicity as the key stressors responsible for increasing similarity among mangrove communities. Since the construction of the Farakka dam in the upstream, both water and soil salinity have been increasing in the Sundarbans (Mirza 1998; Wahid et al. 2007). The average soil salinity has already increased by 60% since 1980 (Aziz & Paul 2015). As a result, hyposaline areas are transforming into mesosaline areas and mesosaline areas are transforming into hypersaline areas (Ghosh et al. 2016). Despite the ongoing ban on logging (Sarker et al. 2011), opportunistic tree felling is common (Iftekhar & Islam 2004). This ongoing transformation in habitat conditions coupled with forest exploitation and sea level rise may seriously alter the current biodiversity and species composition in the Sundarbans. Biodiversity maps in Chapter 3 revealed that the spatial coverage of the heterogeneous (distinct) communities gradually declined at all historical time points since 1986. Together, Chapter 3 and Chapter 4 maps confirm that the most diverse and the most distinct communities are now confined to a specific area (Kalabogi) in the Sundarbans while the rest of the ecosystem looks homogeneous in terms of species composition, suggesting further degradation and forest exploitation may transform these remaining biodiversity hotspots into species-poor homogeneous patches.

6.1.3 Quantifying species trait responses to environmental drivers

A variety of approaches — the CWM (Lavorel et al. 2007), the fourth corner correlation (Legendre et al. 1997; Dray & Legendre 2008), the multivariate RLQ (Dolédec et al. 1996; Dray et al. 2014), and the more recent regression approches (Pollock et al. 2012; Jamil et al. 2012; Jamil et al. 2013; Brown et al. 2014; Warton et al. 2015) — are used to disentangle the link between species traits and environmental drivers (known as 'the fourth-corner problem' in community ecology) and to model the link for predicting species, community and ecosystem

responses under future environmental scenarios. The survival of a species in a specific environment is controlled by how its functional traits (morphological or physiological or anatomical) respond to multiple environmental stressors and how the trait themselves interact (Verberk et al. 2013). Therefore, the interplay between multiple plant functional traits, multiple species and multiple environmental drivers may collectively influence species abundance, community composition and ecosystem productivity.

However, current trait-based approaches often look at species, traits and the environment in a fragmented way, and frequently deal with the effect of single (or sometimes several) environmental driver on individual species traits without considering the complex interactions between multiple traits of multiple competing species under a dynamic environment. These shortcomings raise serious concerns (Webb et al. 2010; Verberk et al. 2013; Funk et al. 2017) about how precisely the existing approaches will forecast species, community and ecosystem responses under future environmental conditions. Therefore, we need an integrated quantitative approach that represents the complexity of the connections between traits, species and environmental drivers while developing a predictive model of future forest dynamics. In Chapter 5, I proposed such an integrated approach that models trait-environment relationships for multiple traits, species, and environmental drivers simultaneously while accounting for intraspecific trait variation. In this way, this novel approach resolves the long-lasting 'fourth-corner problem' problem and contributes to the clarification of different theoretical assumptions about how complex forest ecosystems function, determines the environmental drivers of functional traits, and makes predictions about how traits and forest productivity will be affected by the future changes in the environment.

A common assumption in mangrove literature is that a few strong environmental gradients (such as salinity and tidal inundation) shape structural and functional properties of mangrove forests, and regular species sorting along these gradients are responsible for poor species diversity and relatively homogeneous species composition at least at a regional scale (Farnsworth 1998). This reflects the 'habitat filtering' theory (Weiher & Keddy 1995), a widely tested theory for many taxa in diverse ecosystems. An alternative assumption also exists saying fine-scale

variation in habitat conditions in the dynamic inter-tidal zones may cause variability in species composition and functioning which reflects the 'limiting similarity' theory (MacArthur & Levins 1967; Chesson 2000). My proposed integrated Bayesian approach allowed these ecological hypotheses to be tested in a single analysis simultaneously using all available data and revealed that habitat filtering and limiting similarity together explain mangroves' trait responses to the environment with strong influences of within-species variability in trait-trait relationships.

Applying my approach to the Sundarbans, I found severe detrimental effects of increasing salinity, siltation and soil alkalinity, and a significant positive effect of increasing upriver position (i.e. more available freshwater) on height and SLA, indicating trees living in the freshwater-dominated upstream areas have higher resource acquisition and growth rates than those living in the alkaline and highly silted hypersaline environments. In parallel, a plastic enhancement of survival traits — WD and LS — was common in many species. Higher LS is a common adaptation mechanism in many plants to ensure water use efficiency under extended stress (e.g. drought, salinity etc.) periods (Wang et al. 2011). Denser wood confers mechanical stiffness to trees growing under heavily silted saline soils, but needs more biomass investment and is therefore costlier to construct per unit of stem height (Feller et al. 2010). This extra resource investment of trees in structural support leaves less available resource in a plant body that could be used for fitness purposes (such as photosynthesis and primary growth), representing the growth-survival trade-off (Lawson et al. 2015). My integrated approach identified such trade-off in the most abundant species of the ecosystem — *H. fomes*.

Contrary to the common assumption that mangroves show homogeneous functional responses under stress as they are believed to share evolutionarily convergent traits (Farnsworth 1998), I discovered plastic trait responses among the species and the strength of such responses to the environmental drivers varied for both growth and survival traits. For example, while salinity has its greatest negative effect on the height of *H. fomes* and its greatest positive effect on *X. mekongensis* LS, pH has no significant effect on the height of any of the species. But increasing pH significantly affects the SLA of all species with maximum

negative effect on *E. agallocha*. These findings indicate that multiple environmental drivers simultaneously act on traits, and plastic responses of traits and trait-trait interactions differ among different species which might collectively determine the growth and survival of species.

My model predicts that currently the most productive mangrove tree communities are distributed in the freshwater-dominated hyposaline habitats (eastern and northern regions) while the most unproductive communities are distributed in the highly silted hypersaline habitats (western and south-western regions) in the Sundarbans. Biomass productivity in tree communities is closely connected with the community-wide trait values (Grime 1998; Diaz et al. 2007). Hence, higher biomass productivity in the hyposaline habitats than the silted hypersaline habitats might be related to relatively higher community-wide height and SLA (which together may facilitate greater light capture, photosynthetic rates and net carbon gain) and relatively lower community-wide wood density (resulting in higher stem hydraulic conductivity, photosynthetic carbon gain and lower construction costs per wood volume) in the hyposaline habitats. The relatively nutrient-rich soils (particularly, nitrogen) and biodiverse hyposaline habitats (Chapters 3 & 4) might also contribute to greater biomass productivity in these regions because plants can grow faster in nutrient-rich soils (Pastor et al. 1984; Prado-Junior et al. 2016) and a higher diversity of species offers efficient use of available resources because of higher niche differentiation and interspecific facilitation (Tilman 1999).

Chapter 2 and Chapter 4 showed strong negative effects of increasing salinity and siltation on endemic species abundances and diversity in the Sundarbans. Projected sea level rise (32 cm by 2050) along the Bangladesh coasts (Karim & Mimura 2008) and other aspects of climate change such as increased temperature, monsoon flooding and extended dry season are likely to severely degrade the Sundarbans ecosystem with subsequent effects on species traits and forest productivity. My model-based forecasts show that the biomass productivity of the ecosystem is likely to drop under all projected stress scenarios (10, 20, 30, 40 and 50% increase in salinity and siltation) with a maximum of 30% whole-ecosystem productivity loss under the worst stress scenario by 2050. This productivity loss is mainly related to a significant reduction in community-wide height (36% by 2050)

because of change in species compositiojn and an ecosystem-wide population increase and range expansions of the less-biomass contributing generalists (such as *E. agallocha* and *C. decandra* (Chapters 3 and 5). My species-specific predictions further revealed that every species would lose canopy height and SLA and gain WD and LS under all projected stress conditions, but the rate of loss might vary between the species. Most importantly, the height loss and WD gain could be greatest in the most biomass-contributing species *H. fomes*, suggesting maximum stress on that globally endangered species.

6.2 Practical applications

Chapter 2 specified the environmental requirements of the threatened mangroves and produced species distribution maps. Chapter 5 uncovered how functional responses of different mangrove species vary along the environmental gradients and generated species- and community-level trait maps under current and future environmental conditions. Together, these species-centric and trait-based findings, can help forest managers selecting suitable species and sites for replanting. For example, a significantly stronger negative response of *H. fomes* abundance and canopy height to increasing salinity compared to the responses of the generalists (*E. agallocha* and *C. decandra*) imply for choosing relatively benign upstream habitats for *H. fomes* replanting and planting the generalists or salt-tolerant early-successional species (e.g. *S. apetala*) in the highly degraded barren areas for initial site stabilization.

The process of biotic homogenization has been underway in the Sundarbans resulting in spatial contraction of diverse and distinct mangrove communities in the Sundarbans (Chapter 3). Biodiversity maps revealed that both the historical and contemporary biodiversity hotspots were located at the northern (specifically the Kalabogi region) hyposaline habitats that support the unique association of *X. mekongensis* and *H. fomes*, the two species most at risk of local and global extinction. Therefore, future conservation and protection initiatives should primarily focus on these surviving hotspots because further habitat degradation and exploitation of these threatened species may push them to the brink of extinction.

Establishing coastal protected areas has been common practice in the tropics to conserve forest resources and to offer social and economic benefits to the forest-dependent communities (de Almeida et al. 2016). A PAN (the largest coastal PAN in the world) is also operational in the Sundarbans to confirm completely undisturbed habitats for plants and animals. My species density maps (Chapter 2), biodiversity maps (Chapters 3 and 4) and the forest productivity maps (Chapter 5) have shown that the established PAN does not cover the species density, biodiversity, and forest productivity hotspots. Therefore, this thesis advocate for bringing these hotspots under protected area management to ensure the long-term conservation of the many threatened species living there.

Historical harvesting had a significant negative effect on the abundance of most of the mangroves (Chapter 2) and appeared responsible for the diminishing distinctness of the mangrove communities (Chapter 4). Many rare and endemic plant species including the climax *H. fomes* have faced range contractions or local extirpations over the last three decades (Chapter 3). Although logging has been legally prohibited since 1989 (Sarker et al. 2011), opportunistic harvesting of valuable timber-yielding species (mostly *X. mekongensis* and *H. fomes*) by poachers is common (Iftekhar & Saenger 2008). The BFD has ratified the 'Bangladesh Biodiversity Act 2017' to reduce biodiversity loss and recently initiated the SMART patrol management system to stop this illegal practice in the Sundarbans. My species density and biodiversity maps can guide these valuable protection and monitoring initiatives through tracking individual species populations and community-level diversity changes or predicting changes and recognizing habitats or species that may be affected by future human interventions.

Both mangrove enhancement (reducing biotic and abiotic stresses that caused mangroves' population decline) and mangrove restoration (restoring specific areas where certain mangrove species previously existed) initiatives are regularly taken in the tropical coastal regions to enhance species resistance and resilience to climate change and to offset predicted losses from climate change impacts (Lewis 2005). However, inadequate understanding of which environmental drivers regulate mangroves abundances, composition and functions have resulted in unsuccessful mangrove enhancement and restoration projects in many countries

(Lewis 2005) including the Sundarbans (Islam et al. 2014). This thesis determined the key drivers responsible for spatial variations in mangrove distributions, diversity, and functions in the Sundarbans. For example, salinity and historical harvesting predominantly affect *H. fomes* abundance, siltation, disease, historical harvesting and pH affect the diversity and distinctness of the mangrove communities, and soil salinity, alkalinity, and siltation act simultaneously to limit mangroves' resource acquisitive traits and overall ecosystem productivity. These novel habitat and functional insights and the spatial maps of species, biodiversity, traits, and forest productivity can guide the future mangrove enhancement and restoration initiatives in the Sundarbans.

Also, my proposed integrated approach (Chapter 5) for quantifying trait-environment relationships and predicting ecosystem properties (such as productivity) is not restricted to mangroves. It can be readily applied to any other forest ecosystems of the world (e.g. boreal, temperate, and other tropical forests) to address various management and conservation issues therein.

Finally, based on the findings in Chapters 2 — 5, this thesis recommends to —

- Replant globally endangered *H. fo*mes and locally threatened *X. mekongensis* in less saline upstream habitats (Chapter 2).

- Focus protection actions (e.g. regular patrolling, increase the number of resource protection officers and rangers) on the endangered (e.g., *H. fomes*) as well as the rare endemics (e.g. *C. ramiflora, C. manghas and A. cucullata*) whose populations and geographic ranges have substantially declined in recent times (Chapter 3).

- Take extreme caution while implementing nutrient enrichment programs because the mangroves of the Sundarbans may suffer from nutrient toxicity in highly silted hypersaline habitats (Chapter 4).

- Focus future conservation and protection initiatives primarily on the surviving biodiversity hotspots located in the northern Sundarbans (Chapters 3 and 4).

- Extend or establish new protected areas for immediate protection of the remaining species density, biodiversity and forest productivity hotspots in the Sundarbans (Chapters 2, 3, 4 and 5).

- Take initiatives to test the suitability of interventions such as river dredging to increase the freshwater supply in the Sundarbans to reduce the salinity stress on tree growth and productivity of the ecosystem.

6.3 Limitations and future directions

The HSMs of the mangroves (Chapter 2) are data-driven correlative models that do not necessarily reflect the causal relationships between species and environmental conditions. Here, the fitted response curves for each mangrove species only described how its densities were correlated with multiple predictors within their observed environmental ranges. Since these predictors include proxies for competition, these curves do not necessarily reveal the physiological limits (i.e. the fundamental niche) of the mangroves. Future studies may overcome the above limitations by developing mechanistic models (Dormann et al. 2012) that relate physiological (or morphological) traits with habitat data to translate species – environment interaction into fitness components (e.g. survival, growth, reproduction etc.) for predicting species distribution across space and time (Kearney & Porter 2009).

Because of low prevalence ratio (many zeroes) in the dataset, I could not develop HSMs for the 15 rare mangrove species. Future studies can usefully extend their sampling efforts beyond the existing PSP network to record these rare mangroves.

As previous environmental data were unavailable, I used ordinary kriging to generate biodiversity (alpha, beta and gamma) maps for four historical time points (Chapter 3). Because this direct interpolation approach does not accommodate environmental and biotic predictors, it might have increased prediction uncertainty (Miller et al. 2007). Chapter 4 used both environmental and biotic variables to model and to produce spatial biodiversity maps. Here, the habitat-based models showed better predictive ability than the covariate-free direct interpolation approach. However, small differences between the approaches in

terms of predictive accuracy demonstrates the utility of direct interpolation approaches when environmental data are unavailable.

Anthropogenic pressures, sea level rise, and natural calamities may alter the already stressed habitats of the mangroves with subsequent changes in the salinity and nutrient levels. Therefore, the mangrove HSMs (Chapter 2), the biodiversity models (Chapter 3) and the trait-based models (Chapter 5) should be updated with new environmental data. I could not incorporate hydroperiod data into my models due to their unavailability which might have affected the predictive accuracy of the models. Hydroperiod (the frequency, duration and depth of tidal inundation) directly regulates salinity and nutrient dynamics in mangrove forest floors, thus, influences mangrove regeneration and growth (Crase et al. 2013). The anticipated sea-level rise in the Bangladesh coast may considerably alter the Sundarbans' regional hydrology. Therefore, future studies should include plot level hydroperiod information when they become available.

Similar to the existing trait-based approaches (Dolédec et al. 1996; Legendre et al. 1997; Lavorel et al. 2007; Pollock et al. 2012; Jamil et al. 2012; Jamil et al. 2013; Dray et al. 2014; Brown et al. 2014; Warton et al. 2015), the proposed Bayesian integrated approach (Chapter 5) did not include species-species interactions. Such inclusion might have contributed to better parameter estimates as species composition and functions of plant communities can be mediated by competition-induced shifts in traits i.e. trait divergence or convergence (Grime 2006; Mayfield & Levine 2010). Nevertheless, my modelling framework can be easily extended to include the abundance of one tree species as a covariate for another (Chapter 2).

I used easily measurable morphological ('soft') traits that are proxies of 'hard' traits (for example, SLA as a proxy of the relative growth rate of plants, Pérez-Harguindeguy et al. 2013). 'Hard' traits directly influence the resource acquisition or conservation or stress tolerance hence the fitness in primary producers (Grime 2001). Therefore, future models incorporating important 'hard' traits may offer a better mechanistic understanding of how species, community and ecosystem will respond to future environmental changes.

6.4 Conclusions

Global climate change, local habitat modifications, and human interventions are acting simultaneously to push the mangrove biome to the brink of extinction. Yet, we have a restricted understanding of how these global and local drivers regulate mangrove populations, composition and functions in space and time. Such fundamental knowledge gaps have obstructed the management and conservation programs across the tropics but particularly in the Sundarbans — a global priority ecosystem that is being impacted simultaneously by climate change, habitat modifications and multiple types of human exploitation. Therefore, the main motivation behind this thesis was to fill such knowledge gaps and to provide a spatially explicit baseline for managing and conserving mangrove populations, biodiversity, and ecosystem functioning in the threatened Sundarbans.

Moving from autecology to synecology and applying species-centric to trait-centric approaches on mangrove field data, this thesis (i) advances our understanding on previously unknown habitat preferences of mangroves and their spatial distributions, (ii) explores spatial and temporal dynamics and the determinants of mangrove biodiversity, and (iii) develops a novel integrated approach that resolves the "fourth-corner problem" and contributes to the clarification of different theoretical assumptions about species functional responses under stress, specifies the environmental drivers of functional traits, and generates predictions about how traits and forest productivity will be affected by future changes in environmental conditions.

The findings of this thesis have important management and conservation implications. Results on species habitat suitability and functional trait analyses, together, can guide regional forest managers in selecting suitable species and sites for replanting. The ecosystem-wide decline of diversity and distinctness of the mangrove communities and range contractions or local extirpations of many rare and endemic species over the last three decades suggest for extending the existing protected area network as they currently do not cover the remaining species density and biodiversity hotspots. In addition to providing a basis for designing spatially explicit and cost effective field inventories and monitoring programs, my species, biodiversity, traits, and forest productivity maps can guide the forest protection, habitat enhancement and restoration initiatives in the Sundarbans.

Finally, this thesis points for possible improvements in several areas. The correlative HSMs and the habitat-based biodiversity models can be updated to mechanistic models by incorporating physiological or morphological traits for predicting species distribution across space and time. The integrated approach for quantifying trait – environment relationships could be extended to account for species-species interactions and should incorporate physiological traits when available. The HSMs, the biodiversity models and the trait-based models should be updated time to time with new environmental data to account for the spatial and temporal changes in the habitat conditions. Given the roles of hydroperiod in modulating habitat conditions that in turn may limit or favour plant growth and development, I suggest the inclusion of hydroperiod in future models.

Reference List

de Almeida, L.T. et al., 2016. Evaluating ten years of management effectiveness in a mangrove protected area. *Ocean & Coastal Management*, 125, pp.29–37.

Alongi, D.M., 2014. Carbon Cycling and Storage in Mangrove Forests. *Annual Review of Marine Science*, 6(1), pp.195–219.

Alongi, D.M., 2010. Dissolved iron supply limits early growth of estuarine mangroves. *Ecology*, 91(11), pp.3229–3241.

Alongi, D.M., 2015. The Impact of Climate Change on Mangrove Forests. *Current Climate Change Reports*, 1(1), pp.30–39.

Anderwald, P. et al., 2012. Seasonal trends and spatial differences in marine mammal occurrence in Broadhaven Bay, north-west Ireland. *Journal of the Marine Biological Association of the United Kingdom*, 92(08), pp.1757–1766.

Angiolini, C. et al., 2011. Using Multivariate Analyses to Assess Effects of Fluvial Type on Plant Species Distribution in a Mediterranean River. *Wetlands*, 31(1), pp.167–177.

Austin, M.., 2002. Spatial prediction of species distribution: an interface between ecological theory and statistical modelling. *Ecological Modelling*, 157(2-3), pp.101–118.

Aziz, A. et al., 2013. Prioritizing threats to improve conservation strategy for the tiger Panthera tigris in the Sundarbans Reserve Forest of Bangladesh. *Oryx*, 47(4), pp.1–9.

Aziz, A. & Paul, A., 2015. Bangladesh Sundarbans: Present status of the environment and Biota. *Diversity*, 7(3), pp.242–269.

Ball, M.C., 2002. Interactive effects of salinity and irradiance on growth: implications for mangrove forest structure along salinity gradients. *Trees*, 16(2-3), pp.126–139.

Banerjee, K., Gatti, R.C. & Mitra, A., 2017. Climate change-induced salinity variation impacts on a stenoecious mangrove species in the Indian Sundarbans. *Ambio*, 46(4), pp.492–499.

Barbier, E.B. et al., 2011. The value of estuarine and coastal ecosystem services. *Ecological Monographs*, 81(2), pp.169–193.

Baribault, T.W., Kobe, R.K. & Finley, A.O., 2012. Tropical tree growth is correlated with soil phosphorus, potassium, and calcium, though not for legumes. *Ecological Monographs*, 82(2), pp.189–203.

Barton, K., 2015. MuMIn: Multi-model inference. R package version 1.10.5.

Barwell, L.J., Isaac, N.J.B. & Kunin, W.E., 2015. Measuring β - diversity with species abundance data T. Coulson, ed. *Journal of Animal Ecology*, 84(4), pp.1112–1122.

Berger, U. et al., 2008. Advances and limitations of individual-based models to analyze and predict dynamics of mangrove forests: A review. *Aquatic Botany*, 89(2), pp.260–274.

Biswas, S.R. et al., 2007. Do invasive plants threaten the Sundarbans mangrove forest of Bangladesh? *Forest Ecology and Management*, 245(1-3), pp.1–9.

Blasco, F., Aizpuru, M. & Gers, C., 2001. Depletion of the mangroves of Continental Asia. *Wetlands Ecology and Management*, 9, pp.245–256.

Van Bodegom, P.M., Douma, J.C. & Verheijen, L.M., 2014. A fully traits-based approach to modeling global vegetation distribution. *Proceedings of the National Academy of Sciences of the United States of America*, 111(38), pp.13733–8.

Bonthoux, S., Baselga, A. & Balent, G., 2013. Assessing community-level and single-species models predictions of species distributions and assemblage composition after 25 years of land cover change. *PloS one*, 8(1), p.e54179.

ter Braak, C.J.F., Cormont, A. & Dray, S., 2012. Improved testing of species

traits-environment relationships in the fourth-corner problem. *Ecology*, 93(7), pp.1525–1526.

ter Braak, C.J.F., Peres-Neto, P. & Dray, S., 2017. A critical issue in model-based inference for studying trait-based community assembly and a solution. *PeerJ*, 5, p.e2885.

Bremner, J.M. & Breitenbeck, G.A., 1983. A simple method for determination of ammonium in semimicro-Kjeldahl analysis of soils and plant materials using a block digester . *Soi. Sci. Plant Anal.*, 14, pp.905–913.

Brown, A.M. et al., 2014. The fourth-corner solution - using predictive models to understand how species traits interact with the environment N. Yoccoz, ed. *Methods in Ecology and Evolution*, 5(4), pp.344–352.

Bunt, J., 1996. Mangrove Zonation: An Examination of Data from Seventeen Riverine Estuaries in Tropical Australia. *Annals of Botany*, 78(3), pp.333–341.

Bunt, J.S. & Stieglitz, T., 1999. Indicators of mangrove zonality : the Normanby river , N. E. Australia. *Mangrove and Salt Marshes*, 3(2), pp.177–184.

Burnham, K.P. & Anderson, D.R., 2002. *Model Selection and Multimodel Inference: a Practical Information-theoretic Approach, 2nd edn. Springer-Verlag, New York,*

De Cáceres, M. et al., 2012. The variation of tree beta diversity across a global network of forest plots. *Global Ecology and Biogeography*, 21(12), pp.1191–1202.

Cadotte, M.W., Carscadden, K. & Mirotchnick, N., 2011. Beyond species: Functional diversity and the maintenance of ecological processes and services. *Journal of Applied Ecology*, 48(Wilkins 2009), pp.1079–1087.

Carrasquilla-Henao, M. & Juanes, F., 2017. Mangroves enhance local fisheries catches: a global meta-analysis. *Fish and Fisheries*, 18(1), pp.79–93.

Chain-Guadarrama, A. et al., 2017. Potential trajectories of old-growth Neotropical forest functional composition under climate change. *Ecography*, (February), pp.1–14.

Chauvet, M. et al., 2017. Using a forest dynamics model to link community assembly processes and traits structure S. Russo, ed. *Functional Ecology*, 38(1), pp.42–49.

Chave, J. et al., 2009. Towards a worldwide wood economics spectrum. *Ecology Letters*, 12(4), pp.351–366.

Chen, Y. & Ye, Y., 2014. Effects of Salinity and Nutrient Addition on Mangrove Excoecaria agallocha R. P. Niedz, ed. *PLoS ONE*, 9(4), p.e93337.

Chesson, P., 2000. Mechanisms of Maintenance of Species Diversity. *Annual Review of Ecology and Systematics*, 31(2000), pp.343–358.

Chowdhury, M.Q., Kitin, P., et al., 2016. Cambial dormancy induced growth rings in Heritiera fomes Buch.- Ham.: a proxy for exploring the dynamics of Sundarbans, Bangladesh. *Trees*, 30(1), pp.227–239.

Chowdhury, M.Q. et al., 2008. Nature and periodicity of growth rings in two Bangladeshi mangrove species. *IAWA Journal*, 29(3), pp.265-276.

Chowdhury, M.Q., De Ridder, M. & Beeckman, H., 2016. Climatic Signals in Tree Rings of Heritiera fomes Buch.-Ham. in the Sundarbans, Bangladesh N. K. P. Kumaran, ed. *PLOS ONE*, 11(2), p.e0149788.

Connell, J.H., 1978. Diversity in Tropical Rain Forests and Coral Reefs. *Science*, 199(4335), pp.1302–1310.

Crase, B. et al., 2013. Hydroperiod is the main driver of the spatial pattern of dominance in mangrove communities. *Global Ecology and Biogeography*, 22(7), pp.806–817.

Crase, B. et al., 2015. Modelling both dominance and species distribution provides a more complete picture of changes to mangrove ecosystems under

climate change. *Global Change Biology*, 21(8), pp.3005–3020.

Da Cruz, C.C. et al., 2013. Distribution of mangrove vegetation along inundation, phosphorus, and salinity gradients on the Bragança Peninsula in Northern Brazil. *Plant and Soil*, 370(1-2), pp.393–406.

Dangremond, E.M., Feller, I.C. & Sousa, W.P., 2015. Environmental tolerances of rare and common mangroves along light and salinity gradients. *Oecologia*, 179(4), pp.1187–1198.

Danielsen, F. et al., 2005. The Asian tsunami: a protective role for coastal vegetation. *Science (New York, N.Y.)*, 310(October), p.643.

Daru, B.H. et al., 2013. A Global Trend towards the Loss of Evolutionarily Unique Species in Mangrove Ecosystems. *PloS one*, 8(6), p.e66686.

Das, S., 1999. An adaptive feature of some mangroves of Sundarbans, West Bengal. *Journal of Plant Biology*, 42(June), pp.109–116.

Dasgupta, N. et al., 2012. Protein and enzymes regulations towards salt tolerance of some Indian mangroves in relation to adaptation. *Trees*, 26(2), pp.377–391.

Denwood, M.J., 2016. runjags : An R Package Providing Interface Utilities, Model Templates, Parallel Computing Methods and Additional Distributions for MCMC Models in JAGS. *Journal of Statistical Software*, 71(9), pp.1–25.

De Deurwaerder, H. et al., 2016. How are anatomical and hydraulic features of the mangroves Avicennia marina and Rhizophora mucronata influenced by siltation? *Trees - Structure and Function*, 30(1), pp.35–45.

Devictor, V. et al., 2010. Spatial mismatch and congruence between taxonomic, phylogenetic and functional diversity: The need for integrative conservation strategies in a changing world. *Ecology Letters*, 13(8), pp.1030–1040.

Diaz, S. et al., 2007. Incorporating plant functional diversity effects in ecosystem service assessments. *Proceedings of the National Academy of*

Sciences, 104(52), pp.20684–20689.

Díaz, S. et al., 2015. The global spectrum of plant form and function. *Nature*, 529(7585), pp.167–171.

Dolédec, S. et al., 1996. Matching species traits to environmental variables: a new three-table ordination method. *Environmental and Ecological Statistics*, 3(2), pp.143–166.

Donato, D.C. et al., 2011. Mangroves among the most carbon-rich forests in the tropics. *Nature Geoscience*, 4(4), pp.1–5.

Dormann, C.F. et al., 2012. Correlation and process in species distribution models: bridging a dichotomy. *Journal of Biogeography*, 39(12), pp.2119–2131.

Dormann, C.F., 2007. Promising the future? Global change projections of species distributions. *Basic and Applied Ecology*, 8(5), pp.387–397.

Dray, S. et al., 2014. Combining the fourth-corner and the RLQ methods for assessing trait responses to environmental variation. *Ecology*, 95(1), pp.14–21.

Dray, S. & Legendre, P., 2008. Testing the species traits environment relationships: The fourth-corner problem revisited. *Ecology*, 89(12), pp.3400–3412.

Duke, N.C. et al., 2007. A World Without Mangroves? *Science*, 317(5834), p.41b–42b.

Duke, N.C., 2001. Gap creation and regenerative processes driving diversity and structure of mangrove ecosystems. *Wetlands Ecology and Management*, 9(3), pp.267–279.

Duke, N.C., Ball, M.C. & Ellison, J.C., 1998. Factors Influencing Biodiversity and Distributional Gradients in Mangroves. *Global Ecology and Biogeography Letters*, 7(1), p.27.

Duke, N.C., Ball, M.C. & Ellison, J.C., 1998. Factors Influencing Biodiversity and Distributional Gradients in Mangroves. *Global Ecology and Biogeography Letters*, 7(1), p.27.

Elith, J. & Leathwick, J.R., 2009. Species Distribution Models: Ecological Explanation and Prediction Across Space and Time. *Annual Review of Ecology, Evolution, and Systematics*, 40(1), pp.677–697.

Ellison, A.M., 2001. Macroecology of mangroves: large-scale patterns and processes in tropical coastal forests. *Trees*, 16(2-3), pp.181–194.

Ellison, A.M., Farnsworth, E.J. & Merkt, R.E., 1999. Origins of mangrove ecosystems and the mangrove biodiversity anomaly. *Global Ecology and Biogeography*, 8(2), pp.95–115.

Ellison, A.M., Mukherjee, B.B. & Karim, A., 2000. Testing patterns of zonation in mangroves: Scale dependence and environmental correlates in the Sundarbans of Bangladesh. *Journal of Ecology*, 88(5), pp.813–824.

Eskildsen, A. et al., 2013. Testing species distribution models across space and time: high latitude butterflies and recent warming. *Global Ecology and Biogeography*, 22(12), pp.1293–1303.

Farnsworth, E.J., 1998. Issues of Spatial, Taxonomic and Temporal Scale in Delineating Links between Mangrove Diversity and Ecosystem Function. *Global Ecology and Biogeography Letters*, 7(1), p.15.

Faucon, M.-P., Houben, D. & Lambers, H., 2017. Plant Functional Traits: Soil and Ecosystem Services. *Trends in Plant Science*, 22(5), pp.385–394.

Feller, I.C. et al., 2010. Biocomplexity in Mangrove Ecosystems. *Annual Review of Marine Science*, 2(1), pp.395–417.

Ferrier, S. & Guisan, A., 2006. Spatial modelling of biodiversity at the community level. *Journal of Applied Ecology*, 43(3), pp.393–404.

Flowers, T.J., Galal, H.K. & Bromham, L., 2010. Evolution of halophytes:

Multiple origins of salt tolerance in land plants. *Functional Plant Biology*, 37(Sanderson 2003), pp.604–612.

Franklin, J., 2010. *Mapping species distributions*, Cambridge: Cambridge University Press.

Friess, D., 2016. Ecosystem Services and Disservices of Mangrove Forests: Insights from Historical Colonial Observations. *Forests*, 7(9), p.183.

Funk, J.L. et al., 2017. Revisiting the Holy Grail: using plant functional traits to understand ecological processes. *Biological Reviews*, 92(2), pp.1156–1173.

Gardner, T.A. et al., 2012. A framework for integrating biodiversity concerns into national REDD+ programmes. *Biological Conservation*, 154, pp.61–71.

Gasper, J.R., Kruse, G.H. & Hilborn, R., 2013. Modeling of the spatial distribution of Pacific spiny dogfish (Squalus suckleyi) in the Gulf of Alaska using generalized additive and generalized linear models. *Canadian Journal of Fisheries and Aquatic Sciences*, 70(9), pp.1372–1385.

Gaston, K.J. & Fuller, R.A., 2008. Commonness, population depletion and conservation biology. *Trends in Ecology and Evolution*, 23(1), pp.14–19.

Gee, G.W. & Bauder, J.W., 1986. Particle-size analysis. In *Methods of soil analysis. Part 1. Physical and mineralogical methods*. pp. 383–411.

Geller, J.B., Darling, J. a & Carlton, J.T., 2010. Genetic perspectives on marine biological invasions. *Annual review of marine science*, 2, pp.367–93.

Gelman, A. et al., 2004. Bayesian Data Analysis. *Technometrics*, 46, p.696.

Ghosh, A. et al., 2015. The Indian Sundarban Mangrove Forests: History, Utilization, Conservation Strategies and Local Perception. *Diversity*, 7(2), pp.149–169.

Ghosh, M., Kumar, L. & Roy, C., 2017. Climate Variability and Mangrove Cover Dynamics at Species Level in the Sundarbans, Bangladesh. *Sustainability*,

9(5), p.805.

Ghosh, M., Kumar, L. & Roy, C., 2016. Mapping Long-Term Changes in Mangrove Species Composition and Distribution in the Sundarbans. *Forests*, 7(12), p.305.

Gillette, D.P. et al., 2012. Patterns of change over time in darter (Teleostei: Percidae) assemblages of the Arkansas River basin, northeastern Oklahoma, USA. *Ecography*, 35(October 2011), pp.855–864.

Gilman, E.L. et al., 2008. Threats to mangroves from climate change and adaptation options: A review. *Aquatic Botany*, 89(2), pp.237–250.

Giri, C. et al., 2008. Mangrove forest distributions and dynamics (1975–2005) of the tsunami-affected region of Asia. *Journal of Biogeography*, 35(3), pp.519–528.

Giri, C. et al., 2007. Monitoring mangrove forest dynamics of the Sundarbans in Bangladesh and India using multi-temporal satellite data from 1973 to 2000. *Estuarine, Coastal and Shelf Science*, 73, pp.91–100.

Giri, C. et al., 2011. Status and distribution of mangrove forests of the world using earth observation satellite data. *Global Ecology and Biogeography*, 20(1), pp.154–159.

Gopal, B. & Chauhan, M., 2006. Biodiversity and its conservation in the Sundarban Mangrove Ecosystem. *Aquatic Sciences*, 68(3), pp.338–354.

Granger, V. et al., 2015. Mapping diversity indices: not a trivial issue P. Peres-Neto, ed. *Methods in Ecology and Evolution*, 6(6), pp.688–696.

Gransee, a. & Führs, H., 2013. Magnesium mobility in soils as a challenge for soil and plant analysis, magnesium fertilization and root uptake under adverse growth conditions. *Plant and Soil*, 368, pp.5–21.

Grime, J.P., 1998. Benefits of plant diversity to ecosystems: immediate, filter and founder effects. *Journal of Ecology*, 86, pp.902–910.

Grime, J.P. et al., 1997. Integrated Screening Validates Primary Axes of Specialisation in Plants. *Oikos*, 79(2), p.259.

Grime, J.P., 2001. *Plant Strategies, Vegetation Processes and Ecosystem Properties*, John Wiley & Sons, Ltd.

Grime, J.P., 2006. Trait convergence and trait divergence in herbaceous plant communities: Mechanisms and consequences. *Journal of Vegetation Science*, 17(2), pp.255–260.

Grueters, U. et al., 2014. The mangrove forest dynamics model mesoFON. *Ecological Modelling*, 291, pp.28–41.

Guisan, A. et al., 2013. Predicting species distributions for conservation decisions. *Ecology Letters*, 16, pp.1424–1435.

Guisan, A., Edwards, T.C. & Hastie, T., 2002. Generalized linear and generalized additive models in studies of species distributions: setting the scene. *Ecological Modelling*, 157(2-3), pp.89–100.

Guisan, A. & Thuiller, W., 2005. Predicting species distribution: Offering more than simple habitat models. *Ecology Letters*, 8(9), pp.993–1009.

Guisan, A. & Zimmermann, N.E., 2000. Predictive habitat distribution models in ecology. *Ecological Modelling*, 135(2-3), pp.147–186.

Hardie, M. & Doyle, R., 2012. Measuring soil salinity. *Methods in molecular biology (Clifton, N.J.)*, 913, pp.415–25.

Harun-or-Rashid, S. et al., 2009. Mangrove community recovery potential after catastrophic disturbances in Bangladesh. *Forest Ecology and Management*, 257(3), pp.923–930.

Hastie, G. et al., 2005. Environmental models for predicting oceanic dolphin habitat in the Northeast Atlantic. *ICES Journal of Marine Science*, 62(4), pp.760–770.

Heumann, B.W., 2011. Satellite remote sensing of mangrove forests: Recent advances and future opportunities. *Progress in Physical Geography*, 35(1), pp.87–108.

Hijmans, R.J., 2015. raster: Geographic Data Analysis and Modeling. R package version 2.4-18.

Hill, M.O., 1973. Diversity and Evenness: A Unifying Notation and Its Consequences. *Ecology*, 54(2), p.427.

Hirzel, A.H. & Le Lay, G., 2008. Habitat suitability modelling and niche theory. *Journal of Applied Ecology*, 45(5), pp.1372–1381.

Hooper, D.U. et al., 2005. Effects of biodiversity on ecosystem functioning: A consensus of current knowledge. *Ecological Monographs*, 75(1), pp.3–35.

Hoppe-Speer, S.C.L. et al., 2011. The response of the red mangrove Rhizophora mucronata Lam. to salinity and inundation in South Africa. *Aquatic Botany*, 95(2), pp.71–76.

Hossain, M. et al., 2014. Salinity influence on germination of four important mangrove species of the Sundarbans, Bangladesh. *Agriculture and Forestry*, 60(2), pp.125–135.

Howard, R.J. et al., 2015. Plant-plant interactions in a subtropical mangrove-to-marsh transition zone: Effects of environmental drivers. *Journal of Vegetation Science*, 26(6), pp.1198–1211.

Hubbell, S.P., 2001. *The Unified Neutral Theory of Biodiversity and Biogeography*, Princeton University Press.

Hudson, L.N. et al., 2014. The PREDICTS database: a global database of how local terrestrial biodiversity responds to human impacts. *Ecology and Evolution*, 4(24), pp.4701–4735.

Hussain, M.A., Islam, A.K.M.S. & Hasan, M.A., 2013. Changes of the Seasonal Salinity Distribution At the Sundarbans Coast Due To Impact of Climate

Change. In *4th International Conference on Water & Flood Management (ICWFM-2013)*. pp. 637–648.

Hutchinson, G.E., 1957. Cold Spring Harbor Symposia. *Quantitative Biology*, 22, pp.415–427.

Iftekhar, M.S. & Islam, M.R., 2004. Degeneration of Bangladesh's Sundarbans mangroves: a management issue. *International Forestry Review*, 6(2), pp.123–135.

Iftekhar, M.S. & Saenger, P., 2008. Vegetation dynamics in the Bangladesh Sundarbans mangroves: a review of forest inventories. *Wetlands Ecology and Management*, 16(4), pp.291–312.

Islam, M.S. & Wahab, M.A., 2005. A review on the present status and management of mangrove wetland habitat resources in Bangladesh with emphasis on mangrove fisheries and aquaculture. *Hydrobiologia*, 542(1), pp.165–190.

Islam, S., Rahman, M. & Chakma, S., 2014. Plant Diversity and Forest Structure of the Three Protected Areas (Wildlife Sanctuaries) of Bangladesh Sundarbans: Current Status and Management Strategies. In A. Latiff, I. Faridah-Hanum & M. Ozturk, Khalid Rehman Hakeem, eds. *Mangrove Ecosystems of Asia*. pp. 127–152.

IWM, 2003. *Sundarban Biodiversity Conservation Project*,

Jamil, T. et al., 2013. Selecting traits that explain species-environment relationships: a generalized linear mixed model approach F. de Bello, ed. *Journal of Vegetation Science*, 24(6), pp.988–1000.

Jamil, T. et al., 2012. Trait-Environment Relationships and Tiered Forward Model Selection in Linear Mixed Models. *International Journal of Ecology*, 2012, pp.1–12.

Jamil, T., Kruk, C. & Ter Braak, C.J.F., 2014. A unimodal species response

model relating traits to environment with application to phytoplankton communities. *PLoS ONE*, 9(5).

Jarnevich, C.S. & Reynolds, L. V., 2010. Challenges of predicting the potential distribution of a slow-spreading invader: A habitat suitability map for an invasive riparian tree. *Biological Invasions*, 13, pp.153–163.

Jost, L., 2006. Entropy and diversity. *Oikos*, 113(2), pp.363–375.

Jost, L., 2010. Independence of alpha and beta diversities. *Ecology*, 91(7), pp.1969–1974.

Jost, L., 2007a. PARTITIONING DIVERSITY INTO INDEPENDENT ALPHA AND BETA COMPONENTS. *Ecology*, 88(10), pp.2427–2439.

Jost, L., 2007b. Partitioning diversity into independent alpha and beta components. *Ecology*, 88(10), pp.2427–2439.

Karim, M.F. & Mimura, N., 2008. Impacts of climate change and sea-level rise on cyclonic storm surge floods in Bangladesh. *Global Environmental Change*, 18(3), pp.490–500.

Kathiresan, K., 2010. Globally threatened mangrove species in India. *Current Science*, 98(12), p.2010.

Kattge, J. et al., 2011. TRY - a global database of plant traits. *Global Change Biology*, 17(9), pp.2905–2935.

Kearney, M. & Porter, W., 2009. Mechanistic niche modelling: combining physiological and spatial data to predict species' ranges. *Ecology Letters*, 12(4), pp.334–350.

Khoon, G.W. & Eong, O.J., 1995. The use of demographic studies in mangrove silviculture. *Hydrobiologia*, 295, pp.38255–261.

Kleyer, M. et al., 2012. Assessing species and community functional responses to environmental gradients: Which multivariate methods? *Journal of*

Vegetation Science, 23(5), pp.805–821.

Kodikara, K.A.S. et al., 2017. Have mangrove restoration projects worked? An in-depth study in Sri Lanka. *Restoration Ecology*, pp.1–12.

Kraft, N.J.B., Godoy, O. & Levine, J.M., 2015. Plant functional traits and the multidimensional nature of species coexistence. *Proceedings of the National Academy of Sciences*, 112(3), pp.797–802.

Kraft, N.J.B., Valencia, R. & Ackerly, D.D., 2008. Functional Traits and Niche-Based Tree Community Assembly in an Amazonian Forest. *Science*, 322(5901), pp.580–582.

Krauss, K.W. et al., 2008. Environmental drivers in mangrove establishment and early development: A review. *Aquatic Botany*, 89, pp.105–127.

Krauss, K.W. & Ball, M.C., 2013. On the halophytic nature of mangroves. *Trees - Structure and Function*, 27, pp.7–11.

Kronzucker, H.J., Siddiqi, M.Y. & Glass, A.D.M., 1997. Conifer root discrimination against soil nitrate and the ecology of forest succession. *Nature*, 385, pp.59–61.

Kuenzer, C. et al., 2011. *Remote Sensing of Mangrove Ecosystems: A Review*,

Kunstler, G. et al., 2015. Plant functional traits have globally consistent effects on competition. *Nature*, 529(7585), pp.204–207.

Lande, R., 1996. Statistics and Partitioning of Species Diversity, and Similarity among Multiple Communities. *Oikos*, 76(1), p.5.

Laughlin, D.C., 2014. Applying trait-based models to achieve functional targets for theory-driven ecological restoration. *Ecology Letters*, 17(7), pp.771–784.

Lavorel, S. et al., 2007. Assessing functional diversity in the field – methodology matters! *Functional Ecology*, 22(1), pp.134–147.

Lavorel, S. et al., 2011. Using plant functional traits to understand the landscape distribution of multiple ecosystem services. *Journal of Ecology*, 99(1), pp.135–147.

Lawson, J.R., Fryirs, K.A. & Leishman, M.R., 2015. Hydrological conditions explain variation in wood density in riparian plants of south-eastern Australia S. Bonser, ed. *Journal of Ecology*, 103(4), pp.945–956.

Lee, S.Y. et al., 2014. Ecological role and services of tropical mangrove ecosystems: a reassessment. *Global Ecology and Biogeography*, 23(7), pp.726–743.

Legendre, P. & De Cáceres, M., 2013. Beta diversity as the variance of community data: dissimilarity coefficients and partitioning. *Ecology letters*, 16(8), pp.951–63.

Legendre, P., Galzin, R. & Harmelin-Vivien, M.L., 1997. Relating Behavior to Habitat: Solutions to the Fourth-corner Problem. *Ecology*, 78(2), p.547.

Leinster, T. & Cobbold, C.A., 2012. Measuring diversity: the importance of species similarity. *Ecology*, 93(3), pp.477–489.

Lewis, R.R., 2005. Ecological engineering for successful management and restoration of mangrove forests. *Ecological Engineering*, 24(4), pp.403–418.

Liang, S. et al., 2008. Adaptation to salinity in mangroves: Implication on the evolution of salt-tolerance. *Chinese Science Bulletin*, 53(11), pp.1708–1715.

Lovelock, C.E. et al., 2009. Nutrient Enrichment Increases Mortality of Mangroves R. Thompson, ed. *PLoS ONE*, 4(5), p.e5600.

Lovelock, C.E. et al., 2006. Variation in hydraulic conductivity of mangroves: Influence of species, salinity, and nitrogen and phosphorus availability. *Physiologia Plantarum*, 127(Ball 1996), pp.457–464.

Luo, Z., Sun, O.J. & Xu, H., 2010. A comparison of species composition and stand structure between planted and natural mangrove forests in Shenzhen

Bay, South China. *Journal of Plant Ecology*, 3(3), pp.165–174.

Luther, D. a. & Greenberg, R., 2009. Mangroves: A Global Perspective on the Evolution and Conservation of Their Terrestrial Vertebrates. *BioScience*, 59(7), pp.602–612.

MacArthur, R. & Levins, R., 1967. The Limiting Similarity , Convergence , and Divergence of Coexisting Species. *The American Naturalist*, 101(921), pp.377–385.

Mahmood, H., 2015. *Handbook of selected plant species of the Sundarbans and the embankment ecosystem*, SDBC, Sundarbans.

Malik, A., Fensholt, R. & Mertz, O., 2015. Mangrove exploitation effects on biodiversity and ecosystem services. *Biodiversity and Conservation*, 24(14), pp.3543–3557.

Mateo, R.G., Mokany, K. & Guisan, A., 2017. Biodiversity Models: What If Unsaturation Is the Rule? *Trends in Ecology & Evolution*, xx, pp.1–11.

Maurer, B.A. & Mcgill, B.J., 2011. Measurement of species diversity. In A. E. Magurran & B. J. McGill, eds. *Biological diversity: frontiers in measurement and assessment*. pp. 55–65.

Mayfield, M.M. & Levine, J.M., 2010. Opposing effects of competitive exclusion on the phylogenetic structure of communities. *Ecology Letters*, 13(9), pp.1085–1093.

McKee, K.L. & Faulkner, P.L., 2000. Restoration of biogeochemical function in mangrove forests. *Restoration Ecology*, 8(3), pp.247–259.

McKinney, M.L. & Lockwood, J.L., 1999. Biotic homogenization: a few winners replacing many losers in the next mass extinction. *Trends in Ecology & Evolution*, 14(11), pp.450–453.

Mendes, R.S. et al., 2008. A unified index to measure ecological diversity and species rarity. *Ecography*, 31(February), pp.450–456.

Meynard, C.N. et al., 2011. Beyond taxonomic diversity patterns: how do α, β and γ components of bird functional and phylogenetic diversity respond to environmental gradients across France? *Global Ecology and Biogeography*, 20(6), pp.893–903.

Miller, J., 2010. Species Distribution Modeling. *Geography Compass*, 4(6), pp.490–509.

Miller, J., Franklin, J. & Aspinall, R., 2007. Incorporating spatial dependence in predictive vegetation models. *Ecological Modelling*, 202(3-4), pp.225–242.

Mirza, M.M.Q., 1998. Diversion of the Ganges Water at Farakka and Its Effects on Salinity in Bangladesh. *Environmental Management*, 22(5), pp.711–722.

Mitra, A., 2013. *Sensitivity of mangrove ecosystem to changing climate*,

Mitra, A. & Zaman, S., 2016. *Basics of Marine and Estuarine Ecology*, New Delhi: Springer India.

Mod, H.K. et al., 2015. Biotic interactions boost spatial models of species richness. *Ecography*, 38(9), pp.913–921.

Moudrý, V. & Šímová, P., 2013. Relative importance of climate, topography, and habitats for breeding wetland birds with different latitudinal distributions in the Czech Republic. *Applied Geography*, 44, pp.165–171.

Mukhopadhyay, A. et al., 2015. Changes in mangrove species assemblages and future prediction of the Bangladesh Sundarbans using Markov chain model and cellular automata. *Environ. Sci.: Processes Impacts*, 17(6), pp.1111–1117.

Naidoo, G., 2009. Differential effects of nitrogen and phosphorus enrichment on growth of dwarf Avicennia marina mangroves. *Aquatic Botany*, 90(2), pp.184–190.

Naimi, B., 2015. usdm: Uncertainty Analysis for Species Distribution Models. R package version 1.1-15.

Nandy, P. et al., 2007. Effects of salinity on photosynthesis, leaf anatomy, ion accumulation and photosynthetic nitrogen use efficiency in five Indian mangroves. *Wetlands Ecology and Management*, 15(4), pp.347–357.

Nandy, P., Dasgupta, N. & Das, S., 2009. Differential expression of physiological and biochemical characters of some Indian mangroves towards salt tolerance. *Physiology and Molecular Biology of Plants*, 15(2), pp.151–160.

Naskar, S. & Palit, P.K., 2015. Anatomical and physiological adaptations of mangroves. *Wetlands Ecology and Management*, 23(3), pp.357–370.

Nekola, J.C. & White, P.S., 1999. The distance decay of similarity in biogeography and ecology. *Journal of Biogeography*, 26(4), pp.867–878.

Ngole-Jeme, V.M. et al., 2016. Impact of logging activities in a tropical mangrove on ecosystem diversity and sediment heavy metal concentrations. *Journal of Coastal Conservation*, 20(3), pp.245–255.

Olden, J.D., 2006. Biotic homogenization: a new research agenda for conservation biogeography. *Journal of Biogeography*, 33(12), pp.2027–2039.

Olden, J.D. & Poff, N.L., 2003. Toward a mechanistic understanding and prediction of biotic homogenization. *The American naturalist*, 162(4), pp.442–460.

Olden, J.D. & Rooney, T.P., 2006. On defining and quantifying biotic homogenization. *Global Ecology and Biogeography*, 15, pp.113–120.

Olszewski, T.D., 2004. A unified mathematical framework for the measurement of richness and evenness within and among multiple communities. *Oikos*, 104(2), pp.377–387.

Osland, M.J. et al., 2017. Climatic controls on the global distribution, abundance, and species richness of mangrove forests. *Ecological Monographs*, 87(2), pp.341–359.

Ostling, J.L., Butler, D.R. & Dixon, R.W., 2009. The biogeomorphology of

mangroves and their role in natural hazards mitigation. *Geography Compass*, 3, pp.1607–1624.

Pakeman, R.J., 2011. Multivariate identification of plant functional response and effect traits in an agricultural landscape. *Ecology*, 92(6), pp.1353–1365.

Parida, A.K. et al., 2004. Effects of salinity on biochemical components of the mangrove, Aegiceras corniculatum. *Aquatic Botany*, 80(2), pp.77–87.

Parida, A.K. & Das, A.B., 2005. Salt tolerance and salinity effects on plants: a review. *Ecotoxicology and environmental safety*, 60(3), pp.324–49.

Pastor, J. et al., 1984. Aboveground production and N and P cycling along a nitrogen mineralization gradient on Blackhawk Island, Wisconsin. *Ecology*, 65(1), pp.256–268.

Payo, A. et al., 2016. Projected changes in area of the Sundarban mangrove forest in Bangladesh due to SLR by 2100. *Climatic Change*, 139(2), pp.279–291.

Pebesma, E.J., 2004. Multivariable geostatistics in S: the gstat package. *Computers & Geosciences*, 30(7), pp.683–691.

Peres-Neto, P.R., Dray, S. & Braak, C.J.F. ter, 2017. Linking trait variation to the environment: critical issues with community-weighted mean correlation resolved by the fourth-corner approach. *Ecography*, (July), pp.1–29.

Pérez-Harguindeguy, N. et al., 2013. New handbook for standardised measurement of plant functional traits worldwide. *Australian Journal of Botany*, 61(3), p.167.

Plummer, M., 2015. JAGS Version 4.0.0 user manual. , (August), pp.0–41.

Polidoro, B.A. et al., 2010. The loss of species: mangrove extinction risk and geographic areas of global concern. *PloS one*, 5(4), p.e10095.

Pollock, L.J., Morris, W.K. & Vesk, P. a., 2012. The role of functional traits in

species distributions revealed through a hierarchical model. *Ecography*, 35(8), pp.716–725.

Possingham, H.P., Bode, M. & Klein, C.J., 2015. Optimal Conservation Outcomes Require Both Restoration and Protection. *PLOS Biology*, 13(1), p.e1002052.

Pottier, J. et al., 2013. The accuracy of plant assemblage prediction from species distribution models varies along environmental gradients R. Field, ed. *Global Ecology and Biogeography*, 22(1), pp.52–63.

Prado-Junior, J.A. et al., 2016. Conservative species drive biomass productivity in tropical dry forests. *Journal of Ecology*, 104(3), pp.817–827.

Purves, D.W. et al., 2008. Predicting and understanding forest dynamics using a simple tractable model. *Proceedings of the National Academy of Sciences*, 105(44), pp.17018–17022.

R Core Team, 2016. R: A language and environment for statistical computing.

Rahaman, S.M.B. et al., 2015. A Spatial and Seasonal Pattern of Water Quality in the Sundarbans River Systems of Bangladesh. *Journal of Coastal Research*, 300(2), pp.390–397.

Rahman, M. et al., 2015. Carbon stock in the Sundarbans mangrove forest: spatial variations in vegetation types and salinity zones. *Wetlands Ecology and Management*, 23(2), pp.269–283.

Raju, J.S.S.N., 2003. Xylocarpus (Meliaceae): A less-known mangrove taxon of the Godavari estuary, India. *Current Science*, 84(7), pp.879–881.

Rakotomavo, A. & Fromard, F., 2010. Dynamics of mangrove forests in the Mangoky River delta, Madagascar, under the influence of natural and human factors. *Forest Ecology and Management*, 259(6), pp.1161–1169.

Rasool, S. et al., 2013. *Ecophysiology and Responses of Plants under Salt Stress* P. Ahmad, M. M. Azooz, & M. N. V. Prasad, eds., New York, NY: Springer New York.

Record, S. et al., 2013. Projecting global mangrove species and community distributions under climate change. *Ecosphere*, 4(3), pp.1–23.

Reef, R., Feller, I.C. & Lovelock, C.E., 2010. Nutrition of mangroves. *Tree physiology*, 30(9), pp.1148–60.

Reeve, R. et al., 2016. How to partition diversity. *arXiv*, 1404.6520(v1), pp.1–9.

Reich, P.B., 2014. The world-wide ?fast-slow? plant economics spectrum: a traits manifesto H. Cornelissen, ed. *Journal of Ecology*, 102(2), pp.275–301.

Reich, P.B., Walters, M.B. & Ellsworth, D.S., 1997. From tropics to tundra: Global convergence in plant functioning. *Proceedings of the National Academy of Sciences*, 94(25), pp.13730–13734.

Rényi, a, 1961. On measures of entropy and information. *Entropy*, 547(c), pp.547–561.

Richards, D.R. & Friess, D.A., 2016. Rates and drivers of mangrove deforestation in Southeast Asia, 2000–2012. *Proceedings of the National Academy of Sciences*, 113(2), pp.344–349.

Ricklefs, R.E., Schwarzbach, A.E. & Renner, S.S., 2006. Rate of Lineage Origin Explains the Diversity Anomaly in the World's Mangrove Vegetation. *The American Naturalist*, 168(6), pp.805–810.

Ricotta, C. et al., 2016. Measuring the functional redundancy of biological communities: a quantitative guide P. Peres-Neto, ed. *Methods in Ecology and Evolution*, (2014).

Robinson, C. & Schumacker, R., 2009. Interaction effects: centering, variance inflation factor, and interpretation issues. *Multiple Linear Regression Viewpoints*, 35(1), pp.6–11.

Rosado, B.H.P. et al., 2016. Changes in plant functional traits and water use in Atlantic rainforest: evidence of conservative water use in spatio-temporal scales. *Trees*, 30(1), pp.47–61.

Le Roux, P.C. et al., 2013. Horizontal, but not vertical, biotic interactions affect fine-scale plant distribution patterns in a low-energy system. *Ecology*, 94(3), pp.671–682.

Le Roux, P.C. et al., 2014. Incorporating dominant species as proxies for biotic interactions strengthens plant community models. *Journal of Ecology*, 102(3), pp.767–775.

Saenger, P., 2002. *Mangrove Ecology, Silviculture and Conservation*, Dordrecht: Springer Netherlands.

Sandilyan, S. & Kathiresan, K., 2012. Mangrove conservation: a global perspective. *Biodiversity and Conservation*, 21(14), pp.3523–3542.

Sardans, J. & Peñuelas, J., 2015. Potassium: a neglected nutrient in global change. *Global Ecology and Biogeography*, 24(3), pp.261–275.

Sarker, S.K., Deb, J.C. & Halim, M. a., 2011. A diagnosis of existing logging bans in Bangladesh. *International Forestry Review*, 13(4), pp.461–475.

Scheiter, S., Langan, L. & Higgins, S.I., 2013. Next-generation dynamic global vegetation models: learning from community ecology. *New Phytologist*, 198(3), pp.957–969.

Shangguan, W. et al., 2014. A global soil data set for earth system modeling. *Journal of Advances in Modeling Earth Systems*, 6(1), pp.249–263.

Shannon, C.E. & Weaver, W., 1949. The Mathematical Theory of Communication. *The mathematical theory of communication*, 27(4), p.117.

Sherman, R.E., Fahey, T.J. & Battles, J.J., 2000. Small-scale disturbance and regeneration dynamics in a neotropical mangrove forest. *Journal of Ecology*, 88(1), pp.165–178.

Siddiqi, N.A., 2001. *Mangrove forestry in Bangladesh*, Institute of Forestry and Environmental Sciences, University of Chittagong, Chittagong, Bangladesh.

Siddiqui, A.S.M.H. & Khair, A., 2012. Infestation Status of Heart Rot Disease of Pasur (Xylocarpus mekongensis), Tree in the Sundarbans. *The Indian Forester*, 138(2).

Simpson, E.H.., 1948. Measurement of diversity. *Nature*, 163, p.688.

Siple, M.C. & Donahue, M.J., 2013. Invasive mangrove removal and recovery: Food web effects across a chronosequence. *Journal of Experimental Marine Biology and Ecology*, 448, pp.128–135.

Slik, J.W.F. et al., 2015. An estimate of the number of tropical tree species. *Proceedings of the National Academy of Sciences*, 112(24), pp.7472–7477.

Smart, S.M. et al., 2006. Biotic homogenization and changes in species diversity across human-modified ecosystems. *Proceedings of the Royal Society B: Biological Sciences*, 273(1601), pp.2659-2665.

Smolik, M.G. et al., 2010. Integrating species distribution models and interacting particle systems to predict the spread of an invasive alien plant. *Journal of Biogeography*, 37(3), pp.411–422.

Socolar, J.B. et al., 2015. How Should Beta-Diversity Inform Biodiversity Conservation? *Trends in Ecology and Evolution*, 31(1), pp.67–80.

Soudzilovskaia, N. a. et al., 2013. Functional traits predict relationship between plant abundance dynamic and long-term climate warming. *Proceedings of the National Academy of Sciences*, 110(45), pp.18180–18184.

Spiegelhalter, D.J. et al., 2002. Bayesian measures of model complexity and fit. *Journal of the Royal Statistical Society: Series B (Statistical Methodology)*, 64(4), pp.583–639.

Swenson, N.G. et al., 2012. Phylogenetic and functional alpha and beta diversity in temperate and tropical tree communities. *Ecology*, 93(sp8), pp.S112–S125.

Thampanya, U., Vermaat, J.E. & Terrados, J., 2002. The effect of increasing

sediment accretion on the seedlings of three common Thai mangrove species. *Aquatic Botany*, 74(4), pp.315–325.

Tilman, D., 1999. The ecological consequences of changes in biodiversity: a search for general principles. *Ecology*, 80(5), pp.1455–1474.

Tomlinson, P.B., 1986. *The botany of mangroves*, Cambridge University Press.

Triest, L., 2008. Molecular ecology and biogeography of mangrove trees towards conceptual insights on gene flow and barriers: A review. *Aquatic Botany*, 89(2), pp.138–154.

Tuomisto, H., 2010a. A diversity of beta diversities: straightening up a concept gone awry. Part 1. Defining beta diversity as a function of alpha and gamma diversity. *Ecography*, 33(1), pp.2–22.

Tuomisto, H., 2010b. A diversity of beta diversities: straightening up a concept gone awry. Part 2. Quantifying beta diversity and related phenomena. *Ecography*, 33(1), pp.23–45.

Twilley, R.R. & Rivera-Monroy, V.H., 2005. Developing performance measures of mangrove wetlands using simulation models of hydrology, nutrient biogeochemistry, and community dynamics. *Journal of Coastal Research*, (SI 40), pp.79-93.

Veech, J.A. & Crist, T.O., 2010. Toward a unified view of diversity partitioning. *Ecology*, 91(7), pp.1988–92.

Verberk, W.C.E.P., van Noordwijk, C.G.E. & Hildrew, a. G., 2013. Delivering on a promise: integrating species traits to transform descriptive community ecology into a predictive science. *Freshwater Science*, 32(2), pp.531–547.

Violle, C. et al., 2007. Let the concept of trait be functional! *Oikos*, 116(January), pp.882–892.

Violle, C. et al., 2014. The emergence and promise of functional biogeography. *Proceedings of the National Academy of Sciences*, 111(38), pp.13690–13696.

Vovides, A.G. et al., 2014. Morphological plasticity in mangrove trees: salinity-related changes in the allometry of Avicennia germinans. *Trees*, 28(5), pp.1413–1425.

Wahid, S.M., Babel, M.S. & Bhuiyan, A.R., 2007. Hydrologic monitoring and analysis in the Sundarbans mangrove ecosystem, Bangladesh. *Journal of Hydrology*, 332(3-4), pp.381–395.

Wang, L. et al., 2010. Differentiation between true mangroves and mangrove associates based on leaf traits and salt contents. *Journal of Plant Ecology*, 4(4), pp.292–301.

Wang, L. et al., 2011. Differentiation between true mangroves and mangrove associates based on leaf traits and salt contents. *Journal of Plant Ecology*, 4(4), pp.292–301.

Ward, R.D. et al., 2016. Impacts of climate change on mangrove ecosystems: a region by region overview. *Ecosystem Health and Sustainability*, 2(4), pp.1–25.

Warton, D.I., Shipley, B. & Hastie, T., 2015. CATS regression - a model-based approach to studying trait-based community assembly. *Methods in Ecology and Evolution*, 6(4), pp.389–398.

Washington, W., Kathiresan, K. & Bingham, B.L., 2001. *Biology of mangroves and mangrove Ecosystems*,

Webb, C.T. et al., 2010. A structured and dynamic framework to advance traits-based theory and prediction in ecology. *Ecology Letters*, 13(3), pp.267–283.

Weiher, E. et al., 1999. Challenging Theophrastus: A common core list of plant traits for functional ecology. *Journal of Vegetation Science*, 10(5), pp.609–620.

Weiher, E. & Keddy, P.A., 1995. Assembly Rules , Null Models , and Trait Dispersion : New Questions from Old Patterns. *Oikos*, 74(1), pp.159–164.

Westoby, M. & Wright, I.J., 2006. Land-plant ecology on the basis of functional traits. *Trends in Ecology & Evolution*, 21(5), pp.261–268.

Whittaker, R., 1960. Vegetation of the Siskiyou Mountains, Oregon and California. *Ecological Monographs*, 30(3), pp.279–338.

Whittaker, R.H., 1972. Evolution and Measurement of Species Diversity. *Taxon*, 21(2/3), p.213.

Wisz, M.S. et al., 2013. The role of biotic interactions in shaping distributions and realised assemblages of species: implications for species distribution modelling. *Biological reviews of the Cambridge Philosophical Society*, 88(1), pp.15–30.

Wood, S.N., 2011. Fast stable restricted maximum likelihood and marginal likelihood estimation of semiparametric generalized linear models. *Journal of the Royal Statistical Society: Series B (Statistical Methodology)*, 73(1), pp.3–36.

Wood, S.N., 2006. *Generalized Additive Models: An Introduction with R.*, Chapman and Hall/CRC.

Wright, I.J. et al., 2004. The worldwide leaf economics spectrum. *Nature*, 428(6985), pp.821–827.

Appendices

Appendix 1 Published paper based-on the results of Chapter 2.

Are we failing to protect threatened mangroves in the Sundarbans world heritage ecosystem?

Swapan K. Sarker[1,4,*]**, Richard Reeve**[1]**, Jill Thompson**[2]**, Nirmal K. Paul**[3] **and Jason Matthiopoulos**[1]

[1] Institute of Biodiversity, Animal Health and Comparative Medicine, University of Glasgow, Glasgow G12 8QQ, United Kingdom
[2] Centre for Ecology & Hydrology, Bush Estate, Penicuik, Midlothian, EH26 0QB, United Kingdom
[3] Management Plan Division, Bangladesh Forest Department, Khulna — 9100, Bangladesh
[4] Department of Forestry and Environmental Science, Shahjalal University of Science & Technology, Bangladesh

[*] Corresponding author: s.sarker.1@research.gla.ac.uk

Abstract

The Sundarbans, the largest mangrove ecosystem in the world, is under threat from historical and future human exploitation and sea level rise. Limited scientific knowledge on the spatial ecology of the mangroves in this world heritage ecosystem has been a major impediment to conservation efforts. Here, for the first time, we report on habitat suitability analyses and spatial density maps for the four most prominent mangrove species — *Heritiera fomes*, *Excoecaria agallocha*, *Ceriops decandra* and *Xylocarpus mekongensis*. Globally endangered *H. fomes* abundance declined as salinity increased. Responses to nutrients, elevation, and stem density varied between species. *H. fomes* and *X. mekongensis* preferred upstream habitats. *E. agallocha* and *C. decandra* preferred down-stream and mid-stream habitats. Historical harvesting had negative influences on *H. fomes*, *C. decandra* and *X. mekongensis* abundances. The established protected area network does not support the most suitable habitats of these threatened species. We, therefore, recommend a reconfiguration of the network to include these suitable habitats and ensure their immediate protection. These novel habitat insights and spatial predictions can form the basis for future forest studies and spatial conservation planning, and have implications for more effective conservation of the Sundarbans mangroves and the many species that rely on them.

Introduction

The mangrove biome, spanning over 137,760 km^2 of coastal areas in 118 countries is under severe threat. Nearly 50% of the biome has been lost since the 1950s because of inadequate habitat protection, and large-scale habitat alteration[1]. If the current rate of mangrove loss continues, the whole mangrove biome will disappear in the next 100 years[2]. There are only 70 mangrove species worldwide, compared to between 40,000 and 53,000 tropical forest tree species[3]. Already 16% of mangrove species are critically endangered, endangered or vulnerable and 10% are near-threatened[4]. More than 40% of the mangrove-endemic vertebrates are now also at risk of extinction due to habitat loss[5].

The Sundarbans stretches along the coast of Bangladesh (6,017 km^2) and India (4,000 km^2) and forms the largest single block of halophytic mangrove forest in the world. This unique ecosystem provides the breeding and nursing habitats for diverse marine organisms, houses the last habitats of many endangered animals e.g. Royal Bengal tiger (*Panthera tigris*) and Ganges river dolphin (*Platanista gangetica*), supports the livelihoods of about 3.5 million coastal dwellers and helps reduce the death toll of tsunamis and cyclones[6] in the area. It was designated a Ramsar site under the Ramsar Convention in 1992[7]. UNESCO declared the Sundarbans a World Heritage Site in 1997, because of its 'Outstanding Universal Value', biological diversity and the ecosystem services the area provides[7].

Historical human pressures (i.e. over-exploitation, dam construction, shrimp and salt farming, and regular oil spills) have severely degraded the Sundarbans ecosystem by depleting forest tree stock[8]. Sundarbans is a sea-dominated delta, where freshwater river flows help to modulate salt-water toxicity and keep the ecosystem suitable for mangrove trees. Ganges' freshwater flow into the Sundarbans has dropped from 3700 m^3 s^{-1} to 364 m^3 s^{-1} since the construction of the Farakka dam in India[9] in 1974. In addition, the rate of sea level rise (SLR) along the Bangladesh coast (5.93 mm yr^{-1}) in the last century was substantially higher than the global average (1.0 – 2.0 mm yr^{-1})[10]. The National Adaptation Program of Action has projected 32 cm and 88 cm of SLR by 2050 and 2100, respectively. The Sundarbans as an already stressed ecosystem is likely to be less resilient to the impact of climate change.

In Sundarbans, the population of the globally endangered species, *H. fomes*, is estimated to have declined by 76% since 1959 and about 70% of the remaining *H. fomes* trees are affected by the 'top dying' disease[11]. Dramatic declines in other dominant mangrove species (e.g. *E. agallocha* and *X. mekongensis*) have also been reported[12]. We have limited understanding of the current spatial distributions of *C. decandra*, a globally near-threatened species[7]. Future climate scenarios (in particular for SLR) and ongoing habitat degradation may alter the current spatial distributions of these mangrove species and forest community composition.

A limited understanding of mangrove spatial distributions and mangrove species habitat requirements has reduced the success of conservation initiatives in many countries[13], including Bangladesh[14]. Only recently have coastal mangrove distributions been modelled at global[15] and regional[16] scales and we are now in urgent need of Habitat Suitability Models (HSMs), based on fine-scale species abundance and environmental data to assist us in protecting threatened ecosystems such as the Sundarbans. HSMs and their outputs (i.e. habitat maps)

are widely used during different phases of resource management and spatial conservation planning[17]. These maps are also used to identify areas appropriate for establishing protected areas, evaluate threats to those areas, and design reserves[18]. For example, a baseline distribution map of the mangrove species could be an important tool for the forest managers to make decisions on future mangrove planting and forest protection via tracking population changes over time.

In this study, we use tree counts and environmental data collected from a network of 110 permanent sample plots distributed across the entire Sundarbans to generate spatially explicit baseline information on the distribution and habitat preferences of the four most abundant mangrove species i.e. *Heritiera fomes*, *Excoecaria agallocha*, *Ceriops decandra* and *Xylocarpus mekongensis*. We identify the key environmental variables related to their spatial distribution and generated species-specific spatial density maps using both geostatistical and regression approaches. We then demonstrated the potential applications of these habitat insights and spatial maps for future forest studies, spatial conservation planning and biodiversity protection and monitoring programs.

Materials and methods

Study system.   The Bangladesh Sundarbans (21°30′ − 22°30′N, 89° 00′ – 89°55′E) is part of the world's largest river delta at the Ganges-Brahmaputra estuary (Fig. 1). Geologically, the Sundarbans is of recent origin (about 7000 years old) and was formed through the silt deposition by the Ganges-Brahmaputra river system[19]. The young, slightly calcareous soil is finely textured, poorly drained, rich in alkali metal contents, and with no distinct horizon in the sediment deposits[7]. Of its total area (6017km^2), about 69% is land and the rest comprises rivers, small streams and canals[9]. A major portion of this forest is washed by the tide twice a day and the water level is related to the combined effects of the seawater tides in the Bay of Bengal and freshwater input from the Ganges. During the monsoon (June–September), freshwater flow increases and during the dry season (October to May), fresh water flow sharply drops because of the reduced water influx from the Ganges. The climate is humid, maritime and tropical. Mean annual precipitation is 1700 mm (range: 1474 to 2265 mm); and mean maximum annual temperature is between 29.4°–31.3°C (range: 9.3° to 40° C)[20].

Tree surveys.   The Bangladesh Forest Department (BFD) established a network of 120 permanent sample plots (PSPs) in the Sundarbans in 1986 for monitoring biodiversity and forest stock (Fig. 1). Of these, 110 PSPs (120 x 20 m (0.2. ha), divided into 5 20 x 20 m sub-quadrats) were positioned to represent the ecological zones (i.e. freshwater, moderately saline, and saltwater zones), and the forest types[12]. The remaining relatively smaller sized 10 PSPs (20 x 10 m) were established to monitor ground vegetation mainly in the south-western Sundarbans, and were not considered in this study. The BFD tagged with a unique tree number and measured every tree with stem diameter ≥ 4.6 cm (recorded at 1.3 m from the ground). The height of each tree was also recorded. In this study, we used BFD's last tree data (2008 − 2013) for 91 PSPs, and the tree data we collected (January − June 2014) for 19 PSPs.
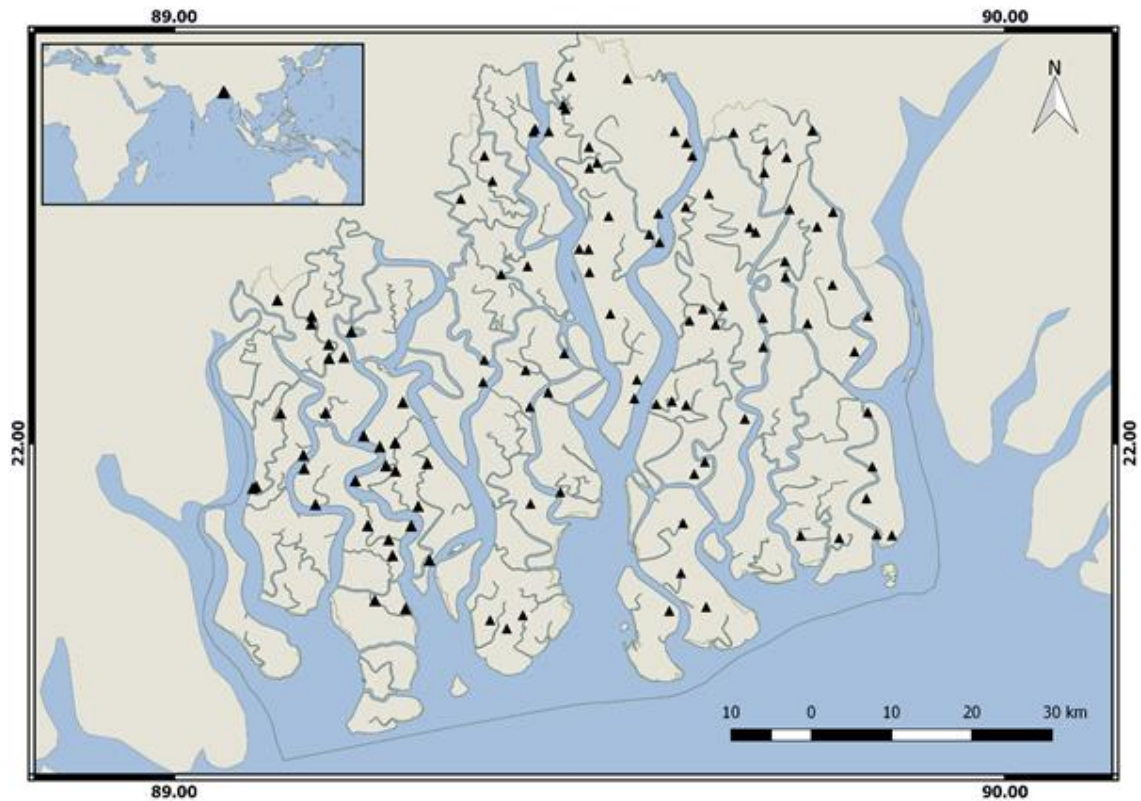
Figure 1. Sampling sites (triangles) in the Sundarbans, Bangladesh.

Environmental data.   We collected environmental data from all 110 PSPs during January – June 2014. We adopted a soil sampling design (Supplementary Figure S1), collected 9 soil samples (to account for the within plot variation in soil parameters) from each PSP to a depth of 15 cm in polyethylene bags using a cylindrical soil core sampler of 5 cm in diameter for laboratory analysis. For soil texture analysis (percentage of sand, slit and clay), we used the hydrometer method[21]. We determined soil salinity (as electrical conductivity — EC) in a 1:5 distilled water:soil dilution[22] using a conductivity meter (Extech 341350A-P Oyster). Soil pH and oxidation reduction potential (ORP) were measured in the field using digital soil pH and ORP (Extech RE300 ExStik) meters. Soil ammonium concentration (NH_4) was determined following the Kjeldahl method[23]. We measured total phosphorus (P) using the molybdovanadate method and a 721-spectrophotometer. Soil potassium (K), magnesium (Mg), iron (Fe), zinc (Zn), copper (Cu), and sulphide concentrations were measured using an atomic absorption spectrophotometer (AA-7000). We analyzed each soil sample and then averaged (9 samples) the results. Five elevation (above-average sea level) readings for each PSP were extracted from the digital elevation model with accuracy (i.e. accuracy at pixel level) ±1 m for the Sundarbans region available in BFD[24]. We then averaged these 5 readings to minimize the error related to the digital elevation model. A proportional distance from the river-sea interface was used to calculate and classify "upriver position" (henceforth, URP) of each PSP[25]. Here 'downstream' represents the lower third (0 — 33% upriver from sea) of the estuarine system, 'intermediate' represents the middle third (34 — 66% upriver from sea), and 'upstream' represents the upper third (67 — 100% upriver from sea). This scheme is useful to understand each mangrove's habitat preference along the downstream (seawater dominated river system) - upstream (freshwater dominated river system) gradient.

Covariate selection for mangrove HSMs. To construct a biologically informative covariate set for our HSMs, we followed the conceptual framework developed for mangroves[26]. This comprises three broad categories of variables (i.e. resources, regulators and hydroperiod) that are believed to control mangrove forest structure and function[27,28,29]. Resources (i.e. nutrients) are depleted by mangrove trees and their availability is linked to tree productivity and indirect competition among individual trees. Here, we used soil NH_4, P, K, Mg, Fe, and Zn based upon the detailed explanation of nutrient requirements of mangroves available in the mangrove literature[28]. Regulators are non-resource variables that influence mangrove growth. We employed soil salinity as our main regulator. Hydroperiod (the duration, frequency and depth of inundation) is recognized as an important determinant of mangrove distribution[29]. Sundarbans PSP-based hydroperiod data are not available, so we used PSP elevation as a proxy that reflects the likely variation in hydroperiod across the area. We also included URP of each PSP as a predictor to account for the influence of the river systems on each mangrove's distributions along the downstream — upstream gradient.

The relative abundance of one mangrove species might influence the abundance of another via biotic interactions i.e. competition or facilitation[30] and each individual tree interacts with the trees (both conspecifics and heterospecifics) that are in its neighbourhood through multiple concurrent interactions[31]. Given the super-dominance of *E. agallocha* and *H. fomes* (see Tree surveys section) and tree structural complexities (i.e. multiple stems in *C. decandra*, large below ground biomass for modified root systems in *H. fomes*, *C. decandra*, and *X. mekongensis*) in the ecosystem which might have increased tree measurement (i.e. diameter, height) errors, we initially considered two alternative measures of abundance: 1) density of all stems (including stems on multiple stemmed individual) for each plot, and 2) total basal area (including stems on multiple stemmed individual) for each plot as biotic variables. HSMs of species with basal area as a covariate had lower explanatory and predictive powers, compared to models with density of all stems. Therefore, we selected density of all stems for each plot (henceforth, DAS) as the biotic variable. We acknowledge that the salinity-stressed western and southern habitats of the Sundarbans have many small diameter (with stunted growth) *E. agallocha* and *H. fomes* trees[32] that may not compete. Disentangling biotic influences from abiotic effects in structuring ecological communities and regulating single species distributions is still an open problem[33]. However, the inclusion of stem densities as a simple proxy of biotic interaction is known to enhance the explanatory and predictive power of HSMs for other forest systems[34,33].

The Sundarbans has a long exploitation history[7]. The government banned tree harvesting in 1989[35]. About 3.5 million people depend on Sundarbans resources (e.g. fish, non-timber forest products, honey) for their livelihoods and illegal tree harvesting is common[19]. Therefore, we included historical harvesting (henceforth, HH) as a covariate in our models because of its potential influence on present tree densities in the PSPs. HH represents the number of illegally harvested trees (detected by counting stumps) in each PSP from the first census (1986) to the last census (2014).

We checked for multi-collinearity in our set of candidate covariates by employing Variance Inflation Factors (VIF) through a stepwise model selection procedure. We

used the *vifstep* function of 'usdm' package[36] in R 3.2.2[37], which first calculates VIF for all covariates, then eliminates the one with highest VIF that exceeds the threshold of 2.5 and repeats the procedure until no covariate with VIF > 2.5 remains. This led to the removal of Zn from our covariate set (Supplementary Table S1).

Habitat modelling. We used generalized additive models[38] (GAMs) with a Poisson likelihood and a log-link because of their ability to handle complex, non-monotonic relationships between the response and the predictor variables[39]. Moreover, by using non-parametric smoothing functions, GAMs can often construct biologically insightful relationships between response and covariates without a-priori hypotheses[17]. Smoothed responses used cubic basis splines implemented within the 'mgcv' package[40] in R.

We used the 'dredge' function in the 'MuMIn' package[41] to fit all possible candidate models with all possible combinations of covariates and ranked the resulting models by the Akaike Information Criterion (AIC)[42]. We then obtained the relative support for each model by calculating the ΔAIC (difference between the AIC value for the best model and the AIC value for each of the other models). Kullback–Leibler information loss is minimal between models with ΔAIC ≤ 2 [42]. We therefore used the 'ΔAIC ≤ 2' criterion to select our confidence set of models for each mangrove species. We then calculated Akaike weights (AICw) to examine relative support for each model in the confidence set. AICw values range from 0 to 1 and the sum of all AICw across the confidence set is 1. When there was only one model with ΔAIC ≤ 2, it was unambiguous that it outperformed all possible candidate models. When there were multiple competing models, we used AIC-weighted model averaging on the parameter estimates of these models to reduce model selection uncertainty and bias. These averaged parameter estimates were used to predict the abundance of the mangroves species across the entire Sundarbans. Relative Importance (RI) of each covariate was identified by summing the AICw of the models in which the covariate was included. RI values range between 0 and 1, where 0 indicates that the target covariate is never included in the competing models, 1 indicates inclusion of the covariate in all the competing models. We ranked the covariates based on their RI values. Residual diagnostic plots for the best GAMs did not indicate violations of the Poisson dispersion assumption.

We measured goodness-of-fit of the models using the R^2 (coefficient of determination) statistic between the observed and estimated abundance values. For validation purposes, we partitioned our dataset into a calibration and validation subsets. Our calibration dataset included 88 PSPs (80% of the full data) and the validation data set included 22 PSPs (20%). The validation dataset was randomly chosen to cover the whole region and was used to examine the predictive power of the fitted models via the R^2 statistic applied to the model's predictions for the validation data. We also mapped the actual and predicted abundances of both calibration and validation set to check for any spatial patterns of prediction errors.

Spatial mapping. We mapped densities of the mangrove species over the entire Sundarbans using two different approaches: 1) direct interpolation of plot-level raw abundance using geostatistical methods, and 2) habitat-based predictions from our HSMs. Both of these approaches were used because environmental data

collection is demanding, whereas tree abundance measurements are taken regularly at the PSPs, and it is   useful to know how close the predictions of the habitat model were compared to simple interpolation methods. To directly interpolate individual mangrove species abundances, we used Ordinary kriging (OK), a widely-used interpolation technique.

The model-averaged predictions from our confidence set of GAMs were used to develop the mangrove habitat maps based on interpolated covariate surfaces. The size of each grid-cell of the interpolated surface was 625 m^2 (25mx25m). Covariate surfaces for generating predictions from the habitat model were constructed by OK using the 'gstat' package[43] in R. A protected area network comprising three Wildlife Sanctuaries (WS) – East WS, West WS, and South WS has been operational since 1960. We superimposed the protected area network on the habitat maps to assess the existing network's ability to support density hotspots of the mangrove species. We compared the predictive abilities of the direct and habitat-based approaches using the normalized root mean square error (NRMSE) statistic derived from the leave-one-out cross-validation procedure. For normalization, the root mean square error statistic was divided by the range of the actual species abundances. Both habitat-based and direct predictions of the mangrove tree abundances were mapped using the 'raster' package[44] in R. We further mapped the prediction discrepancy between these two approaches, to look for any spatial patterning in the prediction errors.

Results

Tree surveys.   A single survey of each of the 110 PSP's carried out between 2008 − 2014 gave a total of 49409 trees of 19 species from 13 families and 19 genera (Table 1). The most abundant mangrove was *E. agallocha* (59.69% of total trees), followed by *H. fomes* (30.89%), *C. decandra* (6.12%), and *X. mekongensis* (0.82%). The rest of the 15 species were extremely rare comprising only 2.49% of the total count.

Habitat models.   The most parsimonious GAMs for estimating species abundances explained the variability of *H. fomes* (68%), *E. agallocha* (84%), *C. decandra* (73%), and *X. mekongensis* (75%) (Table 2). Soil salinity, K, total density of individuals (DAS), upriver position (URP) and historical harvesting (HH) were included in the best GAMs of all species. Mg and Fe were included (RI = 1.00) in the best GAMs for *H. fomes*, *E. agallocha* and *X. mekongensis*, with P (RI = 1.00) for *H. fomes*, *E. agallocha*, and *C. decandra*, and also elevation (RI = 1.00) for *H. fomes* and *X. mekongensis*. The partial response plots of the best GAM (Fig. 2) indicated that *H. fomes* abundance decreased with increasing soil salinity (> 7 dS m^{-1}). In contrast, increasing salinity was associated with increasing abundances of *E. agallocha* (> 7 dS m^{-1}), *C. decandra* (> 6.2 dS m^{-1}), and *X. mekongensis* (> 7 dS m^{-1}).

Table 1. Taxonomy and global conservation status of the mangrove species censused in the 110 permanent sample plots in the Bangladesh Sundarbans. *IUCN global population trend, † Not assessed for the IUCN Red List, LC = Least concern, DD = Data deficient, NT = Near threatened, VU= Vulnerable, EN = Endangered, D = Decreasing.

Latin name	Local name	Family	IUCN conservation status	Global population trend*
Aegiceras corniculatum (L.) Blanco	Khalshi	Myrsinaceae	LC	D
Amoora cucullata Roxb.	Amur	Meliaceae	NA†	NA
Avicennia officinalis L.	Baen	Avicenniaceae	LC	D
Bruguiera sexangula (Lour.) Poiret	Kakra	Rhizophoraceae	LC	D
Cerbera manghas L.	Dagor	Apocynaceae	NA	NA
Ceriops decandra (Griffith) Ding Hou	Goran	Rhizophoraceae	NT	D
Cynometra ramiflora L.	Singra	Fabaceae	NA	NA
Excoecaria agallocha L.	Gewa	Euphorbiaceae	LC	D
Excoecaria indica (Willd.) Müll.Arg.	Batul	Euphorbiaceae	DD	D
Heritiera fomes Buch.-Ham.	Sundri	Malvaceae	EN	D
Intsia bijuga (Colebr.) Kuntze	Bhaela	Leguminosae	VU	D
Lumnitzera racemosa Willd.	Kirpa	Combretaceae	LC	D
Hypobathrum racemosum (Roxb.) Kurz	Narikali	Rubiaceae	NA	NA
Pongamia pinnata (L.) Pierre	Karanja	Leguminosae	LC	Stable
Rhizophora mucronata Lam.	Jhana	Rhizophoraceae	LC	D
Sonneratia apetala Buch-Ham.	Keora	Lythraceae	LC	D
Talipariti tiliaceum (L.) Fryxell	Bhola	Malvaceae	NA	NA
Tamarix dioica Roxb.	Nona Jhao	Tamaricaceae	NA	NA
Xylocarpus granatum Koen.	Dhundal	Meliaceae	LC	D
Xylocarpus mekongensis Pierre	Passur	Meliaceae	LC	D

Table 2. Results of generalized additive models (GAMs) built for the four major mangrove species of the Bangladesh Sundarbans. DE = deviance explained, RI = relative variable importance in the model selection process. Covariates: soil salinity, elevation above average-sea level (ELE), soil NH_4, total phosphorus (P), potassium (K), magnesium (Mg), iron (Fe), upriver position (URP), density of all stems for each plot (DAS) and historical harvesting (HH).

Species	Model rank	Salinity	ELE	NH₄	P	K	Mg	Fe	URP	DAS	HH	ΔAIC	ΔAICw	Adj-R²	DE (%)
H. fomes	1	+	+	−	+	+	+	+	+	+	+	0.00	0.99	0.67	68
	RI	1.0	1.0	0.0	1.0	1.0	1.0	1.0	1.0	1.0	1.0				
E. agallocha	1	+	−	+	+	+	+	+	+	+	+	0.00	0.66	0.83	84
	2	+	+	−	+	+	+	+	+	+	+	1.39	0.33		
	RI	1.0	0.67	0.67	1.0	1.0	1.0	1.0	1.0	1.0	1.0				
C. decandra	1	+	−	+	+	+	−	−	+	+	+	0.00	0.46	0.65	73
	2	−	+	+	+	+	−	−	+	+	+	0.53	0.35		
	3	+	+	+	+	+	−	−	+	+	+	1.84	0.18		
	RI	0.65	0.65	1.0	1.0	1.0	0.0	0.0	1.0	1.0	1.0				
X. mekongensis	1	+	+	−	−	+	+	−	+	+	+	0.00	0.75	0.84	75
	RI	1.0	1.0	0.0	0.0	1.0	1.0	0.0	1.0	1.0	1.0				

Figure 2. Effects of covariates inferred from our best GAMs fitted to the abundances of the four prominent mangrove species in the Sundarbans. The solid line in each plot is the estimated spline function (on the scale of the linear predictor) and shaded areas represent the 95% confidence intervals. Estimated degrees of freedom are provided for each smoother following the covariate names. Zero on the y-axis indicates no effect of the covariate on mangrove abundances (given that the other covariates are included in the model). Covariate units: soil salinity = dS m^{-1}, elevation = m (above average-sea), NH$_4$ = gm Kg^{-1}, P = mg Kg^{-1}, K = gm Kg^{-1}), Mg = gm Kg^{-1}, Fe = gm Kg^{-1}, URP = % upriver, DAS = density of all stems for each plot, and historical harvesting (HH) = total number of harvested trees in each plot since 1986.

The response of the mangrove species varied for different nutrients. High abundance of *H. fomes* was associated with low chemical concentrations of P (< 30 mg Kg^{-1}), K (< 6 gm Kg^{-1}), Mg (< 2.75 gm Kg^{-1}) and Fe (< 30 gm Kg^{-1}). In contrast, high *E. agallocha* abundance was associated with relatively high concentrations of P (> 30 mg Kg^{-1}), K (> 6 gm Kg^{-1}), Mg (> 2.75 gm Kg^{-1}), and Fe (> 30 gm Kg^{-1}), and low concentrations of NH$_4$ (< 0.70 gm Kg^{-1}). High *C. decandra* abundance was related to high K (> 5 gm Kg^{-1}) and low NH$_4$ (< 0.70 gm Kg^{-1}) and P (< 30 mg Kg^{-1}) concentrations. High *X. mekongensis* abundance was related to low K (< 5 gm Kg^{-1}) and Mg (< 1.60 gm Kg^{-1}).

H. fomes and *X. mekongensis* showed preferences for elevated sites. *H. fomes* abundance showed a decreasing trend after a certain value of the biotic variable DAS (> 500 trees/0.2 ha), while *E. agallocha*, *C. decandra* and *X. mekongensis* showed positive responses to increasing DAS. With increasing URP, the abundances of *E. agallocha* (URP > 65%) and *C. decandra* (URP > 50%) sharply decreased, indicating their high preference for down- and mid-stream habitats. In contrast, *H. fomes* and *X. mekongensis* abundances increased with increasing URP (> 50%, indicating their preference for upstream habitats). High historical harvesting of trees was related to low abundances of *H. fomes*, *C. decandra* and *X. mekongensis*. In contrast, *E. agallocha* had high abundance in the sites that experienced high historical harvesting.

The predictive abilities of the GAMs (fitted to the calibration data and applied to the validation data) were R^2 = 0.75 for *H. fomes*, R^2 = 0.78 for *E. agallocha*, and R^2 = 0.51 for *C. decandra*. The predictive ability of the *X. mekongensis* GAMs was somewhat lower (R^2 = 0.24) than for the other mangroves species (possibly due to high densities in few upstream areas and overall low abundance in the entire region). When GAMs were used to estimate mangrove abundances for all 110 PSPs, we observed a strong association (*H. fomes*, R^2 = 0.67; *E. agallocha*, R^2 = 0.83; *C. decandra*, R^2 = 0.65; *X. mekongensis*, R^2 = 0.84) between the actual and estimated abundances. Spatial maps of the actual and estimated abundances of the mangroves (both calibration and validation datasets) looked similar and the residuals did not show spatial clustering (Supplementary Figures S2 & S3).

Spatial distribution maps.   Habitat maps of the mangrove species based on GAMs, and direct interpolation (kriging raw abundances) are presented in Fig. 3 and 4. GAMs for *E. agallocha* had better predictive accuracies than direct interpolation (Supplementary Table S2). For *H. fomes*, *C. decandra* and *X. mekongensis*, both of these methods had almost identical predictive performances. Habitat mapping uncertainties related to these methods are presented in Supplementary Figure S4.

Overall, these maps indicate that the *H. fomes* density hotspots were confined to the eastern Sundarbans. *E. agallocha* density was highest in the north-western region, intermediate in the southern and eastern regions, and lowest in the northern and north-eastern regions. *C. decandra* density was highest in the western and southern regions, intermediate in the central region, and lowest in the northern and north-eastern regions. *X. mekongensis* density was highest in some specific areas in the northern (Kalabogi and Koyra) and north-western (Koikhali) regions. All the three protected areas – East WS, West WS, and South WS are distributed in the downstream areas (adjacent to the Bay of Bengal) (Fig. 3), and do not support the density hotspots for any of these mangrove species.
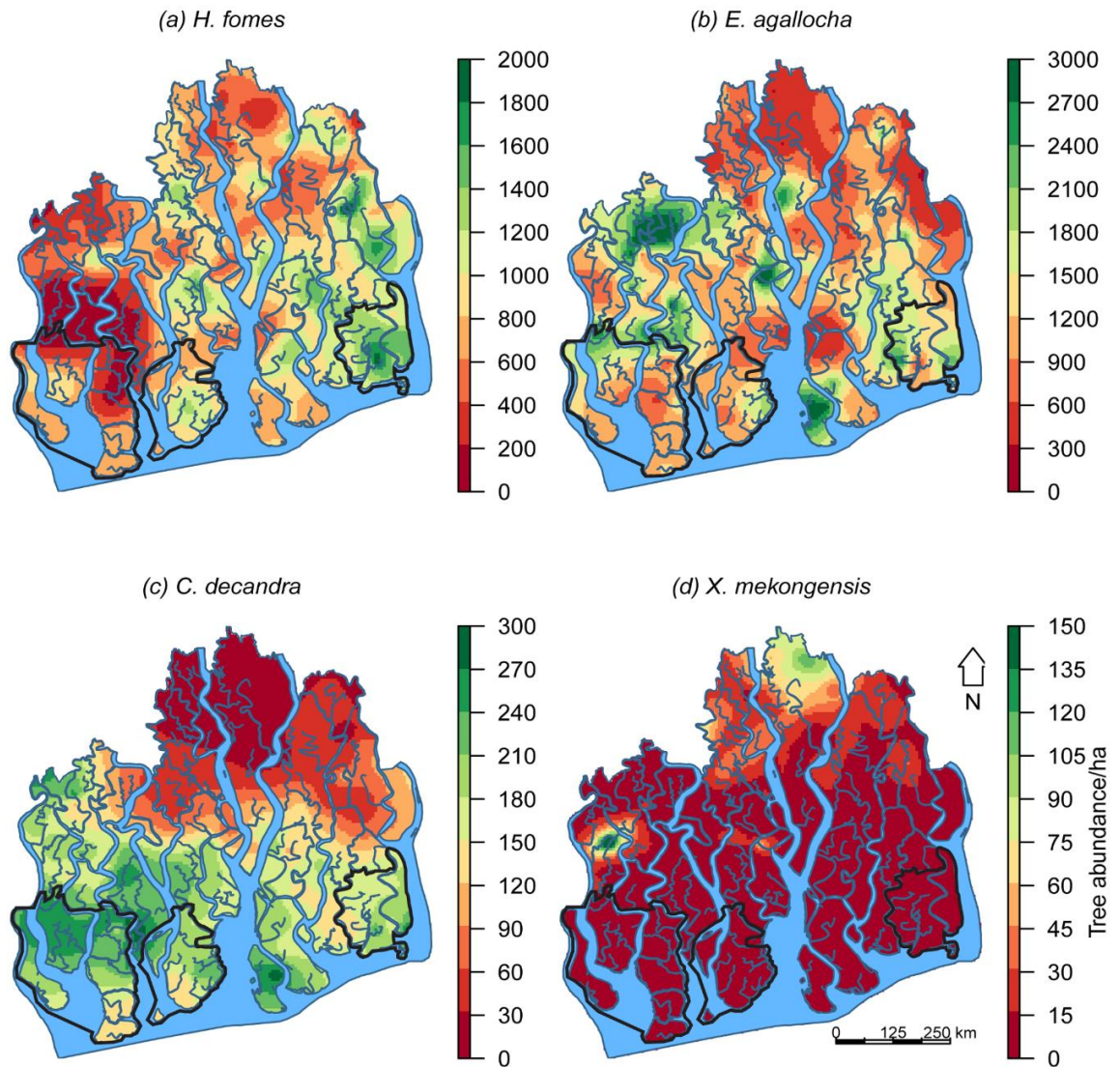
Figure 3. Spatial density ha^{-1} of the mangrove species in the Sundarbans based on habitat-based models (GAMs). Areas inside the bold black lines represent the three protected areas.

Discussion

Our study is the first to quantify mangrove habitat suitability and to determine the key drivers regulating spatial distributions of the mangrove species in the Sundarbans world heritage ecosystem. The high explanatory and predictive power of these HSMs confirm their potential usefulness for constructing regional habitat maps to aid mangrove conservation initiatives. In addition, their ability to reveal mangroves' responses to environmental and biotic predictors provides novel insights into the underlying ecology of these poorly understood but threatened mangrove species.

Extreme salt stress impedes growth and development of many mangroves[45] and the structural development of mangrove forests tends to be limited by high levels of salinity[46]. In the Sundarbans, the response of the mangrove species varies steeply across the salinity gradient (Fig. 2). In the Sundarbans *H. fomes* shows a

clear negative response (high density in the less saline and freshwater rich eastern habitats) and the three other mangroves (*E. agallocha, C. decandra* and *X. mekongensis*) show clear positive responses to increasing soil salinity with high densities in hyper-saline western and southern habitats (Fig. 3 & 4).
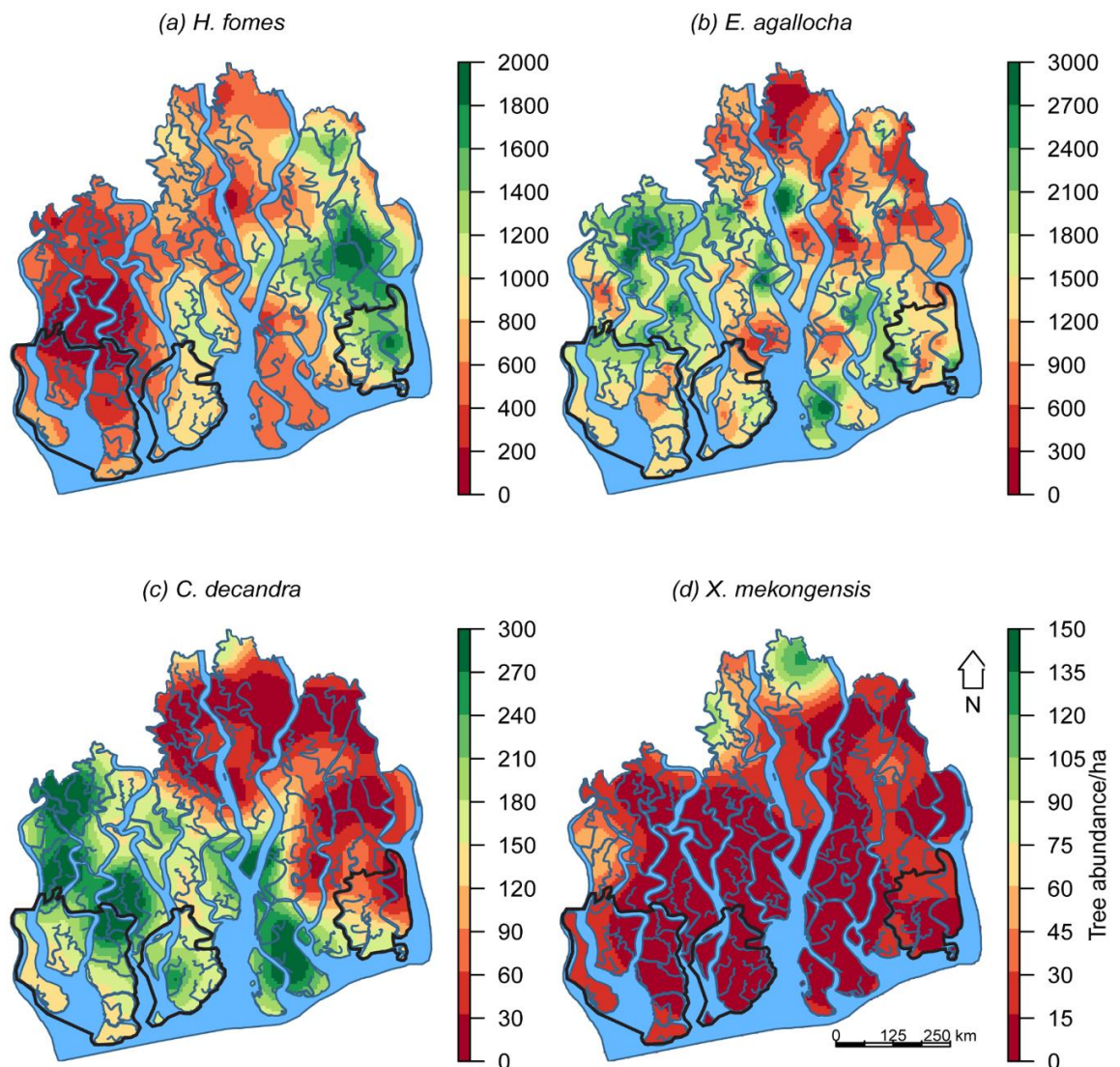
Figure 4. Spatial density ha^{-1} of the mangrove species in the Sundarbans based on geostatistical technique (OK). Areas inside the bold black lines represent the three protected areas.

Our results indicate that the magnitude of response to nutrients varies across mangrove species. *E. agallocha* and *C. decandra* are able to grow abundantly in the NH_4-poor habitats. Limited soil P is a key constraint for forest productivity in tropical ecosystems[47]. *E. agallocha* prefers relatively P-rich habitats (> 30 mg Kg^{-1}). In contrast, *H. fomes* grows abundantly in the P limited sites (< 30 mg Kg^{-1}). Soil K is considered as the key macro-nutrient that can modulate salinity-induced drought stress by improving the water uptake and retention capacity of plants[48]. Relatively higher densities of *E. agallocha*, and *C. decandra* in the highly saline and relatively K-rich habitats (north-western and southern Sundarbans) indicate that these species might have developed strategies for efficient utilization of K in salinity stressed habitats. Fe and Mg are required for successful mangrove growth because of their roles in metabolic and physiological processes[49]. *E. agallocha*

clearly prefers Fe-rich habitats, whilst *H. fomes* prefers Fe-poor habitats. The Mg preference range of *E. agallocha* (> 2.75 gm Kg^{-1}) is somewhat higher than that of *H. fomes* (< 2.75 gm Kg^{-1}) and *X. mekongensis* (< 1.60 gm Kg^{-1}). This disparity may be related to mechanisms (e.g. the distribution and chemical properties of the source rock material, the weathering process, and salinity levels) that control availability of Mg to plants[50]. It is worth remembering that in this study the fitted response curves for each mangrove species only describes how its densities are correlated with multiple predictors within their observed environmental ranges. Since these predictors include proxies for competition, these curves do not necessarily reveal the physiological limits (i.e. the fundamental niche) of the mangroves.

Although the Sundarbans is a deltaic swamp with a narrow elevation gradient (0.50 m – 4.0 m above mean sea level), it is characterized by diverse elevation values. The western zone is more elevated than the eastern zone because of tectonic activity and higher sediment deposition. This variation may be responsible for variable inundation levels in the mangrove habitats with consequent differences in soil salinity and available nutrients, and may ultimately have forced the mangrove trees to be distributed in distinct zones[51]. This hypothesis was tested[8] using randomization tests and data from 11 sampling stations in the Sundarbans, and the researchers in that study concluded that the mangroves of the Sundarbans show no distributional patterns along the elevation gradient (i.e. absence of zonation). In contrast, our results show that *H. fomes* (> 2.00 m) and *X. mekongensis* (> 2.75 m) show clear preference for elevated sites (Fig.2). We were able to reveal these patterns because of our larger sample size of 110 PSPs distributed over the entire region, and our multivariate and nonlinear modelling methodology.

DAS i.e. density of all stems for each plot (with maximum RI (~1) scores) was retained in the species best GAMs, indicating the strength of adding biotic variables in environmental data driven HSMs. *H. fomes* abundance tends to fall when the DAS value is > 500 trees/0.2 ha, indicating the super dominance of generalists (i.e. *E. agallocha* – shows positive linear response to DAS) and disturbance specialists (i.e. *C. decandra*). The negative association of *H. fomes* with *E. agallocha* and *C. decandra* was observed in a previous study in the Sundarbans[8]. Conversely, the abundance of *X. mekongensis* is higher in the highly-populated habitats. Indeed, these are the northern *X. mekongensis* hotspots (Fig. 3) where *X. mekongensis* is positively associated with *H. fomes* and *Bruguiera gymnorrhiza*. Although our correlative inferences might not necessarily reflect the causal mechanisms of biotic interactions (competition or facilitation) on species distributions, they do help improve explanatory and predictive power of HSMs and form the basis for more mechanistic studies.

URP, representing the downstream-upstream gradient, was retained in all of the selected GAMs with maximum RI score (~1), indicating the influence of river systems on the spatial distribution of mangroves. The river system covers about 1700 km^2 (with maximum river width of 10 km) and continually change channels. Erosion and compensatory accretion are common along the river banks. The freshwater supply from these rivers mainly control the amount of alluvium deposit in the forest floor, which in turn regulate the availability of plant nutrients[7]. The negative response of *E. agallocha* and *C. decandra* abundances to increasing URP indicate their preference for habitats distributed between the downstream to

intermediate positions (0 – 66% upriver from the sea – Bay of Bengal). Conversely, *H. fomes* and *X. mekongensis's* clear positive response to URP (> 50%) would support a characterization of these species as upland specialists. These disparities in mangrove habitat preferences along the downstream-upstream gradient may be related to the change in regional hydrology since the construction of the Farakka dam (1974) on the Ganges in India which has silted up most of its southbound distributaries heading towards the Sundarbans' river system. As a result, the carrying capacities of the major river (e.g. Sibsa and Posur) systems have radically changed with about 60% reduction in the freshwater flow[9].

H. fomes is now facing extinction in the Indian Sundarbans and Myanmar[52]. The Bangladesh Sundarbans now supports the sole remaining viable population of this globally endangered mangrove[19]. Our *H. fomes* habitat map (Fig. 3) indicates that the eastern region of the Sundarbans supports the highest *H. fomes* populations, the central and northern regions support intermediate densities, and the mangrove is almost absent in the western region. This may indicate historical range contraction of the species even in the Bangladesh Sundarbans as palynological evidence suggests its past dominance in the western region[20]. The sharp negative response of *H. fomes* to increasing intensity of historical tree harvesting (Fig. 2) indicates that this has been one of the main target species for illegal harvesting. In fact, *H. fomes* stem density has declined by 50% (1960s – 1990s) all over the Sundarbans because of habitat degradation and mass exploitation[12]. *H. fomes* prefers freshwater dominated habitats and shows a negative response to increased soil salinity. Therefore, the highest abundances in the eastern region may be related to its proximity to the freshwater dominated Baleshwar River. However, the freshwater supply to the eastern zone has been decreasing because of heavy siltation in the internal channels[9]. Our findings lead us to conclude that further harvesting and decreases in freshwater supply (i.e. increased salinity) could push this species over the brink of extinction.

E. agallocha habitat maps indicate this species' wide distribution across the entire Sundarbans, except the upstream-dominated northern region. Contrary to *H. fomes*, *E. agallocha* is a salt tolerant fast growing and reproducing species with high ability to colonize open and degraded habitats[53]. *E. agallocha* abundance increased in the sites with high historical harvesting intensity (Fig. 2). Tropical cyclones and tree mortality have created large forest gaps in the Sundarbans and the amount of open areas has been increasing by 0.05% each year[19]. Hence, we assume that these conditions may favour *E. agallocha* to increase its density and expand its range even to the upstream dominated northern region.

C. decandra hotspots are now distributed in the south and south-western zones (Fig. 3*). C. decandra* and other dwarf species have been replacing about 0.4% of the forest area every year[20]. Intermediate *C. decandra* densities in the central and south-eastern regions provide clear indication of its landward range expansion. Interestingly, although *C. decandra* belongs to the 'Near Threatened' status globally, its populations seem to be increasing and the species may be expanding its landward range.

High-density populations of *X. mekongensis* are restricted to few specific areas of the Sundarbans in the northern (Kalabogi and Koyra) and north-western (Koikhali) regions (Fig. 3). The distribution of the species is patchy in the rest of the ecosystem. *X. mekongensis* abundances show sharp negative response to

increasing historical harvesting intensity (Fig. 2). This has been the target species for illegal felling since colonial regime because of its high timber price in the black market[54]. At present, most of the *X. mekongensis* trees (64%) are infected by the heart rot disease[55]. Hence, *X. mekongensis* is under severe pressure in the Sundarbans, and could be at higher risk of local extinction.

The existing protected area network (East, West, and South Wildlife Sanctuaries) does not include the hotspots of any of these threatened species (Fig. 3). Our habitat maps advocate the immediate protection of the remaining suitable habitats (hotspots) of *H. fomes* and *X. mekongensis*, the two species most at risk of local and global extinction. According to the Bangladesh Wildlife Preservation Order 1973 (amended in 1974) these sanctuaries were established to ensure completely undisturbed habitat for the protection of wildlife, vegetation, soil and water[14]. The capacity of these sanctuaries to conserve biodiversity with limited physical and technological resources, has been highly disputed[14]. Given the circumstances, a preventative approach involving the design of a new or extended network of protected areas with improved logistics support is a plausible option offering expediency and cost effectiveness over long term forest restoration projects[56].

The usefulness of HSMs in guiding species habitat restoration, protection, and replanting projects is well documented. Although identifying the potential existence of environmental stressors should be the first step in reforestation and restoration planning, a limited understanding of mangroves habitat requirements has limited the success of such initiatives in many countries[13]. In the Sundarbans, past replanting campaigns (based on educated guesses) were also unsuccessful[14]. In this context, the regional HSMs of this study with detailed information on the mangroves' habitat requirements, may guide the future restoration and mangrove planting initiatives of the Bangladesh Forest Department. The absence of a persistent soil seed bank of *H. fomes* and *X. mekongensis* in the Sundarbans has recently been identified[53]. Thus, we recommend mangrove planting in the forest gaps, to safeguard these habitats from invasive species[57].

The Sundarbans has a history of extensive exploitation particularly during the 1980s[7]. The government enforced a full logging ban in 1989[35]. Despite such law enforcement, illegal felling of trees is common[19]. Our results also indicate the negative influence of historical harvesting on the populations of the threatened mangrove species. This exploitation is also directly linked with the habitat loss of many mangrove-dependent animals including the globally endangered Royal Bengal tiger[58]. Bangladesh has signed and ratified the World Heritage Convention, Ramsar Convention and the Convention on Biological Diversity[35]. The government of Bangladesh has recently developed the Biodiversity National Assessment and Program of Action 2020 to implement sufficient measures to halt further degradation of biological resources. Therefore, our mangrove distribution maps may guide these valuable protection and monitoring initiatives of the Bangladesh Forest Department to combat illegal logging through recording mangrove population changes or predicting changes and identifying areas (or species) that may be most affected by future harvesting and other human interventions (e.g. settlement and shrimp farming).

Conclusions

This study is the first to make complete inventories in the PSP network established in the 1980s by the Bangladesh government for monitoring biodiversity and forest health, demonstrates the usefulness of habitat modelling as a tool in predicting mangrove abundances and provides novel insights into the underlying ecology of these poorly studied threatened species. The HSMs and complementary habitat maps provide spatially explicit information on the remaining habitats of the threatened mangrove species, and form the baseline for designing cost-effective field inventories, biodiversity assessment and monitoring programs. Most importantly, the Bangladesh Forest Department can readily use the distribution maps in their existing protection and monitoring initiatives designed to combat illegal logging in the Sundarbans. The relative performance of the direct interpolation-based species distribution maps against the habitat-based spatial density maps indicates their usefulness when environmental data are not available. We did not make HSMs for the remaining 15 mangrove species in our data due to their low prevalence. Future studies may usefully extend their sampling efforts beyond the existing PSP network to record these rare mangroves. The projected sea level rise along the Bangladesh coast, which is higher than the global rate, may alter the hydrology of the Sundarbans with subsequent changes in the salinity and nutrient levels in the mangroves' habitats. Therefore, we recommend including hydroperiod as a predictor in future HSMs as these data become available.

References

1. Feller, I. C. *et al*. Biocomplexity in mangrove ecosystems. *Ann. Rev. Mar. Sci.* **2,** 395–417 (2010).

2. Duke, N. C. *et al*. A world without mangroves? *Science* **317,** 41-2 (2007).

3. Slik, J. W. F. *et al*. An estimate of the number of tropical tree species. *Proc. Natl. Acad. Sci.* 201423147 (2015). doi:10.1073/pnas.1423147112

4. Polidoro, B. A. *et al*. The loss of species: mangrove extinction risk and geographic areas of global concern. *PLoS One* **5,** e10095 (2010).

5. Luther, D. A. & Greenberg, R. Mangroves: A Global Perspective on the Evolution and Conservation of Their Terrestrial Vertebrates. *Bioscience* **59,** 602–612 (2009).

6. Giri, C. *et al*. Mangrove forest distributions and dynamics (1975–2005) of the tsunami-affected region of Asia. *J. Biogeogr.* **35,** 519-528 (2008).

7. Siddiqi, N. A. *Mangrove forestry in Bangladesh*. (Institute of Forestry and Environmental Sciences, University of Chittagong, Chittagong, Bangladesh, 2001).

8. Ellison, A. M., Mukherjee, B. B. & Karim, A. Testing patterns of zonation in mangroves: Scale dependence and environmental correlates in the Sundarbans of Bangladesh. *J. Ecol.* **88,** 813–824 (2000).

9. Wahid, S. M., Babel, M. S. & Bhuiyan, A. R. Hydrologic monitoring and analysis in the Sundarbans mangrove ecosystem, Bangladesh. *J. Hydrol.* **332,** 381–395 (2007).

10. Karim, M. F. & Mimura, N. Impacts of climate change and sea-level rise on cyclonic storm surge floods in Bangladesh. *Glob. Environ. Chang.* **18,** 490–500 (2008).

11.   Chowdhury, M. Q. *et al*. Nature and periodicity of growth rings in two Bangladeshi mangrove species. *IAWA J*. **29,** 265–276 (2008).

12.   Iftekhar, M. S. & Saenger, P. Vegetation dynamics in the Bangladesh Sundarbans mangroves: a review of forest inventories. *Wetl. Ecol. Manag*. **16,** 291–312 (2007).

13.   Lewis, R. R. Ecological engineering for successful management and restoration of mangrove forests. *Ecol. Eng*. **24,** 403–418 (2005).

14.   Islam, S., Rahman, M. & Chakma, S. in *Mangrove Ecosystems of Asia* (eds. Latiff, I. Faridah-Hanum, A. & Ozturk, Khalid Rehman Hakeem, M.) 127–152 (2014). doi:10.1007/978-1-4614-8582-7

15.   Record, S., Charney, N. D., Zakaria, R. M. & Ellison, A. M. Projecting global mangrove species and community distributions under climate change. *Ecosphere* **4,** 1–23 (2013).

16.   Crase, B., Vesk, P. A., Liedloff, A. & Wintle, B. A. Modelling both dominance and species distribution provides a more complete picture of changes to mangrove ecosystems under climate change. *Glob. Chang. Biol*. **21,** 3005–3020 (2015).

17.   Guisan, A. & Thuiller, W. Predicting species distribution: Offering more than simple habitat models. *Ecology Letters* **8,** 993–1009 (2005).

18.   Guisan, A. *et al*. Predicting species distributions for conservation decisions. *Ecol. Lett*. **16,** 1424–1435 (2013).

19.   Iftekhar, M. S. & Islam, M. R. Degeneration of Bangladesh?s Sundarbans mangroves: a management issue. *International Forestry Review* **6,** 123–135 (2004).

20.   Gopal, B. & Chauhan, M. Biodiversity and its conservation in the Sundarban mangrove ecosystem. in *Aquatic Sciences* **68,** 338–354 (2006).

21.   Gee, G. W. & Bauder, J. W. in *Methods of soil analysis. Part 1. Physical and mineralogical methods* 383–411 (1986). doi:10.2136/sssabookser5.1.2ed.c15

22.   Hardie, M. & Doyle, R. Measuring soil salinity. *Methods Mol. Biol*. **913,** 415-25 (2012).

23.   Bremner, J. M. & Breitenbeck, G. A. A simple method for determination of ammonium in semimicro-Kjeldahl analysis of soils and plant materials using a block digester . *Soi. Sci. Plant Anal*. **14,** 905–913 (1983).

24.   IWM. *Sundarban Biodiversity Conservation Project*. **1,** (2003).

25.   Duke, N. C., Ball, M. C. & Ellison, J. C. Factors Influencing Biodiversity and Distributional Gradients in Mangroves. *Glob. Ecol. Biogeogr. Lett*. **7,** 27 (1998).

26.   Twilley, R. R. & Rivera-Monroy, V. H. Developing performance measures of mangrove wetlands using simulation models of hydrology, nutrient biogeochemistry, and community dynamics. *J. Coast. Res*. 79-93 (2005). doi:10.2307/25736617

27.   Krauss, K. W. *et al*. Environmental drivers in mangrove establishment and early development: A review. *Aquat. Bot*. **89,** 105-127 (2008).

28.   Reef, R., Feller, I. C. & Lovelock, C. E. Nutrition of mangroves. *Tree Physiol*. **30,** 1148-60 (2010).

29.   Crase, B., Liedloff, A., Vesk, P. A., Burgman, M. A. & Wintle, B. A. Hydroperiod is the main driver of the spatial pattern of dominance in mangrove communities. *Glob. Ecol. Biogeogr*. **22,** 806–817 (2013).

30.   Wisz, M. S. *et al.* The role of biotic interactions in shaping distributions and realised assemblages of species: implications for species distribution modelling. *Biol. Rev. Camb. Philos. Soc.* **88,** 15–30 (2013).

31.   Le Roux, P. C., Lenoir, J., Pellissier, L., Wisz, M. S. & Luoto, M. Horizontal, but not vertical, biotic interactions affect fine-scale plant distribution patterns in a low-energy system. *Ecology* **94,** 671–682 (2013).

32.   Chowdhury, M. Q., Kitin, P., De Ridder, M., Delvaux, C. & Beeckman, H. Cambial dormancy induced growth rings in Heritiera fomes Buch.- Ham.: a proxy for exploring the dynamics of Sundarbans, Bangladesh. *Trees* (2015). doi:10.1007/s00468-015-1292-2

33.   Le Roux, P. C., Pellissier, L., Wisz, M. S. & Luoto, M. Incorporating dominant species as proxies for biotic interactions strengthens plant community models. *J. Ecol.* **102,** 767–775 (2014).

34.   Mod, H. K., le Roux, P. C., Guisan, A. & Luoto, M. Biotic interactions boost spatial models of species richness. *Ecography (Cop.).* **38,** 913–921 (2015).

35.   Sarker, S. K., Deb, J. C. & Halim, M. a. A diagnosis of existing logging bans in Bangladesh. *International Forestry Review* **13,** 461–475 (2011).

36.   Naimi, B. usdm: Uncertainty Analysis for Species Distribution Models. R package version 1.1-15. (2015). at <http://cran.r-project.org/package=usdm>

37.   R Core Team. R: A language and environment for statistical computing. (2015). at <https://www.r-project.org/.>

38.   Wood, S. N. *Generalized Additive Models: An Introduction with R.* (Chapman and Hall/CRC., 2006).

39.   Guisan, A., Edwards, T. C. & Hastie, T. Generalized linear and generalized additive models in studies of species distributions: Setting the scene. *Ecol. Modell.* **157,** 89–100 (2002).

40.   Wood, S. N. Fast stable restricted maximum likelihood and marginal likelihood estimation of semiparametric generalized linear models. *J. R. Stat. Soc. Ser. B Stat. Methodol.* **73,** 3–36 (2011).

41.   Barton, K. MuMIn: Multi-model inference. R package version 1.10.5. (2015). at <http://cran.r-project.org/package=MuMIn>

42.   Burnham, K. P. & Anderson, D. R. *Model Selection and Multimodel Inference: a Practical Information-theoretic Approach, 2nd edn. Springer-Verlag, New York. New York Springer* **60,** (2002).

43.   Pebesma, E. J. Multivariable geostatistics in S: the gstat package. *Comput. Geosci.* **30,** 683–691 (2004).

44.   Hijmans, R. J. raster: Geographic Data Analysis and Modeling. R package version 2.4-18. (2015). at <http://cran.r-project.org/package=raster>

45.   Nandy, P., Das, S., Ghose, M. & Spooner-Hart, R. Effects of salinity on photosynthesis, leaf anatomy, ion accumulation and photosynthetic nitrogen use efficiency in five Indian mangroves. *Wetl. Ecol. Manag.* **15,** 347–357 (2007).

46.   Washington, W., Kathiresan, K. & Bingham, B. L. *Biology of mangroves and mangrove Ecosystems. Advances in Marine Biology* **40,** (2001).

47.   Baribault, T. W., Kobe, R. K. & Finley, A. O. Tropical tree growth is correlated with soil phosphorus, potassium, and calcium, though not for legumes. *Ecol. Monogr*. **82,** 189–203 (2012).

48.   Sardans, J. & Peñuelas, J. Potassium: a neglected nutrient in global change. *Glob. Ecol. Biogeogr*. **24,** 261–275 (2015).

49.   Alongi, D. M. Dissolved iron supply limits early growth of estuarine mangroves. *Ecology* **91,** 3229–3241 (2010).

50.   Gransee, a. & Führs, H. Magnesium mobility in soils as a challenge for soil and plant analysis, magnesium fertilization and root uptake under adverse growth conditions. *Plant Soil* **368,** 5–21 (2013).

51.   Bunt, J. Mangrove Zonation: An Examination of Data from Seventeen Riverine Estuaries in Tropical Australia. *Ann. Bot*. **78,** 333–341 (1996).

52.   Blasco, F., Aizpuru, M. & Gers, C. Depletion of the mangroves of Continental Asia. *Wetl. Ecol. Manag.* **9,** 245–256 (2001).

53.   Harun-or-Rashid, S., Biswas, S. R., Böcker, R. & Kruse, M. Mangrove community recovery potential after catastrophic disturbances in Bangladesh. *For. Ecol. Manage*. **257,** 923–930 (2009).

54.   Raju, J. S. S. N. Xylocarpus (Meliaceae): A less-known mangrove taxon of the Godavari estuary, India. *Curr. Sci*. **84,** 879–881 (2003).

55.   Siddiqui, A. S. M. H. & Khair, A. Infestation Status of Heart Rot Disease of Pasur (Xylocarpus mekongensis), Tree in the Sundarbans. *Indian For*. **138,** (2012).

56.   Possingham, H. P., Bode, M. & Klein, C. J. Optimal Conservation Outcomes Require Both Restoration and Protection. *PLOS Biol*. **13,** e1002052 (2015).

57.   Biswas, S. R., Choudhury, J. K., Nishat, A. & Rahman, M. M. Do invasive plants threaten the Sundarbans mangrove forest of Bangladesh? *For. Ecol. Manage*. **245,** 1–9 (2007).

58.   Aziz, A., Barlow, A. C., Greenwood, C. C. & Islam, A. Prioritizing threats to improve conservation strategy for the tiger Panthera tigris in the Sundarbans Reserve Forest of Bangladesh. *Oryx* **47,** 1–9 (2013).

Chapter 2

Appendix 2A. Stepwise VIF test outputs of the environmental covariates.

Covariates	VIF
Salinity	1.53
NH4	1.63
P	1.32
K	1.35
Mg	2.13
Fe	1.58
Zn	2.60
Elevation	1.09
URP	1.07

Appendix 2B. Semivariograms for the major mangrove species in the Sundarbans.

(a) *Heritiera fomes*
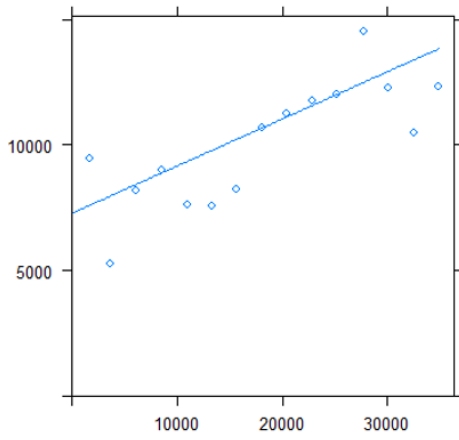
(b) *Excoecaria agallocha*
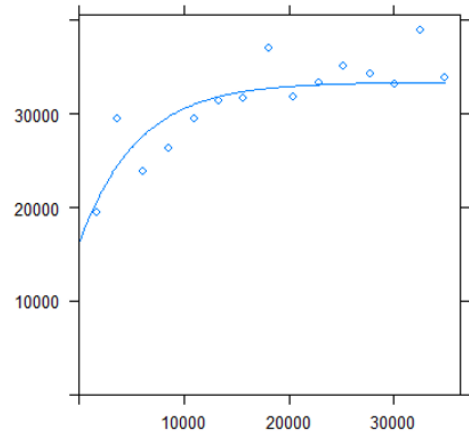
(c) *Ceriops decandra*

(d) *Xylocarpus mekongensis*

Semivariance

Distance (m)
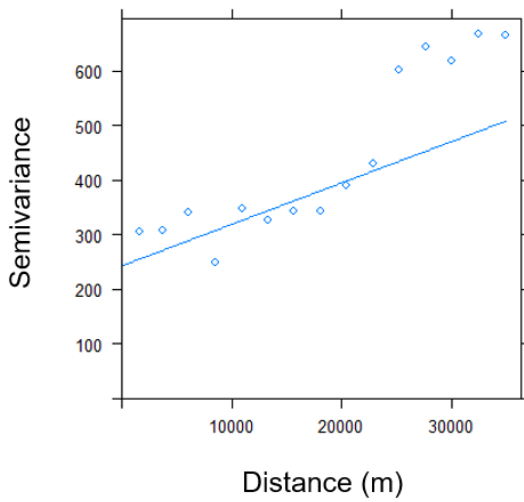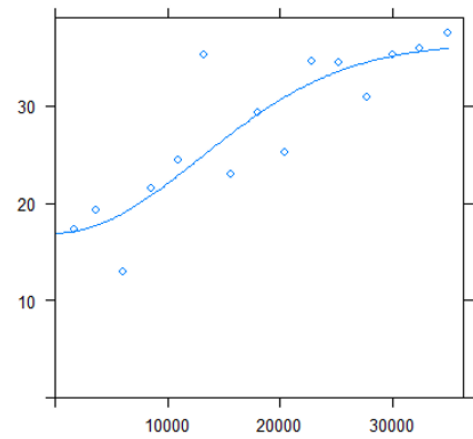
Appendix 2C. Semivariograms for the covariates.

(a) Soil salinity

(b) pH

(c) NH$_4$

(d) P

(e) K

(f) Mg

(f) Fe

(g) Historical harvesting

Semivariance

Distance (m)
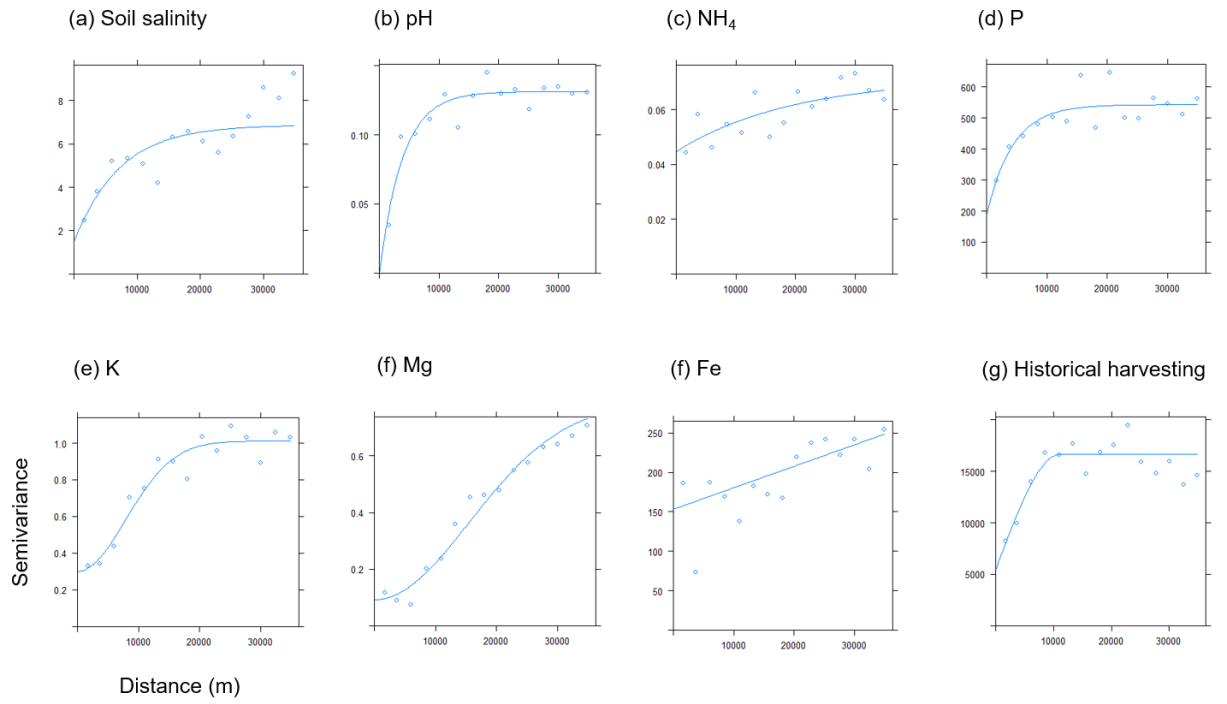
Appendix 2D. Covariate surfaces constructed using Ordinary kriging. HH = historical harvesting (the number of trees harvested since 1986).
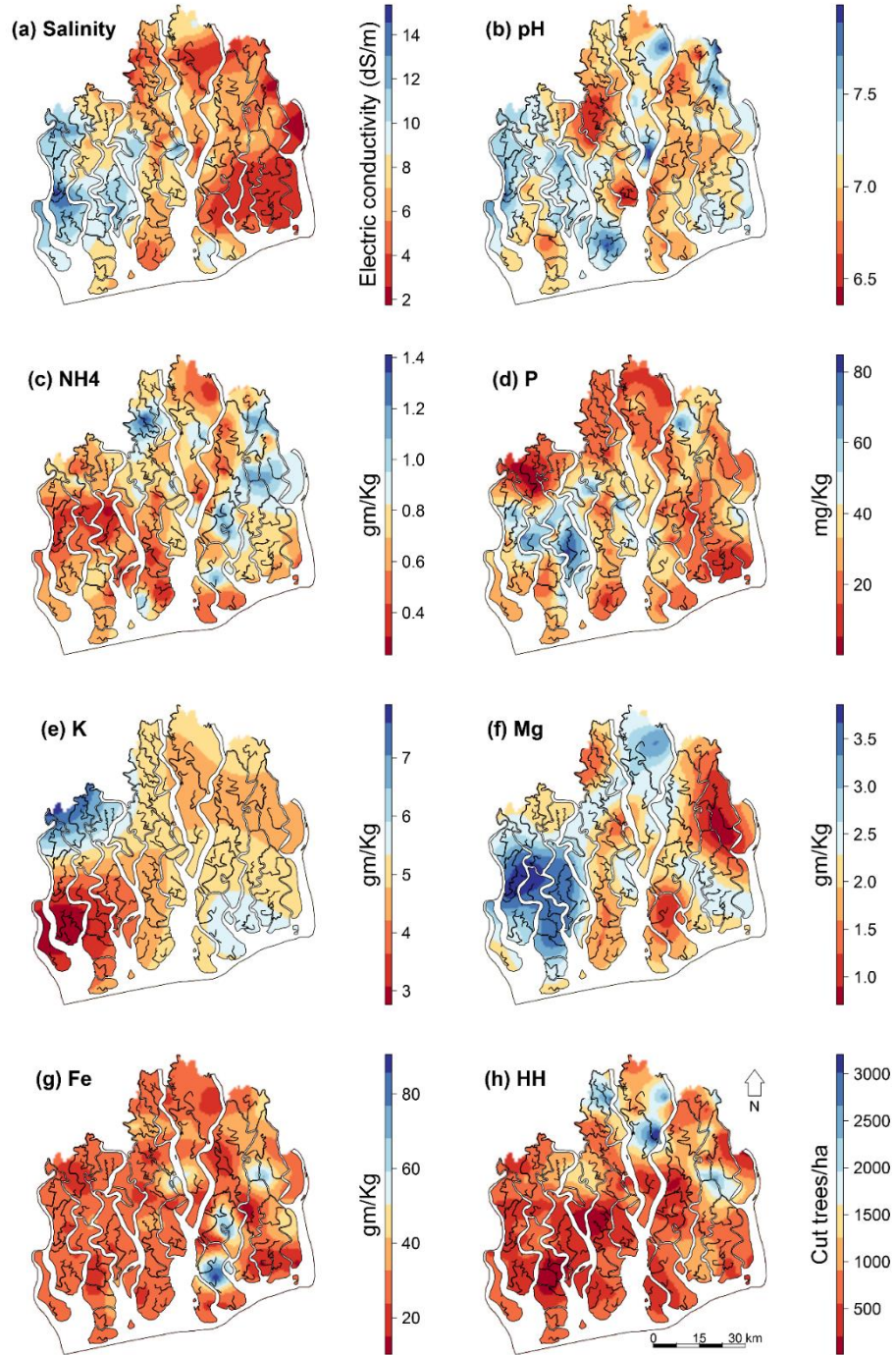
Appendix 2E. Spatial distributions of the actual and estimated abundances of the four species, and uncertainties.
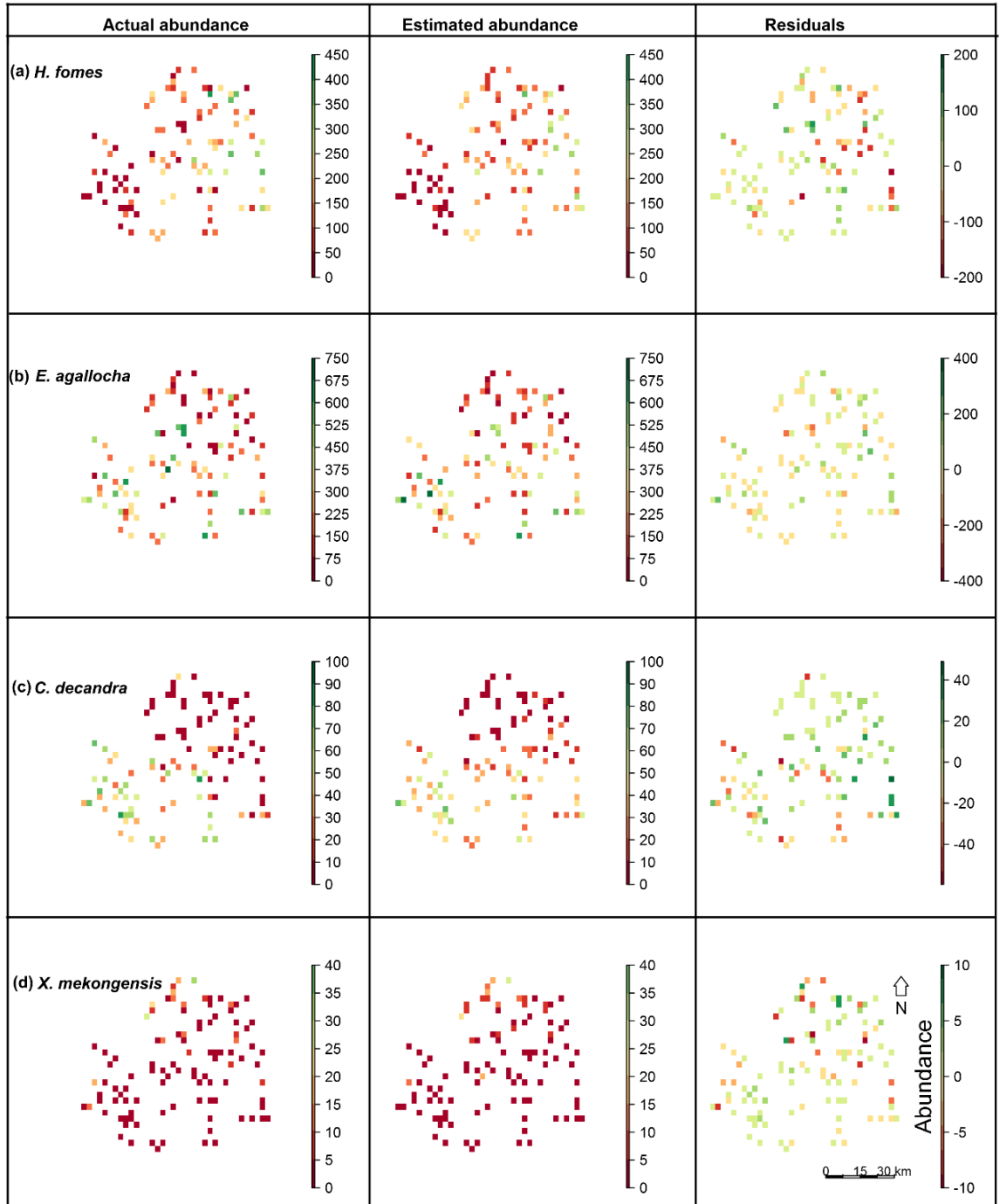
Appendix 2F. Spatial distributions of the actual and estimated abundances of the four species, and uncertainties when the habitat models were applied to the validation data set.
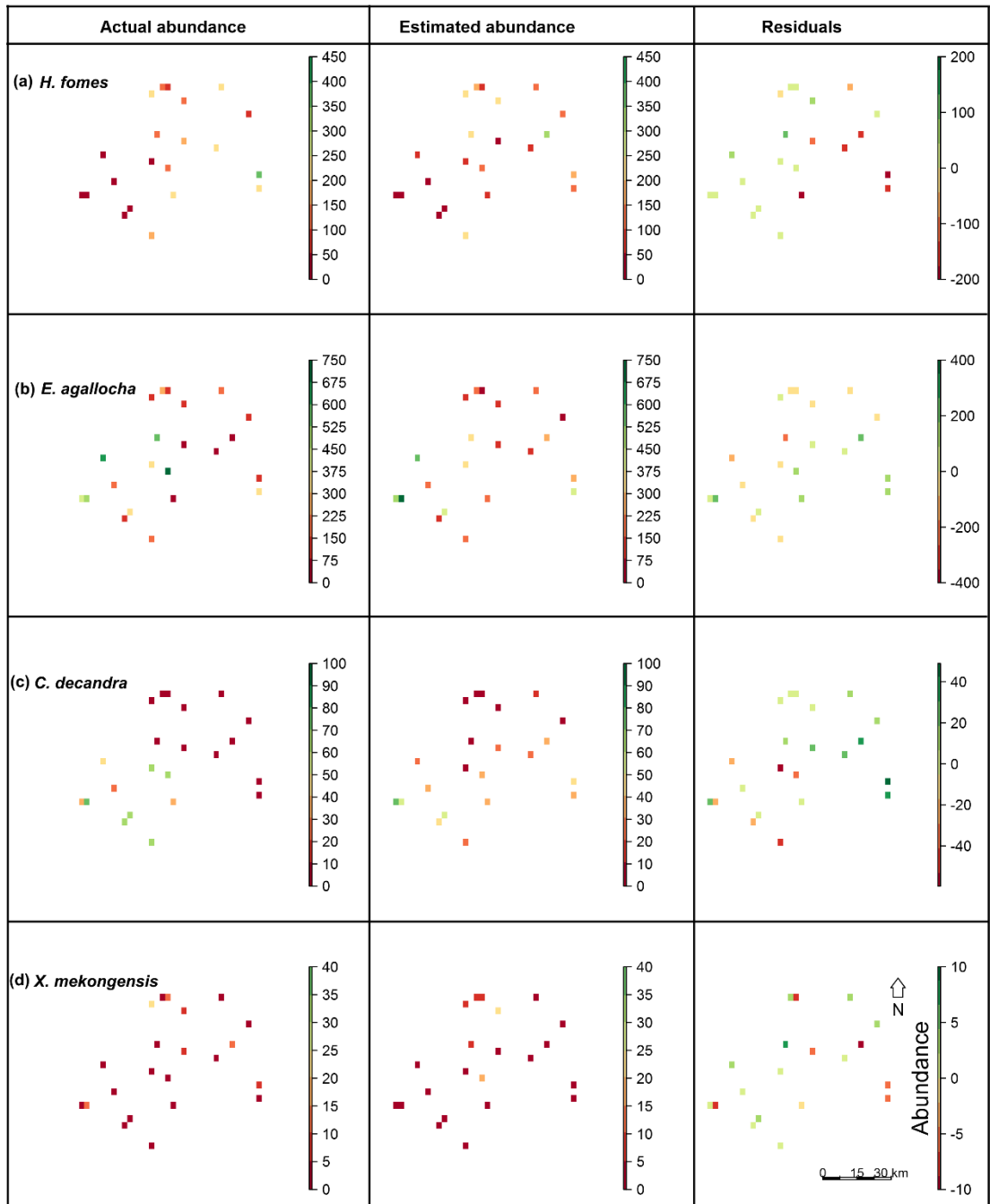
Chapter 3

Appendix 3A. Semivariograms for alpha diversity (viewpoint parameters, q = 0, 1 and 2) in the Sundarbans in four time points since 1986.
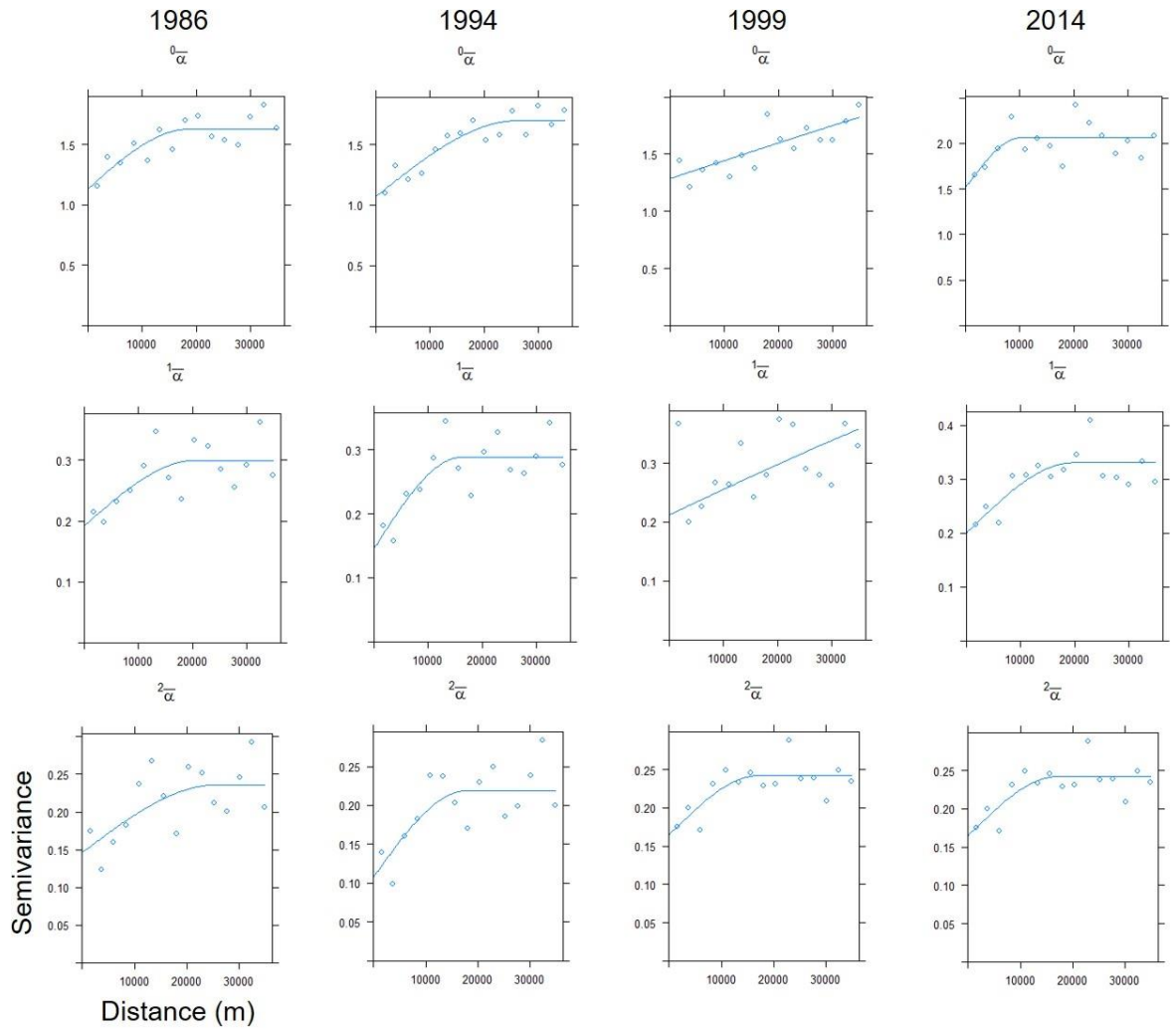
Appendix 3B. Semivariograms for beta diversity (viewpoint parameters, q = 0, 1 and 2) in the Sundarbans in four time points since 1986.
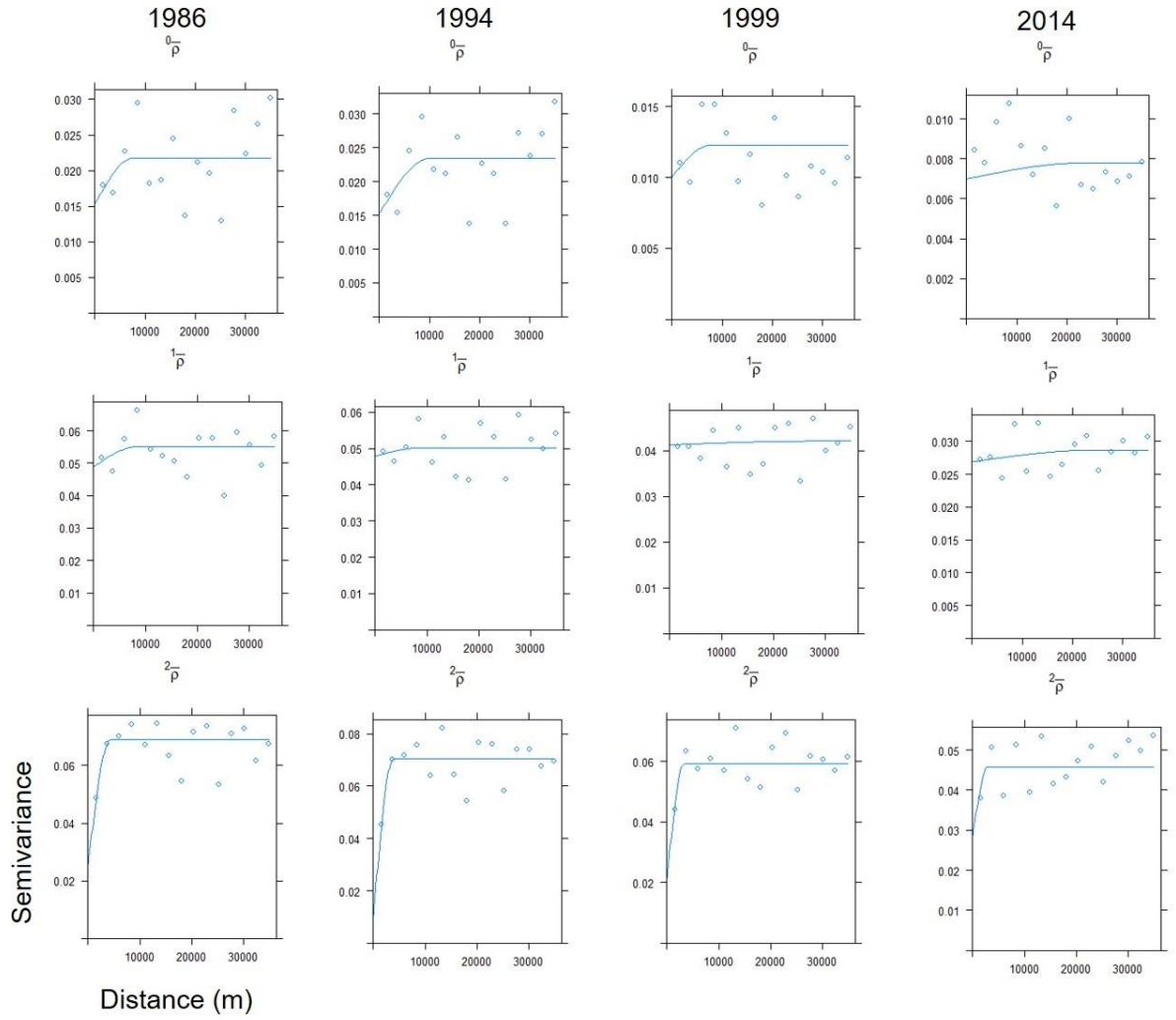
Appendix 3C. Semivariograms for gamma diversity (viewpoint parameters, q = 0, 1 and 2) in the Sundarbans in four time points since 1986.
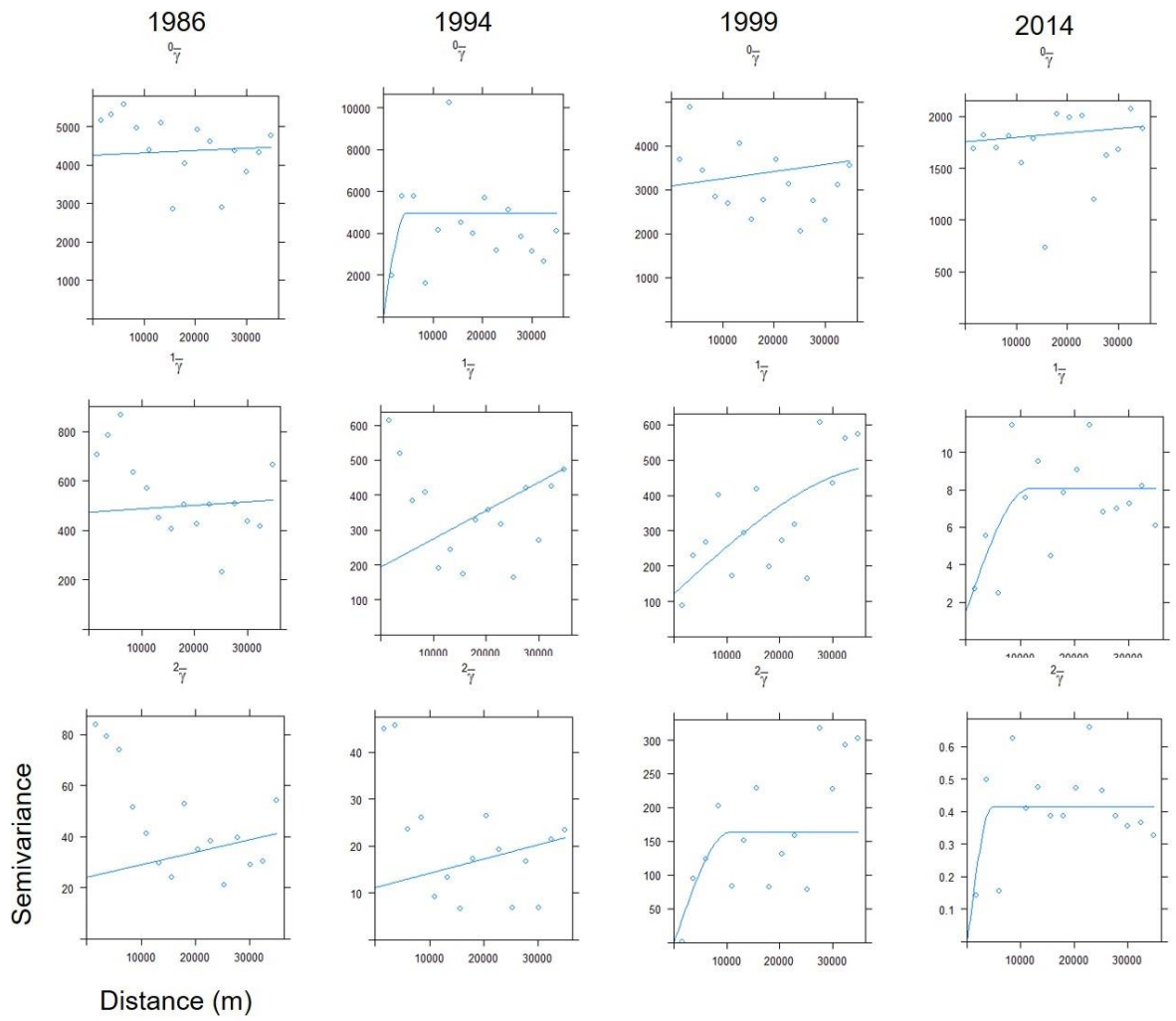
Appendix 3D. Spatial subcommunity alpha, beta, and gamma diversities (viewpoint parameter, $q = 0$) in the ecological zones of the Sundarbans in four time points since 1986.
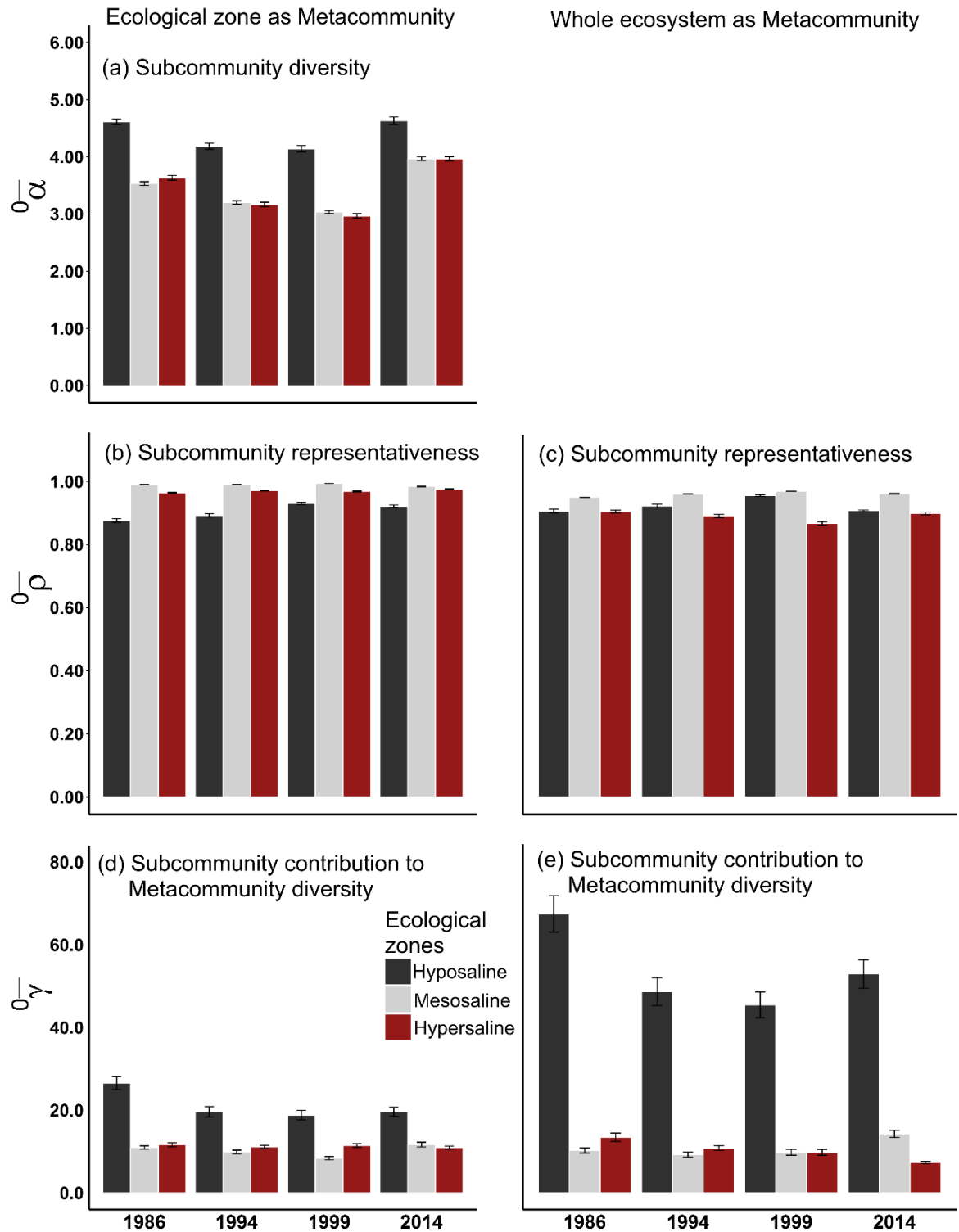
Appendix 3E. Spatial subcommunity alpha, beta, and gamma diversities (viewpoint parameter, $q = 2$) in the ecological zones of the Sundarbans in four time points since 1986.
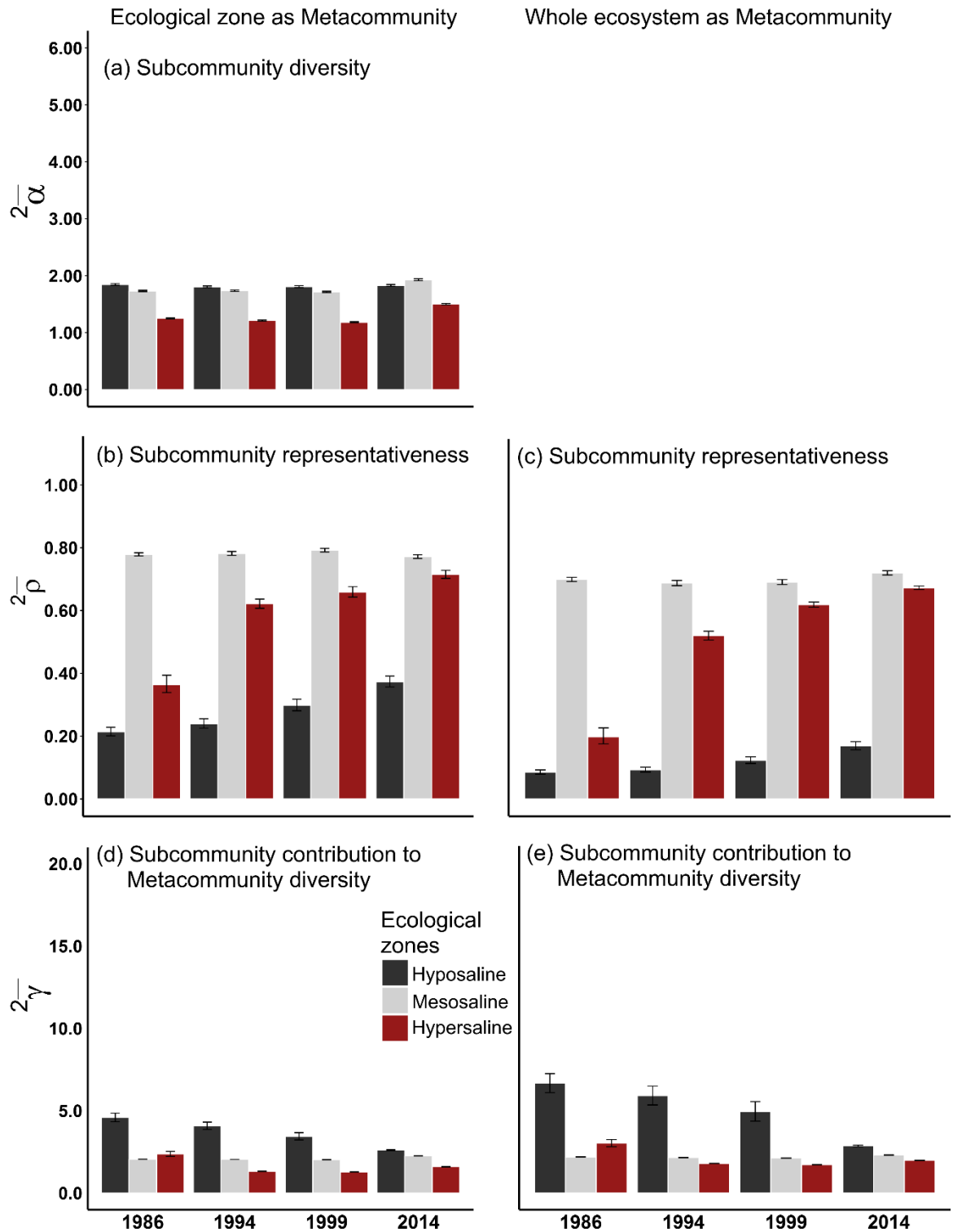
Appendix 3F. Temporal dynamics in subcommunity and zonal beta ($\overline{\rho}$) diversity during 1986 — 2014 for viewpoint parameter, $q = 0$, 1, and 2.
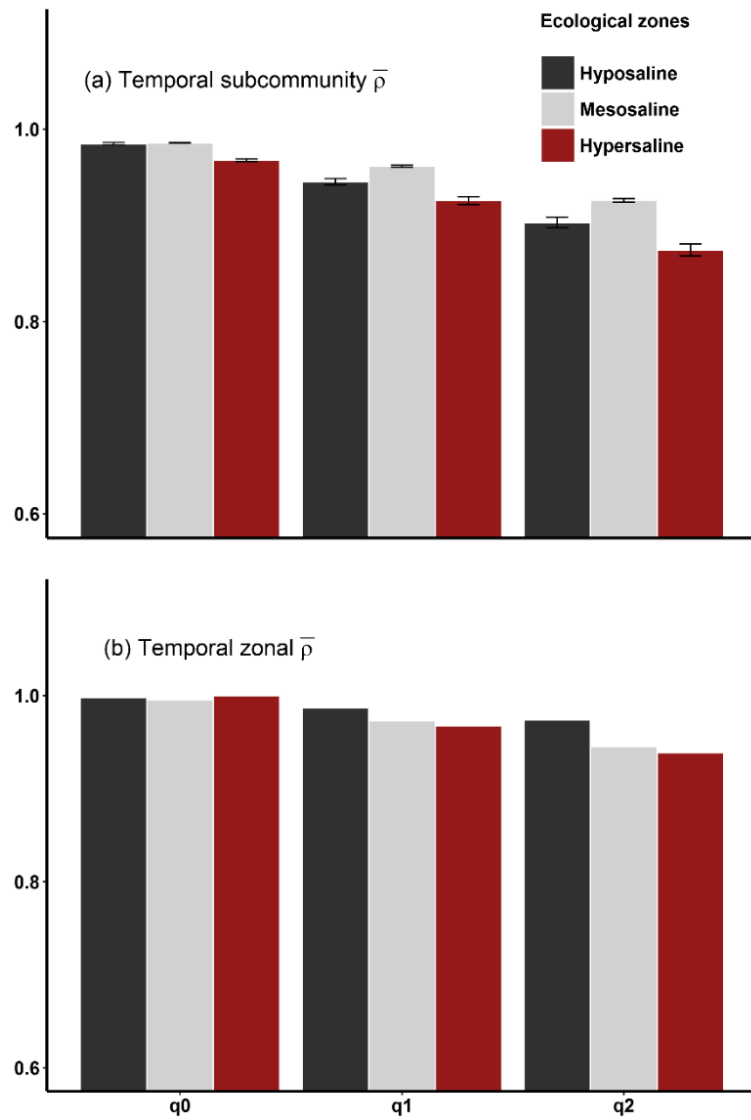
Appendix 3G. Spatial distributions of subcommunity alpha, beta and gamma diversities (for viewpoint parameter, $q = 0$) over the entire Sundarbans generated through ordinary kriging. The black contours represent the three protected areas.
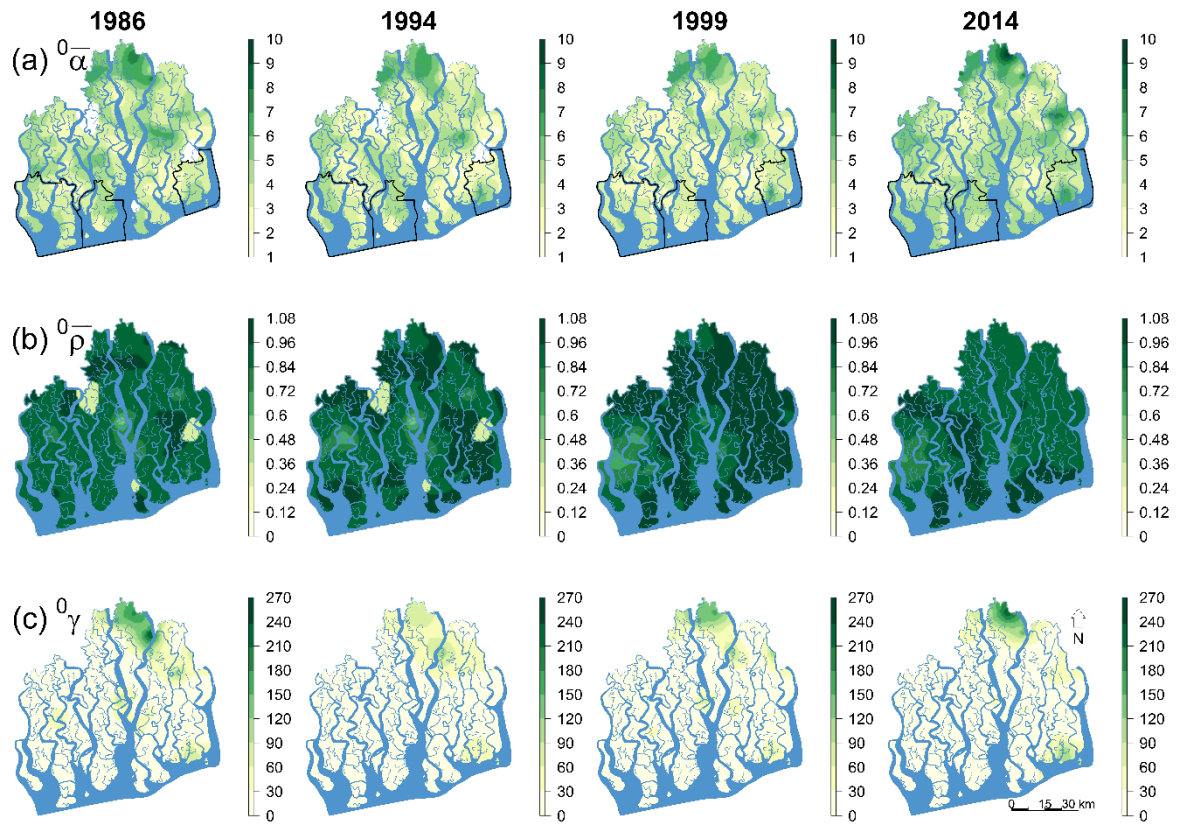
Appendix 3H. Spatial distributions of subcommunity alpha, beta and gamma diversities (for viewpoint parameter, $q = 2$) over the entire Sundarbans generated through ordinary kriging. The black contours represent the three protected areas.
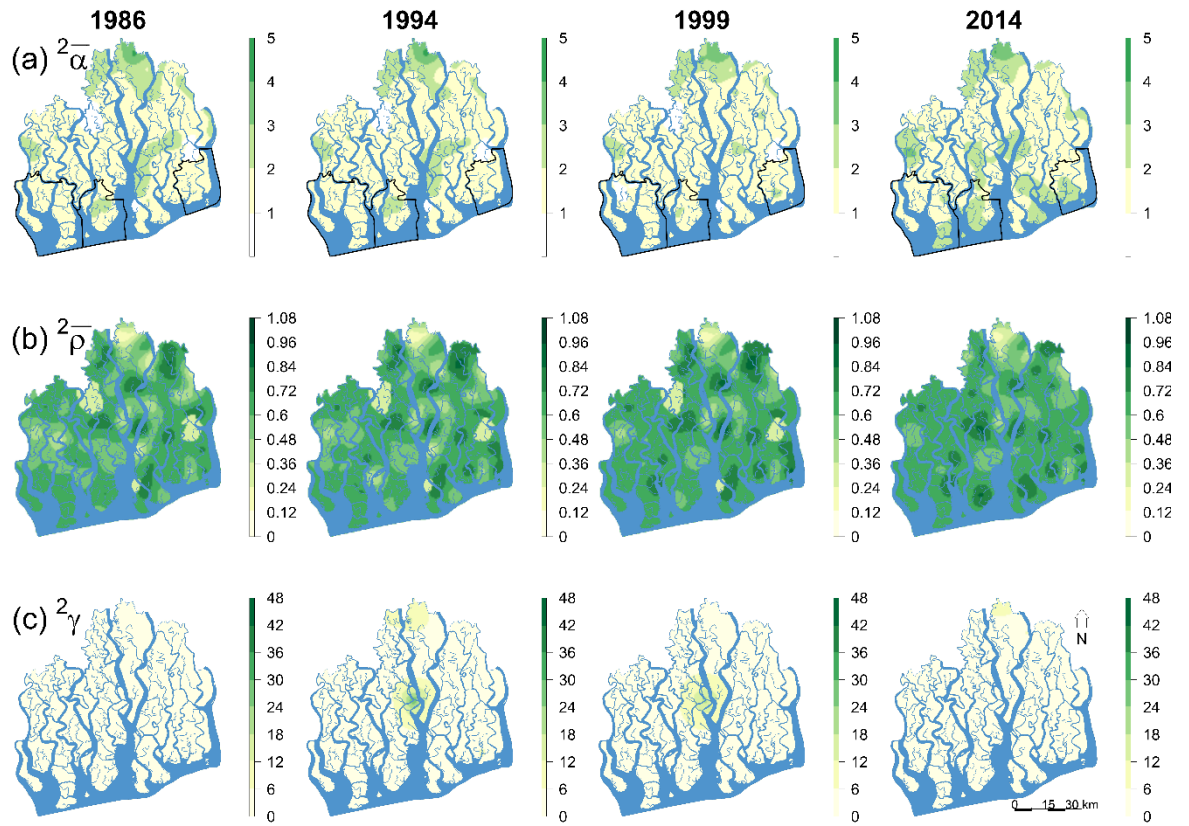
Chapter 4

Appendix 4A. Correlation (expressed as Pearson correlation coefficients) between the covariates.

	HH	DR	Elevation	K	DP	NH$_4$	P	pH	Salinity	Silt	CS	URP
DR	0.02											
Elevation	-0.07	0.09										
K	0.13	0.10	0.25									
DP	-0.18	0.02	0.16	0.11								
NH$_4$	0.3	-0.09	0.02	0.18	-0.06							
P	-0.18	-0.19	-0.05	-0.37	-0.02	-0.12						
pH	-0.01	0.00	-0.02	-0.13	-0.05	-0.18	-0.08					
Salinity	-0.22	-0.16	-0.02	-0.16	0.12	-0.29	0.28	-0.03				
Silt	0.09	0.09	0.11	0.11	0.04	0.01	0.02	0.06	-0.05			
CS	-0.16	-0.10	0.09	0.25	0.16	-0.04	-0.02	0.04	0.12	0.08		
URP	0.49	0.15	0.00	0.16	-0.22	0.15	-0.15	-0.15	-0.14	-0.03	-0.35	
ORP	0.06	0.04	0.01	0.20	-0.03	0.25	0.02	-0.89	-0.09	0.03	0.00	0.17

Appendix 4B. Stepwise VIF test outputs of the environmental covariates. The covariate short-hands are: community size (CS), upriver position (URP), salinity, distance to riverbank (DR), historical harvesting (HH), acidity (pH), silt concentration, disease prevalence (DP), soil total phosphorus (P), soil potassium (K), elevation above average-sea level (ELE), and soil NH4.

Covariates	VIF
CS	1.33
URP	1.65
Salinity	1.29
DR	1.13
HH	1.50
pH	2.43
Silt	1.09
DP	1.14
P	1.32
K	1.5
Elevation	1.12
NH_4	1.27
ORP	5.58

Appendix 4C. Results of GAMs for nine diversity measures. Summaries of model fit in rightmost three columns are only shown for the confidence set models i.e. models with $\Delta AIC_c \leq 2$. + symbol indicates that the covariates were retained and – symbol indicates that the covariates were not retained in the confidence set models for each biodiversity index. The covariate short-hands are: community size (CS), upriver position (URP), salinity, distance to riverbank (DR), historical harvesting (HH), acidity (pH), silt concentration, disease prevalence (DP), soil total phosphorus (P), soil potassium (K), elevation above average-sea level (ELE), and soil NH4.

		CS	URP	Salinity	DR	HH	pH	Silt	DP	P	K	ELE	NH4	AICc	ΔAICc	AICcw
Alpha		+	+	--	+	--	--	--	--	--	--	--	--	362.58	0.00	0.16
	$^0\bar{\alpha}$	+	+	--	--	--	--	--	--	--	--	--	--	362.92	0.34	0.14
		+	+	--	+	+	--	--	--	--	--	--	--	363.25	0.67	0.12
		+	+	--	--	+	--	--	--	--	--	--	--	363.29	0.72	0.11
		+	+	--	--	+	--	--	--	--	+	--	--	363.64	1.07	0.09
		+	+	--	--	--	--	--	--	--	+	--	--	363.83	1.26	0.09
		+	+	--	+	--	--	--	--	--	+	--	--	363.96	1.39	0.08
		+	+	--	+	--	--	+	--	--	--	--	--	364.10	1.53	0.08
		+	+	--	+	+	--	--	--	--	+	--	--	364.14	1.56	0.07
		+	+	--	+	--	--	--	+	--	--	--	--	364.51	1.93	0.06
	$^1\bar{\alpha}$	+	+	--	+	+	+	+	--	+	+	--	--	118.89	0.00	0.42
		+	+	+	+	+	+	+	--	--	--	--	--	120.35	1.46	0.20
		+	+	--	+	+	--	+	--	+	+	--	--	120.42	1.53	0.20
		+	+	--	+	--	+	+	--	+	+	--	--	120.60	1.70	0.18
	$^2\bar{\alpha}$	+	+	+	--	--	+	--	--	+	--	+	--	96.88	0.00	0.28
		+	+	--	--	--	--	--	--	+	+	--	--	97.57	0.69	0.20
		+	+	--	+	--	--	--	--	+	+	--	--	98.18	1.30	0.15
		+	+	--	--	--	--	--	--	+	+	+	--	98.34	1.46	0.14
		+	+	--	--	--	+	--	--	+	+	--	--	98.59	1.71	0.12
		+	+	--	--	+	--	--	--	+	+	--	--	98.72	1.83	0.11
Beta		+	--	+	+	--	--	--	+	--	+	--	--	-247.97	0.00	0.12
	$^0\bar{\rho}$	--	+	+	+	--	--	--	+	+	--	--	--	-247.79	0.17	0.11
		+	--	+	--	--	--	--	+	--	+	--	--	-247.53	0.43	0.09
		+	--	+	--	--	--	--	+	+	--	--	--	-247.50	0.46	0.09
		+	--	+	+	--	--	--	+	+	--	--	--	-247.44	0.53	0.09
		+	--	+	+	--	--	--	+	+	+	--	--	-247.26	0.71	0.08
		--	--	+	--	--	--	--	+	--	+	--	--	-247.06	0.91	0.07
		+	--	+	--	--	--	--	+	+	+	--	--	-246.99	0.98	0.07
		+	--	+	+	--	--	--	--	+	+	--	--	-246.73	1.23	0.06
		+	--	+	+	--	--	--	+	--	--	--	--	-246.73	1.24	0.06
		--	+	+	+	--	--	--	+	+	+	--	--	-246.61	1.36	0.06
		--	--	+	--	--	--	--	+	+	+	--	--	-246.29	1.67	0.05
		+	+	+	--	--	--	--	+	+	--	--	--	-246.06	1.91	0.04
	$^1\bar{\rho}$	+	+	+	--	+	--	+	+	--	--	--	--	-105.82	0.00	0.15

		+	+	+	--	+	+	--	+	--	--	--	--	-105.60	0.21	0.14
		+	+	+	+	+	+	--	+	+	--	--	--	-105.56	0.25	0.13
		+	+	+	+	+	+	--	+	--	--	--	--	-105.31	0.51	0.12
		+	+	+	--	+	--	--	+	--	--	--	--	-104.99	0.83	0.10
		+	+	+	--	+	+	--	+	+	--	--	--	-104.66	1.16	0.08
		+	+	--	--	+	--	--	+	--	--	--	--	-104.50	1.32	0.08
		+	+	+	--	--	--	+	+	--	--	--	--	-104.21	1.60	0.07
		+	+	+	--	+	--	+	+	+	--	--	--	-104.21	1.61	0.07
		+	+	--	--	+	--	+	+	--	--	--	--	-104.00	1.81	0.06
	$^2\overline{\rho}$	+	+	+	--	+	+	+	+	+	+	+	--	-61.93	0.00	0.37
		+	+	+	+	+	+	+	+	+	+	--	+	-61.55	0.39	0.30
		+	+	+	--	+	+	+	+	--	--	--	--	-60.37	1.56	0.17
		+	+	--	+	+	--	+	--	+	--	--	+	-60.20	1.73	0.16
Gamma	$^0\gamma$	+	+	--	+	--	+	--	+	--	--	--	--	786.94	0.00	0.12
		+	+	--	+	--	+	--	+	--	--	--	+	787.16	0.22	0.11
		+	+	--	+	--	--	--	+	--	--	--	+	787.53	0.59	0.09
		+	+	--	+	--	+	--	+	--	--	+	--	787.54	0.60	0.09
		+	+	+	+	+	+	--	+	--	--	--	--	787.99	1.06	0.07
		+	+	--	+	--	+	+	+	--	--	--	--	788.01	1.08	0.07
		+	+	+	+	+	+	+	+	--	--	--	+	788.09	1.15	0.07
		+	+	+	+	--	--	+	--	--	--	--	--	788.15	1.22	0.07
		+	+	--	+	+	+	--	+	--	--	--	--	788.20	1.26	0.06
		+	+	+	+	--	+	+	+	--	--	--	--	788.24	1.30	0.06
		+	+	--	+	--	+	+	+	+	--	--	--	788.73	1.79	0.05
		+	+	+	+	--	+	+	+	--	--	+	--	788.74	1.80	0.05
		+	+	+	+	--	+	+	+	+	--	--	--	788.78	1.85	0.05
		+	+	--	+	+	+	--	+	--	--	+	--	788.92	1.99	0.04
	$^1\gamma$	+	+	+	+	+	+	+	--	+	--	+	+	279.25	0.00	0.65
		+	+	+	+	+	+	+	+	--	--	--	--	280.51	1.26	0.35
	$^2\gamma$	+	+	+	+	+	+	+	--	--	--	--	--	98.50	0.00	0.28
		+	+	--	+	+	--	+	--	+	+	--	--	98.58	0.08	0.27
		+	+	+	+	+	+	+	--	+	+	--	--	98.90	0.40	0.23
		+	+	+	+	+	--	+	--	+	+	--	--	99.05	0.55	0.21

Appendix 4D. Effects of covariates inferred from my best GAMs fitted to the biodiversity measures for $q = 0$.
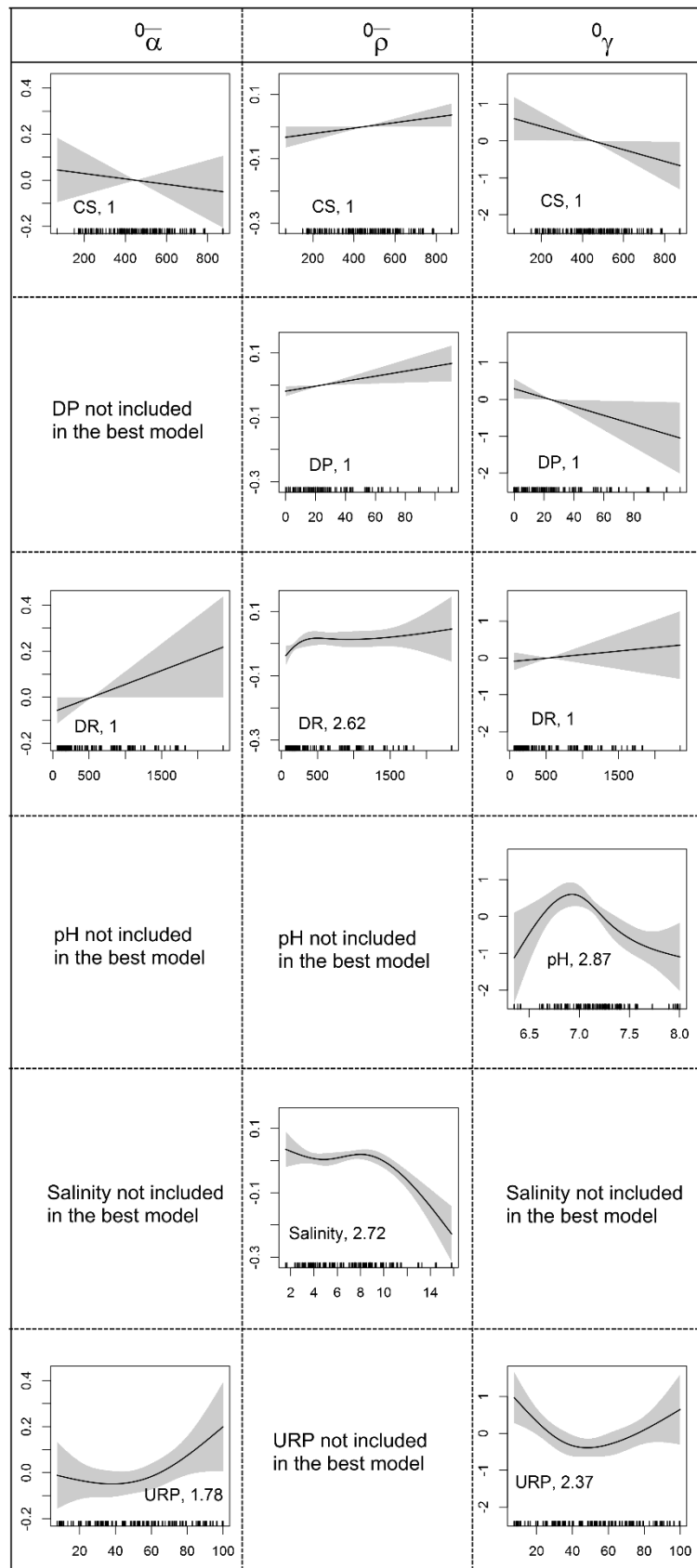
Appendix 4E. Effects of covariates inferred from my best GAMs fitted to the biodiversity measures for $q = 2$.
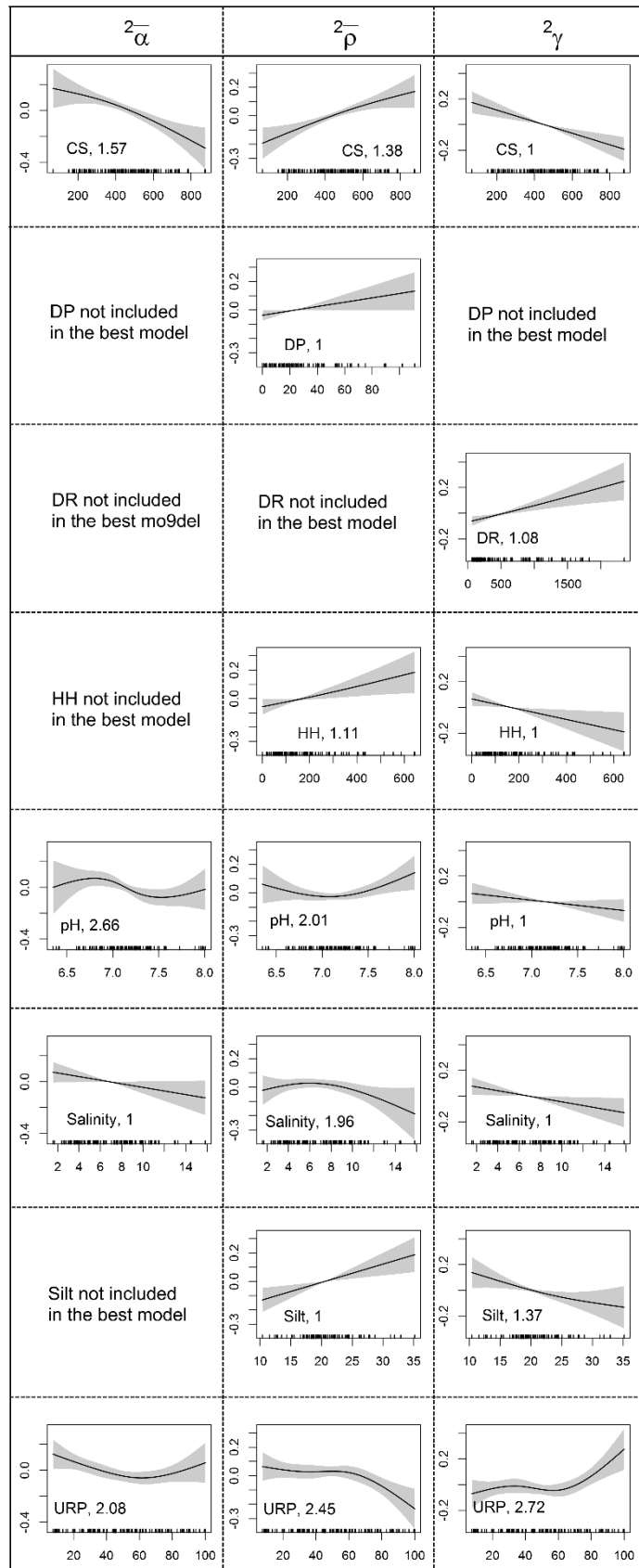
Chapter 5

Appendix 5A. Goodness of fit plots employing regressions of observed trait values vs. the posterior mean of the predicted trait values from the best model (Model VIII) for canopy height (A), SLA (B), wood density (C) and leaf succulence (D).
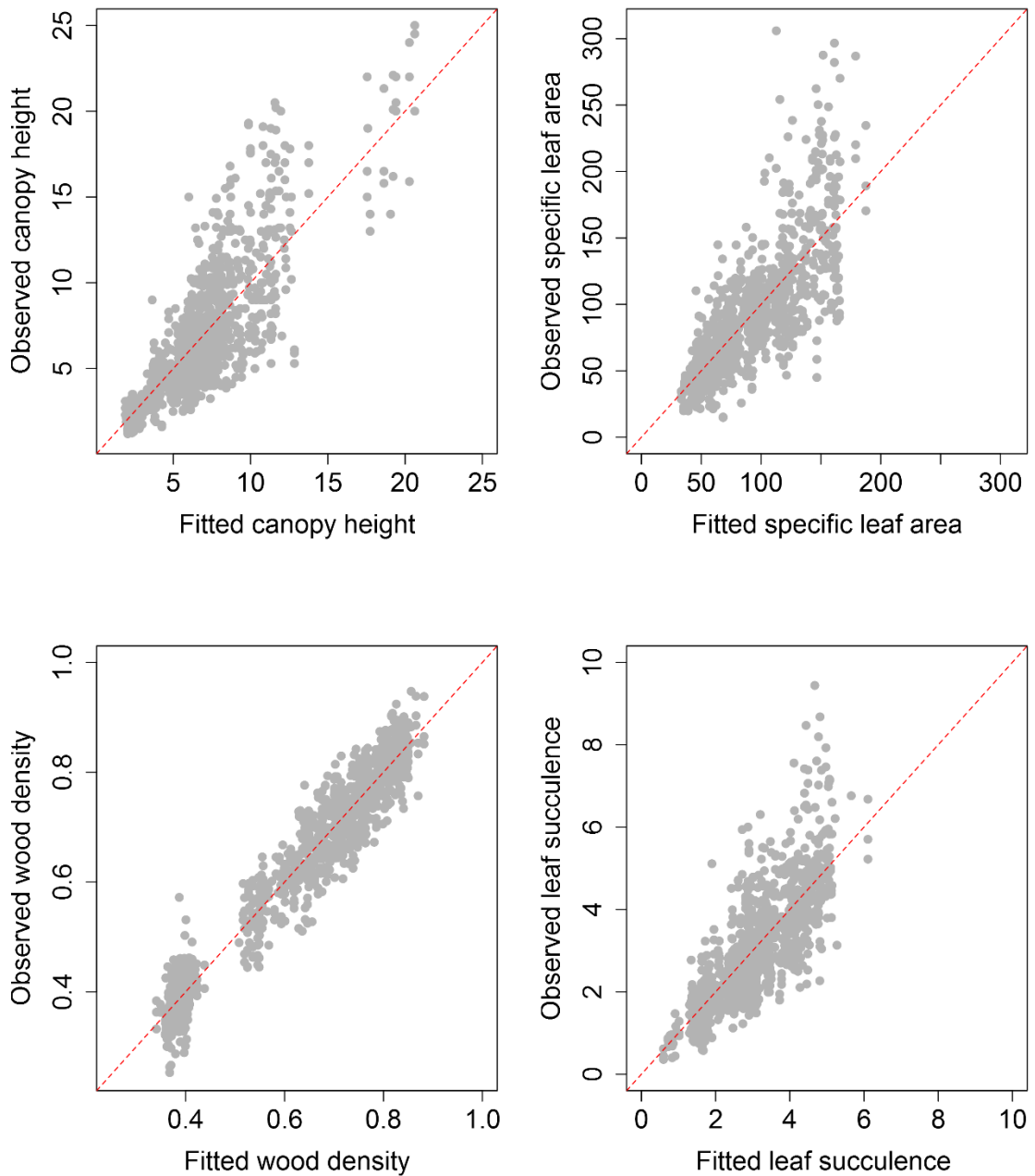
Appendix 5B. Different viewpoints of possible deterioration in terms of overall ecosystem productivity, under five future stress scenarios, E1 to E5, representing a 10% to 50% increase in both salinity and siltation for the whole Sundarbans ecosystem by 2050. A) The posterior probability of deterioration of the whole ecosystem in terms of productivity. B) The proportion of grid cells across the whole ecosystem where the expected (mean) response is a deterioration of overall ecosystem productivity. C) The posterior probability of deterioration of any individual grid cell, averaged across all grid cells in Sundarbans.
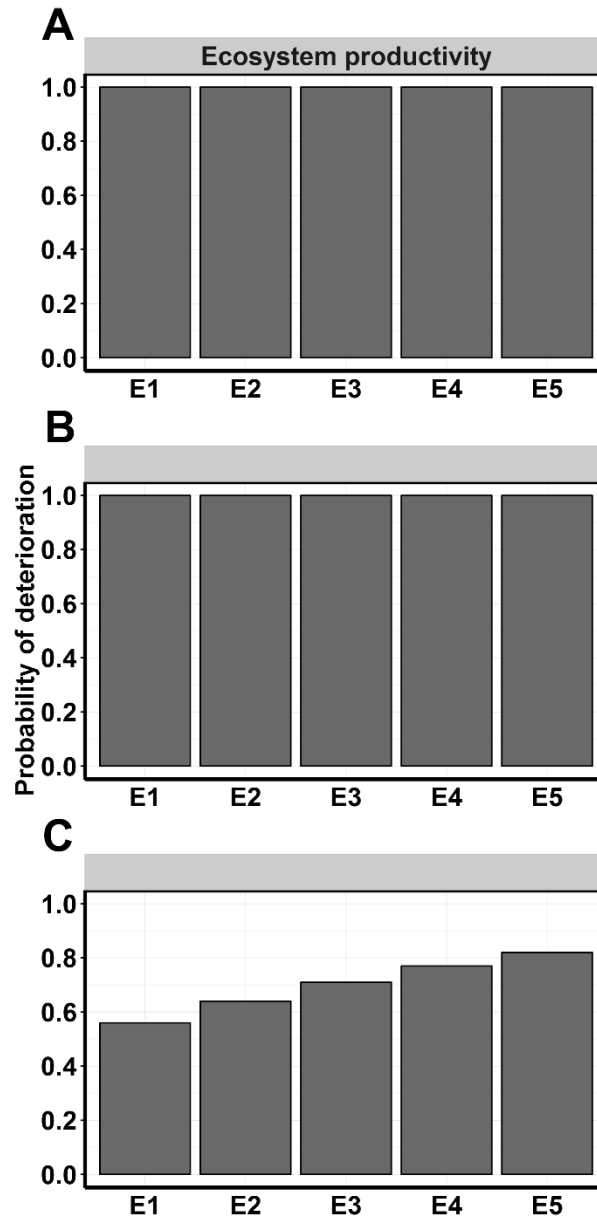
Appendix 5C. Different viewpoints of possible deterioration in terms of community traits, under five future stress scenarios, E1 to E5, representing a 10% to 50% increase in both salinity and siltation for the whole Sundarbans ecosystem by 2050. A) The posterior probability of deterioration of the whole ecosystem in terms of community traits: CH, SLA, WD and LS; B) The proportion of grid cells across the whole ecosystem where the expected (mean) response is a deterioration in terms of the community traits; C) The posterior probability of deterioration of any individual grid cell, averaged across all grid cells in the Sundarbans in terms of the community traits. Decreases in CH and SLA and increases in LS and WD are considered to be deteriorations in the traits.
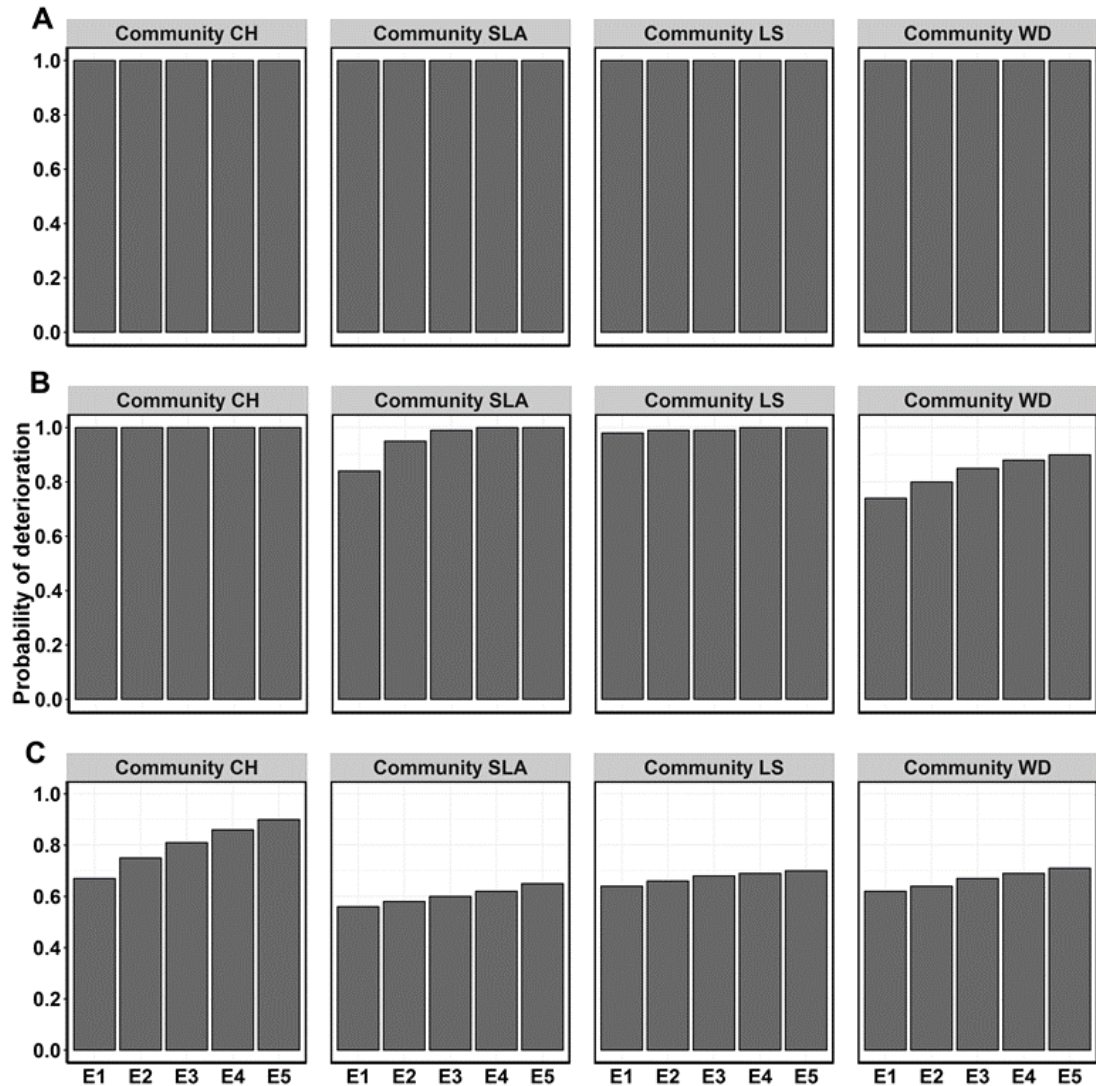
Appendix 5D. Different viewpoints of possible deterioration in terms of each of the traits of the individual species, under five future stress scenarios, E1 to E5, representing a 10% to 50% increase in both salinity and siltation for the whole Sundarbans ecosystem by 2050. A) The posterior probability of deterioration of traits (CH, SLA, WD and LS) for four prominent tree species across the entire ecosystem; B) The proportion of grid cells across the whole ecosystem where the expected (mean) response is a deterioration for each of the traits of the individual species; C) The posterior probability of deterioration of any individual grid cell, averaged across all grid cells in the Sundarbans in terms of each of the traits of the individual species. Decreases in CH and SLA and increases in LS and WD are deteriorations in the traits.
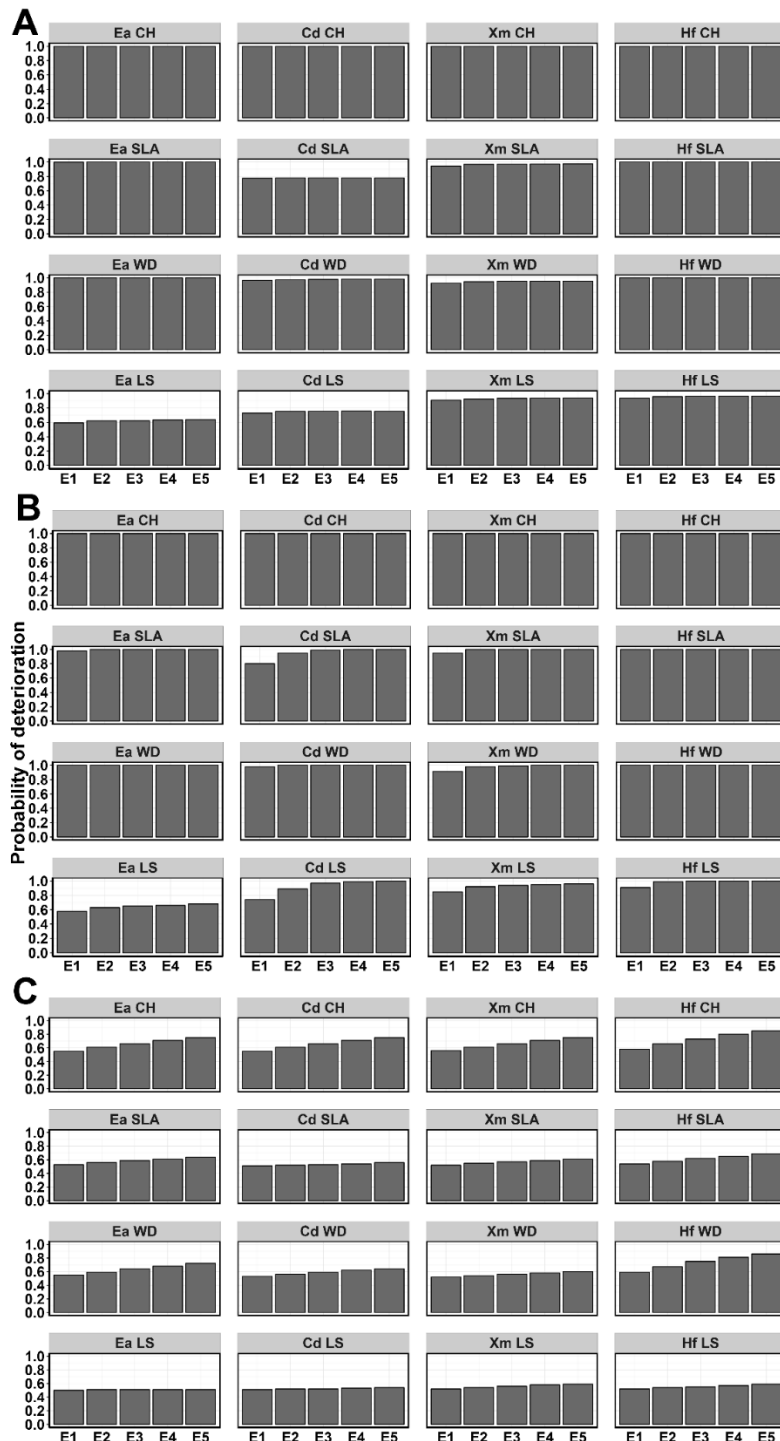
Appendix 5E. Current and future (2050) density distributions of four mangrove tree species in the Sundarbans (Chapter 2).

Current tree density **2050 tree density**

(a) *H. fomes*

(b) *E. agallocha*

(c) *C. decandra*

(d) *X. mekongensis*
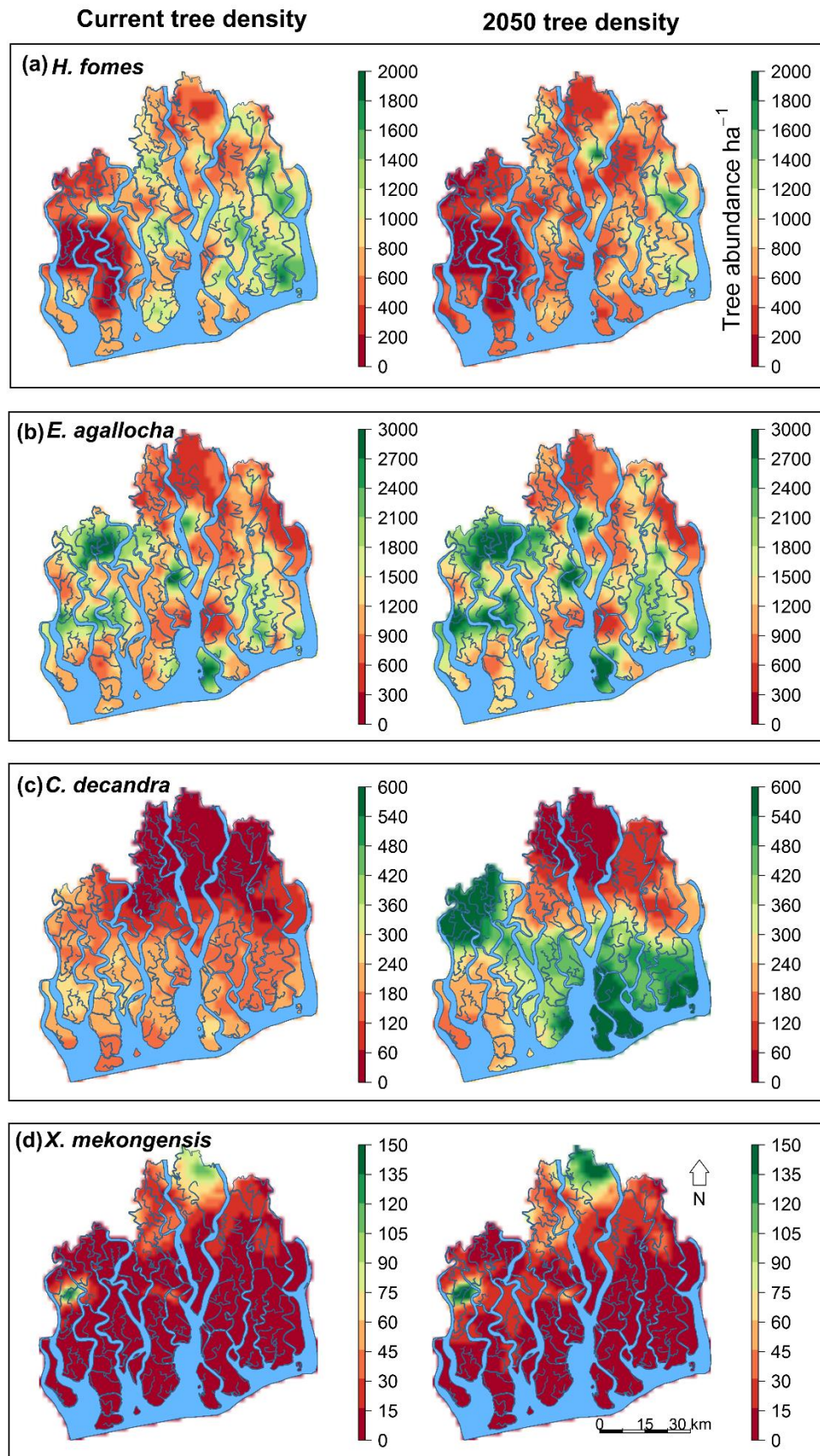
Appendix 5F. R code for the trait-based models

```
##### DATA & LIBRARY IMPORT ####

library(xlsx)
library(runjags)
library(sqldf)
library(XLConnect)
library(XLConnectJars)
library(data.table)
library(rjags)

# Data arrangement
db <- dbConnect(SQLite(), dbname="Test.sqlite.JAGS") # database

# Importing excel raw data
wb <- loadWorkbook("data.xlsx")
setMissingValue(wb, value = "NA")

Tables <- readWorksheet(wb, sheet = getSheets(wb))

names(Tables) = c("ENVIRONMENT", "SPECIES", "TRAIT")    # Names of the data frames
str(Tables)      # structure of Tables
names(Tables)    # Names of the elements of Tables

# Incerting tables into database

with(Tables, {
  dbWriteTable(conn = db, name = "ENVIRONMENT", value = ENVIRONMENT, row.names = FALSE, overwrite=TRUE)
  dbWriteTable(conn = db, name = "SPECIES", value = SPECIES, row.names = FALSE,overwrite=TRUE)
  dbWriteTable(conn = db, name = "TRAIT", value = TRAIT, row.names = FALSE,overwrite=TRUE)
})

## # Creation of overall species, environment and trait data frame
sp.en.traits <- dbGetQuery(db,"SELECT ENVIRONMENT_TRAIT,TRAIT.SPECIES_TRAIT, ENVIRONMENT.NH4, ENVIRONMENT.P,
ENVIRONMENT.K, ENVIRONMENT. SALINITY, ENVIRONMENT.SILT, ENVIRONMENT.PH,ENVIRONMENT.URP,
          ENVIRONMENT.HH, TRAIT.HEIGHT, TRAIT.SLA,TRAIT.WD,TRAIT.SC

          FROM ENVIRONMENT JOIN TRAIT ON ENVIRONMENT.ENVIRONMENT_ENVIRONMENT =
TRAIT.ENVIRONMENT_TRAIT
          WHERE TRAIT.SLA IS NOT NULL AND TRAIT.WD IS NOT NULL AND TRAIT.SC IS NOT NULL AND

          SPECIES_TRAIT IN ('E_agallocha','H_fomes','C_decandra','X_mekongensis','A. officinalis','A_cucullata',
          'B_sexangula','C_ramiflora','S_apetala')") # species that occurred in > 5% of the plots.

n<-length(sp.en.traits[,1]) # Sample size
vmax<-4 # Number of traits to be considered

# Standardizing trait variables

CH<-((sp.en.traits$CH-mean(sp.en.traits$CH))/sd(sp.en.traits$CH))
SLA<-((sp.en.traits$SLA-mean(sp.en.traits$SLA))/sd(sp.en.traits$SLA))
WD<-((sp.en.traits$WD-mean(sp.en.traits$WD))/sd(sp.en.traits$WD))
LS<-((sp.en.traits$LS-mean(sp.en.traits$LS))/sd(sp.en.traits$LS))

traits<-as.matrix(cbind(CH,SLA,WD,LS)) # trait matrix

# Standardizing trait variables

NH4<-((sp.en.traits$NH4-mean(sp.en.traits$NH4))/sd(sp.en.traits$NH4))
P<-((sp.en.traits$P-mean(sp.en.traits$P))/sd(sp.en.traits$P))
K<-((sp.en.traits$K-mean(sp.en.traits$K))/sd(sp.en.traits$K))
SALINITY<-((sp.en.traits$SALINITY-mean(sp.en.traits$SALINITY))/sd(sp.en.traits$SALINITY))
SILT<-((sp.en.traits$SILT-mean(sp.en.traits$SILT))/sd(sp.en.traits$SILT))
PH<-((sp.en.traits$PH-mean(sp.en.traits$PH))/sd(sp.en.traits$PH))
URP<-((sp.en.traits$URP-mean(sp.en.traits$URP))/sd(sp.en.traits$URP))
HH<-((sp.en.traits$HH-mean(sp.en.traits$HH))/sd(sp.en.traits$HH))
```

```
########################################################################
# JAGS Model 1: TER (trait-environment relationship) and
# TTR (trait-trait # relationship) are fixed across the species
########################################################################
model1<-"
model
{
  for( i in 1:n)
  {
  # Linear predictors for individual traits
  ch[i]   <-
a[1,1]+a[1,2]*NH4[i]+a[1,3]*P[i]+a[1,4]*K[i]+a[1,5]*SALINITY[i]+a[1,6]*SILT[i]+a[1,7]*PH[i]+a[1,8]*URP[i]+a[1,9]*HH[i]
  sla[i]   <-
a[2,1]+a[2,2]*NH4[i]+a[2,3]*P[i]+a[2,4]*K[i]+a[2,5]*SALINITY[i]+a[2,6]*SILT[i]+a[2,7]*PH[i]+a[2,8]*URP[i]+a[2,9]*HH[i]
  wd[i]   <-
a[3,1]+a[3,2]*NH4[i]+a[3,3]*P[i]+a[3,4]*K[i]+a[3,5]*SALINITY[i]+a[3,6]*SILT[i]+a[3,7]*PH[i]+a[3,8]*URP[i]+a[3,9]*HH[i]
  ls[i]    <-
a[4,1]+a[4,2]*NH4[i]+a[4,3]*P[i]+a[4,4]*K[i]+a[4,5]*SALINITY[i]+a[4,6]*SILT[i]+a[4,7]*PH[i]+a[4,8]*URP[i]+a[4,9]*HH[i]

  # Definition of the likelihood
  mu[i,1]<-ch[i]
  mu[i,2]<-sla[i]
  mu[i,3]<-wd[i]
  mu[i,4]<-ls[i]

  traits[i,]~dmnorm(mu[i,], omega[,])
  }

  # PRIORS

  # Setting up of the regression coefficients matrix

  averagetau ~ dgamma(0.0001,0.01)

  for(k in 1:9) # Number of coefficients per trait
  {

  for( j in 1:vmax) # Number of traits
  {
  a[j,k] ~ dnorm(0,averagetau)

  }
  }

  # Precision matrix
  # Setting up of the variances vector (the diagonal of the var-cov matrix)
  for( j in 1:vmax)
  {
  sigma[j,j]~dgamma(0.01,0.01) # mean 1 variance high
  }

  # Setting up of the lower diagonal part of var-cov matrix
  for( j in 2:vmax)
  {
  for(k in 1:(j-1))
  {
  sigma[j,k]~dnorm(0,0.01)
  }
  }

  # Mirroring of the lower diagonal by the upper diagonal of the var-cov matrix
  for( j in 1:(vmax-1))
  {
  for(k in (j+1):vmax)
  {
  sigma[j,k]<-sigma[k,j]
  }
  }

  omega<-inverse(sigma) # Conversion of var-cov matrix into precision matrix

  # data # n, vmax, traits, NH4, P, K, SALINITY, SILT, PH, URP, HH
  # monitor # a, averagetau, sigma

}
"
# Model1 outputs
init.model1<-run.jags(model1, n.chains=2, burnin=4000, sample=10000,modules=c("glm","dic"))
extend.init.model1<-extend.jags(init.model1, sample=20000)
```

```
print(extend.init.model1)
dic.extend.init.similar<-extract(extend.init.model1, what='dic') # DIC, pD


##########################################################################
# Model 2: TTR varies across the species
##########################################################################
species<-as.integer(factor(sp.en.traits$SPECIES)) # species as factors

model2<-"
model
{
 for( i in 1:n)
 {
 # Linear predictors for individual traits
 ch[i]  <-
a[1,1]+a[1,2]*NH4[i]+a[1,3]*P[i]+a[1,4]*K[i]+a[1,5]*SALINITY[i]+a[1,6]*SILT[i]+a[1,7]*PH[i]+a[1,8]*URP[i]+a[1,9]*HH[i]
 sla[i]  <-
a[2,1]+a[2,2]*NH4[i]+a[2,3]*P[i]+a[2,4]*K[i]+a[2,5]*SALINITY[i]+a[2,6]*SILT[i]+a[2,7]*PH[i]+a[2,8]*URP[i]+a[2,9]*HH[i]
 wd[i]  <-
a[3,1]+a[3,2]*NH4[i]+a[3,3]*P[i]+a[3,4]*K[i]+a[3,5]*SALINITY[i]+a[3,6]*SILT[i]+a[3,7]*PH[i]+a[3,8]*URP[i]+a[3,9]*HH[i]
 ls[i]   <-
a[4,1]+a[4,2]*NH4[i]+a[4,3]*P[i]+a[4,4]*K[i]+a[4,5]*SALINITY[i]+a[4,6]*SILT[i]+a[4,7]*PH[i]+a[4,8]*URP[i]+a[4,9]*HH[i]

 # Definition of the likelihood
 mu[i,1]<-ls[i]
 mu[i,2]<-sla[i]
 mu[i,3]<-wd[i]
 mu[i,4]<-ls[i]

 traits[i,]~dmnorm(mu[i,], omega[species[i],,])
 }

 # PRIORS

 # Setting up of the regression coefficients matrix

 averagetau ~ dgamma(0.0001,0.01)

 for(k in 1:9) # Number of coefficients per trait
 {

 for( j in 1:vmax) # Number of traits
 {
 a[j,k] ~ dnorm(0,averagetau)

 }
 }

 # Precision matrix
 # Setting up of the variances vector (the diagonal of the var-cov matrix)

 tauvar~dgamma(1.00, 1.00)

 for( j in 1:vmax)
 {
 for (m in 1:9)
 {
 sigma[m,j,j]~dgamma(1, 0.01) # mean 1 variance high
 }
 }
 # Setting up of the lower diagonal part of var-cov matrix
 for( j in 2:vmax)
 {
 for(k in 1:(j-1))
 {
 for (m in 1:9)
 {
 sigma[m,j,k]~dnorm(0,tauvar)
 }
 }
 }
 # Mirroring of the lower diagonal by the upper diagonal of the var-cov matrix
 for( j in 1:(vmax-1))
 {
 for(k in (j+1):vmax)
 {
 for (m in 1:9)
 {
```

```
sigma[m,j,k]<-sigma[m,k,j]

}
}
}
for (m in 1:9)
{
omega[m,1:vmax,1:vmax]<-inverse(sigma[m,1:vmax,1:vmax]) # Conversion of var-cov matrix into precision matrix
}
# data # n, vmax, traits, NH4, P, K,SALINITY, SILT, PH, URP, HH, species
# monitor # a, sigma, tauvar

}
"
```

model2 outputs

```
init.model2<-run.jags(model2, n.chains=2, burnin=4000, sample=10000,modules=c("glm","dic"))
extend.init.model2<-extend.jags(init.model2, sample=20000)
print(extend.init.model2)
dic.extend.init.model2<-extract(extend.init.model2, what='dic') # DIC, pD
```

```
####################################################################
# Model 3: TER varies across the species
####################################################################
model3<-"
model
{
  for( i in 1:n)
  {
  # Linear predictors for individual traits
ch[i]<-
a[1,1,species[i]]+a[1,2,species[i]]*NH4[i]+a[1,3,species[i]]*P[i]+a[1,4,species[i]]*K[i]+a[1,5,species[i]]*SALINITY[i]+a[1,6,species[i]]*SILT[i]+a[1,7,species[i]]*PH[i]+a[1,8,species[i]]*URP[i]+a[1,9,species[i]]*HH[i]
  sla[i]<-
a[2,1,species[i]]+a[2,2,species[i]]*NH4[i]+a[2,3,species[i]]*P[i]+a[2,4,species[i]]*K[i]+a[2,5,species[i]]*SALINITY[i]+a[2,6,species[i]]*SILT[i]+a[2,7,species[i]]*PH[i]+a[2,8,species[i]]*URP[i]+a[2,9,species[i]]*HH[i]
  wd[i] <-
a[3,1,species[i]]+a[3,2,species[i]]*NH4[i]+a[3,3,species[i]]*P[i]+a[3,4,species[i]]*K[i]+a[3,5,species[i]]*SALINITY[i]+a[3,6,species[i]]*SILT[i]+a[3,7,species[i]]*PH[i]+a[3,8,species[i]]*URP[i]+a[3,9,species[i]]*HH[i]
  ls[i] <-
a[4,1,species[i]]+a[4,2,species[i]]*NH4[i]+a[4,3,species[i]]*P[i]+a[4,4,species[i]]*K[i]+a[4,5,species[i]]*SALINITY[i]+a[4,6,species[i]]*SILT[i]+a[4,7,species[i]]*PH[i]+a[4,8,species[i]]*URP[i]+a[4,9,species[i]]*HH[i]

  # Definition of the likelihood
  mu[i,1]<-ch[i]
  mu[i,2]<-sla[i]
  mu[i,3]<-wd[i]
  mu[i,4]<-ls[i]

  traits[i,]~dmnorm(mu[i,], omega[,])
  }

  # PRIORS

  # Setting up of the regression coefficients matrix

  tau.b ~ dgamma(0.0001,0.01)

  for(k in 1:9) # Number of coefficients per trait
  {

  for(j in 1:vmax) # Number of traits
  {

  for (m in 1:9)
  {
  a[j,k,m] ~ dnorm(0,tau.b)
  }
  }
  }

  # Precision matrix
  # Setting up of the variances vector (the diagonal of the var-cov matrix)
  for( j in 1:vmax)
  {
  sigma[j,j]~dgamma(0.01,0.01) # mean 1 variance high
  }

  # Setting up of the lower diagonal part of var-cov matrix
```

```
for( j in 2:vmax)
{
for(k in 1:(j-1))
{
sigma[j,k]~dnorm(0,0.01)
}
}

# Mirroring of the lower diagonal by the upper diagonal of the var-cov matrix
for( j in 1:(vmax-1))
{
for(k in (j+1):vmax)
{
sigma[j,k]<-sigma[k,j]
}
}
omega<-inverse(sigma) # Conversion of var-cov matrix into precision matrix
# data # n, vmax, traits, NH4, P, K,SALINITY, SILT, PH, URP, HH, species
# monitor # a,tau.b,sigma

}
"
# model3 outputs
init.model3<-run.jags(model3, n.chains=2, burnin=4000, sample=10000,modules=c("glm","dic"))
extend.init.model3<-extend.jags(init.model3, sample=20000)
print(extend.init.model3)
dic.extend.init.model3<-extract(extend.init.model3, what='dic') # DIC, pD

######################################################################
# Model 4:TER varies around a common mean
######################################################################
model4<-"
model
{
  for( i in 1:n)
  {
   # Linear predictors for individual traits
  ch[i] <-
a[1,1,species[i]]+a[1,2,species[i]]*NH4[i]+a[1,3,species[i]]*P[i]+a[1,4,species[i]]*K[i]+a[1,5,species[i]]*SALINITY[i]+a[1,6,species[i]]*SILT[i]+a[1,7,species[i]]*PH[i]+a[1,8,species[i]]*URP[i]+a[1,9,species[i]]*HH[i]
   sla[i]<-
a[2,1,species[i]]+a[2,2,species[i]]*NH4[i]+a[2,3,species[i]]*P[i]+a[2,4,species[i]]*K[i]+a[2,5,species[i]]*SALINITY[i]+a[2,6,species[i]]*SILT[i]+a[2,7,species[i]]*PH[i]+a[2,8,species[i]]*URP[i]+a[2,9,species[i]]*HH[i]
   wd[i] <-
a[3,1,species[i]]+a[3,2,species[i]]*NH4[i]+a[3,3,species[i]]*P[i]+a[3,4,species[i]]*K[i]+a[3,5,species[i]]*SALINITY[i]+a[3,6,species[i]]*SILT[i]+a[3,7,species[i]]*PH[i]+a[3,8,species[i]]*URP[i]+a[3,9,species[i]]*HH[i]
   ls[i] <-
a[4,1,species[i]]+a[4,2,species[i]]*NH4[i]+a[4,3,species[i]]*P[i]+a[4,4,species[i]]*K[i]+a[4,5,species[i]]*SALINITY[i]+a[4,6,species[i]]*SILT[i]+a[4,7,species[i]]*PH[i]+a[4,8,species[i]]*URP[i]+a[4,9,species[i]]*HH[i]

   # Definition of the likelihood
   mu[i,1]<-ch[i]
   mu[i,2]<-sla[i]
   mu[i,3]<-wd[i]
   mu[i,4]<-ls[i]

   traits[i,]~dmnorm(mu[i,], omega[,])
   }

  # PRIORS

  # Setting up of the regression coefficients matrix

  averagetau ~ dgamma(0.0001,0.01)
  tau.a ~ dgamma(0.0001,0.01)

  for(k in 1:9) # Number of coefficients per trait
  {
  for(j in 1:vmax) # Number of traits
  {
  averagea[j,k] ~ dnorm(0,averagetau)
  for (m in 1:9)
  {
  a[j,k,m] ~ dnorm(averagea[j,k],tau.a)
  }
  }
  }

  # Precision matrix
```

```
# Setting up of the variances vector (the diagonal of the var-cov matrix)

tauvar~dgamma(1.00, 1.00)

for( j in 1:vmax)
{
sigma[j,j]~dgamma(1, 0.01) # mean 1 variance high
}

# Setting up of the lower diagonal part of var-cov matrix
for( j in 2:vmax)
{
for(k in 1:(j-1))
{
sigma[j,k]~dnorm(0,tauvar)
}
}

# Mirroring of the lower diagonal by the upper diagonal of the var-cov matrix
for( j in 1:(vmax-1))
{
for(k in (j+1):vmax)
{
sigma[j,k]<-sigma[k,j]
}
}
omega<-inverse(sigma) # Conversion of var-cov matrix into precision matrix
# data # n, vmax, traits, NH4, P, K,SALINITY, SILT, PH, URP, HH, species
# monitor # a, averagetau, sigma,tau.a, tauvar

}
"
# model4 outputs
init.model4<-run.jags(model4, n.chains=2, burnin=4000, sample=10000,modules=c("glm","dic"))
extend.init.model4<-extend.jags(init.model4, sample=20000)
print(extend.init.model4)
dic.extend.init.model4<-extract(extend.init.model4, what='dic') # DIC, pD

#######################################################################
# Model 5: TER varies around the common mean for each trait
#######################################################################
model5<-"
model
{
  for( i in 1:n)
  {
  # Linear predictors for individual traits
  ch[i] <-
a[1,1,species[i]]+a[1,2,species[i]]*NH4[i]+a[1,3,species[i]]*P[i]+a[1,4,species[i]]*K[i]+a[1,5,species[i]]*SALINITY[i]+a[1,6,species[i]]*SILT[i]+a[1,7,species[i]]*PH[i]+a[1,8,species[i]]*URP[i]+a[1,9,species[i]]*HH[i]
  sla[i]<-
a[2,1,species[i]]+a[2,2,species[i]]*NH4[i]+a[2,3,species[i]]*P[i]+a[2,4,species[i]]*K[i]+a[2,5,species[i]]*SALINITY[i]+a[2,6,species[i]]*SILT[i]+a[2,7,species[i]]*PH[i]+a[2,8,species[i]]*URP[i]+a[2,9,species[i]]*HH[i]
  wd[i] <-
a[3,1,species[i]]+a[3,2,species[i]]*NH4[i]+a[3,3,species[i]]*P[i]+a[3,4,species[i]]*K[i]+a[3,5,species[i]]*SALINITY[i]+a[3,6,species[i]]*SILT[i]+a[3,7,species[i]]*PH[i]+a[3,8,species[i]]*URP[i]+a[3,9,species[i]]*HH[i]
  ls[i] <-
a[4,1,species[i]]+a[4,2,species[i]]*NH4[i]+a[4,3,species[i]]*P[i]+a[4,4,species[i]]*K[i]+a[4,5,species[i]]*SALINITY[i]+a[4,6,species[i]]*SILT[i]+a[4,7,species[i]]*PH[i]+a[4,8,species[i]]*URP[i]+a[4,9,species[i]]*HH[i]

  # Definition of the likelihood
  mu[i,1]<-ch[i]
  mu[i,2]<-sla[i]
  mu[i,3]<-wd[i]
  mu[i,4]<-ls[i]

  traits[i,]~dmnorm(mu[i,], omega[,])
  }

  # PRIORS

  # Setting up of the regression coefficients matrix

  averagetau ~ dgamma(0.0001,0.01)

  for(j in 1:vmax) # Number of traits
  {
  tau[j] ~ dgamma(0.0001,0.01)
```

```
  for(k in 1:9) # Number of coefficients per trait
  {
  averagea[j,k] ~ dnorm(0,averagetau)

for (m in 1:9)
  {
  a[j,k,m] ~ dnorm(averagea[j,k],tau[j])
  }
  }
  }

  # Precision matrix
  # Setting up of the variances vector (the diagonal of the var-cov matrix)

  tauvar~dgamma(1.00, 1.00)

  for( j in 1:vmax)
  {
  sigma[j,j]~dgamma(1, 0.01) # mean 1 variance high
  }

  # Setting up of the lower diagonal part of var-cov matrix
  for( j in 2:vmax)
  {
  for(k in 1:(j-1))
  {
  sigma[j,k]~dnorm(0,tauvar)
  }
  }

  # Mirroring of the lower diagonal by the upper diagonal of the var-cov matrix
  for( j in 1:(vmax-1))
  {
  for(k in (j+1):vmax)
  {
  sigma[j,k]<-sigma[k,j]
  }
  }
  omega<-inverse(sigma) # Conversion of var-cov matrix into precision matrix
  # data # n, vmax, traits, NH4, P, K,SALINITY, SILT, PH, URP, HH, species
  # monitor # a, averagea, sigma,tau, tauvar

}
"
" # model5 results

init.model5<-run.jags(model5, n.chains=2, burnin=4000, sample=10000,modules=c("glm","dic"))
extend.init.model5<-extend.jags(init.model5, sample=20000)
print(extend.init.model5)
dic.extend.init.model5<-extract(extend.init.model5, what='dic') # DIC, pD

####################################################################
# Model 6: TER varies around the common mean for each environmental driver
####################################################################
model6<-"
model
{
  for( i in 1:n)
  {

  # Linear predictors for individual traits
  ch[i] <-
a[1,1,species[i]]+a[1,2,species[i]]*NH4[i]+a[1,3,species[i]]*P[i]+a[1,4,species[i]]*K[i]+a[1,5,species[i]]*SALINITY[i]+a[1,6,s
pecies[i]]*SILT[i]+a[1,7,species[i]]*PH[i]+a[1,8,species[i]]*URP[i]+a[1,9,species[i]]*HH[i]
  sla[i]<-
a[2,1,species[i]]+a[2,2,species[i]]*NH4[i]+a[2,3,species[i]]*P[i]+a[2,4,species[i]]*K[i]+a[2,5,species[i]]*SALINITY[i]+a[2,6,s
pecies[i]]*SILT[i]+a[2,7,species[i]]*PH[i]+a[2,8,species[i]]*URP[i]+a[2,9,species[i]]*HH[i]
  wd[i] <-
a[3,1,species[i]]+a[3,2,species[i]]*NH4[i]+a[3,3,species[i]]*P[i]+a[3,4,species[i]]*K[i]+a[3,5,species[i]]*SALINITY[i]+a[3,6,s
pecies[i]]*SILT[i]+a[3,7,species[i]]*PH[i]+a[3,8,species[i]]*URP[i]+a[3,9,species[i]]*HH[i]
  ls[i] <-
a[4,1,species[i]]+a[4,2,species[i]]*NH4[i]+a[4,3,species[i]]*P[i]+a[4,4,species[i]]*K[i]+a[4,5,species[i]]*SALINITY[i]+a[4,6,s
pecies[i]]*SILT[i]+a[4,7,species[i]]*PH[i]+a[4,8,species[i]]*URP[i]+a[4,9,species[i]]*HH[i]

  # Definition of the likelihood
  mu[i,1]<-ch[i]
  mu[i,2]<-sla[i]
  mu[i,3]<-wd[i]
  mu[i,4]<-ls[i]
```

```
traits[i,]~dmnorm(mu[i,], omega[,])
}

# PRIORS

# Setting up of the regression coefficients matrix

averagetau ~ dgamma(0.0001,0.01)

for(k in 1:9) # Number of coefficients per trait
{

tau[k] ~ dgamma(0.0001,0.01)

for(j in 1:vmax) # Number of traits
{

averagea[j,k] ~ dnorm(0,averagetau)

for (m in 1:9)
{
a[j,k,m] ~ dnorm(averagea[j,k],tau[k])
}
}
}

# Precision matrix
# Setting up of the variances vector (the diagonal of the var-cov matrix)

tauvar~dgamma(1.00, 1.00)

for( j in 1:vmax)
{
sigma[j,j]~dgamma(1, 0.01) # mean 1 variance high
}

# Setting up of the lower diagonal part of var-cov matrix
for( j in 2:vmax)
{
for(k in 1:(j-1))
{
sigma[j,k]~dnorm(0,tauvar)
}
}

# Mirroring of the lower diagonal by the upper diagonal of the var-cov matrix
for( j in 1:(vmax-1))
{
for(k in (j+1):vmax)
{
sigma[j,k]<-sigma[k,j]
}
}
omega<-inverse(sigma) # Conversion of var-cov matrix into precision matrix
# data # n, vmax, traits, NH4, P, K,SALINITY, SILT, PH, URP, HH, species
# monitor # a, averagea, sigma,tau, tauvar

}
"
# model6 outputs
init.model6<-run.jags(model6, n.chains=2, burnin=4000, sample=10000,modules=c("glm","dic"))
extend.init.model6<-extend.jags(init.model6, sample=20000)
print(extend.init.model6)
dic.extend.init.model6<-extract(extend.init.model6, what='dic') # DIC, pD

###################################################################
# Model 7: TER varies around the common mean for each trait and environmental driver
###################################################################
model7<-"
model
{
  for( i in 1:n)
  {
  # Linear predictors for individual traits
  ch[i] <-
a[1,1,species[i]]+a[1,2,species[i]]*NH4[i]+a[1,3,species[i]]*P[i]+a[1,4,species[i]]*K[i]+a[1,5,species[i]]*SALINITY[i]+a[1,6,s
pecies[i]]*SILT[i]+a[1,7,species[i]]*PH[i]+a[1,8,species[i]]*URP[i]+a[1,9,species[i]]*HH[i]
```

```
  sla[i]<-
a[2,1,species[i]]+a[2,2,species[i]]*NH4[i]+a[2,3,species[i]]*P[i]+a[2,4,species[i]]*K[i]+a[2,5,species[i]]*SALINITY[i]+a[2,6,s
pecies[i]]*SILT[i]+a[2,7,species[i]]*PH[i]+a[2,8,species[i]]*URP[i]+a[2,9,species[i]]*HH[i]
  wd[i] <-
a[3,1,species[i]]+a[3,2,species[i]]*NH4[i]+a[3,3,species[i]]*P[i]+a[3,4,species[i]]*K[i]+a[3,5,species[i]]*SALINITY[i]+a[3,6,s
pecies[i]]*SILT[i]+a[3,7,species[i]]*PH[i]+a[3,8,species[i]]*URP[i]+a[3,9,species[i]]*HH[i]
  ls[i] <-
a[4,1,species[i]]+a[4,2,species[i]]*NH4[i]+a[4,3,species[i]]*P[i]+a[4,4,species[i]]*K[i]+a[4,5,species[i]]*SALINITY[i]+a[4,6,s
pecies[i]]*SILT[i]+a[4,7,species[i]]*PH[i]+a[4,8,species[i]]*URP[i]+a[4,9,species[i]]*HH[i]

  # Definition of the likelihood
  mu[i,1]<-ch[i]
  mu[i,2]<-sla[i]
  mu[i,3]<-wd[i]
  mu[i,4]<-ls[i]

  traits[i,]~dmnorm(mu[i,], omega[,])
  }

  # PRIORS

  # Setting up of the regression coefficients matrix

  averagetau ~ dgamma(0.0001,0.01)

  for(k in 1:9) # Number of coefficients per trait
  {

  for(j in 1:vmax) # Number of traits
  {

  tau[j,k] ~ dgamma(0.0001,0.01)

  averagea[j,k] ~ dnorm(0,averagetau)

  for (m in 1:9)
  {
  a[j,k,m] ~ dnorm(averagea[j,k],tau[j,k])
  }
  }
  }

  # Precision matrix
  # Setting up of the variances vector (the diagonal of the var-cov matrix)

  tauvar~dgamma(1.00, 1.00)

  for( j in 1:vmax)
  {
  sigma[j,j]~dgamma(1, 0.01) # mean 1 variance high
  }

  # Setting up of the lower diagonal part of var-cov matrix
  for( j in 2:vmax)
  {
  for(k in 1:(j-1))
  {
  sigma[j,k]~dnorm(0,tauvar)
  }
  }

  # Mirroring of the lower diagonal by the upper diagonal of the var-cov matrix
  for( j in 1:(vmax-1))
  {
  for(k in (j+1):vmax)
  {
  sigma[j,k]<-sigma[k,j]
  }
  }
  omega<-inverse(sigma) # Conversion of var-cov matrix into precision matrix
  # data # n, vmax, traits, NH4, P, K,SALINITY, SILT, PH, URP, HH, species
  # monitor # a, averagea, sigma,tau, tauvar
}
"
# model7 outputs
init.model7<-run.jags(model7, n.chains=2, burnin=4000, sample=10000,modules=c("glm","dic"))
extend.init.model7<-extend.jags(init.model7, sample=20000)
print(extend.init.model7)
dic.extend.init.model7<-extract(extend.init.model7, what='dic') # DIC
```

```
#####################################################################
# Model 8: TTR varies across the species
#####################################################################
model8<-"
model
{
  for( i in 1:n)
  {
  # Linear predictors for individual traits
   ch[i] <-
a[1,1,species[i]]+a[1,2,species[i]]*NH4[i]+a[1,3,species[i]]*P[i]+a[1,4,species[i]]*K[i]+a[1,5,species[i]]*SALINITY[i]+a[1,6,s
pecies[i]]*SILT[i]+a[1,7,species[i]]*PH[i]+a[1,8,species[i]]*URP[i]+a[1,9,species[i]]*HH[i]
   sla[i]<-
a[2,1,species[i]]+a[2,2,species[i]]*NH4[i]+a[2,3,species[i]]*P[i]+a[2,4,species[i]]*K[i]+a[2,5,species[i]]*SALINITY[i]+a[2,6,s
pecies[i]]*SILT[i]+a[2,7,species[i]]*PH[i]+a[2,8,species[i]]*URP[i]+a[2,9,species[i]]*HH[i]
   wd[i] <-
a[3,1,species[i]]+a[3,2,species[i]]*NH4[i]+a[3,3,species[i]]*P[i]+a[3,4,species[i]]*K[i]+a[3,5,species[i]]*SALINITY[i]+a[3,6,s
pecies[i]]*SILT[i]+a[3,7,species[i]]*PH[i]+a[3,8,species[i]]*URP[i]+a[3,9,species[i]]*HH[i]
   ls[i] <-
a[4,1,species[i]]+a[4,2,species[i]]*NH4[i]+a[4,3,species[i]]*P[i]+a[4,4,species[i]]*K[i]+a[4,5,species[i]]*SALINITY[i]+a[4,6,s
pecies[i]]*SILT[i]+a[4,7,species[i]]*PH[i]+a[4,8,species[i]]*URP[i]+a[4,9,species[i]]*HH[i]

   # Definition of the likelihood
   mu[i,1]<-ch[i]
   mu[i,2]<-sla[i]
   mu[i,3]<-wd[i]
   mu[i,4]<-ls[i]

   traits[i,]~dmnorm(mu[i,], omega[species[i],,])
  }

   # PRIORS

   # Setting up of the regression coefficients matrix

   averagetau ~ dgamma(0.0001,0.01)

   for(k in 1:9) # Number of coefficients per trait
   {

   tau[k] ~ dgamma(0.0001,0.01)

   for(j in 1:vmax) # Number of traits
   {

   averagea[j,k] ~ dnorm(0,averagetau)

   for (m in 1:9)
   {
   a[j,k,m] ~ dnorm(averagea[j,k],tau[k])
   }
   }
   }

   # Precision matrix
   # Setting up of the variances vector (the diagonal of the var-cov matrix)

   tauvar~dgamma(1.00, 1.00)

   for( j in 1:vmax)
   {
   for (m in 1:9)
   {
   sigma[m,j,j]~dgamma(1, 0.01) # mean 1 variance high
   }
   }
   # Setting up of the lower diagonal part of var-cov matrix
   for( j in 2:vmax)
   {
   for(k in 1:(j-1))
   {
   for (m in 1:9)
   {
   sigma[m,j,k]~dnorm(0,tauvar)
   }
   }
   }
   # Mirroring of the lower diagonal by the upper diagonal of the var-cov matrix
```

```
for( j in 1:(vmax-1))
{
for(k in (j+1):vmax)
{
for (m in 1:9)
{
sigma[m,j,k]<-sigma[m,k,j]

}
}
}
for (m in 1:9)
{
omega[m,1:vmax,1:vmax]<-inverse(sigma[m,1:vmax,1:vmax]) # Conversion of var-cov matrix into precision matrix
}
# data # n, vmax, traits, NH4, P, K,SALINITY, SILT, PH, URP, HH, species
# monitor # a, averagetau, sigma, tauvar

}
"
# model8 outputs
init.model8<-run.jags(model8, n.chains=2, burnin=4000, sample=10000,modules=c("glm","dic"))
extend.init.model8<-extend.jags(init.model8, sample=20000)
print(extend.init.model8)
dic.extend.init.model8<-extract(extend.init.model8, what='dic') # DIC, pD


####################################################################
# Model 9: TTR varies around a common mean
####################################################################
model9<-"
model
{
  for( i in 1:n)
  {

  # Linear predictors for individual traits
  ch[i] <-
a[1,1,species[i]]+a[1,2,species[i]]*NH4[i]+a[1,3,species[i]]*P[i]+a[1,4,species[i]]*K[i]+a[1,5,species[i]]*SALINITY[i]+a[1,6,s
pecies[i]]*SILT[i]+a[1,7,species[i]]*PH[i]+a[1,8,species[i]]*URP[i]+a[1,9,species[i]]*HH[i]
  sla[i]<-
a[2,1,species[i]]+a[2,2,species[i]]*NH4[i]+a[2,3,species[i]]*P[i]+a[2,4,species[i]]*K[i]+a[2,5,species[i]]*SALINITY[i]+a[2,6,s
pecies[i]]*SILT[i]+a[2,7,species[i]]*PH[i]+a[2,8,species[i]]*URP[i]+a[2,9,species[i]]*HH[i]
  wd[i] <-
a[3,1,species[i]]+a[3,2,species[i]]*NH4[i]+a[3,3,species[i]]*P[i]+a[3,4,species[i]]*K[i]+a[3,5,species[i]]*SALINITY[i]+a[3,6,s
pecies[i]]*SILT[i]+a[3,7,species[i]]*PH[i]+a[3,8,species[i]]*URP[i]+a[3,9,species[i]]*HH[i]
  ls[i] <-
a[4,1,species[i]]+a[4,2,species[i]]*NH4[i]+a[4,3,species[i]]*P[i]+a[4,4,species[i]]*K[i]+a[4,5,species[i]]*SALINITY[i]+a[4,6,s
pecies[i]]*SILT[i]+a[4,7,species[i]]*PH[i]+a[4,8,species[i]]*URP[i]+a[4,9,species[i]]*HH[i]

  # Definition of the likelihood
  mu[i,1]<-CH[i]
  mu[i,2]<-sla[i]
  mu[i,3]<-wd[i]
  mu[i,4]<-sc[i]

  traits[i,]~dmnorm(mu[i,], omega[species[i],,])
  }
  # PRIORS
  # Setting up of the regression coefficients matrix

  averagetau ~ dgamma(0.0001,0.01)

  for(k in 1:9) # Number of coefficients per trait
  {

  tau[k] ~ dgamma(0.0001,0.01)

  for(j in 1:vmax) # Number of traits
  {

  averagea[j,k] ~ dnorm(0,averagetau)

  for (m in 1:9)
  {
  a[j,k,m] ~ dnorm(averagea[j,k],tau[k])
  }
  }
  }
```

```
# Precision matrix
# Setting up of the variances vector (the diagonal of the var-cov matrix)

tauvar~dgamma(1.00, 1.00)

tau.c~dgamma(0.0001,0.01)

for( j in 1:vmax)
{
for (m in 1:9)
{
sigma[m,j,j]~dgamma(1, 0.01) # mean 1 variance high
}
}
# Setting up of the lower diagonal part of var-cov matrix
for( j in 2:vmax)
{
for(k in 1:(j-1))
{

avsigma[j,k]~dnorm(0,tauvar)

for (m in 1:9)
{
sigma[m,j,k]~dnorm(avsigma[j,k],tau.c)
}
}
}
# Mirroring of the lower diagonal by the upper diagonal of the var-cov matrix
for( j in 1:(vmax-1))
{
for(k in (j+1):vmax)
{
for (m in 1:9)
{
sigma[m,j,k]<-sigma[m,k,j]

}
}
}
for (m in 1:9)
{
omega[m,1:vmax,1:vmax]<-inverse(sigma[m,1:vmax,1:vmax]) # Conversion of var-cov matrix into precision matrix
}
# data # n, vmax, traits, NH4, P, K,SALINITY, SILT, PH, URP, HH, species
# monitor # a, averagea,sigma,tauvar,tau.c
}
"

# model9 outputs
init.model9<-run.jags(model9, n.chains=2, burnin=4000, sample=10000,modules=c("glm","dic"))
extend.init.model9<-extend.jags(init.model9, sample=20000)
print(extend.init.model9)
dic.extend.init.model9<-extract(extend.init.model9, what='dic') # DIC, pD
```